الجمهورية الجزائرية الديمقراطية الشعبية

République Algérienne Démocratique et Populaire

Ministère de L'Enseignement Supérieur et de la Recherche Scientifique

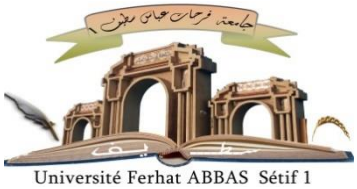

UNIVERSITÉ FERHAT ABBAS - SETIF1

FACULTÉ DE TECHNOLOGIE

THÈSE

Présentée au Département d'Electrotechnique

Pour l'obtention du diplôme de

DOCTORAT

Domaine : Sciences et Technologie

Filière: Automatique **Option: Automatique et systèmes**

Par

ATTIK Nadjah

THÈME

Contribution à la modélisation et au contrôle des systèmes à énergies renouvelable, application sur un système hybride PV/Éolien/système de stockage

Soutenue le 15/03/2023 devant le Jury:

RAHMANI Lazhar	Professeur	Univ. Ferhat Abbas Sétif-1	Président
BADOUD Abd Essalam	Professeur	Univ. Ferhat Abbas Sétif-1	Directeur de Thèse
MERAHI Farid	M.C.A	Univ. Ferhat Abbas Sétif-1	Co-Directeur de Thèse
KESSAL Abdelhalim	Professeur	Univ. Bordj Bou Arreridj	Examinateur
BERRABAH Fouad	M.C.A	Univ. M'sila	Examinateur

الجمهورية الجزائرية الديمقراطية الشعبية

PEOPLE'S DEMOCRATIC REPUBLIC OF ALGERIA

MINISTRY OF HIGHER EDUCATION AND SCIENTIFIC RESEARCH

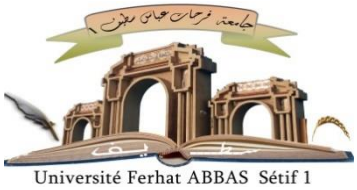

UNIVERSITY FERHAT ABBAS SETIF -1-

FACULTY OF TECHNOLOGY

THESIS

Submitted at Faculty of Technology

This thesis is submitted in fulfillment of the requirement for the degree

PhD

Field: Sciences and Technology

Specialty: Electrical Engineering

Option: Automatic & systems

By

Nadjah ATTIK

Contribution to the modeling and control of renewable energy systems, application to a hybrid PV/wind/storage system

Doctoral Committee:

RAHMANI Lazhar	Professor	University of Ferhat Abbas Sétif-1	President
BADOUD Abd Essalam	Professor	University of Ferhat Abbas Sétif-1	Supervisor
MERAHI Farid	M.C.A	University of Ferhat Abbas Sétif-1	Co-supervisor
KESSAL Abdelhalim	Professor	University of Bordj Bou Arreridj	External Examiner
BERRABAH Fouad	M.C.A	University of M'sila	External Examiner

2023

DEDICATION

I dedicate my dissertation work to my family and my friends.

A special feeling of gratitude to my loving parents,

whose words of encouragement and push for tenacity ring in my ears.

Nadjah Attik

Acknowledgements

This dissertation is not only a result of my own dedication and perseverance, but is largely a credit to the patience and helpful people that I have worked with and to the supporting and understanding people that I have lived with over these past years. I would like to take this opportunity to express my gratitude to everyone who contributed to this work.

First and foremost, I would like to express my respect and sincere gratitude to both of my advisor, **Mr. Abed Essalam BADOUD** Associate Professor at the University of Setit-1 and my co-supervisor **Mr. Farid MERAHI** Associate MCA at the University of Setit-1. Without their invaluable guidance, encouragement, insightful comments and extraordinary patience, this work would never have been possible.

I also wish to express my sincere appreciation to professor **Lazar RAHMANI** for their support to make this research a success.

I would like to thank **Dr. Abdelbaset LAIB,** for his help during the simulation of the theoretical system.

I would like to thank again President of jury **Mr. Lazar RAHMANI** Associate Professor at the University of Setit-1, I would like to thank the members of the jury, **Mr. Abdelhalim KESSAL** Associate Professor at the University of Bordj Bou Arreridj and **Mr. Fouad BENRABAH** Professor at the University of M'sila.

My deepest thanks go to my dearest parents for their hard work and great sacrifices to see that their daughter got a good education, and above all, for always being there for me. I would also like to thank my brothers, my sister, my cousin and all my family for their love and encouragement over the years.

I also extend thanks to the **future Dr Mansouri Sofia** for her continuous encouragement.

I want to express my gratitude to the Automatic Laboratory of Setif, Electrical Engineering Department,University of Setif, Algeria.

I thank my colleagues and friends for being there for me in the difficult moment. To anyone and everyone else who have offer me encouragement, loving reproach, constructive criticism, quality time, a shoulder on which to lean, a place of rest, or avenue to be of doctor.

Table of content

Chapter 01: General Introduction-

An overview of renewable energy sources (Solar and Wind)

1.1 Context ..... .01
1.2 Global access to electricity ..... .02
1.3 Progress in renewable energy ..... .02
1.4 Wind and solar surpass 10% ..... .03
1.5 Analysis of solar and wind energy potential in Algeria ..... .04
1.6 Electrical storage ..... .07
1.7 Energy and Hybrid Systems ..... .07
1.8 Socio-economic interests of the subject ..... .08
1.9 Dissertation motivation and the main contributions ..... .12
1.10 Owverview of the chapters ..... .13
1.11 Thesis Limitations ..... .16
References ..... .16

Chapter 02: Design of an Effective Control for Grid-Connected PV System

2.1 Introduction 19
2.2 State of the art: Power control and emerging PV converter technology ..... .21
2.2.1 Power control for PV side control ..... .21
2.2.2 Classification of MPPT methods ..... .22
A- First MPPT method classification ..... .22
B- Second MPPT method classification ..... .22
C- Other control strategies ..... .24
2.2.3 Power control for grid side control ..... .24
2.2.4 Control structure of DC-link voltage ..... .24
2.2.4.1 DC-link voltage value ..... .25
2.2.5 Control Structure of Grid Connected PV Inverter ..... .25
A1- Linear controllers ..... .25
B1- Non-linear controllers ..... .26
C1- Robust controllers ..... .26
D1- Adaptive controllers ..... .26
E1- Predictive controllers ..... .27
F1- Intelligent controllers ..... .27
2.2.6 Grid synchronization methods ..... .28

2.3 Design of dual-stage three-phase grid-connected PV system..... .29
2.3.1 PV generator ..... .29
2.3.2 Static converters for systems PV connected to the network..... .30
2.3.2.1 Static converters DC-DC ..... .31
2.3.2.2 Boost converter ..... .32
2.3.2.3 DC-link ..... .34
2.3.2.4 Static converters DC/AC ..... .34
A2- Centralized inverters ..... .34
B2- String inverters..... .34
C2- Multi-string inverters..... .35
D2- AC modules ..... .35
E2- Other control strategies..... .35
F2- Multilevel inverters..... .36
2.3.3 Filters for connection to the electricity network ..... .37
2.4 Originality of work carried out ..... .37
2.4.1 PV side power control (DC-DC control) ..... .38
2.4.2 Grid side power control (DC-AC control) ..... .38
2.5 Design of the Feedforward-Fuzzy logic controller for DC-link voltage..... .39
2.6 Simplified FCS-MPC of grid-connected NPC..... .41
2.6.1 Modeling of three-level NPC inverter ..... .41
2.6.2 Control model of three-level NPC inverter ..... .43
2.6.3 Dynamic model of NPC inverter with RL filter ..... .45
2.6.4 Cost function..... .46
2.6.5 Grid synchronization ..... .48
2.7 Simulation results..... .49
2.7.1 Performance comparison of applied FF-FL and PI regulators for DC-Link ..... .49
2.7.2 Synchronization..... .51
2.7.3 Voltage balancing..... .52
2.7.4 THD discussion 53
2.8 Conclusion ..... .54
References 55

Chapter 03: Comparative Study between PI and Fuzzy Logic-PI Based MPPT Strategy for PMSG Variable-Speed Wind Turbine Generation Systems

3.1 Introduction 63
3.2 Background of wind energy systems, generators and power control algorithms..... 64

3.2.1 Background of wind energy system..... 64
3.2.1.1 Angle of Attack..... 65
3.2.1.2 Types of WES..... 66
First category..... 66
Second category..... 67
3.2.2 Background of wind generators..... 68
3.2.3 Background of wind energy control algorithms..... 69
3.2.3.1 MPPT Control Algorithms for a based WECS..... 69
Main classical maximum power control methods..... 71
Wind energy background..... 71
A-Tip Speed Ratio (TSR) Control..... 72
B-Power Signal Feedback (PSF) Control..... 72
C-Optimal Torque Control (OTC)..... 72
D-Perturb and Observation Control..... 73
3.2.3.3 Advanced methods of MPPT Controls..... 74
A1 Fuzzy control..... 74
B1 Sliding mode control..... 75
C1 Neural network (NN)-based MPPT algorithm..... 75
D1 Adaptive MPPT algorithml..... 75
E1 Multivariable perturb and observe (MVPO) MPPT algorithm..... 76
3.2.3.4 Grid Side Control..... 76
3.2.3.5 Other control strategies..... 76
3.2.3.6 AC Voltage Regulator..... 77
A2 Two-level converters..... 77
B2 Three-level converters..... 78
C2 Multi-level converters..... 78
D2 Bidirectional back-to-back two-level power converter..... 78
E2 Unidirectional power converters..... 79
F2 Matrix Converter..... 79
G2. Z-source converter..... 80
H2. Cycloconverter..... 81
3.2.3.7 Control methods for PMSG..... 81
3.3 Modeling of the wind turbine conversion chain based on PMSG..... 83
3.3.1 Wind model..... 83
3.3.2 Aerodynamic model..... 84

3.3.3 Mechanic model 85
3.3.4 Modeling of PMSG 87
3.4 System description for the proposed system for PMSG 89
3.4.1 Generator side controller 90
3.4.1.1 MPPT based PI control 90
3.4.1.2 MPPT based FL-PI control 91
3.5 Model of three phase rectifier 93
3.6 Result and discussion 94
3.7 Conclusion 98
References 100

Chapter 04: Grid Energy Storage Technology

4.1 Introduction 106
4.2 Grid energy storage 106
4.2.1 Pros of grid energy storage 107
4.2.2 Cons of grid energy storage 108
4.3 Energy storage technologies 109
4.3.1 Battery Energy Storage 109
4.3.2 Supercapacitors 109
4.3.3 Pumped hydro energy storage 110
4.3.4 Compressed air energy storage (CAES) 110
4.3.5 Thermal energy storage (TES) 110
4.3.6 Flywheel 110
4.3.7 Hybridization of energy storage systems HESS 111
4.3.8 Hydrogen storage 111
4.4 Specific requirements of grid energy storage 111
4.4.1 Types of batteries 112
4.4.2 Battery Characteristics 113
4.4.3 Battery Bank Size Calculation 114
4.5 Control of Bidirectional DC-DC Converter for Battery Storage 115
4.5.1 Model analysis 116
4.5.2 Design of battery control 117
4.6 Battery testing charging and discharging 118
4.6.1 Discharging mode 118
4.6.1Charging mode 119
4.6.1 Stop mode 120

4.7 Battery testing storage system simulation 120
4.8 Conclusion 121
References 122

Chapter 05: Grid-connected Hybrid Renewable Energy System based PV/Wind

5.1 Introduction 125
5.2 Synthesis of hybrid systems architectures with PV, WES sources and batteries connected to the grid 125
5.2.1DC-Coupled systems 126
5.2.2AC-Coupled systems 127
5.2.3 The proposed configuration of hybrid system 127
5.2.4 What services can batteries provide in our work? 128
5.3 Originality of the proposed configuration 129
5.3.1 Hybrid PV-WES-side Power Control 130
5.3.2 Hybrid grid-side Power Control 130
5.3.3 Hybridization of the WT / PV power 130
5.4 Simulation results and discussions 131
5.4.1 Dynamic behavior of hybrid PV-WT 131
5.4 Conclusion 136
References 137

Chapter 06 : General Conclusion and Perspectives

6.1 Report of the thesis ..... .138
6.2 Perspectives ..... .141

List of Figures

Figures of Chapter 01:

Fig.1.1 Global access to electricity by country in 2021…….. 02

Fig.1.2 Share of energy from renewable sources in gross electricity consumption, 2020. 03

Fig.1.3 Wind and solar generated a tenth of global electricity……... 04

Fig.1.4 Objectives of the updated renewable energy program in Algeria by 2030…… 05

Fig.1.5 (a) Annual average of global horizontal solar irradiation in Algeria, (b) Annual average of wind in Algeria……. 06

Fig.1.6 (a) Solar electricity production (b) Wind electricity production…… 07

Fig.1.7 Global scheme of the proposed hybrid system……... 12

Figures of Chapter 02:

Fig.2.1 First classification of MPPT technique……. 22

Fig.2.2 Second classification of MPPT technique…… 23

Fig.2.3 classification of a few linear controllers used in power electronics……. 25

Fig.2.4 Classification of a few non-linear controllers used in power electronics……. 26

Fig.2.5 Classification of a few robust controllers used in power electronics…… 26

Fig.2.6 Classification of a few adaptive controllers used in power electronics…… 27

Fig.2.7 Classification of predictive control methods used in power electronics……... 27

Fig.2.8 The intelligent controller methods used in power electronics…….. 28

Fig.2.9 Diagram of grid connected photovoltaic system…….. 29

Fig.2.10 Equivalent circuit of a photovoltaic cell…….. 30

Fig.2.11 DC-DC Boost converter…… 32

Fig.2.12 PV inverter configurations (a)-Centralized inverters, (b)-String Inverters, (c)-Multi-string Inverters, (d)-AC modules…….. 35

Fig.2.13 Configurations of inverters connected to the network…….. 36

Fig.2.14 Global system configuration and control…….. 38

Fig.2.15 DC- Link voltage control…….. 39

Fig.2.16 FLC membership functions inputs & output…… 41

Fig.2.17 Structure of three-level NPC inverter……... 42

Fig.2.18 Predictive current control for the NPC inverter…… 44

Fig.2.19 (a) Tree-level voltage source inverter. (b) Switching and voltage vectors of the inverter…… 45

Fig.2.20 Diagram algorithm for FS-MPC……... 48

Fig.2.21 Simulation results of three-level NPC inverter (**a.** Irradiation, **b.** PV power, **c.** DC-voltages, **d.** Grid current **e.** Zoom of grid current, **f.** Grid voltage, **g.** Zoom of grid voltage and its reference, **h.** Grid voltage and current) ..…….. 52
Fig.2.22 Simulation results of three-level NPC inverter (a. Grid current and its reference, **b.** Line voltage, **c.** Phase voltages, **d.** Active and reactive power 53
Fig.2.23 DC-voltage balancing of NPC inverter (a) $V_{c1}+ V_{c2}$, (b), V_{c1} & V_{c2} (c)& V_{c1}-V_{c2}……. 52
Fig.24 THDs (%)……...……... 53

Figures of Chapter 03:

Fig.3.1 General description of a wind turbine system……. 64
Fig.3.2 The major components of a wind turbine…… 65
Fig.3.3 The angle of attack with respect to the blade…….. 66
Fig.3.4 Different control schemes in WES…….. 69
Fig.3.5 Wind turbine control strategy based on four speed regions…… 71
Fig.3.6 TSR, PSF, OTC and P&O control methods…… 73
Fig.3.7 Fuzzy control MPPT block…….. 75
Fig.3.8 Pitch Adjustment …… 77
Fig.3.9 Yaw Adjustment……. 77
Fig.3.10 Classification of Different Control Techniques for PMSM Drive……. 83
Fig.3.11 Simplified scheme of wind turbine……. 83
Fig.3.12 Power coefficient as a function of the TSR ..…….. 85
Fig.3.13 The mechanical coupling between the turbine and the electrical machine…. 85
Fig.3.14 Block diagram of the turbine model…… 86
Fig.3.15 Equivalent circuit of PMSG in the synchronous frame……... 88
Fig.3.16 Block diagram of the GSAP model in the reference d q……. 89
Fig.3.17 Global schematic on the generator side …….. 89
Fig.3.18 PI-based MPPT control……...……... 91
Fig.3.19 Fuzzy-based MPPT control…… 91
Fig.3.20 Membership functions of the various variables……... 92
Fig.3.21 Power electronic generator side converter for wind turbine system…….. 93
Fig.3.22 Basic switching vectors and sectors…… 94
Fig.3.25 Simulation result……. 98

Figures of Chapter 04:

Fig.4.1	Bidirectional DC-DC……..	116
Fig.4.2	Battery control…….	117
Fig.4.3	a. Voltage curve in charging mode, b. SOC curve in charging mode and c. Battery voltage characteristic for different charge currents……	118
Fig.4.4	a. Voltage curve in discharging mode, b. SOC curve in discharging mode and c. Battery voltage characteristic for different discharge currents…….	119
Fig.4.5	a. battery current, b. Voltage curve c. Battery SOC characteristic……..	120

Figures of Chapter 05:

Fig.5.1	HRES configuration with common DC-bus……	126
Fig.5.2	HRES configuration with common AC-bus……	127
Fig.5.3	Synoptic diagram of the hybridization of PV-Wind including storage power plant…….	128
Fig.5.4	Architecture of the power hybrid system……	130
Fig.5.5	Simulation results for constant temperature……	134
Fig.5.6	Simulation results for variable temperature……	134
Fig.5.7	Simulation result for the voltage balancing……	135
Fig.5.8	THDs of HRES……	136

List of Tables

Tables of Chapter 02:

Table.2.1 Comparison of DC-DC converter topologies for high power applications….. 31

Table.2.2 FL control rules……. 41

Table.2.3 Switching states for an NPC converter $\forall\, x \in \{a, b, c\}$…… 42

Table.2.4 Parameters characterizing the PV system connected to the network……. 53

Tables of Chapter 03:

Table.3.1 Features compression of Fixed- Speed (FS-WECS) and Variable-Speed Wind Turbine (VS-WECS)…… 66

Table.3.2 Features compression of horizontal and vertical axis wind turbine…….. 67

Table.3.3 Different types of generators used in WECS……. 68

Table.3.4 Summary of MPPT control algorithms…….. 74

Table.3.5 Fuzzy rules inference matrix…….. 92

Table.3.8 Parameters for a WECS……. 99

Tables of Chapter 04:

Table.4.1 Main chemistries for different battery types…….. 112

List of Abreviations

AC/DC:	Alternative Current to Direct Current
AC:	Alternating Current
BMS:	Battery Management System
BSOC:	Battery State Of Charge
CAES:	Compressed Air Energy Storage
CPI:	Common Point of Interconnection
DC/AC:	Direct Current to Alternative Current
DC/DC:	Direct Current to Direct Current
DC:	Direct Current
DFIG:	Doubly Fed Induction Generator
DOD:	Depth Of Discharge
DPC :	Direct Power Control
DTC :	Direct Torque Control
EMSs:	Energy Management Systems
ESS:	Energy Storage System
FCS-MPC:	Finite Control Set Model Predictive Control
FF-FL:	Feed Forward -Fuzzy Logic
FL:	Fuzzy Logic
FLC:	Fuzzy Logic Control
FL-PI:	Fuzzy Logic - Proportional Integral
FOC:	Field Oriented Control
FS-WECS:	Fixed Speed-Wind Energy Conversertion System
GHG:	Green House Gas
GSC:	Grid Side Converter
HAWT:	Horizontal Axis Wind Turbine
HCM:	Hill Climbing Method
HESS:	Hybridization of Energy Storage Systems
HRES:	Hybrid Renewable Energy System
HS:	Hybrid System
HVAC:	High Voltage AC
IC :	Incremental Conductance
IEA:	International Energy Agency
IEEE :	Institute of Electrical and Electronics Engineering

IGBA : Insulated Gate Bipolar Transistor

LAES: liquid Air Energy Storage

LQG: Linear Quadratic Gaussian

MATLAB®: Matrix Laboratory

MC: Matrix Converter

MPC: Model Predictive Control

MPPT: Maximum Power Point Tracking

MSC: Machine Side Converter

MVPO: MultiVariable Perturb and Observe

NN: Neural Networks

NPC: Neutral Point Clamped

OTC: Optimal Torque Control

P&O: Perturb and Observe

PF: Power Factor

PFL: Partial Feedback Linearization

PHES: Pumped Hydro Energy Storage

PI: Proportional Integral

PLL: Phase Locked Loop

PMSG: Permanent Magnet Synchronous Generator

PSF: Power Signal Feedback

PSO: Particle Swarm Optimization

PV: Photovoltaïc

PVG: Photovoltaïc Generator

PWM: Pulse Width Modulation

RCC: Ripple Correlation Control

RE: Renewable Energy

RES: Renewable Energy System

RSC: Rotor Side Converter

SCHB: Series Connected H-Bridge

SCIG: Squirrel-Cage Induction Generator

SKTM: The Algerian company of electricity and renewable energies

SMC: Sliding Mode Controller

SOC: State Of Charge

SVM: Space Vector Modulation

SVPWM: Space Vector Pulse Width Modulation

TES: Thermal Energy Storage

THD: Total Harmonic Distortion

THh: Terawatt-houts

TSR: Tip Speed Ratio

VAWT: Vertical Axis Wind Turbine

VSC: Voltage Source Converter

VS-WECS: Variable-Speed-Wind Energy Conversertion System

VVC: Voltage Vector Control

WECS: Wind Energy Conversion System

WES: Wind Energy System

WG: Wind Generator

WRIG: Wound Rotor Induction Generator

WRSG: Wound Rotor Syncronous Generator

WT: Wind Turbine

WTG: Wind Turbine Generator

ZSC: Z-source converter

List of Acronymes :

I_{gm}^{*}	[A]	Estimated amplitude of grid current
I_{PVg}	[A]	Contribution current by FF from PV array
I_{loss}	[A]	Loss current
$V_{\max}$	[V]	The amplitude of CPI line voltage
δ	-	Constant
i_{ga}, i_{gb}, i_{gc}	[A]	The measured grid current
v_{ga}, v_{gb}, v_{gc}	[V]	The measured grid voltage
λ	-	The weighting factor
g	-	Cost function
V_{dc}^{*}	[V]	The reference DC link voltage
C1&C2	[µF]	DC capacitors
f	[HZ]	Grid frequency
Vmp	[V]	Voltage at maximum power
Imp	[A]	Current at maximum power
Pmp	[W]	Maximum power
Voc	[V]	Open circuit voltage
Isc	[I]	Short circuit current
Ns	-	Total number of cells in series
Np	-	Total number of cells in parallel
Nps	-	Total number panels in series
Npp	-	Total number panels in parallel
I_o	[A]	The reverse saturation curent of the diode
V_t	[V]	The thermal voltage of the PV module
n	-	The diode ideality factor
D	-	The pulse width modulator duty cycle
P	[W]	Active power
Q	[VAR]	Reactive power
β	Degree (º)	Blade pitch angle
TSR	-	Tip speed ratio or λ (Lambda)
ρ	(Kg/m^2)	Air density

A_1	m/s	The average value of the wind speed
a_k	-	Harmonic amplitude of the order k
ω_k	[Rad/s]	Pulse harmonic of order k
v_w	[m/s]	Wind speed
A	[m^2]	Wind turbine blades swept area
C_p	-	Power coefficient
Ct	-	Coefficient of torque
T_t	[N.m]	The aerodynamic torque
T_{em}	[N.m]	Electromagnetic torque supplied by the generator
J_m	[kg.m^2]	Inertia of the machine
J	[kg.m^2]	Inertia of the turbine
f_m	|N.m/s]	Coefficient of friction of the machine
f	|N.m/s]	Friction of the blades
J_{Tot}	[kg.m^2]	Total inertia
f_{Tot}	|N.m/s]	Total friction coefficient
φ_{abc}	[Wb]	The flows of the axes (a, b, c)
φ_f	[Wb]	Flux of the permanent magnet
M	[mH]	PMSG mutual inductance
ω_p	[rd/s]	Electric angular velocity or electric pulsation
Ω	[rd/s]	Mechanical angular speed
P	-	Pairs of poles
T_m	[N.m]	Engine torque driving the PMSG
T_f	[N.m]	Friction torque
V_{in}	[V]	The input voltage
V_{out}	[V]	The output voltage
Ts	[µs]	The switching time period
R	[Ω]	Filter resistance
L	[mH]	Filter inductance
V	[V]	The voltage vector generated by the NPC inverter
$i_\alpha^*(k)$, $i_\beta^*(k)$	[A]	he real and imaginary components of the reference current vector

$C_{p\max}$	-	The maximum value of the power coefficient
λ_{opt}	-	The optimal tip speed ratio
ω_{opt}		Optimum rotor speed
T_{opt}	[N.m]	Optimum torque
R	[m]	Blade radius
Ω_t	[rd/s]	The angular speed of the rotor
$\begin{bmatrix} v_a & v_b & v_c \end{bmatrix}^t$	[V]	Stator phase voltage vector
$\begin{bmatrix} i_a & i_b & i_c \end{bmatrix}^t$	[A]	Current vector of the stator phases
$\begin{bmatrix} \varphi_a & \varphi_b & \varphi_c \end{bmatrix}^t$	[Wb]	Vector of the total fluxes
R_s	[Ω]	The resistance of the stator phases
Ls	[mH]	The inductance of the stator phases
Lc	[mH]	The cyclic inductance
ω_p	[rd/s]	Electric velocity or electric pulsation
S_a, S_b,S_c	-	Switching state of the converter
N_{bs}	-	Number of batteries connected in series,
V_{bn}	[V]	Nominal voltage of a battery
$E_{bat,\max}$	[Wh]	Maximum authorized storage energy
$E_{bat,\min}$	[Wh]	Minimum authorized storage energy

.

Chapter 01: General Introduction-

An overview of renewable energy sources (Solar and Wind)

1.1 Context 01
1.2 Global access to electricity 02
1.3 Progress in renewable energy 02
1.4 Wind and solar surpass 10% 03
1.5 Analysis of solar and wind energy potential in Algeria 04
1.6 Electrical storage 07
1.7 Energy and Hybrid Systems 07
1.8 Socio-economic interests of the subject 08
1.9 Dissertation motivation and the main contributions 12
1.10 Owverview of the chapters 13
1.11 Thesis Limitations 16
References 16

Chapter 1 : General Introduction- An overview of renewable energy sources (Solar and Wind)



1.1 Context

Environmental degradation, global warming and air pollution are the results, effects and taxes of the standard living improvement tied to the energy demand growth, which is currently satisfied with fossil fuels. According to studies, by 2030, energy demand will have increased by 45% [1]. This increase in demand is a result of demographic changes such as population expansion, unequal wealth distribution across many nations, economic welfare, and numerous other ecological factors that support the continued use of fossil fuels [1-3]. The depletion of traditional fossil fuel reserves and the rise in energy demand result in price rises, which encourage energy suppliers to seek for alternative energy sources supported by governmental programs like solar and wind sources.

The current economic incentives alone are insufficient to inject energy conservation initiatives since renewable energy sources are rarely competitive with conventional energy sources [1]. This is due to the economic, financial, political, geographical, and technological obstacles that face a fast, large-scale, global development and deployment of Wind, Water, Solar and Geothermal as sources of energy. Despite all sciences toward renewable energy, development is taking the track and the evolution of renewable sources is becoming perceptible. [1-3]

1.2 Global access to electricity

In both urban and rural settings, electricity became a necessity for a comfortable living. It is crucial to the most important aspects of daily living, such as recreation, travel, instruction, and healthcare. However, according to the International Energy Agency (IEA), billion people, representing 14% of the world's population, lacked access to electricity in 2021[1]. Fig.1.1, the world population's map with access to electricity, shows that these people without access to electricity live in developing countries, especially in sub-Saharan Africa and South Asia [2]. Most of these countries show a discrepancy in the electrification rate between rural and urban areas [3][19].

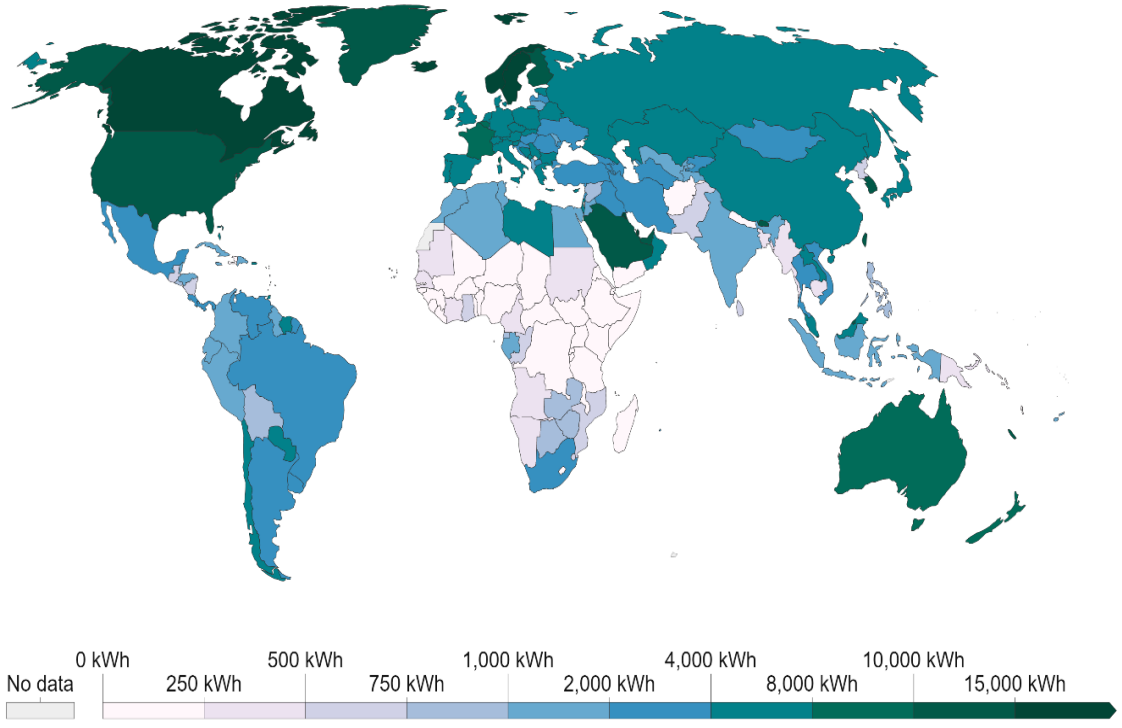

Fig. 1.1 Global access to electricity by country in 2021 [19]

Energy poverty, or a lack of access to power, is the biggest economic barrier since it keeps individuals from participating in the contemporary economy. People continue to live in darkness. So, how are these energy issues being resolved? Currently, most nations have access to electricity at a rate of 100%, while many more have rates of above 95%. The majority of the world's populous nations, such China, Brazil, and the United States, are included in literature [1], [3].

1.3 Progress in renewable energy

Due to ongoing technology developments, cost reductions, and a growth in energy demand, renewable energy has become a feasible option for supplying electricity in developing countries. The growth in electricity generated from renewable energy sources during the period 2011 to 2020

largely reflects an expansion in three renewable energy sources across the world, principally wind power, hydraulic energy and solar power. In 2021, renewable energy sources made up 37.5 % of gross electricity consumption in the world, up from 34.1 % in 2019 [2-5], [19] and [20].

Wind and hydro power accounted for more than two-thirds of the total electricity generated from renewable sources (36% and 33 %, respectively). The remaining one-third of electricity generated was from solar power (14 %), solid biofuels (8 %) and other renewable sources (8 %) [19,20]. Solar power is the fastest-growing source in 2011, it accounted for 1 %. This means that the growth in electricity from solar power has been dramatic, rising from just 7.4 TWh in 2008 to 144.2 TWh in 2020 [20]. The growth in electricity from RE power has been rising from 110.1 GWs in 2011 to 278.3 GW in 2020, as illustrated the share of energy from renewable sources in electricity and presented in Fig.1.2.

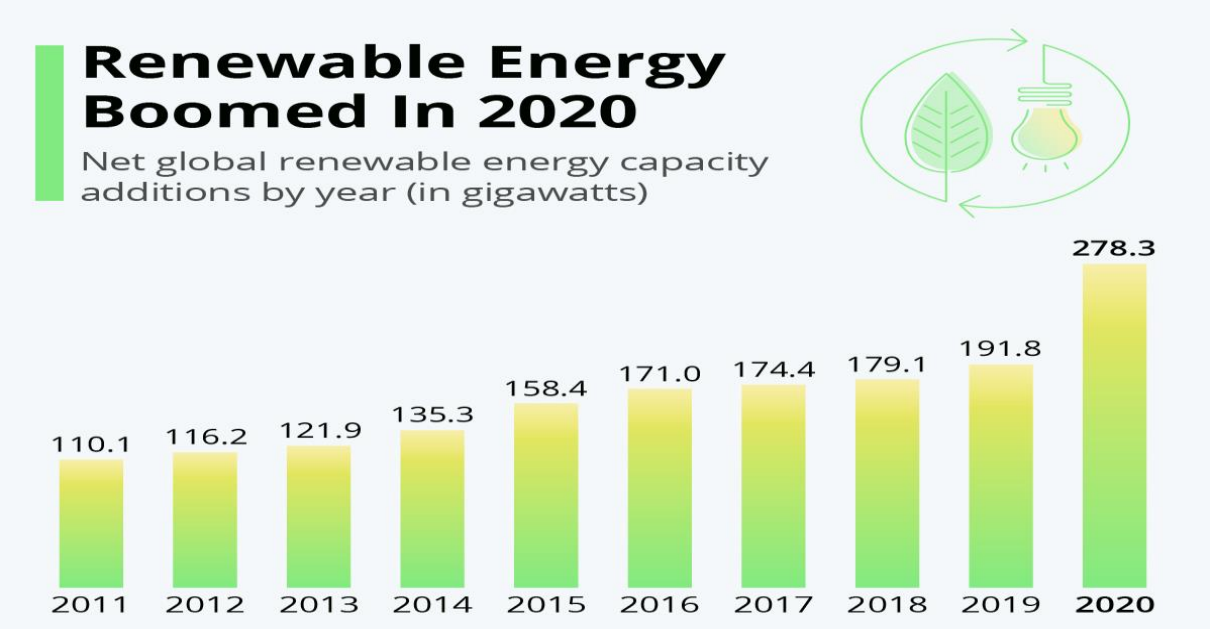

Fig.1.2 Share of energy from renewable sources in gross electricity consumption, 2020 [20]

1.4 Wind and solar surpass 10%

Ten percent (10%) of the electricity in the world comes from solar and wind energy. They make up the fourth-largest source of power globally and are the most appealing alternatives to fossil fuels due to their unbounded availability, low cost, and lack of pollution. Wind and solar energy conversion systems are more environmentally friendly, small size, self-sustaining, and able to be located closer to clients than centralized power facilities like coal, etc. However, because these renewable energy sources are intermittent and unpredictable, there may occasionally be changes in the amount of power generated [1-6]. Miss matching between power generation and load power causes a deviation from the desired voltage and frequency in power supply, their individual use may not be practical at all sites. The outputs of wind turbines and PV systems depend on variables like wind speed, solar radiation, temperature etc. that people cannot control [21]. Therefore,

combining the deployment of both of these technologies into a linked autonomous system with battery storage and grid support can be more successful at meeting energy needs without sacrificing efficiency and dependability. These are often termed as hybrid systems because of the involvement of two different sources of renewable energy and are especially popular in remote area applications [21]. The graphic shown in Fig.1.3, using IEA data; highlights the scale of the electricity transition.

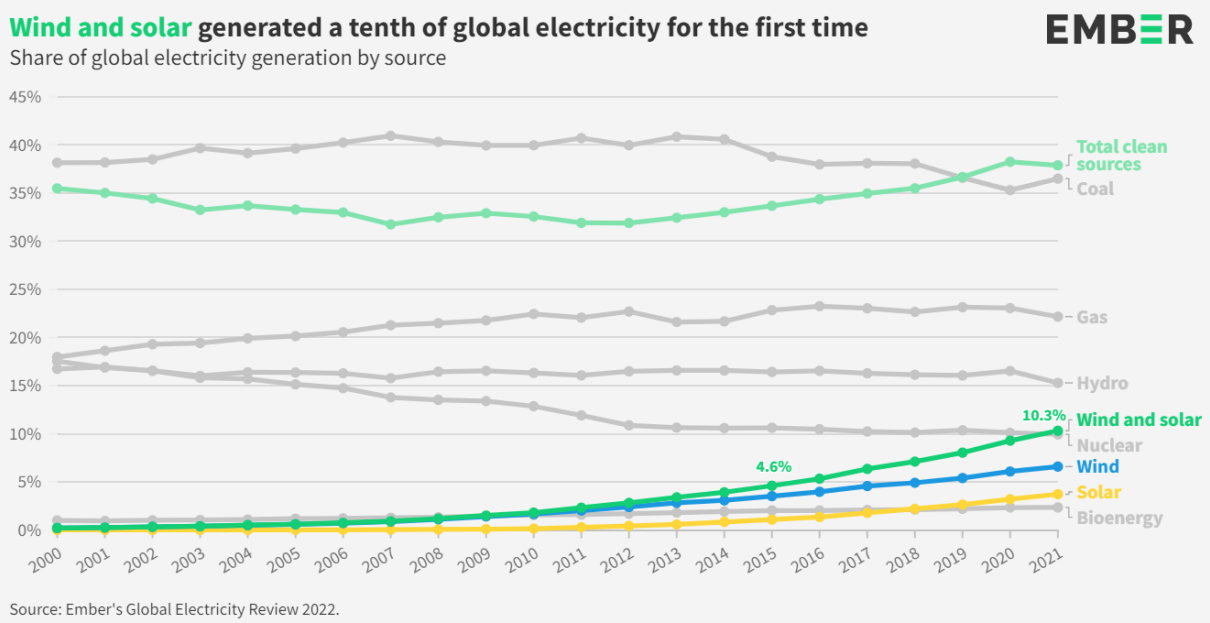

Fig.1.3 Wind and solar generated a tenth of global electricity [21]

1.5 Analysis of solar and wind energy potential in Algeria

Algeria has a sizable surface area of 2.383 million km^2; it is the tenth largest country in the world, making it unique that it experiences a range of topographical conditions and weather patterns. Additionally, it combines three distinct geographic regions: the coastal zone, the highlands (Tell Atlas Mountains), and the desert [1]. Fig.1.4 depicts Algeria's energy mix, with natural gas serving as the primary source of electricity generation [4]. The Algerian government wants to diversify its economy in order to promote sustainable development and lessen the dependency of the electricity sector on fossil fuels [7, 8]. Changing the energy policy to favour power production from renewable energy sources is essential to achieving this goal (RES). Many initiatives are recently done to address these challenges. A hybrid solar-gas station for electricity production with a capacity of 25 MW has been installed in Hassi R'mel. The Algerian company of electricity and renewable energies (SKTM) has installed PV farms in southern regions with a total capacity of 344 MW [4]. Regarding wind energy, a 10 MW wind park has been installed in the province of Adrar [4-8]. Nonetheless, these projects present only a small portion of the electricity produced as depicted in Fig.1.4. Additionally, it is exceedingly difficult to deploy PV and wind power due to the energy's volatility and instability. There have been many ideas put out

in this respect, including RES evaluation [3], energy storage [5], hybrid systems [6], and forecasting of power demand and energy production [7]. Additional research revealed that the anti-correlated solar and wind resources might offer a way to counteract their variations [8, 9]. In order to achieve this, there has been an upsurge in interest in the assessment of complementarity between variable renewable energy sources over the past several years.

The purpose of this work is to close this gap and offer a thorough investigation of the potential existence of solar-wind complementarity from both temporal and spatial perspectives over the Algerian region. Algeria's potential for solar and wind energy has been thoroughly researched in literature. According to revised solar radiation maps for Algeria provided by multiple authors [11], Djanet province was found to have the highest sun radiation resources. Numerous reviewers [3] evaluated Algeria's potential for solar and wind energy. Given the aforementioned, Algeria has enormous potential for solar and wind energy, and assessing its resources is a crucial first step in choosing the best RES locations before making any expenditures. However, there is frequently an imbalance between the demand and supply of power from RES, raising serious questions about the system dependability [18], in particular, during the end of the day when solar energy production declines and typically the demand for electricity rises [19]. The evaluation of the synergy between solar and wind energy, along with the identification of ideal locations for future installations, could be a huge help in overcoming the aforementioned difficulties. Additionally, avoiding an oversized system, lowering renewable curtailment, and reducing the capacity of the storage energy system can all be facilitated by the complementary nature of solar and wind resources [8], [20, 21].

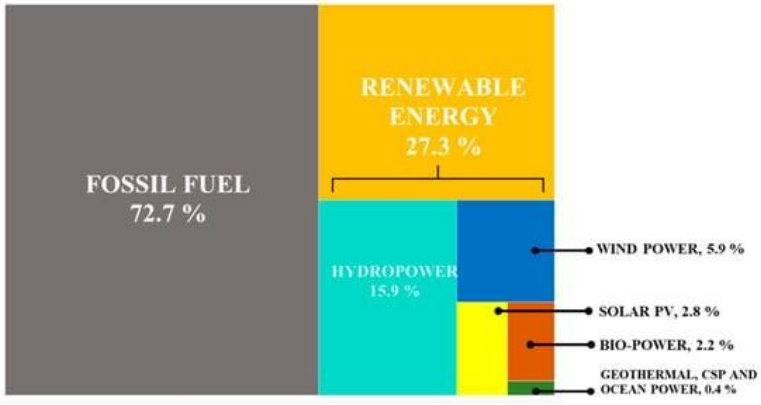

Fig.1.4 Algeria's energy mix by 2021[22]

As shown in Fig.1.5 (a), Algeria has a significant potential for solar energy that is different from other countries. Over the majority of the national land, the total annual solar energy is about two MWh on a horizontal layout by one square meter. Additionally, it appears that southern regions provide more potential than others for the use of solar resources does to produce the hydrogen. Particularly, Tamanrasset and Illizi, with yearly solar energy potentials of 2.4 and 2.2 MWh/m^2, respectively, have strong solar energy potential. On the coast and at several northern

area sites, particularly in Jijel, El-Taref, and Blida, the minimal quantity of annual solar energy available was rough 1.6 MWh/m^2 [5].

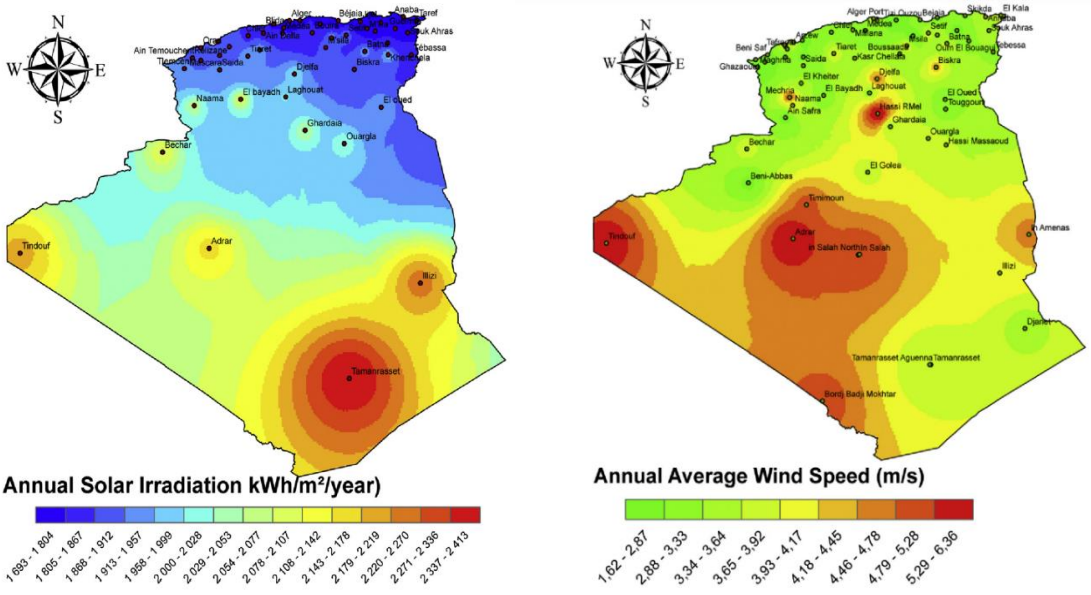

(a) (b)

Fig.1.5 (a) Annual average global solar irradiation in Algeria,
(b) Annual average wind in Algeria [5]

Fig.1.5 (b) shows the annual average wind speed of different regions in Algeria. According to the analysis of wind speed, the average wind speed in Algeria ranges from 1.6 m/s to 6.3 m/s. The regions with the highest wind speeds were Adrar (6.3 m/s), Hassi-R'mel (6.1 m/s), and Tindouf (6.0 m/s). The picturesque windy areas found in Tiaret, Borj-Baji Mokhtar, Djelfa, and Biskra. In the area along the coast, the wind speed is approximately 4 m/s. A speed of 1.6 m/s was recorded in Tizi-Ouzou region as the slowest (northern region). Therefore, we note that the wind potential for Maghnia region (northwestern region) is less than 1.4 m/s.

The analysis of solar electricity generation was assumed that the mono-crystalline photovoltaic panels would have an efficiency of 15.28 % and a peak output of 250 W when calculating the electrical energy potential [3-5]. Fig.1.6 (a) shows the regional distribution of electricity produced by solar energy. The findings indicate that Algeria's entire terrain is capable of producing between 250 and 370 GWh/km^2 of solar electricity yearly. With 368.7 GWh/km^2/year, Tamenrasset region continues to dominate in terms of maximal electrical potential. Bechar, located in the far west, comes in third place with an annual mean solar power generation of 321.1 GWh/km^2. A large-scale hydrogen synthesis from solar energy is strongly advised, and the evaluation of solar electricity generation demonstrates the significant potential of solar energy exploitation extensively noticed in the south country. The analysis of wind energy output as shown in Fig.1.6 (b) displays the electrical energy data from the wind turbine model with a 1.5 MW as rated power. As can be seen, the territory's wind energy potential is unevenly distributed. The southern region

of Algeria is said to have a significant potential for energy, and we can find a few distributed in the southwest as well as at the center. The highest annual mean wind electricity production is estimated in Hassi R'mel region (Laghouat) with 1074.8 GWh/ km^2, while the lowest value is given in the site of Tizi-Ouzou, equal to 48 GWh/km^2/year. Annually, less than 900 GWh/km^2 is predicted wind turbine electricity generation in the rest of the country, which is nevertheless quite respectable and encourages the use of wind energy [5].

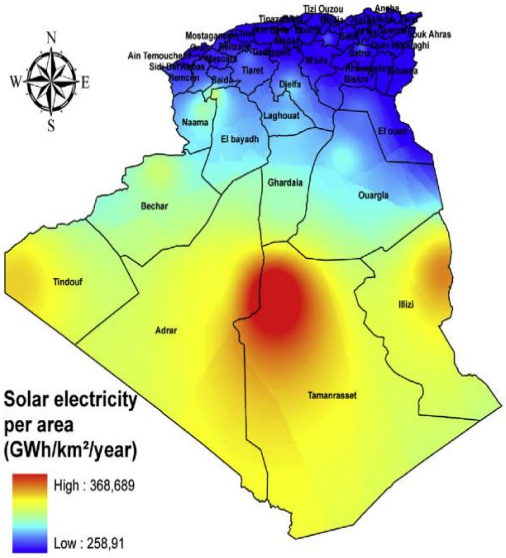

Fig.1.6 (a) Solar electricity production [5]

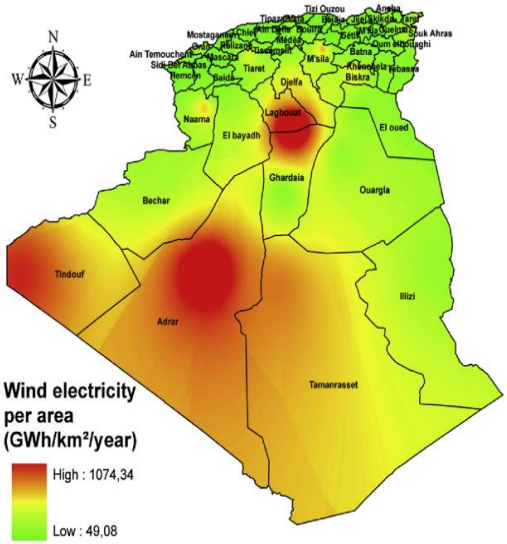

Fig.1.6 (b) Wind electricity production [5]

1.6 Electrical storages

Unfortunately, because of their interruptions, renewable sources are largely dependent on the climatic environment and cannot be reliable for user applications [10]. Devices technologies are urged to achieve the maximum levels of efficiency due to the need of reliable storage for renewable sources. Depending on the battery type and its intended use, modern battery design techniques demand a smart charging method [9,10]. Nevertheless, by using different types of renewable sources, the problem of energy discontinuity could be solved by selecting systems that back up each other in such a way that the demand of power is permanent and unbroken. PV and wind generation are both time dependent and variable but, are highly correlated, which make them ideal for a dual-sourced hybrid system.

1.7 Energy and hybrid system

Humanity requires three types of energy forms in order to satisfy their life. These forms are mechanical, electrical, and thermal energy. The electrical form of energy is the most preferable; it can be easily transported, converted, and stored. For this reason, industries compete to design the best solution for the end user. The science behind manufacturing renewable energy source components is growing toward maturity. High system efficiency is the target of all manufacturers and consumers [17, 18]. Manufacturer of solar panels is going forward to design the highest

efficient panels, also manufacturer of power converters and semi-conductors are immersed to design the fastest and lossless switching components, as well, manufacturer of wind energy system (WES) is plunged into designing the perfect design with the longest lifetime. Electrical storage device technologies are encouraged to reach the highest efficiency due to the need of reliable storage for renewable sources [1-3]. Thus, the Hybrid Systems (HS) and their management techniques are becoming the gravity center of the renewable energy science.

A power flow control of photovoltaic-wind-battery Hybrid Renewable Energy System (HRES) for stand-alone or supplying the electrical grid are used to balance the power generation and load power. Several hybridization possibilities of power sources can be obtained to produce more powers with both reliability and security of power generation systems.

Beside the unsynchronized generation peaks with demand peaks, renewable distributed generators are usually backed up with energy storage to minimize the fluctuations in their generated power and to synchronize the generation peaks with the demand peaks. However, energy storage devices are expensive [10-13]. A key element in increasing the profitability of batteries is to extend its lifetime by developing a battery management system (BMS) that can manage the battery operation carefully under all circumstances without violating its design limits [10]. Another key element in increasing the overall system profitability is to optimize the scheduling and operation of the system when it operates in grid-connected mode.

1.8 Socio-economic interests of the subject

Energy plays a fundamental role in socio-economic development and human welfare of a country. Energy access is a prerequisite for the realization of a country's socio-economic development. The availability of energy is enough to open up opportunities for people to carry out productive activities and work more effectively, so they can contribute to economic and social progress. The economic and social progress that occurs will drive demand for increasingly quality energy [10-12]. The availability of electricity is very important, because it can trigger the emergence of productive economic activities. Enough lighting at night provides opportunities for children to learn, read books and do school work. People can access information via television or access to the internet. Besides that, there is also access to electricity, besides being able to support activities in the primary sector (agriculture, fisheries and livestock) that already exist in the village, but also the presence of electricity can trigger the emergence of secondary sectors, such as trade and tourism in the village. So that access to electricity is not just to provide access of village community to electricity, but also in the broader sense that the emergence of electricity in rural areas is important because it can encourage existing economic growth and move potential sectors to be developed in the village [12-16].

Every sector of modern civilisation is dependent on energy, which comes from various energy sources such as nuclear energy, renewable plants and fossil fuels (coal, oil and natural gas). The combustion of fossil fuels emits a huge amount of greenhouse gases (GHGs) such as carbon dioxide, sulphur dioxide, and nitrogen dioxide that harm the atmosphere and the health of the population [15-17]. Therefore, there is an acute need for a power generation system, which is reliable, and sustainable that overcomes various problems related to the existing power system. Renewable energy sources can play an important role in reducing global warming and they are clean and environmentally friendly [9], [10-12].

Electrical energy generation from wind and PV sources is considered as being the most promising renewable energy and is, therefore, to be developed to replace coal, oil, gas, and even nuclear based production [14-16]. However, any process of energy transformation from one form into another usable form is complex. Naturally, includes a certain number of economic and environmental features of different kinds operation of large-scale renewable energy requires space where the resource is available that requires a good management planning and the electrical networks will also be adapted and managed to promote decentralized production) [15]. The obtained techno-economic and environmental results allow reaching an objective judgment regarding the studied system.

Recently, hybrid power systems using RES are becoming popular due to their potential benefits on the environment [12-16]. Thus, the development of hybrid systems for renewable energy conversion will undoubtedly help to solve many social problems, especially in poor countries, and open up vast commercial [12].

In [6], the authors have investigated to the adoption of technologies designed to exploit hybrid renewable (solar, wind, biomass and small hydro) energy systems at the rural level. It is centred on around the establishment of rural energy centers to improve the basic living environment. It is found out that the standard of living of rural peoples will be increased by utilizing renewable energy sources as a hybrid renewable energy system. After the establishment of the rural energy centers, employment opportunities will be increased. The improvement in living standard will stop the migration of peoples from rural area to the township will be stopped. As a result, social as well as the economic conditions of the villages will improve. HRES are more reliable for the development of rural, remote areas in the developing countries.

Besides that, in [13] the authors proposed an optimization methodology for minimum life cycle cost of a HRES based on solar photovoltaic, wind and biomass power. Biomass power seeks to take advantage of locally available forest woody biomass in the form of wood chips to provide energy in periods when the PV and wind power generated are not enough to satisfy demand [13]. The results show that a HRES combining the selected three sources of renewable energy could be

installed in a rural township; such a system would have benefits in terms of energy autonomy and environmental quality improvement, as well as in term of job opportunity creation.

Authors in [17] conducted a study to determine the optimal operating cost of hybrid grid-connected system to supply a residential load. Economically, the results showed that hybrid energy systems are more beneficial than systems with one source. Other different research papers showed systems potential and performance. These studies were focused on different aspects of PV, wind sources either connected to grid systems or considered as standalone systems [9], [11-14], [16-19]. From the literature review, most of the existing research related to the hybrid grid-connected system did not include real utility grid prices for purchasing energy from the grid. One very important missing aspect is to study the potential of using PV/Wind hybrid system connected to utility grid considering real grid prices.

The recent development in the socio-economic area, motivations, issues, system configuration, and planning methodologies using different objectives to evaluate the performance of HRES with isolated and grid-connected mode is discussed in [14]. The planning and design of low-cost energy solution for HRES including numerous technology options and availability of energy resources, reliability, and sensibility analysis are very difficult task. Therefore, the use of simulation software platform, such as HOMER, HYBRID 2, RETScreen, SOME, and RAPSYS, is making it easier to decide the possible configuration of the system and its analysis.

An extensive research has been conducted worldwide in the area of RE but the techno-economic assessments of different RE sources in Algeria received more less attention. In [16], the authors describe the technical and economic analysis of hybrid solar/wind energy source for the site of Tlemcen-Algeria. The result shows that the use of a wind system as a back-up system with a photovoltaic system increases the cost of the hybrid system for the site of Tlemcen. Due to the dominance of solar energy at the Tlemcen site over wind energy, there is a positive economic trend in the usage of photovoltaic systems with wind energy. For the first time in Algeria, recent research conducted in [8] contributed to the evaluation of the geographical and temporal complementarity between solar and wind resources at various timeframes. Additionally, the results of this analysis are presented in the form of maps, which can be used to identify potential sites for future investments in solar-wind hybrid systems. It is confirmed that Algeria contains a huge potential of solar and wind energy, accounted to a maximum annual sum of 2.38 MWh/m^2/year, and 3.33 MWh/m^2/year, respectively. Moderate complementarity levels are observed on the daily timescale in the coastal and highland regions. While the southern part of the country has the highest resources of sustainable energy, it is characterized by high levels of similarity over all time intervals [8], [16]. This similarity indicates that the solar and wind power sources supplying local loads (mostly

off-grid) will still have to rely on energy storage technologies, demand side management, or dispatching generators.

The proposed HS structure is a grid-connected hybrid system composed of a PV panel, a wind and batteries. All these components share one DC bus.

1. The application of MPPTs to the sources forms the foundation of the suggested strategy. In order to drive the PV panels and wind turbine to produce their maximum power, MPPTs are utilized. These extra parts are crucial in keeping the DC bus voltage at a constant level so that the current flows automatically from the source to the grid.

2. Subsequently, the block diagram of hybrid PV/wind system for its grid connection is presented in Fig .1.7. The PV arrays power system with DC-DC boost converter is connected to the DC bus, the wind power is also connected to DC bus through AC-DC rectifier. In grid tied operation mode, the grid side inverter is responsible for stable DC bus voltage and injects only active power to the grid with zero reactive power.

3. Batteries from various aspects including design features, advantages, disadvantages, and environmental impacts are assessed. This review reaffirms that batteries are efficient, convenient, reliable and easy-to-use energy storage systems (ESSs). In addition, it confirms that battery self life and use life are limited. A large amount and wide range of raw materials, including metals and non-metals, are used to produce batteries. The industrial battery can generate considerable amounts of environmental pollutants (e.g., hazardous waste, greenhouse gas emissions and toxic gases) during different processes such as mining, manufacturing, use, transportation, collection, storage, treatment, disposal and recycling. Battery use at a large scale or grid-scale, which is widely anticipated, will have significant social and environmental impacts. Hence, it must be compared carefully with alternatives in terms of sustainability, while focusing on research to quantify externalities and reduce risk. Alternatives such as pumped hydro and compressed air energy storage must be encouraged because of their low environmental impact compared to different types of batteries.

4. In the end, we performed the hybridization phase of two systems (PV, Wind turbine) at the DC bus, the collected power is moving to the network through a single inverter.

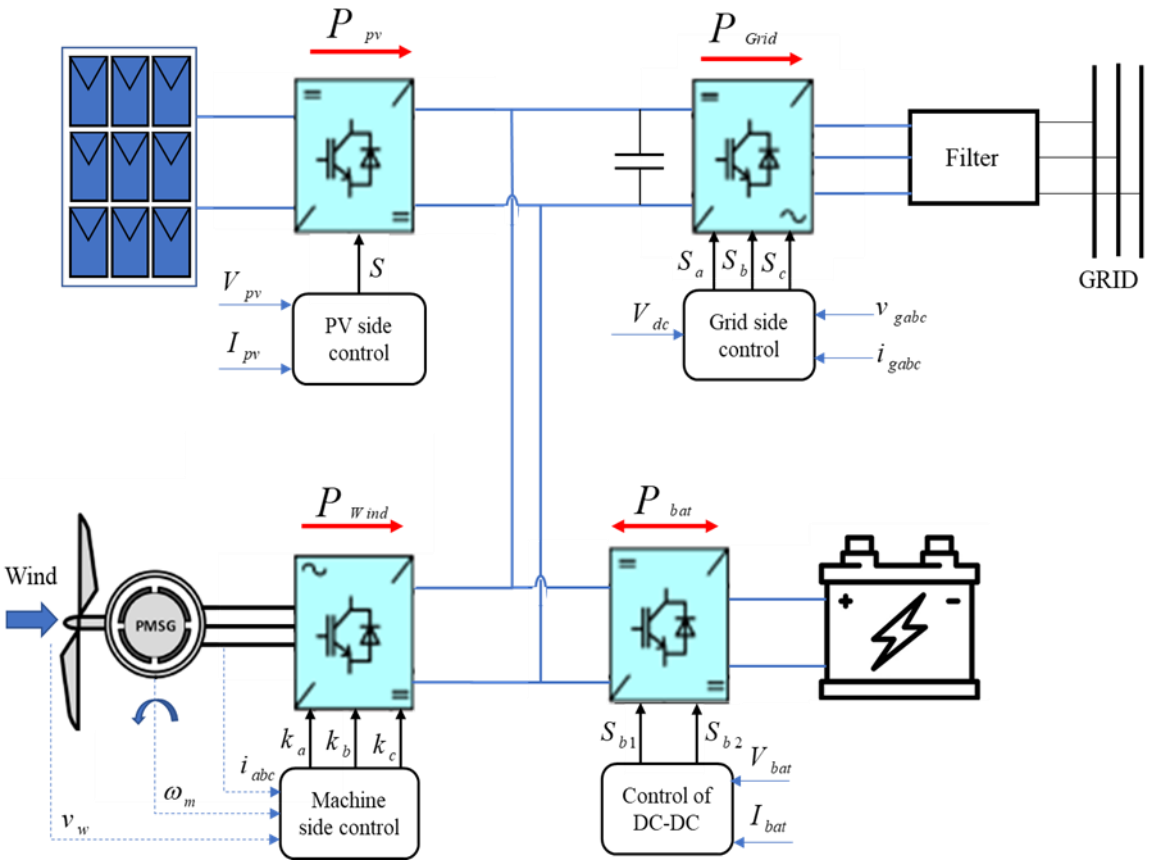

Fig.1.7 Global scheme of the proposed hybrid system

1.9 Dissertation motivation and the main contributions

The significant shift in energy demand from conventional to renewable energy sources is what motivated this study [4]. Countries are forced to create efficient solutions for energy mix due to the depletion of conventional supplies. It requires a novel normative approach in organizing for supporting research on different energy resources. Combining solar photovoltaic systems with strategy requires large storage capacity, which is expensive. However, the hybrid systems solve the problem [18]. Under this objective, different types of hybrid systems (photovoltaic/wind) for electricity supplying have been demonstrated in a large number of pilot and concrete projects.

Solar and wind energy are omnipresent, which sometimes requires the hybridization of these two systems. Hybrid solar-wind power systems uses two renewable energy sources will improve system efficiency and power reliability and reduce energy storage requirements [4-6].

The problems of power converters interfacing PV-wind hybrid system with the electrical grid involves some major drawbacks appear in simulation studies such as an important overshoot in the steady state, the long response time, a bad power quality and a bad THD that exceeds IEEE standards (< 5%). In purpose to address these issues, different contributions are proposed and will be presented under different categories. The contributions on power maximization of solar and wind turbines, DC-link control and get a better synchronization between three pathways of the

system (Production/Transport/Synchronization with the network) aim to reduce energy losses by using new control algorithms, which increases production and provides more economic income.

That's why in this context two novel approaches have been proposed in order to overcome these drawbacks. As a first step, a poor tracking of the DC-link regulator is particularly apparent when the solar irradiance varies severely or suddenly. This problem leads us to develop the extension of DC-link control using the Feed Forward based Fuzzy Logic (FF-FL) to improve its transient performance. More development in term of minimization error, fuzzy is used to compensate the DC-link losses with remarkable improved performances, which are noted by setting DC-link voltage reference. Where the DC-link voltage was adapted by adjusting reference DC-link voltage according to CPI (common point of interconnection). The grid side converter enables to control the active and reactive power flow injected into the grid with improving the output power quality by reducing the total harmonic distortion (THD). Another task is dedicated to control the connection to the grid using three-level converter in order to achieve high voltage using low voltage switching devices. In this case, Neutral Point Clamped (NPC) has been proposed to provide high output power to feed the PV source into an existing three-phase power grid via an RL filter. Therefore, the second proposed approach deals principally with the behavior of grid currents variation, Finite Control Set-Model Predictive Control (FCS-MPC) has been proposed to exhibit the high dynamic efficiency for multilevel converters that keeps a unit power factor and maximizes the energy harvested from the hybrid system.

1.10 Overview of the chapters

The content of this thesis is divided into six chapters. This first chapter is restricted to a brief introduction to the subjects related to this thesis. This chapter presents an overview of the integration of renewable energy resources. It also describes the current global energy demand and growth challenges that the world is currently facing. The literature survey on the global energy scenario and renewable energy integration, and evaluates the spatial which mainly involves solar photovoltaic (PV) and wind energy is presented, and the complementarity between solar and wind energy in Algeria. The chapter also addresses the different contexts of using renewable energy resources (RERs) and grid-connected applications.

Chapter 2 Design of an Effective control for Grid-Connected PV System

This chapter will deal on the novel topology of a DC-link control using Feed Forward-Fuzzy Logic (FF-FL) method to control the first conversion stage. This method is associated with the second stage predictive current control strategy Finite Control Set-Model Predictive Control Strategy (FCS-MPC) applied in a three-phase three-level neutral point clamped inverter based dual-stage grid connected photovoltaic (PV) system. In this chapter, the first processing step will extract the maximum power from PV field to feed the DC-link stage. Boost chopper will adjust

the duty cycle using perturb and observe (P&O) algorithm to track the maximum power (MPPT) in all weather conditions and has preference such as straightforward topology, efficiency… etc. To maintain a suitable power intermission control, it must be checking the DC-link voltage at the reference value then assessment the amplitude of the grid currents. Simple regulators have an extended time to respond and considerable voltage ripples over steady state. Feed Forward overcomes these issues. The selectors of adaptive DC-link voltage controller to assure a high efficiency of PV system with many endeavors have been notified in the technical literature. We propose an adaptive DC-link voltage Feed Forward by adjusting reference DC-link voltage according to CPI (Common Point of Interconnection) voltage. To compensate the current undesirable harmonic together with a unity power factor, the proposed work can perform predictive current control strategy FCS-MPC, which will suggested for the current control of three-phase three-level inverter. A discrete-time model of power conversion systems will be firstly developed. It describes the dynamics of the line currents in a stationary reference frame. Therefore, the FCS-MPC method will be applied to determine the appropriate control-law that minimizes the cost function. The latter will formulate in terms of the errors related to the line currents and DC-voltage mid-point. A multi-step model predictive voltage control method based on (FCS-MPC) will be presented in this chapter. The proposed method is validated on a three-level three-phase voltage source PV inverter. In each control cycle, 27 voltage vectors for inverters are evaluated on line based on predictive model to obtain the optimal switching state. A comparative study of the DC-link control between two methods (FF-FL and PI) with a remarkable improvement was noted in the simulation results, which proves the right choice and the proposed thorough study in order to improve the power quality transmitted in the networks.

Chapter 3 Comparative Study between PI and Fuzzy-PI Based MPPT Strategy for PMSG Variable-Speed Wind Turbine Generation Systems

This chapter will be devoted to wind energies, their captured power, their different types as well as the different structures of the electromechanical converters used in these systems (wind system). The chapter will propose the modeling of the various elements constituting wind turbine part, including the primary source (wind and turbine), the electromechanical converter and ending with the power converter model. Once the entire plant is modeled, we will proceed to its control starting by generator speed control in order to reach the optimal speed allowing the extraction of the maximum power.

The chapter will focus on a comparative analysis of two control methods to extract the maximum power from Permanent Magnet Synchronous Generator (PMSG) based Wind Energy Conversion System (WECS) under different wind speed conditions. The WECS consists of a wind turbine, a PMSG and AC/DC converter stand-alone mode. The Maximum Power Point Tracking

(MPPT) control technique compares the Proportional Integral (PI) control and Fuzzy Logic Proportional Integral controller (FL-PI). The considered parameters for analysing the efficiency of MPPT controller is the steady state of dynamic response of the system under different wind speed is considered to justify the overall efficiency of the controllers.

The potential to use DC directly from WECS requires proper rectification (from AC to DC) of power when considered for DC load or grid applications. In this chapter a converter is designed for rectification of the power developed by the WECS and an attempt is made to apply Space Vector Pulse Width Modulation (SVPWM) for switching of rectifier to obtain a pure DC supply from WECS.

Chapter 4 Grid Energy Storage Technology (GEST)

Fast-ramping grid-level storage is still an immature industry while energy storage technologies have existed for decades. It is experiencing relatively rapid improvements in performance and cost across a variety of technologies. In this innovation cycle, it is important to determine which properties of emerging energy storage technologies are most valuable. Decreased capital cost, increased power capability, and increased efficiency all would improve the value of an energy storage technology. Each has cost implications that vary by application, but there has not yet been an investigation of the marginal rate of technical substitution between storage properties. Energy storage devices will be needed at different locations of the power system, to level the mismatch between renewable power generators, consumption and/or to store the surplus of power from renewable sources for later use during no generation times or low power generation times.

This chapter will give an overview of different storage technologies, review of batteries from various aspects such as design features, advantages, disadvantages, and environmental impacts. Study of the role of batteries and how batteries contribute to environmental pollution, greenhouse gas (GHG) emissions, and harmful effects on public health. In addition, provides a reader who has little to none technical chemistry background with an overview of the working principles of lithium-ion batteries.

Chapter 5 Grid-connected of Hybrid Renewable Energy System based PV/Wind

The last phase of this study is intended for the hybridization of two plants at the DC-bus level. They debit their energies to the network under a single DC-bus and a single inverter.

The chapter is essentially based on performance of wind/PV hybrid system under different perturbation conditions (irradiation, wind and temperature). Wind power system and PV arrays are controlled to reach maximum power output. The DC output of wind and solar PV plants is connected to a common DC-bus. A common inverter suitable for combined output AC capacity is used to convert DC power into AC power.

Chapter 6 General Conclusion and Perspectives

This chapter provides thesis conclusion and some research perspectives in this field.

1.11 Thesis limitations

- The Matlab/Simulink model is incredibly slow to start up. Simulink takes its time at the startup to compile the model. However, the elapsed time is huge; the Simpower systems model in Matlab/Simulink takes a long time in the simulation; sometimes, several minutes especially for the hybrid system.
- Renewable energy sources continue to gain popularity. However, two major limitations exist that prevent widespread adoption, availability of the electricity generated and equipment cost. The downside, however, the cost of equipment needs to create such system. Thus, optimization of the generation, storage in light of capital cost and variability mitigation is imperative to the financial feasibility of grid systems.
- Not only cost and simulation are the problems, the COVID-19 pandemic has altered people's lifestyles. Mostly all activities were conducted entirely online.

References

[1] KARAMI, Nabil. *Control of a hybrid system based PEMFC and photovoltaic panels*. 2013. Doctoral dissertation. Aix-Marseille.

[2] YIMEN, Nasser, TCHOTANG, Theodore, KANMOGNE, Abraham, *et al.* Optimal sizing and techno-economic analysis of hybrid renewable energy systems—A case study of a photovoltaic/wind/battery/diesel system in Fanisau, Northern Nigeria. *Processes*, 2020, vol. 8, no 11, p. 1381.

[3] LAKHDARA, A., BAHI, T., et MOUSSAOUI, A. Study and Management of an Hybrid System Connected to The Network. *J. Electrical Systems*, 2022, vol. 18, no 2, p. 163-172.

[4] CHAKIR, Asmae, TABAA, Mohamed, MOUTAOUAKKIL, Fouad, *et al.* Optimal energy management for a grid connected PV-battery system. *Energy Reports*, 2020, vol. 6, p. 218-231.

[5] RAHMOUNI, Soumia, NEGROU, Belkhir, SETTOU, Noureddine, *et al.* Prospects of hydrogen production potential from renewable resources in Algeria. *International Journal of Hydrogen Energy*, 2017, vol. 42, no 2, p. 1383-1395.

[6] AKELLA, Ashok Kumar et DAS, Somnath. Technical and socio-economic aspects of hybrid renewable energy sources: a step-by-step approach. *International Journal of Applied Engineering Research*, 2017, vol. 12, no 21, p. 11228-11241.

[7] ALHARTHI, Yahya Z., SIDDIKI, Mahbube K., et CHAUDHRY, Ghulam M. Techno-economic analysis of hybrid PV/wind system connected to utility grid. In : *2019 IEEE Texas Power and Energy Conference (TPEC)*. IEEE, 2019. p. 1-6.

[8] GUEZGOUZ, Mohammed, JURASZ, Jakub, CHOUAI, Mohamed, *et al.* Assessment of solar and wind energy complementarity in Algeria. *Energy Conversion and Management*, 2021, vol. 238, p. 114170.

[9] MURUGAPERUMAL, K. et RAJ, P. Ajay D. Vimal. Feasibility design and techno-economic analysis of hybrid renewable energy system for rural electrification. *Solar Energy*, 2019, vol. 188, p. 1068-1083.

[10] KHAN, Faizan A., PAL, Nitai, et SAEED, Syed H. Optimization and sizing of SPV/Wind hybrid renewable energy system: A techno-economic and social perspective. *Energy*, 2021, vol. 233, p. 121114.

[11]RACHMAWATIE, D., RUSTIADI, E., FAUZI, Aad, *et al*. Analysis of the socio-economic impact of renewable energy hybrid electricity utilization for rural community development (case study: Pantai Anyar, Yogyakarta special region, Indonesia). In : *IOP Conference Series: Earth and Environmental Science*. IOP Publishing, 2019. p. 012013.

[12]AGRAWAL, Monika, SAXENA, Bharat Kumar, et RAO, K. V. S. Techno-Economic Analysis of a Grid-Connected Hybrid Solar–Wind Energy System. In : *Green Buildings and Sustainable Engineering*. Springer, Singapore, 2019. p. 81-92.

[13] GONZÁLEZ, Arnau, RIBA, Jordi-Roger, et RIUS, Antoni. Optimal sizing of a hybrid grid-connected photovoltaic–wind–biomass power system. *Sustainability*, 2015, vol. 7, no 9, p. 12787-12806.

[14]BOHRE, Aashish Kumar, SAWLE, Yashwant, et ACHARJEE, Parimal. Optimal design and techno-socio-economic analysis of hybrid renewable system for gird-connected system. In : *Renewable Energy Systems*. Academic Press, 2021. p. 653-686.

[15] NURUNNABI, Md, ROY, Naruttam Kumar, et MAHMUD, Md Apel. Investigating the environmental and socio-economic impacts of grid-tied photovoltaic and on-shore wind systems in Bangladesh. *IET Renewable Power Generation*, 2018, vol. 12, no 9, p. 1082-1090.

[16] CHADEL, Asma, CHADEL, Meriem, AILLERIE, Michel, *et al*. Technical and economic analysis of hybrid solar/wind energy source for the site of Tlemcen-Algeria. *Energy Procedia*, 2017, vol. 119, p. 29-37.

[17] TÜRKAY, Belgin Emre et TELLI, Ali Yasin. Economic analysis of standalone and grid connected hybrid energy systems. *Renewable energy*, 2011, vol. 36, no 7, p. 1931-1943.

[17] MANWELL, J. F., *et al.* Hybrid energy systems. *Encyclopedia of energy*, 2004, vol. 3, no 2004, p. 215-229.

[18] STOYANOV, Ludmil. *Etude de différentes structures de systèmes hybrides à sources d'énergie renouvelables*. 2011. Doctoral dissertation. Université Pascal Paoli.

[19] Ritchie, Hannah, Max Roser, et Pablo Rosado. « Energy ». *Our World in Data*, 28 novembre 2020. https://ourworldindata.org/energy-access.

[20]https://www.statista.com/chart/24856/net-global-renewable-capacity-additions/

[21] « Wind and Solar Generated 10% of Global Electricity in 2021 - a World First ».

[22] https://renewablesnow.com/news/algeria-to-invite-investors-for-renewables-programme-by-summer-end-516370/

Chapter 02: Design of an Effective Control for Grid-Connected PV System

2.1 Introduction 19
2.2 State of the art: Power control and emerging PV converter technology ..... .21
2.2.1 Power control for PV side control ..... .21
2.2.2 Classification of MPPT methods ..... .22
A- First MPPT method classification ..... .22
B- Second MPPT method classification ..... .22
C- Other control strategies ..... .24
2.2.3 Power control for grid side control ..... .24
2.2.4 Control structure of DC-link voltage ..... .24
2.2.4.1 DC-link voltage value ..... .25
2.2.5 Control Structure of Grid Connected PV Inverter ..... .25
A1- Linear controllers ..... .25
B1- Non-linear controllers ..... .26
C1- Robust controllers ..... .26
D1- Adaptive controllers ..... .26
E1- Predictive controllers ..... .27
F1- Intelligent controllers ..... .27
2.2.6 Grid synchronization methods ..... .28
2.3 Design of dual-stage three-phase grid-connected PV system ..... .29
2.3.1 PV generator ..... .29
2.3.2 Static converters for systems PV connected to the network ..... .30
2.3.2.1 Static converters DC-DC ..... .31
2.3.2.2 Boost converter ..... .32
2.3.2.3 DC-link ..... .34
2.3.2.4 Static converters DC/AC ..... .34
A2- Centralized inverters ..... .34
B2- String inverters ..... .34
C2- Multi-string inverters ..... .35
D2- AC modules ..... .35
E2- Other control strategies ..... .35
F2- Multilevel inverters ..... .36
2.3.3 Filters for connection to the electricity network ..... .37
2.4 Originality of work carried out ..... .37
2.4.1 PV side power control (DC-DC control) ..... .38
2.4.2 Grid side power control (DC-AC control) ..... .38
2.5 Design of the Feedforward-Fuzzy logic controller for DC-link voltage ..... .39
2.6 Simplified FCS-MPC of grid-connected NPC ..... .41
2.6.1 Modeling of three-level NPC inverter ..... .41
2.6.2 Control model of three-level NPC inverter ..... .43
2.6.3 Dynamic model of NPC inverter with RL filter ..... .45
2.6.4 Cost function ..... .46
2.6.5 Grid synchronization ..... .48
2.7 Simulation results ..... .49
2.7.1 Performance comparison of applied FF-FL and PI regulators for DC-Link ..... .49
2.7.2 Synchronization ..... .51
2.7.3 Voltage balancing ..... .52
2.7.4 THD discussion 53
2.8 Conclusion ..... .54
References 55

Chapter 2 Design of an Effective Control for Grid-Connected PV System



Abstract

A two-stage photovoltaic grid-connected modeling and control approaches are presented in this chapter focuses on updating grid control and regulations. In addition, an overview of recent control strategies for PV side control, grid side control and the phase locked loop (PLL) with a grid synchronization technique is discussed briefly. A complete mathematical model is discussed for each component of the system.

Analytically, the aim is to study a photovoltaic system connected to the electrical supply network from its exploited maximum power. The MPPT of the photovoltaic system is integrated with the boost controller.

The DC-link control is based on Feed Forward with Fuzzy Logic (FF-FL), the FLC is designed with minimum membership functions and fuzzy rules to enhance the voltage source inverter. A three-level Neutral Point Clamped (NPC) voltage source inverter for grid connected photovoltaic (PV) systems is proposed using a Finite Control Set Model Predictive Control (FCS-MPC), which is a genetic approach for predictive control of multilevel inverters allows to control the active and reactive powers without parameter tuning. Both of (FF-FL & FCS-MPC) allow to achieve grid-tied current injection with low total harmonic distortion (THD) of the current, unity power factor and balancing the capacitor voltages. The simulation model is implemented in a MATLAB/Simulink environment.

2.1 INTRODUCTION

In the last decades there has been growing concern about energy resources, as energy consumption trend does not seem to be sustainable, this situation has led to research in renewable energies [1], [2]. Nowadays, photovoltaic energy can be the most well-established renewable energy. Solar photovoltaic energy is following its path in terms of installed power increase and applications (grid connection instead of stand-alone systems) [1], [3]. This work contributes not only to the energy development of cities or environmental problem, especially of air pollution, but also to power converters and control.

To carry out this research, we asked ourselves the following question:

1. How to achieve interconnection of the photovoltaic system to the electrical grid?

The proposed hypotheses are such as:

1. It is necessary to concentrate our forces in order to increment the PV system's performances. In order to reach this last aspect, it is important to note that the output characteristic of a photovoltaic array is nonlinear and changes with solar irradiation and the cell's temperature. Therefore, a Maximum Power Point Tracking (MPPT) technique is needed to draw peak power from the solar array in order to maximize the produced energy.
2. The purpose of the DC link voltage controller is to preserve the DC-link voltage at its reference value according to the (CPI) and to provide the reference grid current. This controller achieved the transfer of the active power flow, drawn from the photovoltaic generator, to the utility network.
3. Inverters have several exciting features that make them the best for solar panels. Grid-tied PV inverters have an added functionality besides converting the solar energy from DC to AC.
4. With the use of Phase Locked Loop PLL, the inverters voltage and current and that of the grid are maintained and operated synchronously.
5. A filter is often used to interconnect an inverter to the utility grid in order to filter the harmonics produced by the inverter.

The power delivered by the PV system of one or more photovoltaic panels depends on the irradiance, temperature, and the current drawn from the cells. A two-stage circuit topology is proposed, wherein the first stage is a boost converter, which serves for maximum power point tracking [2], [5-7]. Maximum Power Point Tracking (MPPT) algorithm is used to extract the maximum power from the PV systems which will be injected to the electrical grid. The second stage is a grid tied voltage source converter (VSC), which not only feeds extracted solar photovoltaic (PV) energy into the three-phase distribution system but also serves for harmonics mitigation, reactive power compensation and grid current regulation [8], [9].

There are two main power circuits in the proposed topology. The duty ratio for the boost converter is decided on the basis of the MPPT control algorithm [10]. The input voltage of the boost converter is continuously adjusted such that the PV array operates at MPP [11-14]. The output of the boost converter is connected to the DC-link of the voltage source converter (VSC). The DC link voltage of the VSC is adjusted in real time considering the CPI voltage [15-17]. Therefore, with the proposed control approach, both input and output voltages of the boost converter are adjusted in real time. Moreover, the proposed control algorithm also presents a solution for balancing grid currents. Hence, the currents injected by the VSC are controlled such that the grid currents are always balanced and sinusoidal at unity power factor [16], [18]. For proper control of output currents of the VSC, the DC link voltage is kept constant (higher than the amplitude of CPI line voltage) [16].

Higher power usually requires higher voltages. In order to maintain currents at an acceptable level, isolation voltage limit of PV panels constrains the number of series-connected panels in a PV array, thus limiting its maximum DC voltage level [18-21]. Therefore, multilevel inverters appear to be a very good solution for solar applications, as a PV arrays concatenation is straight forward to each level of the DC-link. In this scenario, power control of multilevel inverters for photovoltaic applications has recently been considered. Several methods for power control of multilevel inverters have already been presented. Nowadays, the most popular Modal Predictive Control MPC method is obviously the FCS-MPC [24], [22-27]. Among the possible switching states of the converter, it applies at each sampling time only one switching state that should be the most appropriate one according to a performance criterion. Accordingly, the switching states are considered as control inputs. On the other side, based on the discrete-time state-space model of the power conversion system, the system's behavior is predicted over a finite horizon. The predicted variables are therefore utilized to formulate a cost-function which minimizes specific constraints. Accordingly, the appropriate control-law is the one that minimizes the cost-function [26-29]. Note that the FCS-MPC allows formulating the control variables and constraint into a single control-law which is indeed a very important benefit [26]. Recently, multilevel inverters are becoming increasingly used as an active interface for grid connected PV systems, this is because of their superior features such as higher voltage operation, good power quality, reduced common mode voltage and low voltage stress on power semiconductors. In this chapter, a discrete-time state-space model of the power conversion system is firstly developed [30]. It describes the dynamics of the currents in a stationary reference frame and the one of the DC-bus capacitor voltage. Therefore, the FCS-MPC method is applied to determine the appropriate control-law that minimizes the cost function.

On the other hand, a simple MPPT (P&O) and a DC-link control method based on the Feed Forward-Fuzzy logic (FF-FL) control concept are proposed which allow directly the DC link voltage control. DC-link neutral-point balance is also achieved by means of the predictive control algorithm, which considers the redundant switching states of the NPC converter. The proposed methods are evaluated by numerical simulations and carried out under a grid voltage conditions.

2.2 State of the art: Power control and emerging PV converter technology

In recent years, grid connected renewable energy system has emerged with its simplicity, reliability and durability. The ranges of grid tie inverters are classified as small scale as several tens of kilowatts and large scale as hundreds of megawatts [31]. Accordingly, the standard interconnection with the grid is made higher extent in improving its power system reliability [32], [33], efficiency and cost. Moreover, the working of grid connected inverter primarily depends on robustness in control strategy [34], even working in abnormal grid conditions such as deviation of voltage and frequency. The control of solar photovoltaic (PV) systems has recently attracted a lot of attention. Over the past few years, many control objectives and controllers have been reported in the literature. Two main objectives can be identified, the first is a PV side control to obtain the maximum available PV power with MPPT algorithm control and the second objective is the grid side control. The grid side control includes three main steps of control: DC-link voltage control, current control and grid synchronization. This review focuses on different power control algorithms for grid-connected photovoltaic system [17], [35].

2.2.1 Power control for PV side control

In recent decades, photovoltaic generation systems have increased rapidly, with the explosive growth of power electronics technology contributing to the large installation of power electronic devices, their influence on the power system operation has drawn more attention [36-38]. In view of such a circumstance, it is also necessary to optimize the control techniques of grid-tied PV inverters since the function under low voltage faults are so much different from that under normal conditions. To be precise, the key problems to be considered include the over current due to a sudden decrease in voltage, the sudden surge in DC-link voltage because of the imbalance between input and output power [39]. In the literature, several control methods were developed to enhance the inverter output under the asymmetrical faults and reduce generation losses [40-41]. Due to high solar panel cost, the investment in solar energy systems is still high [23]. Consequently, considering the first investments for any installed energy plant, the objective is to extract maximum energy production from the capacity provided. Several studies have suggested the use of two stages PV generation system [42-44]. A DC-DC converter is conventionally used as the first stage that serves the objective of the MPPT [15].

2.2.2 Classification of MPPT methods

In the DC-DC stage, the maximum power should be extracted from the PV source [24]. The converter in this stage operates as a matching circuit because of the nonlinear characteristics of the PV source and also elevates the PV voltage for proper grid connection [46], [47]. Many MPPT techniques have been addressed in the literature [41-43]. Indeed, they differ from each other based on several factors, including methodology, efficiency, tracking speed, required sensors, complexity, cost, range of effectiveness, convergence speed, correct tracking when irradiation and/or temperature change with the hardware needed for the implementation or popularity [48]. The maximum power point tracking control classification can be mainly divided into many types [47], [49-51]. A big number of MPPT method classifications and designs are available in the literature [11-13], each classification has its own specifications, limitations and applications.

A-First MPPT method classification

A growing number of MMPT classification of tracking technique classification has been applied to MPPT algorithms. Therefore, in literature, many pieces of research have classified the MPPT algorithms based on their conventional or intelligent control schemes [10-13], [38-59], as shown in Fig.2.1:

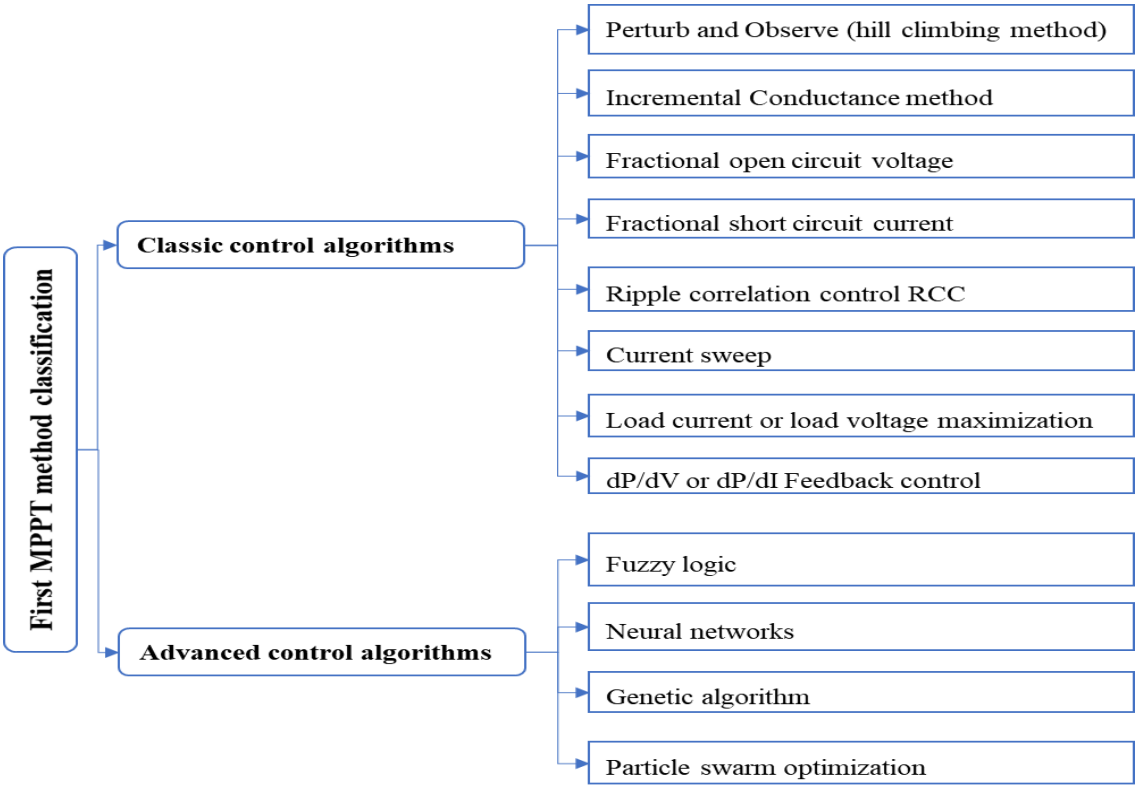

Fig.2.1 First classification of MPPT technique

B-Second MPPT method classification

Since the starts of PV application as stand-alone and grid-connected systems, researchers start to develop strategies to squeeze the PV panel to absorb the maximum power. There is no evaluation

study that classifies methods since each one can be suitable for an application and not for another. The ease of implementation is an important factor in the deciding which MPPT techniques to use, some techniques are easily implemented with no need for on-site adjustment or calibrations. Other techniques are more complex and their calibration varies with site location and climatic conditions. In this section, tracking methods are categorized by their tracking technique, which are divided into five groups [43], [46-59]. Fig.2.2 illustrates the second classification of the MPPT algorithm.

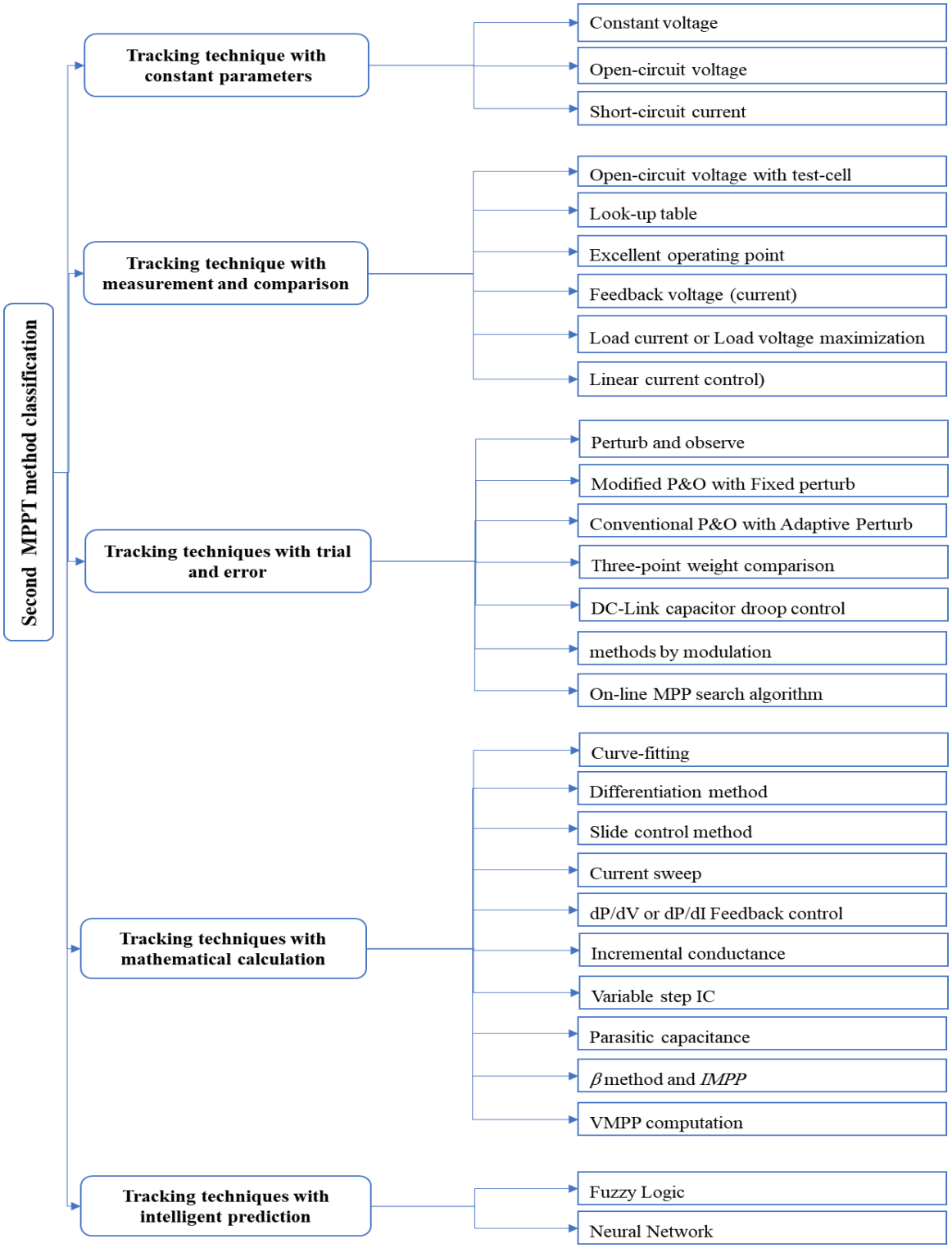

Fig.2.2 Second classification of MPPT technique

C-Other control strategies

Recently, and as a result of the continuous development of controllers, advanced techniques, such as model predictive control (MPC) and optimization techniques are proposed to overcome the limitations of the conventional maximum power point tracking (MPPT) methods [58],[60]. Hybrid MPPT techniques are applied in nature for systems exposed to partial shading conditions caused by nearby buildings or trees, clouds or even smoke [61-64].

2.2.3 Power control for grid side control

The inverter control strategy consists of two main cascaded loops. Typically, a loop which regulates the DC-link voltage and loop which controls the grid current. The current protection and power quality issues are associated with the current control loops [39].

The two-stage PV array connected to the grid will require a constant current injection in the DC-link, which is the output capacitor of the boost converter. A constant current injection will ensure the constant voltage of the DC-link and limited fluctuation in the output voltage variation. Hence, the inverter will get the constant input DC voltage, which is necessary to improve the performance and efficiency of an inverter [16], [60].

2.2.4 Control structure of DC-link voltage

Modeling and theoretical analysis of DC-link voltage control of converter has become an important research topic in modern power electronics. For these restrictions, number of controllers used in DC-link voltage control such as PI controller, PID controller, fuzzy controller, sliding mode controller and so on [14-18]. Any voltage fluctuations across the DC-link produces total harmonic distortion (THD) in grid current, hence decreasing power quality of the system [16], [17]. DC-link acts as a DC bus between boost converter and inverter, ignoring capacitor losses, energy flowing from PVG towards DC-link charges it, consequently increasing voltage across it. Similarly, when grid draws energy, the capacitor discharges reducing voltage across it. The DC-link capacitor is an entity used to improve power quality, monitoring and protection to meet requirements of the grid [60].

Several researchers are showing a three-phase grid tied PV generation system with constant DC-link voltage power [14-16], [18]. However, the configuration in the DC-link voltage of the voltage source converter is adapted with respect to the common point of interconnection (CPI) voltage variation. The DC bus voltage must be greater than the maximum value (peak value) of the line voltage on the AC side of the inverter. The DC-Link voltage must be controlled to a desired value higher than the grid peak voltage to ensure transmission of generated PV power into the grid. For this purpose, almost of researchers use the PI controller and the output of PI generates a reference signal for grid current which is used to achieve power factor control of the grid [64-66]. Recently, many researchers have relied on fuzzy logic technology to tackle the PI controller's

inherent difficulties, such as the response time is slow and the control is unreliable under irradiation changes [16]. Also, an artificial intelligence, particle swarm optimization PSO based DC-Link voltage control for two stage grid connected PV inverter is adopted to optimize the K_p and K_i parameters to regulate the DC-link voltage.

2.2.4.1 DC-Link voltage value

For proper control of VSC output current, the DC link voltage of VSC should be greater than the amplitude of line voltage. Moreover, in order to adaptively adjust the DC link voltage with respect to CPI voltage variation, the reference DC link voltage is adaptively adjusted with the amplitude of CPI voltage [60],[68]. The reference DC link voltage is estimated as:

$$V_{dc}^{*} > \sqrt{3}V_{\max} \tag{2.1}$$

$V_{\max}$: The amplitude of CPI voltage

For proper current control the DC link voltage must be higher than the amplitude of CPI line voltage. Therefore, reference DC link voltage is kept around 10% to 15% higher than the peak of the CPI line voltage.

2.2.5 Control Structure of Grid Connected PV Inverter

The DC–AC converters inject sinusoidal current into the grid controlling the power factor. Therefore, the inverter converts the DC power from the PV generator into AC power for grid injection. One important part of the system PV connected to the grid is its control. The fundamental types of control can be classified into two types: voltage control and current control. The voltage and current of the grid are taken as reference and it is transformed to a mathematical equation with current control structure and given as duty cycle to the inverter. According to the specific operating condition and behavior of the electrical grid, the controllers of PV systems are divided into six categories, which are the linear controllers, the non-linear controllers, the robust controllers, the adaptive controllers, the predictive controllers, and the intelligent controllers [68], [69].

A1-Linear controllers

These controllers are designed based on the features and dynamics of the linear system. The typical feedback control theory is used for analyzing and designing these controllers. A few linear controllers are classified as [60-63]:

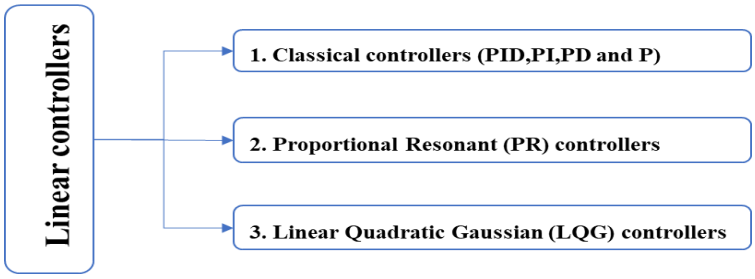

Fig.2.3 classification of a few linear controllers used in power electronics

B1-Non-linear controllers

These controllers have an extraordinary operation compared to the basic controllers [59-61], [64-66]. However, in terms of design and implementation, these controllers are complicated such as:

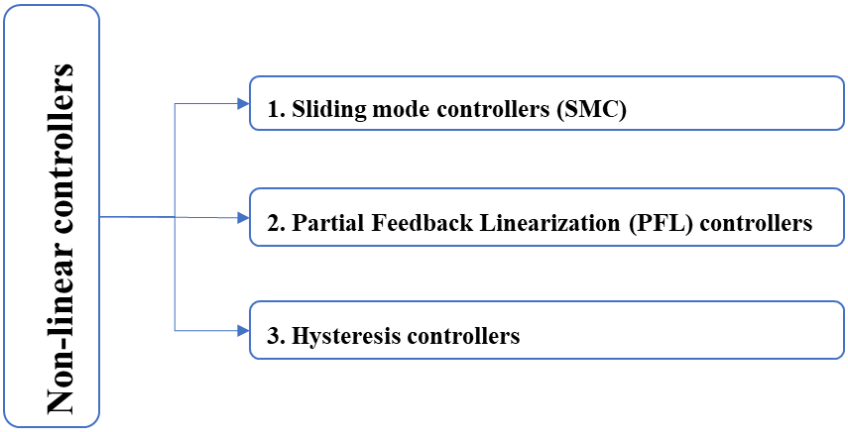

Fig.2.4 Classification of a few non-linear controllers used in power electronics

C1- Robust controllers

A robust control theory approach is utilized in order to design a controller with concern to uncertainties. The goal of these methods is to acquire stability in the occurrence of partial modelling errors as well as robust performance. In the robust control, bounds, clear description, and good criteria must be defined. This controller can promise robust performance and stability of the closed-loop systems, even in the multivariable systems [61], [63-65].

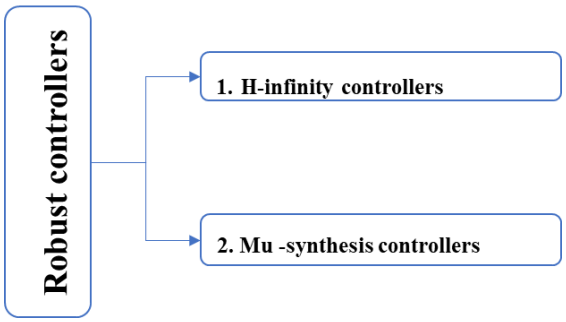

Fig.2.5 classification of a few robust controllers used in power electronics

D1- Adaptive controllers

Adaptive control refers to a control method that is used by a controller that must adapt to a controlled system with varying or uncertain parameters. Adaptive control detects the changes in the functioning of the process and regulates the controlling parameters automatically to compensate for the altering conditions of the process and, in turn, optimizes the loop response.

Conventional controllers adjust linear and non- linear systems over time because of the way they are designed. This approach is useful when operating conditions are fixed with little to no hindrances or changes. However, as soon as these conditions change, conventional controllers stop working. Adaptive control, on the other hand, adapts to changing control parameters and has the

ability to control the process [64], [78]. Adaptive control relies on parameter estimation, which is a part of system identification. There two methods to estimate the parameters:

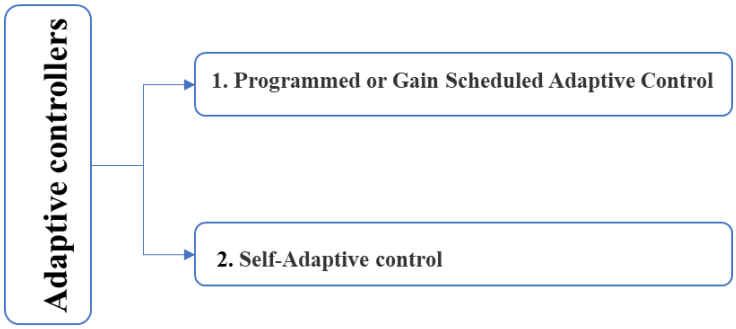

Fig.2.6 classification of a few adaptive controllers used in power electronics

E1- Predictive controllers

The future behavior of controlled parameters is predicted by using a system model in predictive controllers. Based on a predefined optimization criterion, to obtain the optimal actuation the controller utilizes this information. It can be applied to different systems, while a multivariable case can be considered, because of its non-linearities, constraints that can be simply incorporated, and very fast dynamic response. It has also easy implementation. The comparison of classic controller and this controller comparison shows, that an excessive number of calculations are required in the predictive controller [65-72]. Predictive control covers a very wide class of controllers that have found rather recent application in power converters. A classification of different predictive control methods is shown in Fig.2.7.

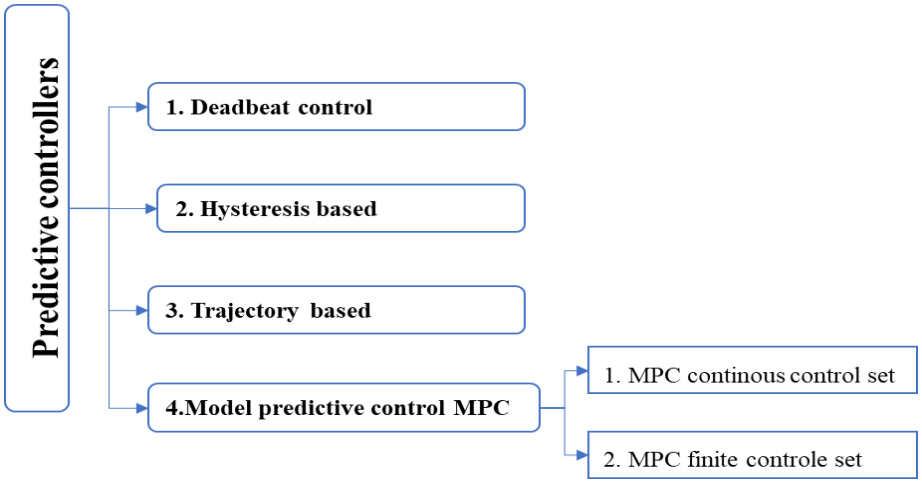

Fig.2.7 Classification of predictive control methods used in power electronics

F1- Intelligent controllers

Intelligent controllers obtain automation through the imitation of biological intelligence. Furthermore, the way biological systems troubleshoot problems are borrowed for the idea. Then, utilized to solve the control problem [61-80]. Fig.2.8 shows the intelligent controller methods.

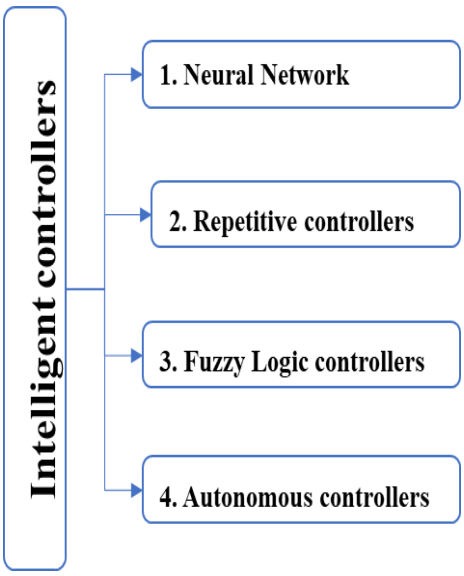

Fig.2.8 The intelligent controller methods used in power electronics

2.2.6 Grid synchronization methods

A power converter is commonly sensitive to the voltage disturbances. Since, its control system might lose controllability on the power signals under distorted conditions. In three phase system, active and reactive powers can be controlled using αβ or dq synchronous frame. The importance of synchronization is defined as the power converter interacts with the grid at the point of common coupling. In order to reduce the undesirable effects and attenuate the voltage disturbances, the synchronization should be properly designed with an accurate phase locked loop (PLL) to create current waveform reference in good quality.

Synchronization is fundamental in the control of the inverters connected to the grid. It consists of the connection of the generated signals with the same parameters of amplitude, phase and frequency of the power grid. In this process PLL techniques are generally used to perform the synchronization. The principal operation of the PLL is tuning the inverter's voltage with a reference voltage measured at the CPI [73-81]. According to the technique employed, the PLL can be categorized as: synchronous reference frame, second-order generalized integrator, quadrature PLL and enhanced PLL [76-81]. Another alternative are synchronization algorithms that do not measure grid voltage. These are based on virtual flow, power instantaneous and observer-based schemes. Generally, classical PLL techniques do not achieve a good phase-angle detection when the voltage grids have large amplitude and phase variations. Robust PLL techniques are required for weak-grid conditions. When there are not ideal conditions at the CPI, although hybrid PLL algorithms may result in a good performance.

2.3 Design of dual-stage three-phase grid-connected PV system

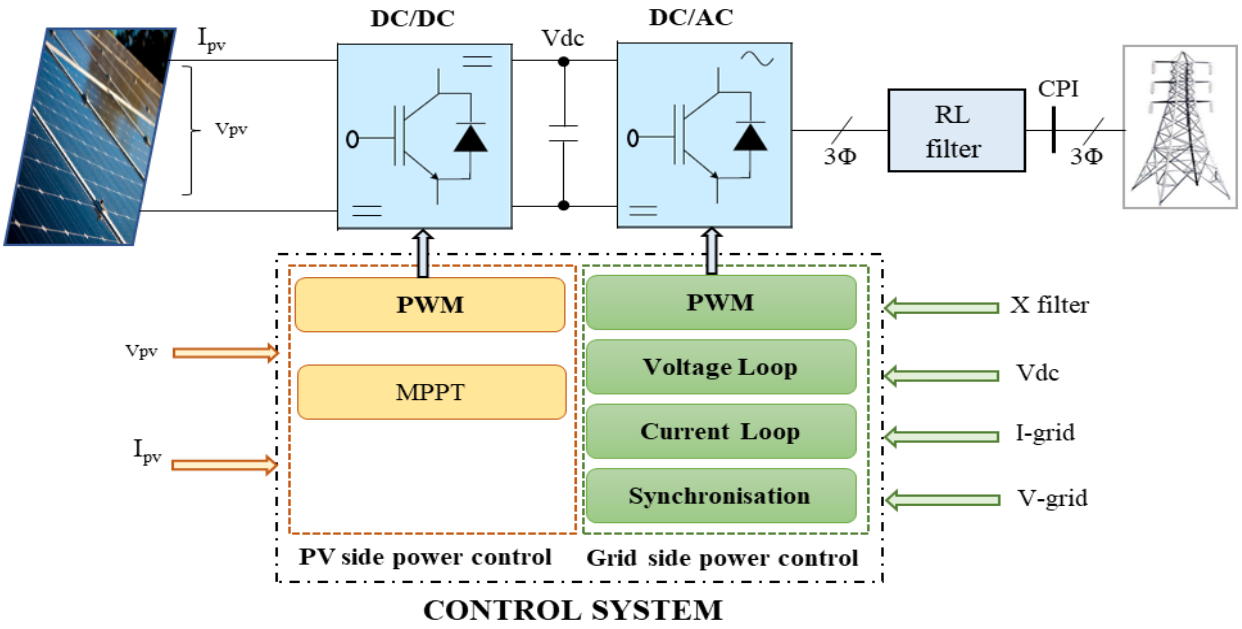

Fig.2.9 Diagram of grid connected photovoltaic system

The configuration of the three-phase solar energy conversion system is shown in Fig.2.9. This section localizes on the control of the three-phase grid connected photovoltaic system. In order to ensure a conversion of PV energy into alternative, electrical energy suitable for the grid, the PV plant connected to the grid is essentially composed of the following elements: the PV module, the DC-DC converter, the PV inverter which converts direct electrical energy into alternating energy. It can be single-phase or three-phase. To well detail the proposed control method later, the basic control components will be introduced first. The DC-DC converter is used to produce the maximum power from PV arrays, the MPPT controller, which has for aim to set the operating point of the PV system to the point of maximum power (MPP), where the maximum power point tracking algorithm (MPPT) is implemented based on perturb and observe (P&O). In addition, this chapter offers a Feed Forward (FF) compensation technique using a signal model of DC-link voltage control. As a consequence, thus the system defeats the problem associated with sudden disturbances. This section proposes an implementation of a neutral point clamped (NPC) three-level voltage source inverter under a robust FCS-MPC [82].

2.3.1 PV generator

A photovoltaic PV generator is the whole assembly of solar cells, connections, protective parts, supports…etc. In the present modeling, we focus only on cell, module and array [60]. Solar cells consist of a p-n junction fabricated in a thin wafer or layer of semiconductor (usually silicon). In the dark, the I-V output characteristic of a solar cell has an exponential characteristic similar to that of a diode [64]. When solar energy (photons) hits the solar cell, with energy greater than the band gap energy of the semiconductor, electrons are knocked loose from the atoms in the material,

creating electron-hole pairs [65]. These carriers are swept apart under the influence of the internal electric fields of the p-n junction and create a current proportional to the incident radiation. When the cell is short circuited, this current flows in the external circuit; when open circuited, this current is shunted internally by the intrinsic p-n junction diode [64].

The circuit diagram in Fig.2.10 presents the photovoltaic cell which consists of the first part with current source model and the luminous flux.

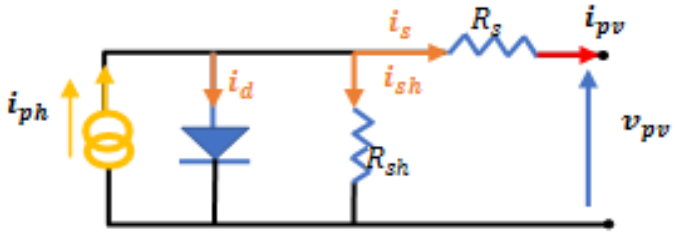

Fig.2.10 Equivalent circuit of a photovoltaic cell

The losses are modeled in the second part by two resistors, series resistor R_s and a shunt resistor R_p, in the middle a diode for the polarization of the cell and the phenomenon of minority carrier recombination.

The current produced by the photovoltaic cell is given by the following equation as in (2.2):

$$i_{PV} = i_{ph} - I_o\left(e^{\frac{v_{pv}+R_s i_{pv}}{nV_t}} - 1\right) - \frac{v_{pv} + R_s i_{pv}}{R_{sh}} \quad (2.2)$$

For the model, it is necessary to add the number of cells in parallel/series forming a module. So, the current of the photovoltaic module is given by (2.3):

$$i_{pv} = N_p i_{ph} - N_p I_o\left(e^{\frac{N_s v_{pv}+(N_s/N_p)R_s i_{pv}}{nN_s V_t}} - 1\right) - \frac{N_s v_{pv} + (N_s/N_p)R_s i_{pv}}{(N_s/N_p)R_{sh}} \quad (2.3)$$

Where:

I_o : the reverse saturation curent of the diode;

V_t : the thermal voltage of the PV module;

n: the diode ideality factor;

N_s : the numbers of PV cells in series;

N_p : the numbers of PV cells in parallels.

2.3.2 Static converters for systems PV connected to the network

Adaptation and conversion of the continuous power produced by the PVG into alternative power adapted to the network are ensured by the static converters which are the DC-DC converters (choppers) and DC-AC converters (inverters).

2.3.2.1 Static converters DC-DC

The table below compares the most DC-DC converter topologies use, including Non-Isolated and Isolated topology, and sets design guidelines for each, based on a logical understanding of their nuances and their response to input voltage variations [18],[67].

Table 2.1 Comparison of DC-DC converter topologies for high power applications

	Topology	Schematic	Power (W)	Efficiency	VOUT/VIN	Maximum Duty Cycle
Non-Isolated Topologies	Buck	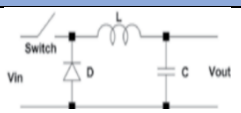	500	85 %	D	0.9
	Boost	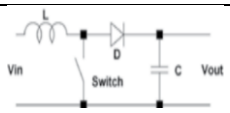	150	70 %	$\frac{1}{1-D}$	0.9
	Buck-Boost	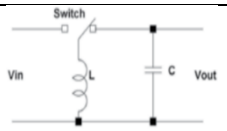	150	70 %	$\frac{-D}{1-D}$	0.9
	SEPIC	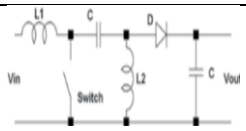	150	75 %	$\frac{D}{1-D}$	0.9
	Ćuk	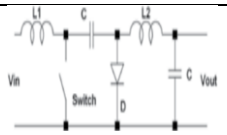	150	75 %	$\frac{-D}{1-D}$	0.9
Isolated Topologies	DCM Flyback	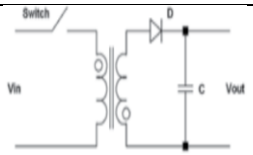	150	75 %	$D*\sqrt{\frac{T*V_{out}}{2*I_{out}*L}}$	0.9
	Forward	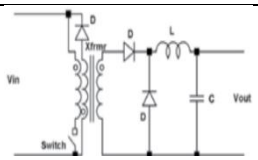	150	75 %	$\frac{2N_{s1}}{N_{p1}}*D$	0.45
	Push-Pull	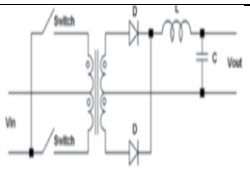	500	80 %	$\frac{N_{s1}}{N_{p1}}*D$	0.45
	Half-Bridge	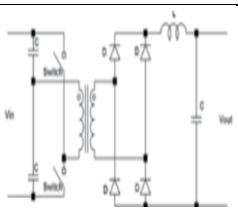	500	85 %	$\frac{N_{s1}}{N_{p1}}*D$	0.45

	Resonant LLC	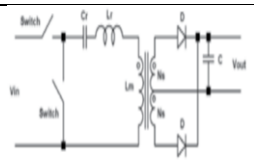	500	90 %	Frequency dependent based on resonant tank transfer function	0.45

Where:

V_{in} : is the input voltage;

V_{out} : is the output voltage;

D: is the pulse width modulator duty cycle;

T: is the switching time period;

L_p: is the secondary inductance;

N_{p1} : is the primary winding;

N_{s1} : is secondary winding.

In addition to two basic topologies mentioned previously, other multilevel converter topologies have been proposed [67], multilevel DC-DC converter systems are used to transform low level DC voltages to larger DC voltages. Different topologies of multilevel DC-DC power converters such as cascaded model, one-to-many model and general multilevel DC-DC converter modules are studied [68].

2.2.3.2 Boost converter

Initially, a boost converter appears the most promising candidate for a series connected, integrated DC/DC converter. A boost characteristic would also allow the maximum power point (MPP) to be always tracked [18].

To maintain the voltage generated at the maximum power level, the boost converter is controlled by the MPPT algorithm to maintain and track the desired output voltage at the maximum power point by adjusting the duty cycle. The inductor and capacitor are applied to maintain the current and voltage ripple within the limit. The boost converter topology is shown in Fig.2.11.

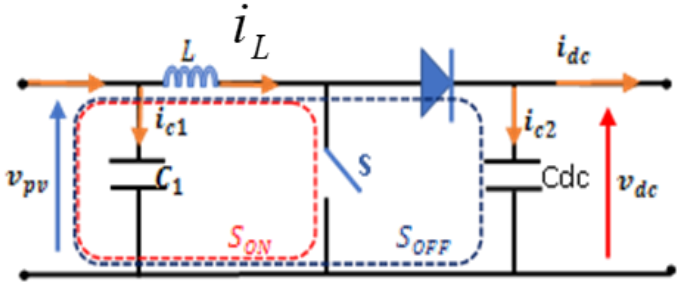

Fig .2.11 DC-DC Boost converter

The principle operating of a boost converter is divided into two distinct phases depending on the state of the switch S. The output voltage of the boost converter is given by the following equations:

State 1: S_{ON}

When the switch S is closed, the current in the inductor will increase, and magnetic energy is stored in the inductor. The diode is open, and the function of the converter described by the following equations as in (2.4):

$$\frac{d}{dt} i_L = \frac{1}{L} v_{pv} \tag{2.4}$$

At the end of ON state, the current i_L has increased by the value expressed Δi_{L-ON} as:

$$\Delta i_{L-ON} = \int_0^{T_{ON}} di_L = \int_0^{D.T} \frac{v_{pv}}{L} dt = \frac{v_{pv}.D.T}{L} \tag{2.5}$$

Where: $T_{ON} = DT$

State 2: S_{OFF}

When the switch S is open, the inductor will be in series with the generator and its voltage will be added to that of the generator. The energy accumulated in the inductor will be transferred to the capacity. The converter is described by the following equations:

$$\frac{d}{dt} i_L = \frac{1}{L}\left(v_{pv} - v_{dc}\right) \tag{2.6}$$

The variation of i_L during the blocked state will therefore be equal to:

$$\Delta i_{L-OFF} = \int_{T_{ON}}^{T_{OFF}} di_L = \int_{D.T}^{T} \frac{(v_{pv} - v_{dc})}{L} dt = \frac{(v_{pv} - v_{dc}).T}{L} - \frac{(v_{pv} - v_{dc}).D.T}{L} \tag{2.7}$$

Where: $T_{OFF} = T$

The energy stored in the components and the current are always equal at the beginning. At the end of each switching cycle, we can write:

$$\Delta i_{L-ON} + \Delta i_{L-OFF} = 0 \tag{2.8}$$

Therefore,

$$\frac{v_{dc}}{v_{pv}} = \frac{1}{1-D} \tag{2.9}$$

With $D \in [0\ 1]$

During operation of the chopper, the transistor (IGBT) will be switched at a constant frequency *f* with a opening time equal to DT and an closing time equal (1- D) T.

Where:

T: is the switching period that is equal to 1/*f*.

2.2.3.3 DC- link

Generally, the DC- link voltage oscillates between two levels depending on the operating climatic conditions, ambient temperature and irradiance. It is governed by the following equation:

$$\frac{dV_{dc}}{dt} = \frac{1}{C_{dc}} i_{C2} \tag{2.10}$$

Where: Cdc = capacitance of the capacitor [F].

2.2.3.4 Static converters DC/AC

Grid-connected photovoltaic power generation systems can be found in different sizes and power levels for different needs and applications [87]. Therefore, the generic PV energy conversion system structure of Fig.2.9 can vary significantly from one plant to another. For simplicity, grid-connected PV systems can be subdivided depending on their power rating: small-scale from a few watts to few tens of kW, medium-scale from a few tens of kW to a few hundreds, and large-scale from a few hundreds of kW to several hundreds of MW. In addition, PV systems can be further classified depending on the PV module arrangement: a single module, a string of modules, multiple strings and arrays [91],[92]. The PV module arrangement also gives the inverter configuration its name, consequently: AC-module inverter, string inverter, multi-string inverter and central inverter, as shown in Fig.2.12.

A2- Centralized inverters

In this model, the central inverter interfaces a whole PV array to the grid though a single inverter [91]. The array is composed of parallel-connected strings. A blocking diode in series to each string is necessary to prevent them from acting as a load when partial shading or mismatch occurs. Because the whole array is connected to a single inverter, this configuration can only provide a single MPPT operation, leading to the lowest MPPT efficiency of all configurations. Nevertheless, it provides a simple structure, reliable and efficient converter, making it one of the most common solutions for large-scale PV plants.

B2- String inverters

In the solar power industry, wiring sets of individual panels together is called stringing. A string solar inverter converts all of the direct current (DC) in strings of panels into usable alternating current (AC). String inverters are also known as central inverters. They have been around for decades, are affordable, and get the job done on most small-scale solar installations **[91], [92].** The string solar inverter structure remains a favorite one in new installations. However, in a common scenario of partial shading, MPP tracking may still not be sufficient to achieve a certain efficiency requirement.

C2- Multi-string inverters

In this structure, a DC-DC converter is implemented for each string for MPP tracking and power combination of different string to a DC bus. Multi-string inverter features the optimal MPP tracking for a single string of PVs. A big power stage works as a grid connected half bridge inverter without transformer. The multi-string inverter is useful when PV strings of different rated power, different orientation is combined. The DC-DC part can be implemented with high-frequency pulse width modulation (PWM) converter to reduce the implementation area [91],[92].

D2- AC modules

The AC module is the integration of the inverter and PV module into one electrical device, it removes the mismatch losses between PV modules since there is only one PV module, as well as supports optimal adjustment between the PV module and the inverter, and hence, the individual MPPT. It includes the possibility of a facilitated enlargement of the system, due to the modular structure. The necessary high voltage-amplification reduce the overall efficiency and increase the price per watt, because of more complex circuit topologies. The present solutions use self-commutated DC–AC [91], [92].

Referring to progressing technologies to transfer to and organize the PV power in the grid, the mainly five configuration concepts available, are presented in Fig.2.12.

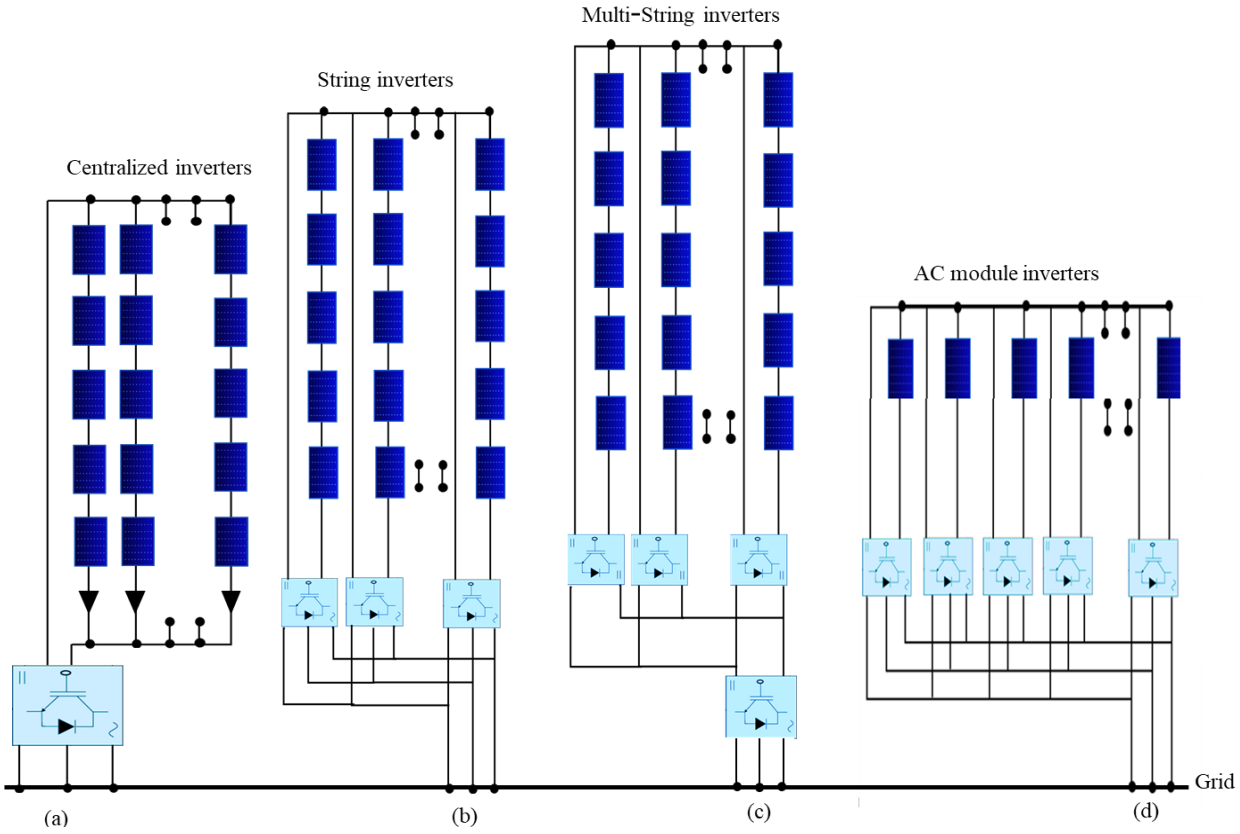

Fig.2.12 PV inverter configurations (a)-Centralized inverters, (b)-String Inverters, (c)-Multi-string Inverters, (d)-AC modules.

E2- Other classification

Another classification of the inverters is made based on the existence or absence of the transformer, as shown in Fig.2.13.

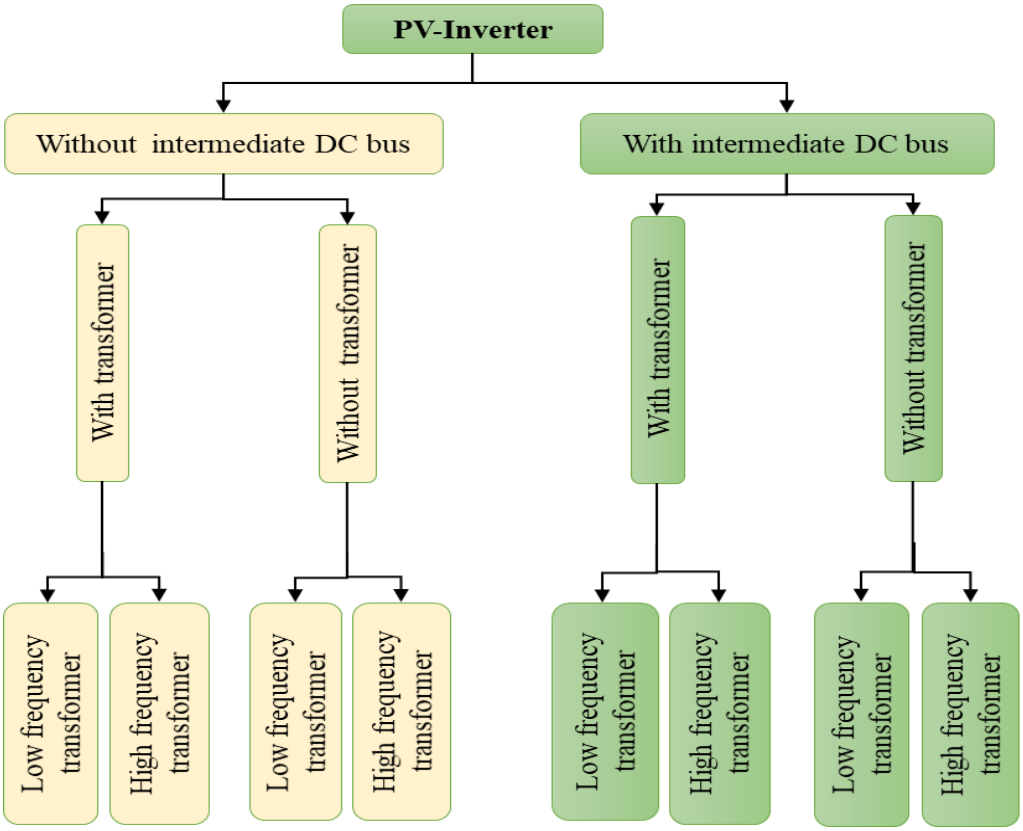

Fig.2.13 Configurations of inverters connected to the network

F2- Multilevel inverters

Today, the decrease in the overall cost of the grid-connected PV system is due to the improvement in the existing grid-connected inverter technologies. In comparison to the simple two-level inverters, multilevel grid-connected inverters offer numerous advantages. The multilevel inverters result in the AC voltage at the inverter's output terminal [93], [94], which comprises of several staircase voltage levels. The staircase sinusoidal waveform resulting from the multilevel inverter is close to an actual and pure sinusoidal wave with low total harmonic distortion. Thus, the filter requirement is reduced and the harmonic distortion is low. Various DC voltage levels can be easily produced due to the modular structure of PV arrays; for these purposes, a new group of multilevel inverters has appeared as the solution for working with higher voltage levels. The most important topologies proposed for multilevel are diode-clamped; capacitor-clamped (flying capacitors); and cascaded. Also, several modulation strategies have been adopted for multilevel inverters [94], [95]. In general, multilevel voltage inverters can be viewed as voltage synthesizers, in which the output voltage is synthesized from several discrete voltage levels.

Advantages

- The main advantage of multilevel converter is the higher voltage handling capability with lower rated devices;
- It has lower switching losses and higher overall efficiency than others;
- Allows a reduction in the size of the filtering elements, which affects the dynamic response of the converter;
- The voltage capacity of the existing devices can be increased many times without the complications of static and dynamic voltage sharing;
- Spectral performance of multilevel waveforms is superior than the two-level counterparts [94],[95].

Disadvantages

- Requires a numbers of semiconductor devices, which increases the complexity of the control circuit;
- The voltage imbalance between the upper and the lower DC-link capacitor;
- Unequal current stress on the semiconductors.

2.3.3 Filters for connection to the electricity network

Filters can be divided in two distinct types: active filters and passive filters. The purpose of the filters of the connection to the electrical network is to eliminate certain harmonics generated by the inverter in order to inject current into the electrical network in compliance with the standards relating to network harmonics and electromagnetic compatibility [96].

2.4 Originality of work carried out

The originality of this work is on the outline control is given with these follow steps technique:

- The boost converter is used as an adaptation stage to realize the MPPT for PV systems, allowing to always recover the maximum of energy. Different types of MPPT algorithms have already been proposed in the literature**,** Perturb and Observe method (P&O) is the most used method in the industry because of its good balancing between the complexity and the reliability of this method.
- For optimal operation, the installation needs a constant DC voltage. The DC voltage regulation V_{dc} implemented by supplying active power on the network. A Feed Forward with Fuzzy Logic (FF-FL) is implemented in DC bus voltage regulation loop in order to reduce voltage fluctuations across the DC bus capacitor and maintain it at its desired value V_{dc} *.
- A phase locked loop (PLL) outputs a unitary signal synchronized in phase and frequency with the input signal. The PLL ensures that the error between the input phase and output phase is kept to a minimum, and the frequency of input and output is the same.

- The predictive control strategy proposed for an NPC multilevel inverter is based on a finite number of possible switching states generated by the static power converter, so the system model is used to predict the future behavior of the variables to be controlled for each switching state. The power converter frame used to interface the PV array with the power grid is shown in Fig.2.14. The first stage consists the boost converter, which will raise the relatively solar voltage to a level suitable for the DC-link. The second stage is three-phase neutral point clamped (NPC) three level converter that runs in a current controlled mode to inject unity power factor current to the grid. An output RL filter is proposed in order to minimize the ripples and switching losses. PLL allowing the phase or output frequency of a system to be slaved to the phase or frequency of the input signal.

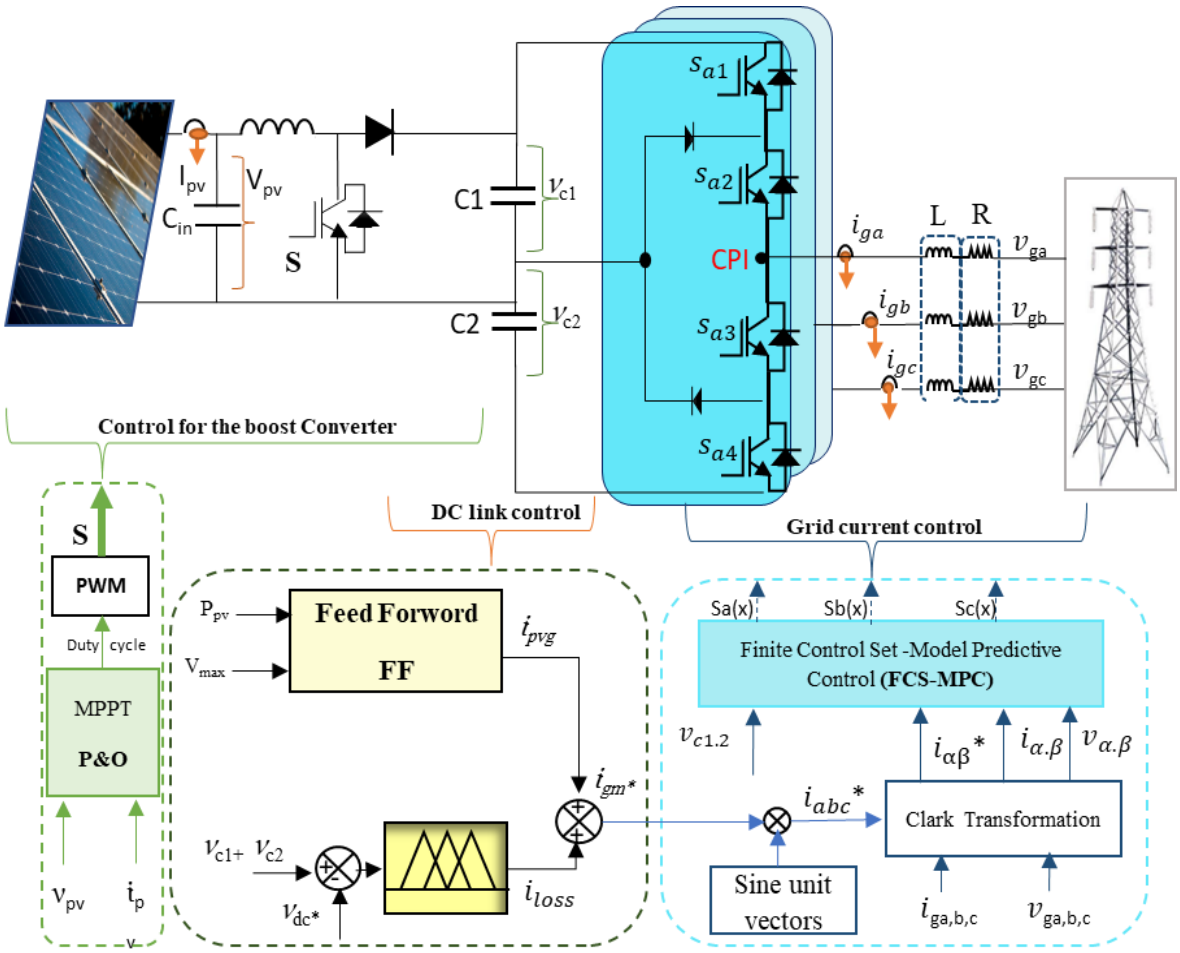

Fig.2.14 Global system configuration and control

2.4.1 PV side power control (DC-DC control)

In purpose to extract the maximum amount photovoltaic energy, the PV system must be able to track the solar array's maximum power point (MPP) that varies with the solar radiation value. For the power setting, it should be noticed that there is not clear reference power since photovoltaic power varies with the solar radiation. However, to extract the maximum photovoltaic power; the photovoltaic generator voltage must be adjusted according to the radiation. This adjustment is

made possible while varying the transistor duty cycle, carrying out a regulation of the generator voltage using P&O algorithm.

2.4.2 Grid side power control (DC-AC control)

In grid side connected control mode, all the available energy that can be extracted from the photovoltaic generator (PVG) is transferred to the grid. The control structure for the grid connected mode is shown in Fig.2.14. The DC-link voltage in the inner loop using Feed forward term based Fuzzy logic control and Finite Control Set Model Predictive Control (FCS-MPC) is used to adjust the inverter output currents in the (αβ) synchronous frame in the other control loop. The reactive power is typically used to zero level in order to obtain the zero-phase angle between voltage and current in order to guarantee the unity power factor (PF≈1). The voltage control of the DC-link acts to supply the active power. The output current controller achieves the voltage reference for an average conversion control method that controls the switches of the grid inverter synchronous with grid is carried out by using a phase locked loop (PLL).

2.5 Design of the Feed Forward-Fuzzy Logic controller (FF-FL) for DC-link voltage

Serval control strategies have been inserted to design DC-link voltage controllers like classical PI controller and fuzzy logic. The application of sliding and integral sliding theories also considered such as an ongoing topic [14-17]. We choose in this chapter a Feed Forward term under a low voltage ripple steady state and fast response time. The block scheme of Feed Forward term with Fuzzy logic FLC is designed with minimum fuzzy rules as illustrated in Fig.2.15.

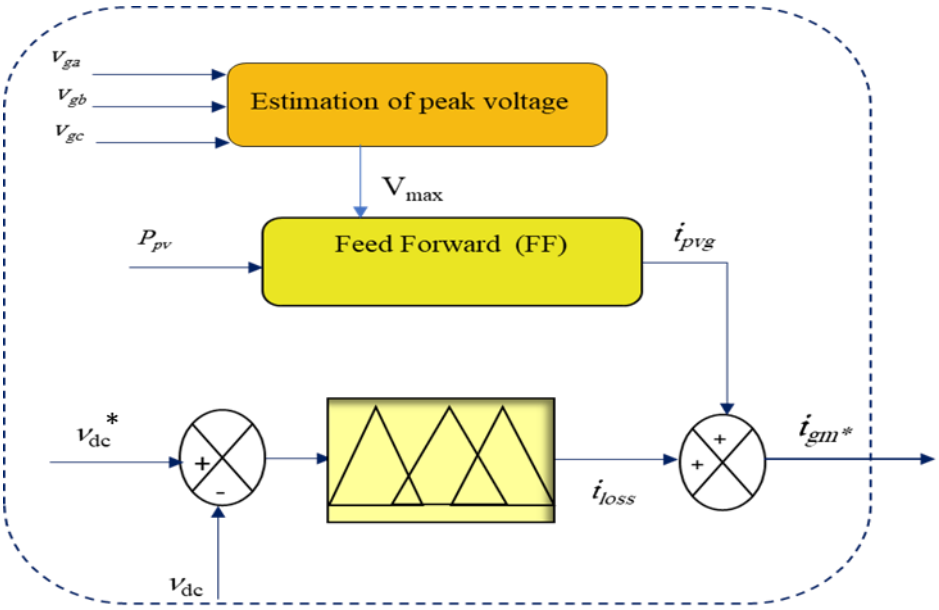

Fig.2.15 DC- Link voltage control

From the above Fig.2.15, the PV power ($P_{pv} = v_{pv} * i_{pv}$). Therefore, the following equation will define the amplitude of grid current I_{gm}*:

$$I_{gm}^{*} = I_{PVg} + I_{loss} \tag{2.11}$$

I_{gm}^{*} : Estimated amplitude of grid current;

I_{PVg} : Contribution current by FF from PV array;

i_{loss}: Loss current.

The amplitude of grid currents consists of two main parts which are the loss component and the contribution from the PV array. The output of Fuzzy logic controller can be considered as loss component in a steady state condition. The amplitude of grid current I_{gm}* is then multiplied with unit vectors to estimate reference grid current [14],[18]. To maintain current necessary to guarantee the excellent operation of the grid interface inverter. A PV Feed Forward term for the PV array contribution to grid current is also estimated to provide fast dynamic response. The PV Feedforward term is estimated as:

$$I_{PVg} = \frac{2P_{pv}}{3\,V_{\max}} \tag{2.12}$$

$$V_{\max} = \sqrt{\frac{2(v_{ga}^2 + v_{gb}^2 + v_{gc}^2)}{3}} \tag{2.13}$$

With:

$V_{\max}$: the amplitude of CPI line voltage

While, the FLC is designed with minimum fuzzy rules to compensate the DC-link voltage losses and to keep the DC-link voltage constant at the desired value regardless the operation conditions. The Fuzzy controller inputs are usually the voltage error e(k) as given in (2.14) and change of error Δe(k) as indicated in (2.15) and (2.15). The two inputs are supplied into FL control unit for Fuzzification. Fig.2.15 represents the offer normalized input membership functions in terms of linguistic variables NB (Negative Big), ZE (zero) and PB (Positive Big) as shown in the following Fig2.16.

Triangular and trapezoidal membership functions are picked in order to lower the computational complexity. The voltage error is the difference between the measured DC-link voltage V_{dc} and the desired referenceV_{dc}^{*}. The reference DC link voltage is adaptively adjusted according to the amplitude CPI (common point of interconnection) voltage. For proper current control the DC-link voltage must be higher than the amplitude of the CPI line voltage. Therefore, reference DC-link voltage is kept around 10% to 15% higher than the peak of CPI line voltage as given in (2.16).

$$e(k) = V_{dc}^{*} - V_{dc} \tag{2.14}$$

The error variation is calculated as:

$$\Delta e(k) = e(k) - e(k-1) \tag{2.15}$$

Where :

$$V_{dc} = v_{c1} + v_{c2}$$

$$V_{dc}^{*} = \delta\sqrt{3}V_{\max} \quad (2.16)$$

Where : $\delta > 1$

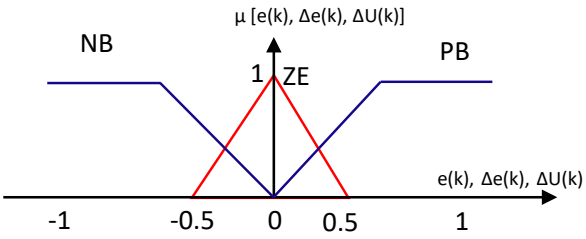

Fig2.16. FLC membership functions inputs & output

From the system behavior study, we can establish the command rules, which connect the output with the input. As we mentioned, each of the two linguistic inputs of the fuzzy controller has three fuzzy sets, which gives a set of nine rules. These can be represented by the inference matrix in Table 2.2.

Table 2.2 FL control rules.

Fuzzy logic Rules		Δe (k)		
		NB	**ZE**	**PB**
e (k)	**NB**	PB	PB	ZE
	ZE	PB	ZE	NB
	PB	ZE	NB	NB

The output of FL controller can be considered as loss component in a steady state condition. The logic for determining this matrix rules is based on global knowledge or qualitative functioning of the system as:

Rule 01: If e is NB & Δe is NB then ΔU is PB

Rule 02: If e is NB & Δe is ZE then ΔU is PB

Rule 03: ……..

……..……..

Rule 09: If e is PB & Δe is PB then ΔU is NB

When the fuzzy output is calculated, it should be transformed into a numeric value. It exists several methods to achieve this transformation, the most used is the center method of gravity.

2.6 Simplified FCS-MPC of grid- connected NPC

2.6.1 Modeling of three-level NPC inverter

This structure consists of three symmetrical arms each converter arm is achieved by using four IGBT switching devices in parallel with two clamping diodes. The DC-link is collected of two

similar capacitors, and their neutral-point (mid-point) is symbolic as z. The neutral-point of the clamping diodes in each phase is connected to z. The net DC-bus voltage is taken equally between the two DC-link capacitors [96-100].

The operation modes for an NPC converter only two switches conduct at any time, and switch pairs (s_{x1}, s_{x3}) and (s_{x2}, s_{x4}) operate in a complementary manner for three-phase applications.

Where: $s_{x1}+s_{x3}=1$ and $s_{x2}+s_{x4}=1$ for all x ∈ {a, b, c}.

The three operating mode output voltages in one phase for a three-phase NPC converter are given as follows:

The input DC branch currents and the output voltages for all possible switching states of converter summarized in Table 2.3 and the possible voltage vectors and switching states in Fig.2.19.

TABLE 2.3. Switching states for an NPC converter ∀ x ∈ {a, b, c}

Voltage levels	Switching state			
	S_{x1}	S_{x2}	S_{x3}	S_{x4}
Vdc	1	1	0	0
Vdc/2	0	1	1	0
0	0	0	1	1

To predict the future behavior of the current and voltage grid, number of switch changes, and DC-link capacitor voltages, a discrete-time model of the inverter is given in the synchronous reference frame. The controller uses all the possible switching states (27) of the inverter for their evaluations and predictions using a cost function [95-97]. Fig.2.17 shows the three-phase converter structure.

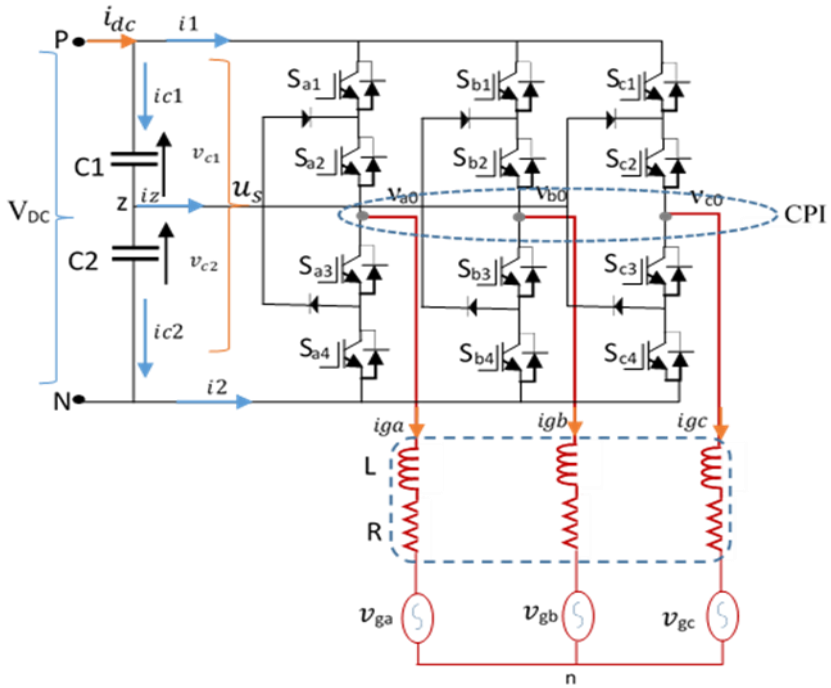

Fig.2.17 Structure of three-level NPC inverter

Advantages

Among the functions performed by the inverter, we cite the following [105]:

- Ensure perfect synchronization with the network;
- Adjust the output voltage to the maximum admissible value for the network;
- Minimize phase shift;
- Reduce the rate of harmonic frequencies in order to have an almost sinusoidal output signal;
- Reduce electromagnetic interference;
- Guarantee the high efficiency of the power transferred to the network;
- Solid state power components block a reverse voltage that is only half voltage of the DC source;
- All phases share the same DC bus;
- The fundamental frequency ensures high efficiency;
- The control method is relatively simple;
- The three-level waveform results in better spectral quality compared to that of a conventional three-phase inverter, which makes passive filters less bulky [101], [102].

Disadvantages

On the other hand, the NPC topology presents several technical difficulties in the cases of great power such as:

- For topologies with more than three levels, loopback diodes can increase the voltage stresses. So, the series diode connections might be required, but it complicates the design and raises questions of reliability and cost of construction;
- This topology requires high switching speed loopback diodes which must be able to withstand full load current [101];
- Different ratings for switching devices are necessary due to their cyclic conduction;
- Maintaining the load balance of capacitors is still an open question for NPC inverter topologies with more than three levels. Although the three-level NPC inverter operates with a high-power factor (PF), it is mainly used in compensation circuits. This is due to the capacity balancing issue [102].

2.6.2 Control model of three-level NPC inverter

Recently, predictive control has gotten more attention and become a very promising control scheme in various power electronics applications. It can be sorted into three prime branches incorporating the continuous control set, Finite Control Set Model Predictive Control (FCS-MPC) [98], [99]. Both of the continuous control set and deadbeat model predictive control needs a modulator at the output stage for switching state generation [98]. However, FCS-MPC takes the

advantage of a limited number of switching actions related to the controlled converter and directly generates the optimal switching state. FCS-MPC can be simply performed by deriving the model of the system under study. Then, the discrete time model of the converter is developed. Further, the predicted control variable is differentiated from its reference value together with other conditions.

The predictive control for the NPC inverter is shown in Fig.2.18. The future values of the currents and voltages in the capacitors are predicted for the 27(3^3) switching states generated by the inverter. For this, it is necessary to measure the present currents and voltages in the capacitors. After obtaining the predictions, a cost function is evaluated for each switching state. The switching state that minimizes the cost function g is selected and applied during the next sampling period [90-94], [98]. FCS-MPC explicitly takes feature of the discrete nature of power converters by specifically comparing the switching state using the error control because the switching state is selected directly from the minimization of the cost function; there is no need for linear controllers and modulators. [95, 96].

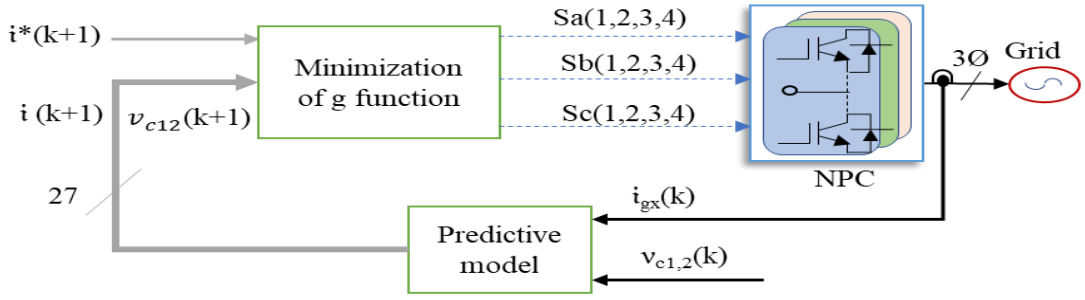

Fig.2.18 Predictive current control for the NPC inverter

In this section, we will detail the algorithm control of the inverter such as the synthesis of the conversion modulators and the connection generators [99]. The studied control device architecture is limited to the inversion of the average conversions equivalent model. The inverter is supposed commendable; the applied external controls to the switches are confused with the open or closed switches idealized states [100-102]. Three-level DC-AC voltage source inverter with switching and voltage vectors with FCS-MPC is clarified in Fig.2.19.

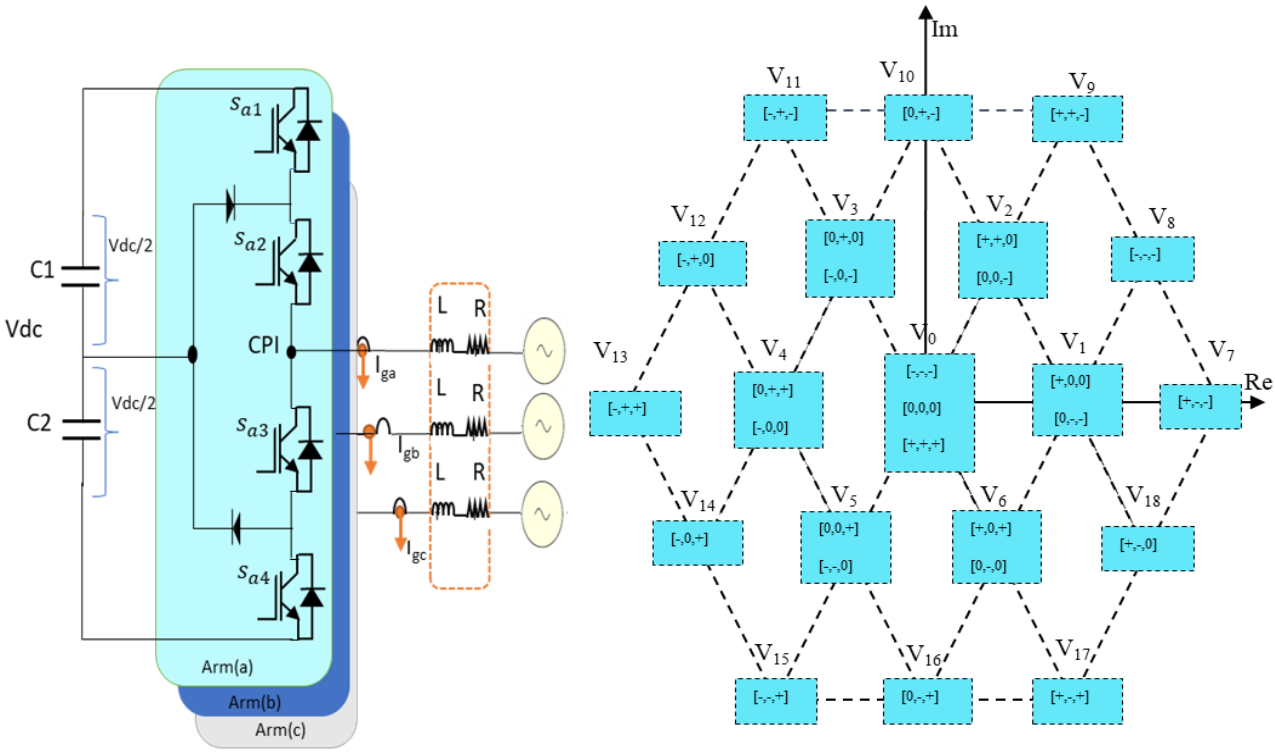

(**a**) (**B**)

Fig.2.19 (**a**) Tree-level voltage source inverter. (**b**) Switching and voltage vectors of the inverter.

2.6.3 Dynamic model of NPC inverter with RL filter

The three-level inverter topology with an RL output filter is illustrated in Fig.2.18**.** A good coupling that can be seen between the phases makes the design of the controller difficult. A completely decoupled model in the αβ frame is used in this work in order to remove this coupling effect. The dynamic equations of the inverter's output voltage with respect to three phases can be written as (2.17):

$$\begin{cases} \dfrac{di_{ga}}{dt} = \dfrac{1}{L}\left[V_{} - v_{g_a}(t) - Ri_{ga}(t)\right] \\ \dfrac{di_{gb}}{dt} = \dfrac{1}{L}\left[V_{} - v_{gb}(t) - Ri_{gb}(t)\right] \\ \dfrac{di_{gc}}{dt} = \dfrac{1}{L}\left[V_{} - v_{gc}(t) - Ri_{gc}(t)\right] \end{cases} \tag{2.17}$$

R:Filter resistance

L :Filter inductance,

V: is voltage vector generated by the NPC inverter

i_{ga}, i_{gb}, i_{gc} : The measured grid current;

v_{ga}, v_{gb}, v_{gc} : The measured grid voltage.

Applying Clarke transformation, the grid currents can be expressed in two-phases (αβ coordinates). Then, the continuous-time state-space equation of the grid results in (αβ) frame, the system model is given by (2.18).

$$\begin{cases} \dfrac{di_{\alpha}}{dt} = \dfrac{1}{L}\left[-Ri_{g\alpha}(t) - v_{g_{\alpha}}(t) + V_{\alpha}\right] \\ \dfrac{di\,\beta}{dt} = \dfrac{1}{L}\left[-Ri_{g\beta}(t) - v_{g\beta}(t) + V_{\beta}\right] \end{cases} \tag{2.18}$$

Using Euler's discretization process as in (2.19):

$$\frac{di(t)}{dt} \approx \frac{i(k+1) - i(k)}{T_s} \tag{2.19}$$

The grid current dynamics can be expressed using Euler's discretization method as:

$$\begin{cases} i_{\alpha}(k+1) = \dfrac{T_s}{L}\left[-Ri_{\alpha}(k) - v_{g_{\alpha}}(k) + V_{\alpha}(k)\right] + i_{\alpha}(k) \\ i_{\beta}(k+1) = \dfrac{T_s}{L}\left[-Ri_{\beta}(k) - v_{g\beta}(k) + V_{\beta}(k)\right] + i_{\beta}(k) \end{cases} \tag{2.20}$$

Finite-set model predictive controller (FCS-MPC) is one between a very wide class of predictive controllers that have attract researchers' interest because of its simplicity, and its ability to include system's non linearity and constraints in the model, avoiding the procedure of linearize the system at any considering the variable, the dynamics of the voltages across the two dc-bus capacitors are expressed in the continuous-time domain as shown in equations (2.21).

$$\begin{cases} \dfrac{Cdv_{c1}}{dt} = i_{c1}(t) \\ \dfrac{Cdv_{c2}}{dt} = i_{c2}(t) \end{cases} \tag{2.21}$$

A discrete-time equation for the DC-link capacitor voltages are obtained by using Euler-forward in order to obtain a discrete-time system representation. Then, the discrete-time DC-link capacitor voltage can be:

$$\begin{cases} v_{c1}(k+1) = v_{ci}(k) + \dfrac{T_s}{c} i_{c1}(k) \\ v_{c2}(k+1) = v_{c2}(k) + \dfrac{T_s}{c} i_{c2}(k) \end{cases} \tag{2.22}$$

Where:

$C_1 = C_2 = C$

2.6.4 Cost function

Since the main objective of the cost feature is to keep track of a given variable and control a multilevel inverter, it is not restricted to just doing that. In addition, one of the FCS-MPC's key advantages is that the cost function embraces any required term that could predict another device variable, system restriction or necessity for the system. This versatility makes it easier for the FCS-

MPC to achieve more control goals that can lead to improve power quality, system efficiency, performances, safety and other potential merit figures. Since, these terms will most likely be of various physical nature (voltage, current, power, losses of switching… etc) [100]. It may lead to coupling effects between variables, or to overestimate the significance of respecting the others in the cost function by one word, rendering their presence invaluable and even uncontrollable. This problem was commonly addressed in MPC by using or weighting factors for each cost function term [71-74]. Depending on the essence of the various terms involved in the cost function formulation, it's classified in different groups in order to facilitate the definition of a weighting factor adjustment technique then could be applied to identical types of cost functions and alike terms. FCS-MPC minimizes the tracking error between both of the reference and predicted grid current by using a cost function defined as (2.23) [101],[102]:

$$g = \left|i_{\alpha}^{*}(k+1) - i_{\alpha}(k+1)\right| + \left|i_{\beta}^{*}(k+1) - i_{\beta}(k+1)\right| + \lambda\left|v_{c1}(k+1) - v_{c2}(k+1)\right| \quad (2.23)$$

$i_{\alpha}(k+1)$, $i_{\beta}(k+1)$: The real and imaginary components of the predicted current vector respectively;

$i_{\alpha}^{*}(k)$, $i_{\beta}^{*}(k)$ he real and imaginary components of the reference current vector;

λ : The weighting factor.

The basic algorithm for predictive control implementation as showed in Fig.2.20 begins to detect the system's state variables V(k) and its reference during a given sampling time k with horizon 1. Using a suitable model finite set model predictive current control (FCS-MPC), it is possible to get the state variables over the next sampling time (k + 1), for each possible input V(k) using the predicted variables compared with its references, a defined cost function g can be optimized. The input V(k) that minimizes the cost function is applied in the next sampling time (k + 1), by the analysis of switching redundancies of the topology in order to reduce the subset of possible inputs [104-106].

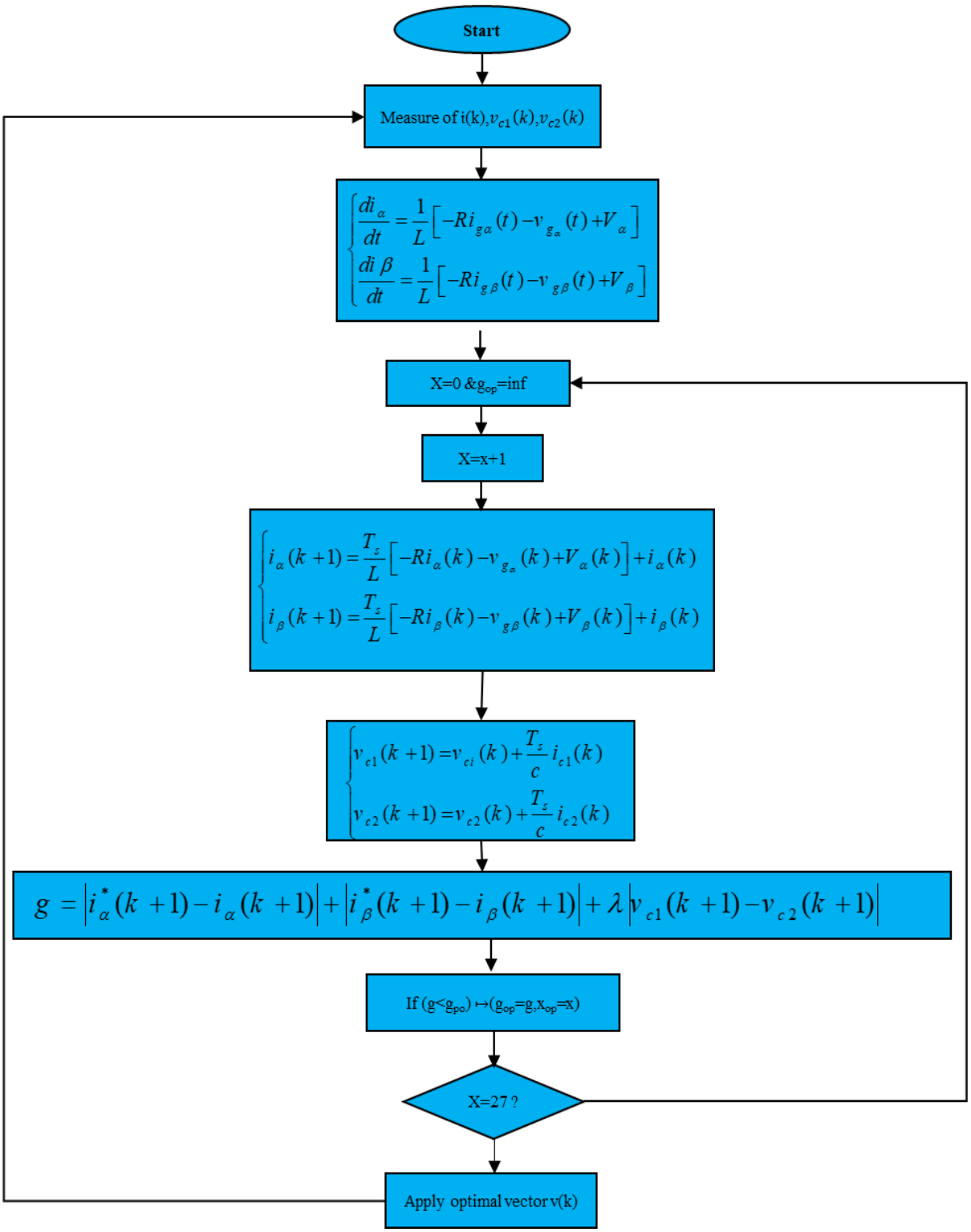

Fig.2.20**.** Diagram algorithm for FCS-MPC

2.6.5 Grid synchronization

In order to reduce the undesirable effects and attenuate the voltage disturbances, the synchronization should be properly designed with an accurate phase locked loop (PLL) to create current waveform reference in good quality. The PLL used in this study is the one chosen synchronous reference frame, this PLL tracks the frequency and phase of a sinusoidal signal to keep the input and output phase difference at zero.

2.7 Simulation results

2.7.1 Performance comparison of applied FF-FL and PI regulators for DC-Link

The overall system of an effective control for grid-connected PV system is given, the chapter has provided an outline of an adaptive DC-link control and a multilevel inverter circuit topology neutral-point clamped (NPC), where the above studied inverter is connected to the grid and controlled via the previously detailed Feed Forward with a Fuzzy Logic FF-FL control and a Finite Set Control Model Predictive Control FCS-MPC algorithms. In order to validate the advantages of the proposed approaches, a simulation of the system has been done on MATLAB/ Simulink. The parameters of the proposed system used in the simulations are summarized in table.2.4.

The purpose from the proposed controller is to deliver a low distorted current to the grid, fast dynamic and a good performance. The quality of the power distributed to the utility grid is governed by standards and international codes IEEE

A brief comparative study based on DC-link control between (FF-FL) & PI to select the optimal method.

With the aim of evaluating the steady-state performance of the proposed FCS-MPC algorithm, simulated evaluations have been estimated. Fig.2.21, Fig.2.22 and Fig.2.23 shows the steady-state results for the proposed FCS-MPC method based on the tree-phase three-level NPC converters.

The results obtained are shown in Fig.2.21. The random changes in solar irradiance (400 W/m^2, 700 W/m^2, 1000 W/m^2…etc), is used in Fig.2.21(a), the photovoltaic power reaches steady state for illumination levels through only the order of a few milliseconds for the two systems as shown in Fig.2.21(b).

For the first control Feed forward with Fuzzy Logic (FF-FL), it can clearly be seen that with FF-FL controller, the DC-voltage follows its reference which is achieved rapidly without overshoot. However, for the second control PI where Fig.2.21(c) shows the DC voltage achieve its reference with an overshoot of 200V to 300V.

For the two control strategies, the level number of the output voltage is three, the grid voltage and current are illustrated in Fig.2.21(d), Fig.2.21(e) and Fig.2.21(f), perfect current reference tracking with the lowest harmonic content as shown in Fig.2.21(g) and Fig.2.21(h). Furthermore, the FCS-MPC algorithm effectively decreases the THD by precisely tracking the reference current. The reactive power is almost kept zero, it means, a quasi-totality injection of the PV array energy as active power into the grid, and a unity power factor operation is ensured since the voltage and current as given in Fig.2.21(e) are kept in phase. Only, the PI effect is seemed clearly at the level of the grid current form, THD and unity power factor.

FF-FL **PI**

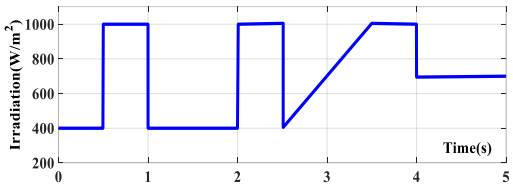

a

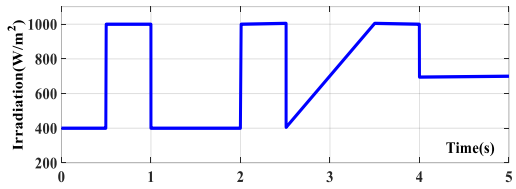

a

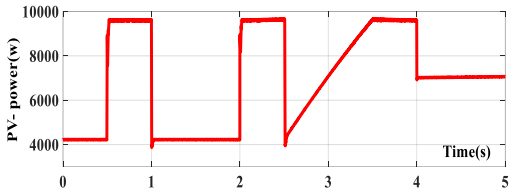

b

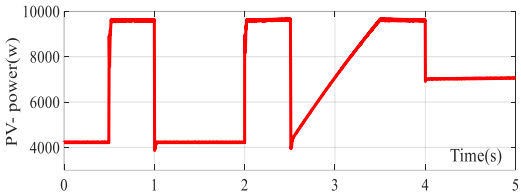

b

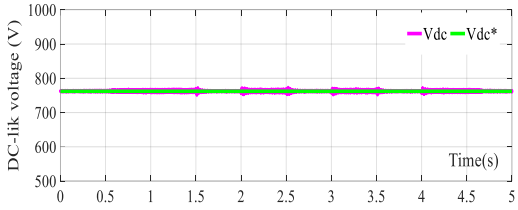

c

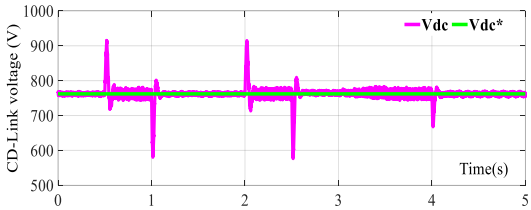

c

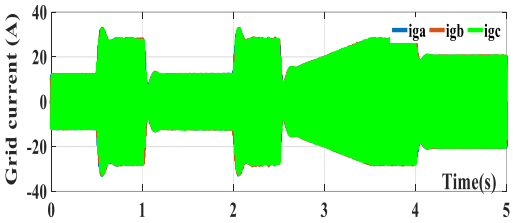

d

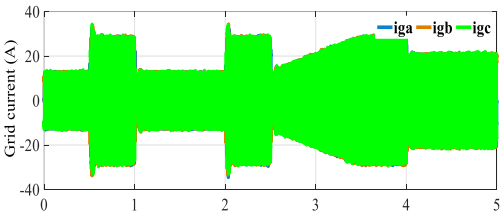

d

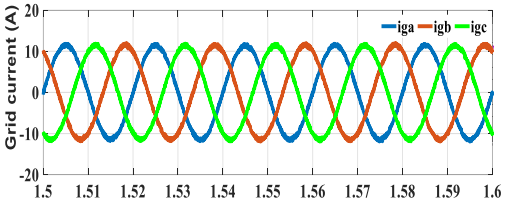

e

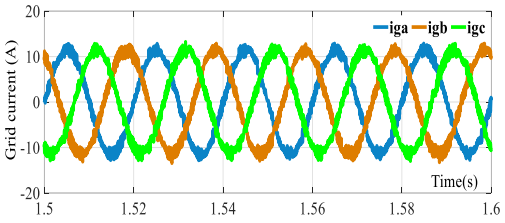

e

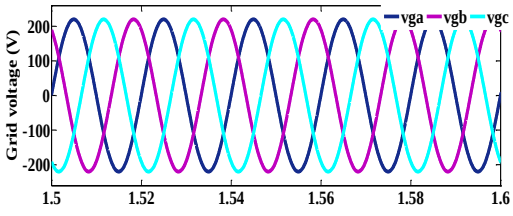

f

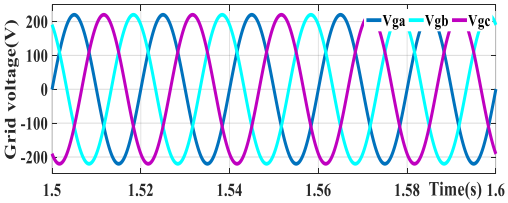

f

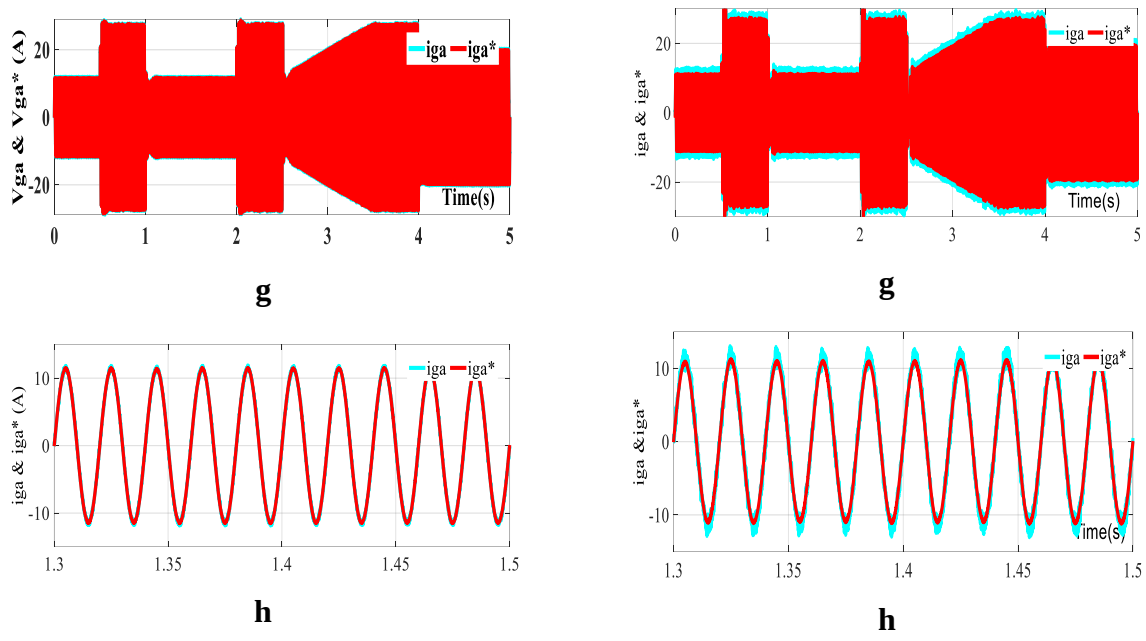

Fig.2.21. Simulation results of three-level NPC inverter (**a.** Irradiation, **b.** PV power, **c.** DC-voltage, **d.** Grid current **e.** Zoom of grid current, **f.** Zoom of grid voltage, **g.** Grid current and its reference, **h.** Zoom of grid current and its reference).

2.7.2 Synchronization

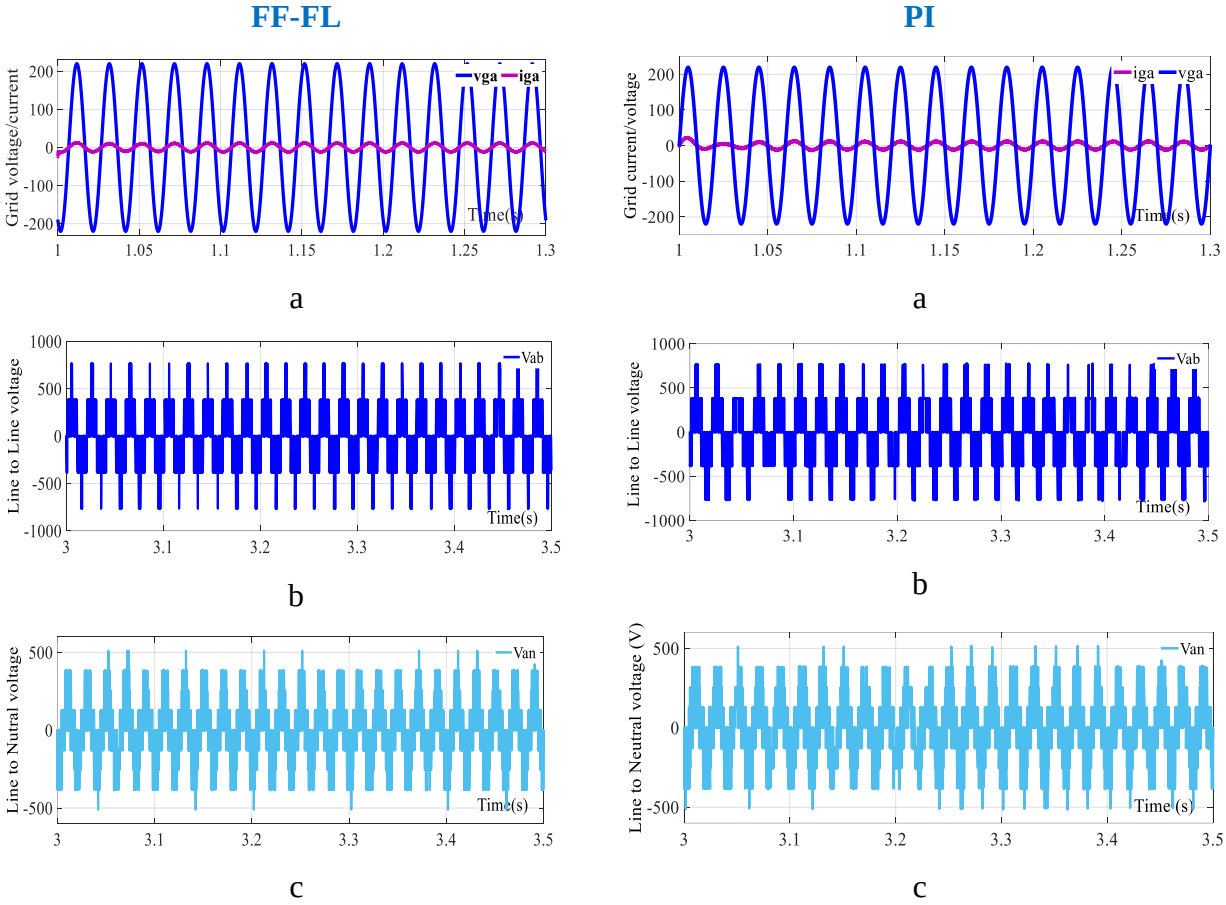

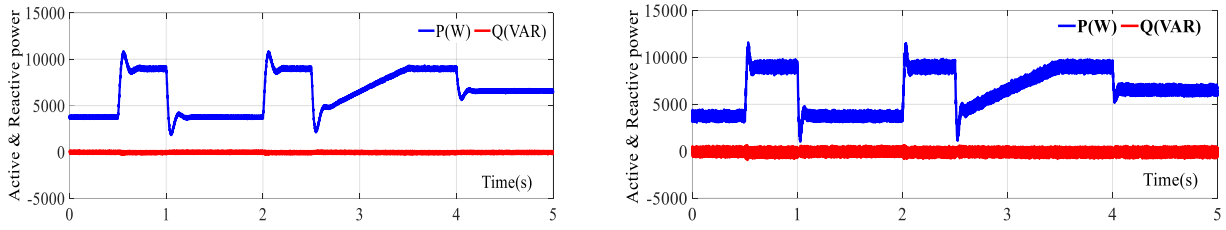

Fig.22 Simulation results of three-level NPC inverter (**a**. Grid current and voltage, **b.** Line voltage, **c.** Phase voltage, **d.** Active and reactive powers.

The three-phase, grid current and voltage is sinusoidal and in phase. The weighting factor affords the highest output performance in terms of the DC-voltage balancing. It can be confirmed by the produced PV power which corresponds to the power injected into the network. Also, that the reactive power is kept to zero, which corresponds to a unit power factor operation.

2.7.3 Voltage balancing

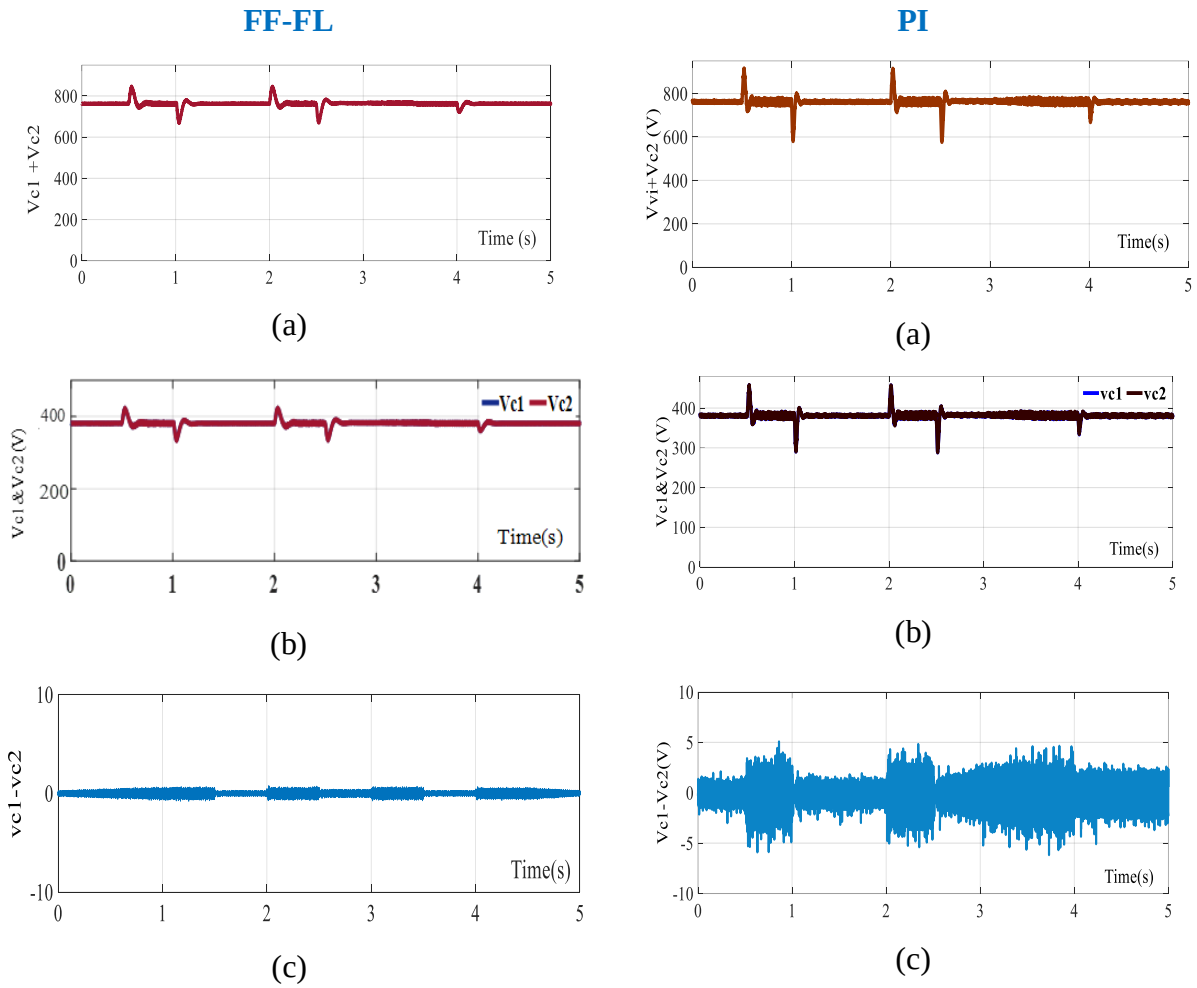

Fig.2.23 DC-voltage balancing of NPC inverter (a) $V_{c1}+ V_{c2,}$ (b)V_{c1} & V_{c2} and (c)& $V_{c1}- V_{c2}$

Multilevel neutral-point clamped (NPC) inverters suffer from the voltage balancing problem,

which seriously hinders its implementation in the industry, a robust finite set predictive control is proposed which can solve this problem. One of the most important sides of the finite set model predictive control method is the simplicity for realizing the voltage balance in the DC link capacitors. This characteristic was tested using the cost function. The method was effective in maintaining voltage balance. Fig.2.23 shows the capabilities of the method. To demonstrate the validity of the proposed voltage balancing, three-level neutral point clamped inverter prototype was built and tested as capacitor voltages vc1 and vc2. We can prove the balancing of the NPC inverter by the three following equations:($v_{c1}+v_{c2}=v_{dc}$) , ($v_{c1}=v_{c2}$) or ($v_{c1}-v_{c2}=0$)

The DC-voltage is balanced by showing the differences between (v_{c1} and v_{c2}) given in Fig.2.23. We note that the presented techniques generate a balanced three-phase current which follows its reference with negligible harmonics.

2.7.4 THD discussion

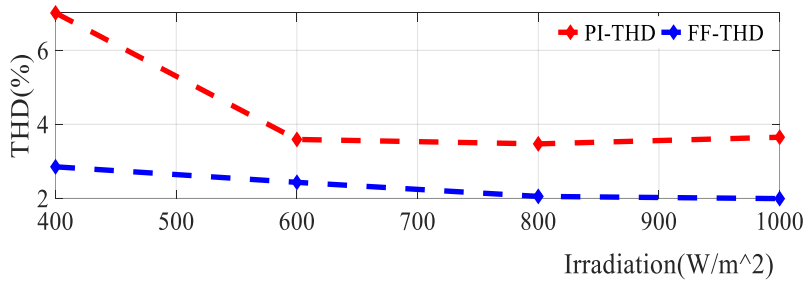

Fig.2.24 THDs (%)

The THD analysis of the grid current in Fig.2.24 shows that the FF-FL and FCS-MPC for the NPC have a real influence, the line current has been controlled properly to inject a pure active power into the grid ensuring a unit power factor operation mode. But in case of PI, THD pass to a limit of the FF-FL. However, the PI controller has some cons such as: the high overshoot, sensitivity with difficulty to define controller gains accurately in nonlinear systems and slow response due to sudden solar irradiation. So, the FL controller is proposed to overcome the disadvantages of the PI controller, it is observed that FL controller provides important advantages over the traditional PI controller like limiting the overshoot and THD.

Table. 2.4 Parameters characterizing the PV system connected to the network.

Parameters of the system PV parameters

Voltage at maximum power	V_{mp}	**28**	**[V]**
Current at maximum power	I_{mp}	2.85	[A]
Maximum power at standard condition	P_{mp}	80	[W]
Open circuit voltage	V_{oc}	3.71	[V]
Short circuit current	I_{sc}	33.1	[A]

Total number of cells in series	Ns	36
Total number of cells in parallel	Np	1
Total number panels in series	Nps	15
Total number panels in parallel	Npp	8

Parameters of the system DC boost parameters

DC capacitors	C1&C2	1550	[µF]
Constant	δ	1.1	

Parameters of the system Grid parameters

Grid resistance	R	**0.1**	**[Ω]**
Grid inductance	L	4	[mH]
Grid Frequency	f	50	[HZ]
Grid peak voltage		220	[V]

Parameters of the system Simulation parameters

MPPT sampling time	**$1e^{-3}$**	**[s]**
FCS-MPC sampling time	$2e^{-5}$	[s]
Weighting factor λ	0.001	

2.8 CONCLUSION

The PV market has experienced in the last decade an exponential growth, becoming an important alternative and clean energy source in many countries. Along with the decrease in price and the increase in efficiency of the PV modules, the PV converter topologies have been continuously changing following more demanding requirements and standards. These regulations are being adapted to a new power system scenario where renewable energy sources are an important part of the energy mix. Nowadays, and meeting these legal requirements, PV converter topologies deal with issues such as high efficiency, high power density, grid code compliance, reliability, long warranties and economic costs. A good number of PV converter topologies can be found in the market for string, multistring, central and AC-module PV applications. Among all these converter topologies, it can be affirmed that one of the most important appearances has been the multilevel converters, mainly the NPC.

A grid-connected PV energy system is studied in this research chapter where the whole system is simulated in Matlab/Simulink environment. The PV array is connected to the grid through the DC/DC boost converter and three-phase multilevel NPC inverter. The maximum power extracted from the PV is achieved using a simple P&O technique. On the other hand, the main function of

the grid side controller is to control the active and reactive power via two control loops which are the inner current control loop and the outer DC-link voltage control loop. The outer DC-link voltage control loop using a hybrid nonlinear control method FF-FL technique in comparison with a conventional PI to control the DC-link voltage. FF-FL has been proposed to increase robustness of the system in different dynamic modes of irradiation. FF-FL provide more effective, accurate and compact tools to control the DC-link voltage in the grid. While the inner control loop, the FCS-MPC algorithm is developed with the aim to achieve a perfect control of the injected powers into the grid using a three-level NPC inverter as part of renewable energy system. The simulation results prove the robust control of DC-voltage, active and reactive power transited to the utility grid.

References

[1] A. K. Traoré, A. Cardenas, M. L. Doumbia, and K. Agbossou, 'Comparative Study of Three Power Management Strategies of a Wind PV Hybrid Stand-alone System for Agricultural Applications', in IECON 2018-44th Annual Conference of the IEEE Industrial Electronics Society, 2018, pp. 1711–1716.1–6.

[2] A. Ghosh and A. Joshi, 'A new approach to load balancing and power factor correction in power distribution system', IEEE Trans. Power Delivery, vol. 15, no. 1, pp. 417–422, Jan. 2000, doi: 10.1109/61.847283.

[3] G. Bandoc, A.-M. S. Florescu, M. Degeratu, and R. Pravalie, 'c', 'Renewable Energy and Environmental Sustainability', vol. 1, p. 29, 2016.

[4] G. Bandoc, A.-M. S. Florescu, M. Degeratu, and R. Pravalie, 'Use of hybrid renewable energy systems for small communities', Renewable Energy and Environmental Sustainability, vol. 1, p. 29, 2016.

[5] M. Cespedes and J. Sun, 'Adaptive control of grid-connected inverters based on online grid impedance measurements', IEEE Transactions on sustainable energy, vol. 5, no. 2, pp. 516–523, 2014.

[6] N. Hamrouni and A. Chérif, 'Modelling and control of a grid connected photovoltaic system', Revue des Energies Renouvelables, vol. 10, no. 3, pp. 335–344, 2007.

[7] S. Sumathi, L. A. Kumar, and P. Surekha (auth.), Solar PV and Wind Energy Conversion Systems: An Introduction to Theory, Modeling with MATLAB/SIMULINK, and the Role of Soft Computing Techniques, 1st ed. Springer International Publishing, 2015. Accessed: Nov. 04, 2021.

[8] S. A. Azmi, M. F. N. Tajuddin, M. F. Mohamed, and L. J. Hwai, 'Multi-loop control strategies of three-phase two-level current source inverter for grid interfacing photovoltaic system', in 2017 IEEE Conference on Energy Conversion (CENCON), 2017, pp. 277–282.

[9] BOLLIPO, Ratnakar Babu, MIKKILI, Suresh, et BONTHAGORLA, Praveen Kumar. Hybrid, optimal, intelligent and classical PV MPPT techniques: A review. CSEE Journal of Power and Energy Systems, 2020, vol. 7, no 1, p. 9-33.

[10] K. Amara et al., 'Improved performance of a PV solar panel with adaptive neuro fuzzy inference system ANFIS based MPPT', in 2018 7th International Conference on Renewable Energy Research and Applications (ICRERA), 2018, pp. 1098–1101.

[11] M. A. Abdourrziq, M. Ouassaid, and M. Maaroufi, 'Single-sensor based MPPT for photovoltaic systems', International Journal of Renewable Energy Research (IJRER), vol. 6, no. 2, pp. 570–579, 2016.

[12] M. A. De Brito, L. P. Sampaio, G. Luigi, G. A. e Melo, and C. A. Canesin, 'Comparative analysis of MPPT techniques for PV applications', in 2011 International Conference on Clean Electrical Power (ICCEP), 2011, pp. 99–104.

[13] J. Suganya and M. C. Mabel, 'Maximum power point tracker for a photovoltaic system', in 2012 International Conference on Computing, Electronics and Electrical Technologies (ICCEET), 2012, pp. 463–465.

[14] H. Suryanarayana and M. K. Mishra, 'Fuzzy logic based supervision of DC link PI control in a DSTATCOM', in 2008 Annual IEEE India Conference, 2008, vol. 2, pp. 453–458.

[15] S. M. Tayebi, H. Hu, and I. Batarseh, 'Advanced DC-Link Voltage Regulation and Capacitor Optimization for Three-Phase Microinverters', IEEE Trans. Ind. Electron., vol. 66, no. 1, pp. 307–317, Jan. 2019, doi: 10.1109/TIE.2018.2823700.

[16] C. Jain and B. Singh, 'A Three-Phase Grid Tied SPV System With Adaptive DC Link Voltage for CPI Voltage Variations', IEEE Transactions on Sustainable Energy, vol. 7, no. 1, pp. 337–344, Jan. 2016, doi: 10.1109/TSTE.2015.2496297.

[17] R. L. de A. Ribeiro, T. de O. A. Rocha, R. M. de Sousa, E. C. dos Santos, and A. M. N. Lima, 'A Robust DC-Link Voltage Control Strategy to Enhance the Performance of Shunt Active Power Filters Without Harmonic Detection Schemes', IEEE Trans. Ind. Electron., vol. 62, no. 2, pp.

[18] AUNG, Thandar et NAING, Tun Lin. DC-link voltage control of DC-DC boost converter-inverter system with PI controller. World Academy of Science, Engineering and Technology International Journal of Electrical and Computer Engineering, 2018, vol. 12, no 11, p. 848-856.

[19] T. Zhao, Q. Zong, T. Zhang, and Y. Xu, 'Study of photovoltaic three-phase grid-connected inverter based on the grid voltage-oriented control', in 2016 IEEE 11th Conference on Industrial Electronics and Applications (ICIEA), Jun. 2016, pp. 2055–2060. doi: 10.1109/ICIEA.2016.7603927.

[20] M. Ahmed, M. Abdelrahem, and R. Kennel, 'Highly Efficient and Robust Grid Connected Photovoltaic System Based Model Predictive Control with Kalman Filtering Capability', Sustainability, vol. 12, no. 11, p. 4542, 2020.

[21] S. Abbasi, A. A. Ghadimi, A. H. Abolmasoumi, M. Reza Miveh, and F. Jurado, 'Enhanced Control Scheme for a Three-Phase Grid-Connected PV Inverter under Unbalanced Fault Conditions', Electronics, vol. 9, no. 8, p. 1247, 2020.

[22] N. Babu P, J. M. Guerrero, P. Siano, R. Peesapati, and G. Panda, 'An Improved Adaptive Control Strategy in Grid-Tied PV System With Active Power Filter for Power Quality Enhancement', IEEE Systems Journal, pp. 1–12, 2020, doi: 10.1109/JSYST.2020.2985164.

[23] M. A. Garnica Lopez, J. L. Garcia de Vicuna, J. Miret, M. Castilla, and R. Guzman, 'Control Strategy for Grid-Connected Three-Phase Inverters During Voltage Sags to Meet Grid Codes and to Maximize Power Delivery Capability', IEEE Trans. Power Electron., vol. 33, no. 11, pp. 9360–9374, Nov. 2018, doi: 10.1109/TPEL.2018.2792478.

[24] R. P. Aguilera, P. Lezana, and D. E. Quevedo, 'Finite-Control-Set Model Predictive Control With Improved Steady-State Performance', IEEE Transactions on Industrial Informatics, vol. 9, no. 2, pp. 658–667, May 2013, doi: 10.1109/TII.2012.2211027.

[25] J. Rodriguez et al., 'State of the Art of Finite Control Set Model Predictive Control in Power Electronics', IEEE Transactions on Industrial Informatics, vol. 9, no. 2, pp. 1003–1016, May 2013, doi: 10.1109/TII.2012.2221469.

[26] Y. Zhang, W. Xie, Z. Li, and Y. Zhang, 'Model Predictive Direct Power Control of a PWM Rectifier With Duty Cycle Optimization', IEEE Transactions on Power Electronics, vol. 28, no. 11, pp. 5343–5351, Nov. 2013, doi:

10.1109/TPEL.2013.2243846.

[27] J. Hong and R. Cao, 'Adaptive Selective Harmonic Elimination Model Predictive Control for Three-Level T-Type Inverter', IEEE Access, vol. 8, pp. 157983–157994, 2020, doi: 10.1109/ACCESS.2020.3020216.

[28] A. Laib, F. Krim, B. Talbi, H. Feroura, and A. Kihal, 'Decoupled active and reactive power control strategy of grid-connected six-level diode-clamped inverters based on finite set model predictive control for photovoltaic application', Revue Roumaine des Sciences Techniques-Serie Electrotechnique et Energetique, vol. 64, no. 1, pp. 51–56, 2019.

[29] R. Beniak, K. Górecki, P. Paduch, and K. Rogowski, 'Reduced Switch Count in Space Vector PWM for Three-Level NPC Inverter', Energies, vol. 13, no. 22, p. 5945, Nov. 2020, doi: 10.3390/en13225945.

[30] J. Rodriguez, S. Bernet, B. Wu, J. O. Pontt, and S. Kouro, 'Multilevel Voltage-Source-Converter Topologies for Industrial Medium-Voltage Drives', IEEE Trans. Ind. Electron., vol. 54, no. 6, pp. 2930–2945, Dec. 2007, doi: 10.1109/TIE.2007.907044.

[31] S. Kouro, J. I. Leon, D. Vinnikov, and L. G. Franquelo, 'Grid-Connected Photovoltaic Systems: An Overview of Recent Research and Emerging PV Converter Technology', EEE Ind. Electron. Mag., vol. 9, no. 1, pp. 47–61, Mar. 2015, doi: 10.1109/MIE.2014.2376976.

[32] L. Ji et al., 'A multi-objective control strategy for three phase grid-connected inverter during unbalanced voltage sag', IEEE Transactions on Power Delivery, 2020.

[33] O. Kukrer, S. Bayhan, and H. Komurcugil, 'Model-Based Current Control Strategy With Virtual Time Constant for Improved Dynamic Response of Three-Phase Grid-Connected VSI', IEEE Trans. Ind. Electron., vol. 66, no. 6, pp. 4156–4165, Jun. 2019, doi: 10.1109/TIE.2018.2863195.

[34] M. İnci and Ö. Türksoy, 'Review of fuel cells to grid interface: Configurations, technical challenges and trends', Journal of cleaner production, vol. 213, pp. 1353–1370, 2019.

[35] C. Mahamat, 'Analyse et commandes des convertisseurs multi-niveaux pour un générateur photovoltaïque connecté au réseau électrique', PhD Thesis, Université Paris-Saclay, 2018.

[36] C. Miron, 'Advanced control for renewable energy systems', PhD Thesis, Lille 1, 2018.

[37] M. A. Hannan, Z. A. Ghani, A. Mohamed, and M. N. Uddin, 'Real-time testing of a fuzzy logic controller based grid-connected photovoltaic inverter system', in 2014 IEEE Industry Application Society Annual Meeting, Vancouver, BC, Canada, Oct. 2014, pp. 1–8. doi: 10.1109/IAS.2014.6978394.

[38] N. Babu P, J. M. Guerrero, P. Siano, R. Peesapati, and G. Panda, 'An Improved Adaptive Control Strategy in Grid-Tied PV System With Active Power Filter for Power Quality Enhancement', IEEE Systems Journal, pp. 1–12, 2020, doi: 10.1109/JSYST.2020.2985164.

[39] A. Kihal, F. Krim, B. Talbi, A. Laib, and A. Sahli, 'A Robust Control of Two-Stage Grid-Tied PV Systems Employing Integral Sliding Mode Theory', Energies, vol. 11, no. 10, p. 2791, 2018.

[40] D. Murillo-Yarce et al., 'A Review of Control Techniques in Photovoltaic Systems', Sustainability, vol. 12, no. 24, p. 10598, 2020.

[41] P. S. Sikder and N. Pal, 'Modeling of an intelligent battery controller for standalone solar-wind hybrid distributed generation system', Journal of King Saud University-Engineering Sciences, 2019.

[42] S. Weckx, C. Gonzalez, and J. Driesen, 'Combined Central and Local Active and Reactive Power Control of PV Inverters', IEEE Transactions on Sustainable Energy, vol. 5, no. 3, pp. 776–784, Jul. 2014, doi: 10.1109/TSTE.2014.2300934.

[43] S. Ouchen, S. Abdeddaim, A. Betka, and A. Menadi, 'Experimental validation of sliding mode-predictive direct power control of a grid connected photovoltaic system, feeding a nonlinear load', Solar Energy, vol. 137, pp.

328–336, 2016.

[44] K. Zeb et al., 'A comprehensive review on inverter topologies and control strategies for grid connected photovoltaic system', Renewable and Sustainable Energy Reviews, vol. 94, pp. 1120–1141, 2018.

[45] H. Abu-Rub, M. Malinowski, and K. Al-Haddad, 'Power Electronics for Renewable Energy Systems, Transportation and Industrial Applications'. Wiley. Accessed: Nov. 04, 2021.

[46] S. K. Kollimalla and M. K. Mishra, 'Variable perturbation size adaptive P&O MPPT algorithm for sudden changes in irradiance', IEEE Transactions on Sustainable Energy, vol. 5, no. 3, pp. 718–728, 2014.

[47] L. M. Elobaid, A. K. Abdelsalam, and E. E. Zakzouk, 'Artificial neural network-based photovoltaic maximum power point tracking techniques: a survey', IET Renewable Power Generation, vol. 9, no. 8, pp. 1043–1063, 2015.

[48] R. B. Koad, A. F. Zobaa, and A. El-Shahat, 'A novel MPPT algorithm based on particle swarm optimization for photovoltaic systems', IEEE Transactions on Sustainable Energy, vol. 8, no. 2, pp. 468–476, 2016.

[49] D. G. Montoya, C. A. Ramos-Paja, and R. Giral, 'Improved design of sliding-mode controllers based on the requirements of MPPT techniques', IEEE transactions on Power Electronics, vol. 31, no. 1, pp. 235–247, 2015.

[50] B. Talbi, F. Krim, T. Rekioua, A. Laib, and H. Feroura, 'Design and hardware validation of modified P&O algorithm by fuzzy logic approach based on model predictive control for MPPT of PV systems', Journal of Renewable and Sustainable Energy, vol. 9, no. 4, p. 043503, Jul. 2017, doi: 10.1063/1.4999961.

[51] S. Khadidja, M. Mountassar, and B. M'hamed, 'Comparative study of incremental conductance and perturb observe MPPT methods for photovoltaic system', in 2017 International Conference on Green Energy Conversion Systems (GECS), Mar. 2017, pp. 1–6. doi: 10.1109/GECS.2017.8066230.

[52] P. Vinay and M. A. Mathews, 'Modelling and analysis of artificial intelligence based MPPT techniques for PV applications', in 2014 International Conference on Advances in Green Energy (ICAGE), Dec. 2014, pp. 56–65. doi: 10.1109/ICAGE.2014.7050144.

[53] H. Renaudineau et al., 'A PSO-Based Global MPPT Technique for Distributed PV Power Generation', IEEE Transactions on Industrial Electronics, vol. 62, no. 2, pp. 1047–1058, Feb. 2015, doi: 10.1109/TIE.2014.2336600.

[54] A. Safari and S. Mekhilef, 'Incremental conductance MPPT method for PV systems', in 2011 24th Canadian Conference on Electrical and Computer Engineering(CCECE), Niagara Falls, ON, Canada, May 2011, pp. 000345–000347. doi: 10.1109/CCECE.2011.6030470.

[55] R. Alik and A. Jusoh, 'An enhanced P&O checking algorithm MPPT for high tracking efficiency of partially shaded PV module', Solar Energy, vol. 163, pp. 570–580, Mar. 2018, doi: 10.1016/j.solener.2017.12.050.

[56] S. Z. Mirbagheri, S. Mekhilef, and S. M. Mirhassani, 'MPPT with Inc. Cond method using conventional interleaved boost converter', Energy Procedia, vol. 42, pp.

[57] H. Boumaaraf, A. Talha, and O. Bouhali, 'A three-phase NPC grid-connected inverter for photovoltaic applications using neural network MPPT', Renewable and Sustainable Energy Reviews, vol. 49, pp. 1171–1179, Sep. 2015, doi: 10.1016/j.rser.2015.04.06624–32, 2013.

[58] A. Lashab, D. Sera, and J. M. Guerrero, 'A dual-discrete model predictive control-based MPPT for PV systems', IEEE Transactions on Power Electronics, vol. 34, no. 10, pp. 9686–9697, 2019.

[59] C. Jain and B. Singh, 'An adjustable DC link voltage-based control of multifunctional grid interfaced solar PV system', IEEE Journal of Emerging and Selected Topics in Power Electronics, vol. 5, no. 2, pp. 651–660, 2016.

[60] N. Karami, 'Control of a hybrid system based PEMFC and photovoltaic panels', PhD Thesis, Aix-Marseille, 2013.

[61] B. Bendib, H. Belmili, and F. Krim, 'A survey of the most used MPPT methods: Conventional and advanced algorithms applied for photovoltaic systems', Renewable and Sustainable Energy Reviews, vol. 45, pp. 637–648, 2015.

[62] M. Seyedmahmoudian et al., 'State of the art artificial intelligence-based MPPT techniques for mitigating partial shading effects on PV systems–A review', Renewable and Sustainable Energy Reviews, vol. 64, pp. 435–455, 2016.

[63] S. S. binti Abd Karim, 'Modelling and Control of a Grid Connected Photovoltaic System', 2014.

[64] H. Yatimi and E. Aroudam, 'Assessment and control of a photovoltaic energy storage system based on the robust sliding mode MPPT controller', Solar Energy, vol. 139, pp. 557–568, 2016.

[65] K. Arulkumar, K. Palanisamy, and D. Vijayakumar, 'Recent advances and control techniques in grid connected PV system–A review', International Journal of Renewable Energy Research, vol. 6, no. 3, pp. 1037–1049, 2016.

[66] S. Fahad, A. J. Mahdi, W. H. Tang, K. Huang, and Y. Liu, 'Particle swarm optimization based DC-link voltage control for two stage grid connected PV inverter', in 2018 International Conference on Power System Technology (POWERCON), 2018, pp. 2233–2241.

[67] B. Karanayil, V. G. Agelidis, and J. Pou, 'Evaluation of DC-link decoupling using electrolytic or polypropylene film capacitors in three-phase grid-connected photovoltaic inverters', in IECON 2013-39th Annual Conference of the IEEE Industrial Electronics Society, 2013, pp. 6980–6986.

[68] J. Zhang and M. Cheng, 'DC link voltage control strategy of grid-connected wind power generation system', in The 2nd International Symposium on Power Electronics for Distributed Generation Systems, Hefei, China, Jun. 2010, pp. 970–975. doi: 10.1109/PEDG.2010.5545825.

[69] T. Nguyen-Van, R. Abe, and K. Tanaka, 'A Digital Hysteresis Current Control for Half-Bridge Inverters with Constrained Switching Frequency', Energies, vol. 10, no. 10, p. 1610, Oct. 2017, doi: 10.3390/en10101610.

[70] J. Rodriguez and P. Cortes, 'Predictive Control of Power Converters and Electrical Drives: Rodriguez/Predictive Control of Power Converters and Electrical Drives'. Chichester, UK: John Wiley & Sons, Ltd, 2012. doi: 10.1002/9781119941446.

[71] Y. Liu, B. Ge, H. Abu-Rub, H. Sun, F. Z. Peng, and Y. Xue, 'Model Predictive Direct Power Control for Active Power Decoupled Single-Phase Quasi-Z -Source Inverter', IEEE Transactions on Industrial Informatics, vol. 12, no. 4, pp. 1550–1559, Aug. 2016, doi: 10.1109/TII.2016.2580001.

[72] X. Gao, W. Tian, X. Liu, Z. Zhang, and R. Kennel, 'Model Predictive Control of a Three-Level NPC Rectifier with a Sliding Manifold Term', in 2018 International Power Electronics Conference (IPEC-Niigata 2018 -ECCE Asia), Niigata, May 2018, pp. 1661–1665. doi: 10.23919/IPEC.2018.8508030.

[73] A. Mora, R. P. Aguilera, R. Cardenas, P. Lezana, and D. D. C. Lu, 'Phase-Shifted Model Predictive Control of a Three-Level Active-NPC Converter', in 2018 IEEE 27th International Symposium on Industrial Electronics (ISIE), Cairns, QLD, Jun. 2018, pp. 270–276. doi:

[74] A. Calle-Prado, S. Alepuz, J. Bordonau, J. Nicolas-Apruzzese, P. Cortes, and J. Rodriguez, 'Model Predictive Current Control of Grid-Connected Neutral-Point-Clamped Converters to Meet Low-Voltage Ride-Through Requirements', IEEE Trans. Ind. Electron., vol. 62, no. 3, pp. 1503–1514, Mar. 2015, doi: 10.1109/TIE.2014.2364459.

[75] X. Guo, M. C. Cavalcanti, A. M. Farias, and J. M. Guerrero, 'Single-Carrier Modulation for Neutral-Point-Clamped Inverters in Three-Phase Transformerless Photovoltaic Systems', IEEE Trans. Power Electron., vol. 28, no. 6, pp. 2635–2637, Jun. 2013, doi: 10.1109/TPEL.2012.2224138.

[76] S. A. A. Fallahzadeh, N. R. Abjadi, and A. Kargar, 'Decoupled Active and Reactive Power Control of a Grid-

Connected Inverter-Based DG Using Adaptive Input–Output Feedback Linearization', Iran J Sci Technol Trans Electr Eng, vol. 44, no. 4, pp. 1369–1378, Dec. 2020, doi: 10.1007/s40998-020-00319-3.

[77] Liming Liu, Hui Li, Yaosuo Xue, and Wenxin Liu, 'Decoupled Active and Reactive Power Control for Large-Scale Grid-Connected Photovoltaic Systems Using Cascaded Modular Multilevel Converters', IEEE Trans. Power Electron., vol. 30, no. 1, pp. 176–187, Jan. 2015, doi: 10.1109/TPEL.2014.2304966.

[78] Z. Lim, 'Active Neutral-Point-Clamped Inverter', in Advanced Multilevel Converters and Applications in Grid Integration, A. I. Maswood and H. D. Tafti, Eds. Chichester, UK: John Wiley & Sons, Ltd, 2018, pp. 275–318. doi: 10.1002/9781119476030.ch14.

[79] V. Yaramasu and B. Wu, 'Model Predictive Decoupled Active and Reactive Power Control for High-Power Grid-Connected Four-Level Diode-Clamped Inverters', IEEE Trans. Ind. Electron., vol. 61, no. 7, pp. 3407–3416, Jul. 2014, doi: 10.1109/TIE.2013.2278959.

[80] R. Vargas, P. Cortés, U. Ammann, J. Rodríguez, and J. Pontt, 'Predictive control of a three-phase neutral-point-clamped inverter', IEEE Transactions on Industrial Electronics, vol. 54, no. 5, pp. 2697–2705, 2007.

[81] C. M. Nirmal Mukundan, P. Jayaprakash, U. Subramaniam, and D. J. Almakhles, 'Binary Hybrid Multilevel Inverter-Based Grid Integrated Solar Energy Conversion System With Damped SOGI Control', IEEE Access, vol. 8, pp. 37214–37228, 2020, doi: 10.1109/ACCESS.2020.2974773.

[82] M. Trabelsi, S. Bayhan, K. A. Ghazi, H. Abu-Rub, and L. Ben-Brahim, 'Finite-Control-Set Model Predictive Control for Grid-Connected Packed-U-Cells Multilevel Inverter', IEEE Trans. Ind. Electron., vol. 63, no. 11, pp. 7286–7295, Nov. 2016, doi: 10.1109/TIE.2016.2558142.

[83] C. Xia, T. Liu, T. Shi, and Z. Song, 'A simplified finite-control-set model-predictive control for power converters', IEEE Transactions on Industrial Informatics, vol. 10, no. 2, pp. 991–1002, 2013.

[84] K. Górecki, K. Rogowski, and R. Beniak, 'Three-level NPC Inverter SVM Implementation on Delfino DSC', IFAC-PapersOnLine, vol. 52, no. 27, pp. 252–256, 2019, doi: 10.1016/j.ifacol.2019.12.647.

[85] H. Hu, F. Feng, and T. Wang, 'Open-circuit fault diagnosis of NPC inverter IGBT based on independent component analysis and neural network', Energy Reports, vol. 6, pp. 134–143, Dec. 2020, doi: 10.1016/j.egyr.2020.11.273.

[86] Y. Liu, H. Abu-Rub, Y. Xue, and F. Tao, 'A Discrete-Time Average Model-Based Predictive Control for a Quasi-Z-Source Inverter', IEEE Trans. Ind. Electron., vol. 65, no. 8, pp. 6044–6054, Aug. 2018, doi: 10.1109/TIE.2017.2787050.

[87] J. Loncarski, V. G. Monopoli, R. Leuzzi, L. Ristic, and F. Cupertino, 'Analytical and Simulation Fair Comparison of Three Level Si IGBT Based NPC Topologies and Two Level SiC MOSFET Based Topology for High Speed Drives', Energies, vol. 12, no. 23, p. 4571, Nov. 2019, doi: 10.3390/en12234571.

[88] M. Hamdi, M. Hamouda, L. Sbita, and K. Al-Haddad, 'FCS-MPC for grid-tied three-phase three-level NPC inverter with experimental validation', in 2017 International Conference on Green Energy Conversion Systems (GECS), 2017, pp. 1–6.

[89] V. Yaramasu and B. Wu, Model Predictive Control of Wind Energy Conversion Systems. Hoboken, NJ, USA: John Wiley & Sons, Inc, 2017.

[90] Laib, ABDELBASET, Fateh Krim, Billel Talbi, HAMZA Feroura, et ABBES Kihal. « Decoupled active and reactive power control strategy of grid-connected six-level diode-clamped inverters based on finite set model predictive control for photovoltaic application ». Revue Roumaine des Sciences Techniques-Serie Electrotechnique et Energetique 64, no 1 (2019): 51–56

[91] NEMA, Savita, NEMA, R. K., et AGNIHOTRI, Gayatri. Inverter topologies and control structure in photovoltaic applications: A review. Journal of Renewable and Sustainable Energy, 2011, vol. 3, no 1, p. 012701.

[92] DESAI, Alpesh, MUKHOPADHYAY, Indrajit, et RAY, Abhijit. Performance Analysis of String and Central Inverter based Ideally Designed Utility scale Solar PV Plant. In : 2020 47th IEEE Photovoltaic Specialists Conference (PVSC). IEEE, 2020. p. 2412-2417. [92] S. Kouro, J. I. Leon, D. Vinnikov, and L. G. Franquelo, 'Grid-Connected Photovoltaic Systems: An Overview of Recent Research and Emerging PV Converter Technology', EEE Ind. Electron. Mag., vol. 9, no. 1, pp. 47–61, Mar. 2015, doi: 10.1109/MIE.2014.2376976.

[93] J. Jung, H. Ku, W. Im and J. Kim, "A Carrier-Based PWM Control Strategy for Three-Level NPC Inverter Based on Bootstrap Gate Drive Circuit," in IEEE Transactions on Power Electronics, vol. 35, no. 3, pp. 2843-2860, March 2020, doi: 10.1109/TPEL.2019.2930088.

[94] W. Jiang, Q. Zhang, M. Mingna and X. Huang, "Low Frequency Harmonics Reduction Discontinuous PWM Strategy With Active Neutral Point Voltage Control for Neutral Point Clamped Three-Level Inverter," in IEEE Access, vol. 8, pp. 179128-179140, 2020, doi: 10.1109/ACCESS.2020.3026668.

[95] Asghar Taheri, Mohammad Hadi Zhalebaghi,A new model predictive control algorithm by reducing the computing time of cost function minimization for NPC inverter in three-phase power grids, ISA Transactions,Vol.71, Part 2, pp.391-402,2017, https://doi.org/10.1016/j.isatra.2017.07.027.

[96] YOFO, Emmanuel et DJONDINÉ, Philippe. Parallel Active Filtering based on a three–phase multicell converter. SCIREA Journal of Electrical Engineering, 2019, vol. 4, p. 48-62.

[97] Kim, J.-C.; Moon, S.-K.; Kwak, S. Direct model-based predictive control scheme without cost function for voltage source inverters with reduced common-mode voltage. Int. J. Electron. 2018, 105, 629–644

[98] LAIB, Abdelbaset, KRIM, Fateh, TALBI, Billel, et al. Improved control for three phase dual-stage grid-connected PV systems based on predictive control strategy. Journal of Control Engineering and Applied Informatics, 2018, vol. 20, no 3, p. 12-23.

[99] SMITH, Cameron, GARGOOM, Ameen, HAQUE, Md Enamul, et al. Model Predictive Control of Grid Connected Solar PV Inverter. In : 2020 Australasian Universities Power Engineering Conference (AUPEC). IEEE, 2020. p. 1-6.

[100] LAIB, Abdelbaset, KRIM, Fateh, TALBI, Billel, et al. A predictive control scheme for large-scale grid-connected PV system using high-level NPC inverter. Arabian Journal for Science and Engineering, 2020, vol. 45, no 3, p. 1685-1701.

[101] KRUG, H.-P., KUME, Tsuneo, et SWAMY, Mahesh. Neutral-point clamped three-level general purpose inverter-features, benefits and applications. In : 2004 IEEE 35th Annual Power Electronics Specialists Conference (IEEE Cat. No. 04CH37551). IEEE, 2004. p. 323-328.

[102] BUSQUETS-MONGE, Sergio, BORDONAU, Josep, BOROYEVICH, Dushan, et al. The nearest three virtual space vector PWM-a modulation for the comprehensive neutral-point balancing in the three-level NPC inverter. IEEE power electronics letters, 2004, vol. 2, no 1, p. 11-15.

Chapter 03: Comparative Study between PI and Fuzzy Logic-PI Based MPPT Strategy for PMSG Variable-Speed Wind Turbine Generation Systems

3.1 Introduction 63
3.2 Background of wind energy systems, generators and power control algorithms 64
3.2.1 Background of wind energy system 64
3.2.1.1 Angle of Attack 65
3.2.1.2 Types of WES 66
- First category 66
- Second category 67
3.2.2 Background of wind generators 68
3.2.3 Background of wind energy control algorithms 69
3.2.3.1 MPPT Control Algorithms for a based WECS 69
3.2.3.2 Main classical maximum power control methods 71
- Wind energy background 71
A-Tip Speed Ratio (TSR) Control 72
B-Power Signal Feedback (PSF) Control 72
C-Optimal Torque Control (OTC) 72
D-Perturb and Observation Control 73
3.2.3.3 Advanced methods of MPPT Controls 74
A1 Fuzzy control 74
B1 Sliding mode control 75
C1 Neural network (NN)-based MPPT algorithm 75
D1 Adaptive MPPT algorithml 75
E1 Multivariable perturb and observe (MVPO) MPPT algorithm 76
3.2.3.4 Grid Side Control 76
3.2.3.5 Other control strategies 76
3.2.3.6 AC Voltage Regulator 77
A2 Two-level converters 77
B2 Three-level converters 78
C2 Multi-level converters 78
D2 Bidirectional back-to-back two-level power converter 78
E2 Unidirectional power converters 79
F2 Matrix Converter 79
G2. Z-source converter 80
H2. Cycloconverter 81
3.2.3.7 Control methods for PMSG 81
3.3 Modeling of the wind turbine conversion chain based on PMSG 83
3.3.1 Wind model 83
3.3.2 Aerodynamic model 84
3.3.3 Mechanic model 85
3.3.4 Modeling of PMSG 87
3.4 System description for the proposed system for PMSG 89
3.4.1 Generator side controller 90
3.4.1.1 MPPT based PI control 90
3.4.1.2 MPPT based FL-PI control 91
3.5 Model of three phase rectifier 93
3.6 Result and discussion 94
3.7 Conclusion 98
References 100

Chapter 3 Comparative Study between FL-PI and PI Based MPPT Strategy for PMSG VS-WTGS



Abstract

This chapter provides a study of generator technologies used in WECS. This study is based on an exhaustive review and the state of the art about the control strategies of WTG systems, a comparison of different converters used in wind conversion system, cost, efficiency, power consumption and control complexity.

In order to achieve the maximum power point tracking (MPPT) for wind power generation systems, this chapter presents an artificial intelligent technique based on the Fuzzy Logic Controller (FLC) to enhance the maximum power point tracking (MPPT) of PMSG-based wind turbine. The FL-PI method is compared with the conventional method of MPPT to clarify the superior features of the proposed technique.

In order to acquire a pure DC supply from WECS, a converter is created in this work for rectification of the power generated by the WECS. Space Vector Pulse Width Modulation (SVPWM) is then attempted to be used for switching the rectifier.

A model of PMSG side control considering two MPPT techniques is conducted using MATLAB/Simulink platform. To reveal the robustness and the feasibility of the control system, it is examined under different wind speed profiles. Basing on the obtained results, good tracking with high accuracy and lower oscillation rate are observed after using FL-PI.

3.1 Introduction

The use of wind turbine generators to produce electrical power is still quite small and limited due to the large dependence on climatic conditions on the one side, and to the random fluctuating behavior of the wind energy on the other side [1]. However, wind energy conversion systems have been gaining board and attracting wide attention as different renewable energy sources due to depletion of fossil fuel reserves and environmental issues as a direct result of fossil fuel sources using. Wind power is becoming more appealing to alternative energy sources due to several factors; mainly its mature and clean aspects, the availability of renewable energy technology, being competitive with conventional power plants, no greenhouse gasses generating that can cause global warming and benefiting the countryside economy. Wind turbines can be installed on farms while occupying only a limited number of farms [1]-[5]. The drawback of this kind of energy source as wind speed changes during the day, wind energy varies continuously despite plentifully. In this way, it is difficult to obtain the full amount of power.

On the other hand, where the generator is operated by electronic power equipment, contain a maximum power point tracker, which adjusts the rotational speed to optimize the output power of the turbine. The amount of wind energy conversion system (WECS) output depends on the precision of the whole system, upon the accuracy, which the peak power points are tracked by WECS's maximum power point tracking (MPPT) controller. In addition, WECS decrease mechanical stresses and acoustic noise and allow the control of both the active and reactive powers [6], [7].

Today, the use of new and the larger wind turbines based on variable-speed operation with pitch control will be developed by manufacturers. These larger turbines use a direct-driven synchronous generator (PMSG) or a doubly fed induction generator (DFIG). In recent years. To incorporate them into the wind system, variable speed-wind energy conversion systems (VS-WECS) are increasingly growing. It dominates technologies in the current wind power industry because they have many benefits, over fixed velocity systems, such as the ability to obtain the control technique of Maximum Power Point Tracking (MPPT) to extract maximum power at different winds speed, higher overall reliability and power quality [7]- [10]. Different type of wind turbine generator has become widespread and commonly used in wind power. However, due to the attractive characteristics of permanent magnet synchronous generators (PMSG) are becoming common variable-speed generation systems with the increased penetration of VS-WECS into power systems around the world, and the use of PMSG in large WTGs is increasing rapidly [11]. It is directly connected to the turbine without a gearbox; it can run at low speeds and more benefits such as, higher reliability and efficiency, noise reduction, and smaller size. [2] This study focusses

on past and advanced concepts, and control methods or techniques applied for wind turbine systems.

In this context, this chapter proposes a control strategy of PMSG-wind energy generation system. WECS model includes Wind Turbine (WT), PMSG and PWM rectifier in generator-side with an intermediate DC circuit. The generator-side rectifier is used to track the maximum power from wind. The proposed approach is based on a comprehensive overview study of the permanent magnet synchronous generator (PMSG) for wind energy generation system. The dynamic model of PMSG is presented, and two maximum power point tracking (MPPT) algorithms have been realized in the aim to compare their performance. A comparison of performances of the conventional PI MPPT and the Fuzzy Logic Proportional Integral (FL-PI) MPPT is presented. Control technique for the presented system is presented and analyzed for generator-side converter. The simulation results carried out using Matlab/Simulink software show the effectiveness of the studied system.

3.2 Background of wind energy systems, generators and power control algorithms

Wind turbine control is necessary to ensure low maintenance costs and efficient performance. The control system also guarantees safe operation [10], optimizes power output, and ensures long structural life. Turbine rotational speed and the generator speed are two key areas that must control for power limitation and optimization [11]. The control strategies sections explain how to manage the areas and which techniques unable to use.

3.2.1 Background of wind energy system

Wind energy conversion system (WECS) converts wind kinetic energy to mechanical energy using wind turbine rotor blades, then the generator converts the mechanical power to electrical power [12]. The resulting electrical power is being fed to the load or electrical network through power electronic converters. The WECS under study consists of a gearless wind turbine coupled to PMSG generator with a generator side converter linked through a DC-link to electrical network side converter. Fig.3.1 summarized the major parts included in the mechanical and electrical power conversion of a typical wind turbine system.

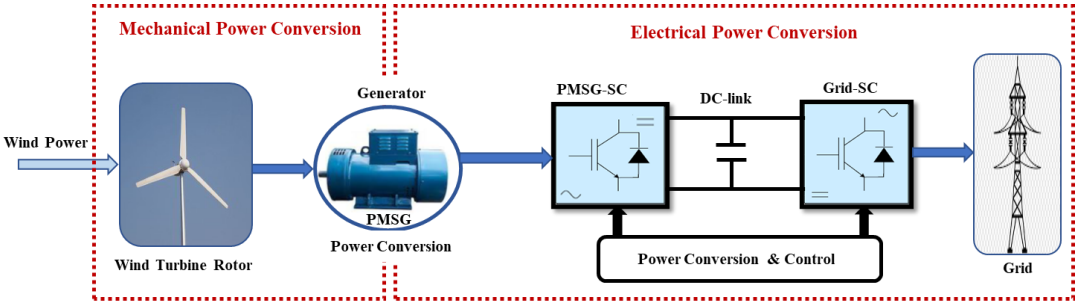

Fig.3.1 Wind turbine system description

The turbine components responsible for these energy conversions are the rotor and the generator. The rotor is the area of the turbine that consists of both the turbine hub and blades. As wind strikes the turbine's blades, the hub rotates due to aerodynamic forces. Then, this rotation is then sent through the transmission system to decrease the revolutions per minute [13]. The transmission system consists of the main bearing, high-speed shaft, gearbox, and low-speed shaft. The ratio of the gearbox determines the rotation division and the rotation speed that the generator sees. This rotation is finally sent to the generator for mechanical-to-electrical conversion. Compared to DFIGs, PMSGs can eliminate the gearbox and slip rings and thus provide a direct drive option [14]. Furthermore, PMSGs have higher efficiency and power density than any other machines. Fig.3.2 shows the major components of a wind turbine: gearbox, generator, hub, rotor, low-speed shaft, high-speed shaft, and the main bearing. The purpose of the hub is to connect the blades' servos that adjust the blade direction to the low-speed shaft. The rotor is the area of the turbine that consists of both the hub and blades. The components are all housed together in a structure called the nacelle.

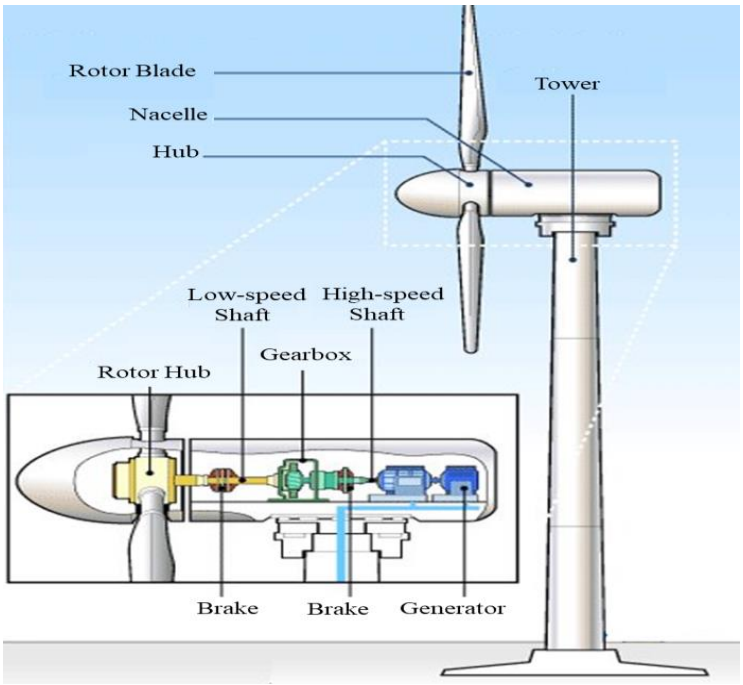

Fig.3.2 Horizontal wind turbine components [57].

3.2.1.1 Angle of Attack

The amount of surface area available for the incoming wind is key to increasing aerodynamic forces on the rotor blades. The angle at which the blade is adjusted is referred to the attack angle of attack α. This angle is measured with respect to the incoming wind direction and the chord line of the blade [15].

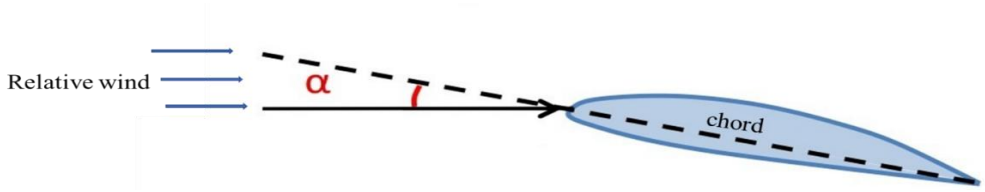

Fig.3.3 Attack angle according to the blade direction

3.2.1.2 Types of WES

WTs are classified into two main categories:

- **First category**

It is characterized first of fixed speed-wind turbines that they are equipped with an induction generator that is directly connected to the grid, with a soft-starter and a capacitor bank for reducing reactive power compensation [16]. They are designed to achieve maximum efficiency at one particular wind speed. Then, Variable speed-wind turbines are designed to achieve maximum aerodynamic efficiency over a wide range of wind speeds. It has a more complicated electrical system than that of a fixed-speed wind turbine [17]. It is typically equipped with an induction or synchronous generator and connected to the grid through a power converter. Table 3.1 gives us the main features compression of Fixed- speed and Variable-speed Wind Turbine.

Table 3.1 Features compression of Fixed- Speed (FS-WECS) and Variable-Speed Wind Turbine (VS-WECS)

Featu	Advantages	Disadvantages
FS-WECS	• Simple, robust and reliable. • Cost of its electrical parts is low.	• Uncontrollable reactive power consumption, mechanical stress and limited power quality control owing to its fixed-speed operation. • All fluctuations in the wind speed are further her transmitted as fluctuations in the mechanical torque and then as fluctuations in the electrical power on the grid.

VS-WECS	• Increased energy capture, improved power quality and reduced mechanical stress on the wind turbine. • The introduction of variable speed-wind turbine types increase the number of applicable generator types and introduces several degrees of freedom in the combination of generator type and power converter type.	• Losses in power electronics, the use of more components and the increased cost of equipment because of the power electronics.

- **Second category**

WTs are the most crucial part of WES. These WTs can be installed either on vertical or on the horizontal axis forming vertical-axis wind turbine (VAWT) or horizontal-axis wind turbine (HAWT) respectively. HAWT type is very commonly used in WES as it has several merits as compare to VAWT like, it has simple configuration especially for higher rates, besides their high efficiency and low cost [10]. Table 3.2 summarizes some features compression of horizontal and vertical axis wind turbine.

Table 3.2 Features compression of horizontal and vertical axis wind turbine [18]

Features	**Vertical Axis** 	**Horizontal Axis** 
Efficiency	Low	High
Tower Height	Small (around 10 m)	Large (around 100 m)
Blades Rotation Speed	Low (3-7 m/sec)	High (5-12 m/sec)
Rotational Blades Area	Small	Large
Maintenance	Simple	Complex
Noise Effect	0-10 dB	5-60 dB
Generator location	Ground Tower	Top Wind
Application	On Shore	Both On and Off Shore

3.2.2 Background of wind generators

The classification of wind electric conversion system is fixed and variable speed type, gearbox or direct driven type, etc. In following the sections, the different configurations of the wind electric generators are presented [18]. Any types of three-phase generator can connect to wind turbine.

Different types of generators which are used with wind turbines, are as follows: asynchronous (induction) generator and synchronous generator, Squirrel cage induction generator (SCIG), Doubly-Fed Induction Generator DFIG and wound rotor induction generator (WRIG) are coming under asynchronous generators. Wound rotor generator (WRSG) and permanent magnet generator (PMSG) are coming under synchronous generator [19-21]. In order to select the adequate generator for our study we have done a comparative study of three main generators, which is illustrated in the table below:

Table 3.3: Different types of generators used in WECS [19]

Generator type	Advantages	Disadvantages
Squirrel-Cage Induction Generator SCIG 	• Simple construction. • Simple maintenance.	• Requires reactive power. • Requires soft-start device for initial connection to the grid.
Doubly-Fed Induction Generator DFIG 	• Attenuated pulsation of wind turbine torque low cost. • Direct connection to the power grid significantly reduced power rating and cost of the converter. • Possible speed regulation for optimal utilization of energy. • Power converter provides reactive power for machine magnetization.	• Direct connection to the grid is somewhat difficult. • Requires an excitation system, slip rings and brushes, and maintenance.

Permanent Magnet Synchronous Generator PMSG 	• No Gearbox. • Simple control of reactive power. • Wide range of speeds. • Simple control.	• Large dimensions and weight, problems with construction, transportation and installation.

3.2.3 Background of wind energy control algorithms

In WES, the effective generation of power can only be obtained by using overall control scheme. These control schemes are based on different subsystems of any wind energy systems; on the bases of this control schemes for WES are divided into three types. The first is maximum power tracking control (MPPT) by using different algorithms; The second one is machine/grid side control and then different control including pitch angle control, stall control and yaw control [10]. Fig.3.4 shows some different control schemes in WES.

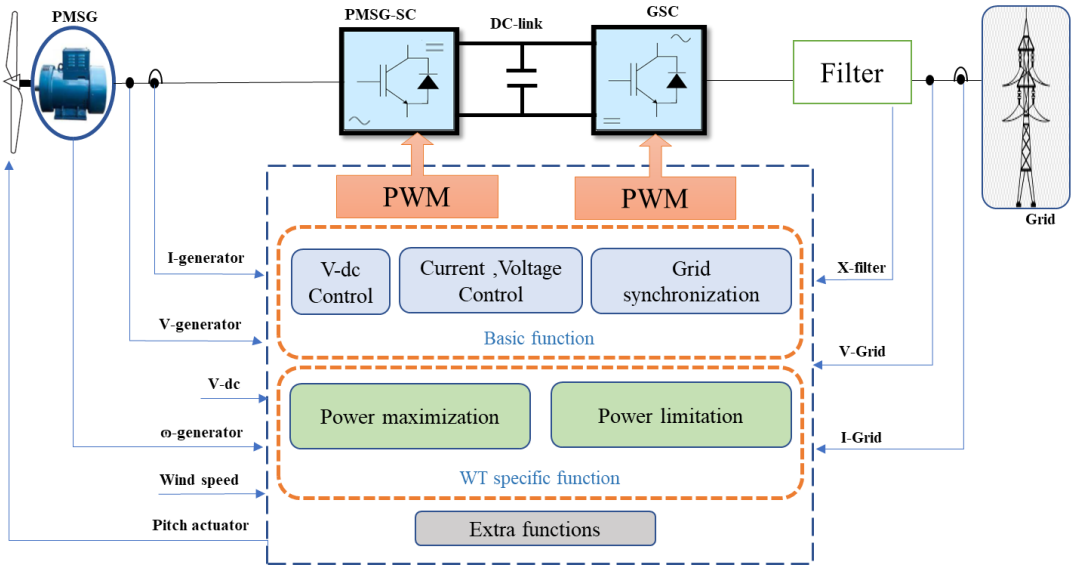

Fig.3.4 Different control of WECS

3.2.3.1 MPPT Control Algorithms for a based WECS

Wind power is the most reliable and developed renewable energy source over past decades. With the rapid penetration of wind generators in the power system, it is very essential to track the maximum available power from wind and wind turbine operates at its maximal energy conversion output. MPPT algorithms plays a vital role in any renewable resource. Wind energy system requires the algorithm to extract as much energy as possible because according to Betz theory only 59.3% of total available [20].

Broadly, a decent variety of publication report on various maximum power point tracking (MPPT) algorithms for a WECS [21]. However, making a choice on an exact MPPT algorithm for

a particular case requires sufficient proficiency because each algorithm has its own merits and demerits. Different available MPPT algorithms are described for extracting maximum power which are classified according to the power measurement (direct or indirect power controller). Merits, demerits and comprehensive comparison of the different MPPT algorithms also highlighted in the terms of complexity, wind speed requirement, prior training, speed responses, etc [25]. Also, the ability to acquire the maximal energy output. This section serves as a proper reference for future MPPT users in selecting appropriate MPPT algorithm for their requirement. The maximum power point tracking control can be mainly divided into two types [26]. They are the conventional control schemes and intelligent control schemes. The conventional control schemes can also be divided into current mode control and speed mode control, which depends on the setting of reference values. The reference values are the active power and electromagnetic torque for current mode control [27-28], and the rotational speed for the speed mode control [29].

Output power from the wind turbine can be controlled to work more effectively within a specific range of the wind speeds bounded by cut-in ($V_{w\text{-}in}$) and cut-out ($V_{w\text{-}out}$) speeds. Out of this range, the turbine should not operate for safety of the turbine as well as generator. The rated power (P-rated) is obtained from the wind turbine at a specific wind speed (V-rated). Consequently, there are four main operating regions as demonstrated in Fig.3.5.

The first and fourth region is below $V_{w\text{-}in}$ and above $V_{w\text{-}out}$ respectively, where the turbine should be disconnected from the grid to prevent it from being driven by the generator. The second region is in between $V_{w\text{-}in}$ and V-rated, where a wind turbine controller starts to operate to extract energy as much as possible by MPPT algorithm. The third region is in between V-rated and $V_{w\text{-}out}$, where it is necessary to restrict the mechanical power generation to the rated power to avoid damage on the turbine. Thus, the MPPT algorithm is required to focus on the second region. Although there are various types of wind turbines, relying upon fixed or variable wind speed, the maximum energy can be extracted only by variable speed wind turbines (VSWT). In contrast to fixed speed wind turbines (FSWT), VSWT needs a partial or full order power converter for power flow control, MPPT control delivering a high quality of power [11–18]. Since these turbines can vary their rotational speed to follow the instantaneous variation in wind speed, they are able to preserve a constant rotational speed to wind speed ratio, called the optimum tip speed ratio (TSR) for which the extracted power is maximized [23]. In addition to this, VSWT can be controlled to minimize the stress on the tower structure, gears and wind generator (WG) shaft, since the blades absorb peaks of WT torque during the variation of the WG speed of rotation, leading to a longer installation life of WECS [18].

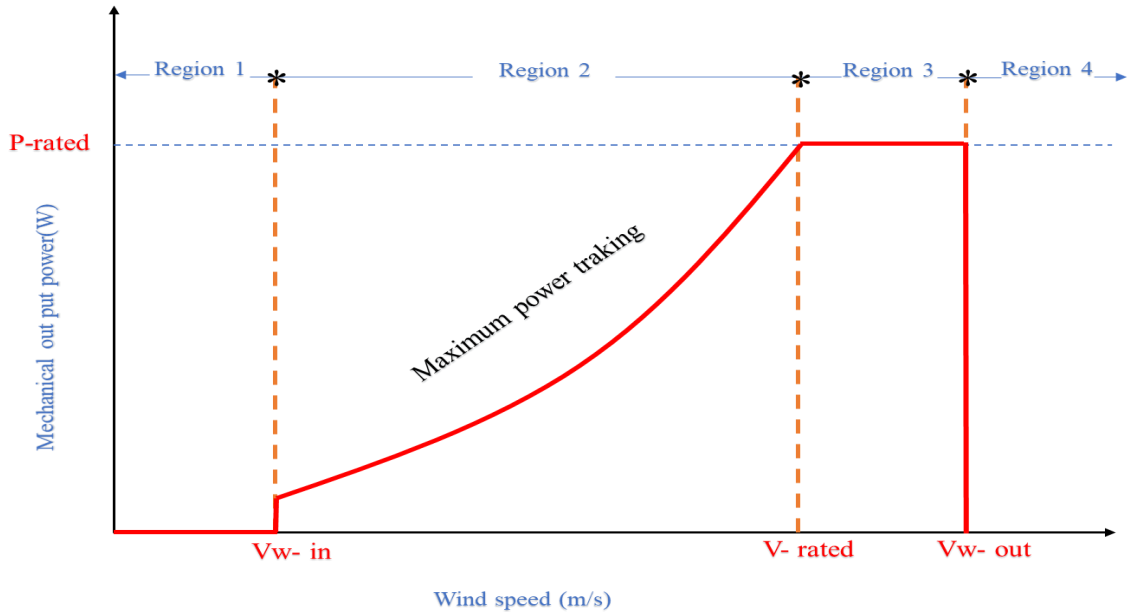

Fig.3.5 Wind turbine control strategy based on four speed zones.

3.2.1.2 Main classical maximum power control methods

The MPPT algorithms are categorized into four types: Tip-Speed ratio control (TSR), Power-Signal feedback (PSF), Hill climb search (HCS) based or Perturb & Observe (P&O) and Optimal Torque Control (OTC) [2].

- **Wind energy background**

The maximum power of a wind turbine at different speeds can be written as:

$$P_{\max} = K_{opt}\Omega_{t-opt}^{3} \tag{3.1}$$

Where

$$K_{opt} = \frac{0.5\pi\ \rho\ C_{p\max}R^{5}}{\lambda_{opt}^{3}} \tag{3.2}$$

$$\Omega_{t-opt} = \frac{\lambda_{opt}v}{R} \tag{3.3}$$

Where R is the turbine radius, v is the wind speed, ρ is the air density, $C_{p\max}$ is the maximum value of the power coefficient, λ_{opt} is the optimal tip speed ratio. Fig.3.6 shows turbine mechanical power as a function of rotor speed at various wind speeds. The power for a certain wind speed is maximum at a certain value of rotor speed called optimum rotor speed Ω_{t-opt}. This is the speed which corresponds to the optimum tip speed ratio λ_{opt}. In order to have maximum possible power, the turbine should always operate at λ_{opt}. This is possible by controlling the rotational speed of the turbine so that it is at the optimum speed of rotation [30].

$$P_{\max} = \Omega_{t-opt}T_{opt} \tag{3.4}$$

Where T_{opt} is the optimum torque value from (3. 3) and (3. 4).

$$T_{opt} = K_{opt}\Omega_{t-opt}^{2} \tag{3.5}$$

In this section, the four MPPT methods are presented and their pros and cons will be discussed.

A Tip Speed Ratio (TSR) Control

TSR control method regulates rotor speed to maintain an optimal TSR and requires measurement of both the wind speed and turbine speed. The optimal TSR for a given wind speed is obtained from the turbine-generator characteristics and varies from system to system.

According to (3.3) and (3.4), the optimal rotational speed λ_{opt} of the wind turbine rotor for a given wind speed can be used to obtain the maximum turbine efficiency and then the maximum mechanical output power of the turbine [31]. The TSR control method regulates the rotational speed of the generator in order to maintain the TSR to an optimum value at which power extracted is its maximum value. This method is simple; However, it requires both the wind speed and the turbine speed to be measured or estimated in real time accurately. Unfortunately, measuring the wind speed flowing in the wind turbine rotor is difficult and increases the complexity and costs in the reality especially for small generating systems [32]. Furthermore, it needs the knowledge of optimum TSR of the turbine, which changes, with variations of the turbine parameters. The block diagram of a PMSG WECS with TSR control is shown in Fig.3.6.

B Power Signal Feedback (PSF) Control

In PSF control, it is required to have the knowledge of the wind turbine's maximum power curve, and track this curve through its control mechanisms. The maximum power curves need to be obtained via simulations or off-line experiment on individual wind turbines or from the datasheet of WT, which makes it difficult to implement with accuracy in practical applications [31]. In this method, reference power is generated using a maximum power data curve or using the mechanical power equation of the wind turbine where wind speed or the rotational speed is used as the input. Fig.3.6 shows the block diagram of a WECS with PSF controller for maximum power extraction. The PSF control block generates the optimal power command P_{opt} which is then applied to the grid side converter control system for maximum power extraction as equation (3.4), using this equation, one could either measure the rotor speed of generator ω to set the reference turbine power P_t [22].

C Optimal Torque Control (OTC)

In the OTC method when the wind speed changes, the generator torque is controlled continuously at the optimum operating point according to (3.5). Fig.3.6 shows the block diagram of OTC MPPT method. The algorithm measures generator rotor speed and computes optimum

torque T_{opt}, the torque that maximizes turbine power. This optimum torque is used as reference torque of a PMSG vector control method [33].

D Perturb and Observation Control

Hill climb search (HCS) methods are used for finding the peak point of the wind turbine power curve without any knowledge about wind turbine's maximum power curve or the information on wind velocity [31], [32]. Perturb and observation (P&O) technique is one of the WECS MPPT methods based on HCS algorithm. The fundamental principle of the P&O algorithm is to detect the change of wind turbine output power P[k]-P[k-l] after a generator speed perturbation $\omega[k]-\omega[k-1]$ and decide the next generator speed perturbation $\omega[k+1]$ according to the variation of P[k]-P[k-l]. First, the generator speed is perturbed by a step change $\Delta\omega[k]$ and then the variations of output power ΔP[k] is observed. If the output power is increasing, the subsequent perturbation will be kept unchanged and the rotor speed will be increased until the optimal rotational speed of the rotor for a specific wind speed is reached and the WECS will operate at or around this point; otherwise, the perturbation direction will be reversed. The principle of perturbation algorithm is illustrated in Fig.3.6 [33].

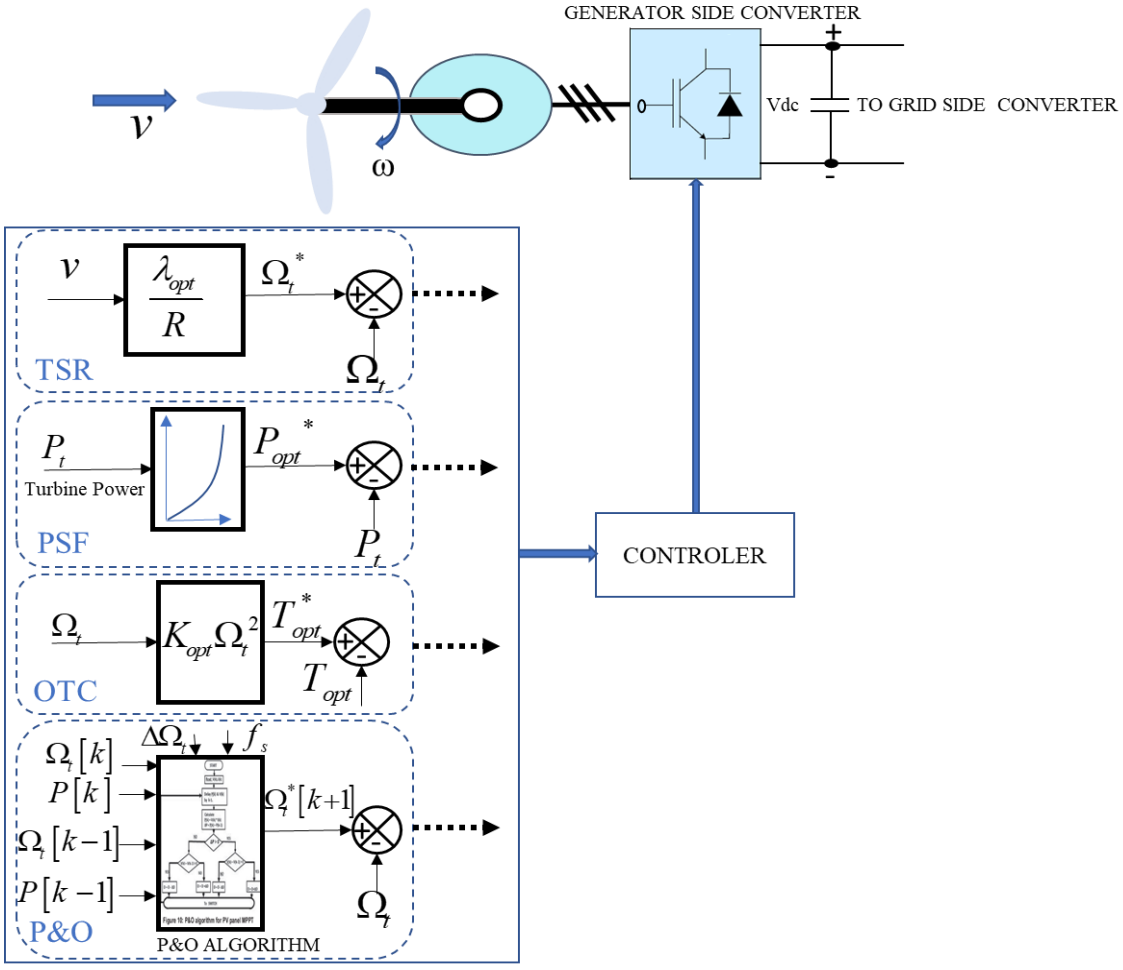

Fig.3.6 TSR, PSF, OTC and P&O control methods

Table 3.4 presents the advantages and drawbacks of each of these MPPT algorithms.

Table 3.4 Summary of MPPT control algorithms [32]

MPPT	Advantages	Disadvantages
(TSR)	• High efficiency and performance with a fast convergence speed. • Its optimal point can be determined theoretically or experimentally.	• High cost of operation especially for small WT systems. • Impossible to have precise wind speed.
(PSF)	• The PSF provides a robust and cost effective maximum power control of The WT. • It is also simple to use with a fast speed of convergence.	• Low efficiency under varying wind conditions since it does not reflect variations in wind speed instantly.
(OTC)	• Very simple to use, fast convergence speed and high efficiency.	• Just like the PSF, the OTC lacks the ability to measure wind speed directly.
(HCS)	• Simple implementation, excellent performance under varying wind conditions and high flexibility.	• It can cause stalling in smaller WTs. • Under a rapid wind change, there is slow response and incorrect detection of direction for maximum power especially in large and medium inertia WTs.

3.2.1.3 Advanced methods of MPPT Controls

The following are the most advanced utilized MPPT control algorithms

A1 Fuzzy control

It overcomes the requirement of a prerequisite mathematical description of the system. The fuzzy will understand the system behavior in the form of rules, and by using these rules the system performance will remain in the desired operating range. Fig.3.7 shows the fuzzy controller for MPPT consisting of fuzzification, rule base and defuzzification blocks [9], [33].

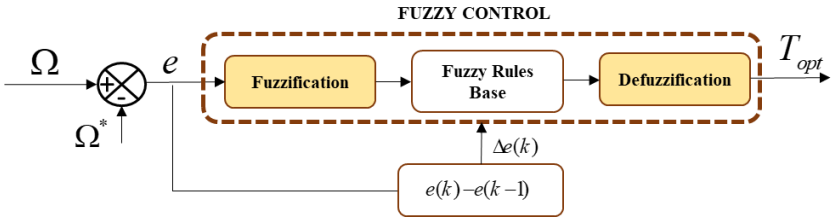

Fig.3.7 Fuzzy control MPPT block

The generator speed is given by ω and the optimal value is referred to as ω^*. The error is given by e and the the error variations is given by Δe. As wind, energy is highly uncertain.

B1 Sliding mode control

When there is any time-varying parameter for a non-linear system, then the sliding mode control (SMC) can be used. Here, the dynamics of the system can be modified through a discrete control signal, which makes the non-linearity to slide along the normal trajectory of the system. In most of the scenario, this SMC is used for variable speed wind turbine [34]. If there is any turbulence and any uncertainties in the system, the sliding model will provide regulated output power, while overcoming the mechanical stresses in the drive train transmission system. The error generated due to reference speed and actual speed is sent through PI controller [35].

C1 Neural network (NN)-based MPPT algorithm

Similar to Fuzzy logic controller, the neural network (NN) has become popular and expanded with the development in soft computing technology [31]. The architecture of a Neural Network consists of three layers: input, hidden, and output layers and the number of nodes in each layer. The input variables can be pitch angle, terminal voltage, output torque, wind speed, rotor speed, etc. or any combination of these variables. The output is generally a reference signal like reference power, rotor speed, reference torque, etc. that is used to drive the power electronic circuit of wind turbine close to the MPP. The convergence of operating point to the peak point depends on the weights assigned to the layers, the type of algorithm used by the hidden layer and the training given to the neural network for a particular system for different input–output patterns.

D1 Adaptive MPPT algorithm

The adaptive MPPT algorithm provides accurate optimal response and can measure the uncertain system parameters. The algorithm requires the wind speed measurement and the knowledge of the system parameters to generate the speed reference from a lookup table [30][31]. In addition, the performance of the algorithm is highly dependent on the selection of the adaptive law for generating the necessary torque reference.

E1 Multivariable perturb and observe (MVPO) MPPT algorithm

The aim of this algorithm is to maximize the generated power output of the wind farm, reducing the requirements of control units and sensors [31]. Such a solution causes the wind power systems economically strong, because the extracted power is same as compared with power classical wind farms, but the number of components required is reduced in MVPO algorithm. To maximize the output power of wind farm, an extension of the P&O algorithm is adopted to optimize currents of all generators present in wind farm [29]. Such a multivariable P&O algorithm, named MVPO, is designed to optimize each generator operating point by using the P&O principle [30].

3.2.3.4 Grid Side Control

The grid-side converter keeps the DC-link voltage fixed and meets the active power demand according to the grid codes. The power quality, synchronization with the grid and grid code compliance can be improved by using grid side control and provides effective active power control. This grid side control can be done using grid side controllers; these controllers so not play any role in energy conversion. Grid side controllers are only responsible for the power quality and synchronization with grid.

3.2.3.5 Other control strategies

WECSs have to cope with the intermittent and seasonal variability of the wind. By this reason, they begin to work when the wind speed is above the cut-in speed so that power is injected into the utility grid; moreover, they include some mechanisms to limit the captured power at high wind speeds to prevent overloading. Manny control strategies can be used for captured power control such as [37, 38]:

- Stall control;
- Pitch control;
- Yaw control.

The stall control is based on a specific design of the blades so that stall occurs when the wind speed exceeds a certain level; it means that the captured power is automatically limited in the rated power range [38-40]. This method is simple, robust and cheap, but it has low efficiency at low wind speed. In case of pitch control, blades can be tuned away from or into the wind as the captured power becomes too high or too low; this is performed by rotating the blades, or part of them, with respect to their longitudinal axes. Below rated wind speed, blades are pitched for optimum power extraction whereas above the rated wind speed blades are pitched to small angle of attack for limiting the power. Advantages of this type of control are good power control performance, assisted start-up and emergency power reduction; The biggest disadvantage is the extra complexity

due to the pitch mechanism. In case of active stall control, the stall is controlled actively by pitching blades to larger angle of attack with wind speed above the rated value [41].

Different control methods to either optimize or limit power output, can control a turbine by controlling the generator speed, blade angle adjustment, and rotation of the entire wind turbine. Blade angle adjustment and turbine rotation are also known respectively, as pitch and yaw control. Yaw control ensures that the turbine is constantly facing into the wind to maximize the effective rotor area and, as a result, power. Because wind direction can vary quickly, the turbine may misalign with the oncoming wind and cause power output losses.

A visual representation of pitch and yaw adjustment is shown in Figures 3.8 and 3.9.

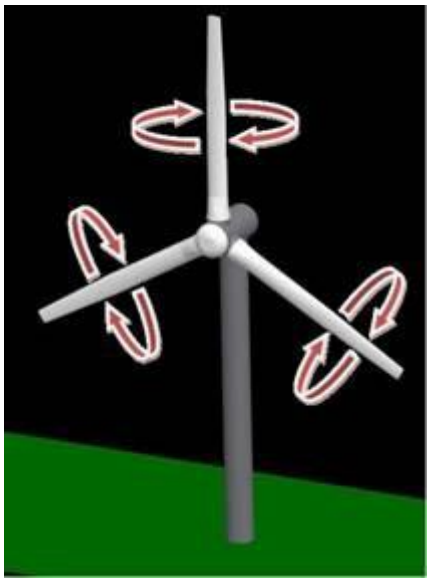

Fig.3.8 Pitch Adjustment [27].

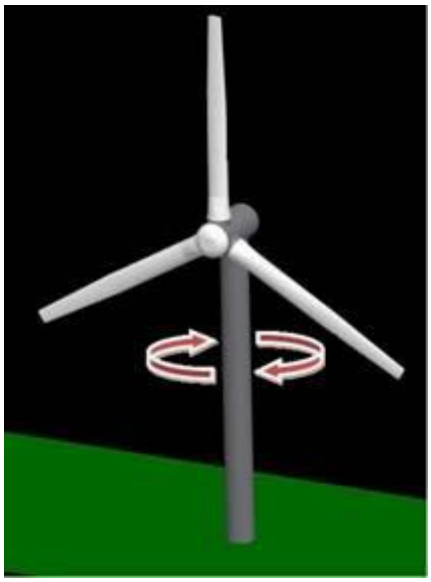

Fig.3.9 Yaw Adjustment [27].

3.2.3.6 AC Voltage Regulator

Power electronics converters are one of the key parts used in WES. In the AC to DC conversion systems is needed hence, voltage regulators or frequency regulators are required. According with the different proposed voltage control topologies can be classified in the following categories:

A2 Two-level converters

The two-level three-phase inverter is a very commonly used topology, that inverter consists of six switches and a capacitor models a ripple-free DC-link voltage. By controlling the switches, Pulse Width Modulation (PWM), and filtering the output, a quasi-sinusoidal waveform is obtained. However, without the filter, the output voltage would be a square wave. To ensure, that short circuits do not occur, dead time is normally incorporated, meaning that two switches in one leg of the inverter is never turned on at the same time [42].

B2 Three-level converters

The three-level inverter is an alternative to the two-level inverter, and have some advantages, that makes it better suited for a medium voltage application. However, a trade-off is that it consists of twice as many transistors as its two-level counterpart. One of the advantages of the three-level inverter is, that the transistors always turn on and off in pairs [42][43]. This means that two switches will always share the full DC-voltage, where two-level inverter switches have to be able to block the full DC-link voltage.

C2 Multi-level converters

Currently there is an increasing interest in multilevel power converters especially for medium to high-power, high voltage-wind turbine applications. Multilevel inverters consist of six or more switches per leg, and the main idea is to create an even higher number of output sinusoidal voltage levels, than the three-level inverter, further decreasing the harmonic content. Since the development of the neutral-point clamped (NPC) three-level converter, several alternative multilevel converter topologies have been reported in the literature [44].

D2 Bidirectional back-to-back two-level power converter

The back-to-back PWM-VSI is a bi-directional power converter consisting of two conventional PWM-VSCs. To achieve full control of the grid current, the DC-link voltage must be boosted to a level higher than the amplitude of the grid line-line voltage. The power flow of the grid side converter is controlled in order to keep the DC-link voltage constant, while the control of the generator side is set to suit the magnetization demand and the reference speed [45]. The advantage of the PWM-VSC is the capacitor decoupling between the grid inverter and the generator inverter. Besides affording some protection, this decoupling offers also separate control of the two inverters, allowing compensation of asymmetry, both on the generator side and on the grid side, independently. The inclusion of a boost inductance in the DC-link circuit increases the component count, but a positive effect is that the boost inductance reduces the demands on the performance of the grid side harmonic filter, and offers some protection of the converter against abnormal conditions on the grid [43], [45].

Pros

- The back-to-back converter is a bidirectional power converter;
- The DC-link voltage can be boosted to achieve full control of the grid current;
- The capacitor between the inverter and rectifier makes it possible to decouple the control of the two inverters, allowing the compensation of asymmetry on both the generator side and the grid side [45];
- The component costs are low.

Cons

- The back-to-back converter consists of two inverters, so the switching losses might be even more pronounced;
- The presence of the heavy and bulky DC-link capacitor increases the costs and reduces the lifetime of the system;
- The switching losses. Every commutation in both the grid inverter and the generator inverter between the upper and lower DC-link branch is associated with a hard switching and a natural commutation [45];
- The combined control of the controlled rectifier and inverter is quite complicated.

E2 Unidirectional power converters

A wound rotor synchronous generator requires a simple diode bridge rectifier for the generator side converter. The diode rectifier is the most common used topology in power electronic applications. For a three-phase system, it consists of six diodes. The diode rectifier can only be used in one quadrant, it is simple and it is not possible to control it. It could be used in some applications with a DC-bus. The variable speed operation of the wind turbine is achieved by using an extra power converter, which fed the excitation winding. The grid side converter will offer a decoupled control of the active and reactive power delivered to the grid and all the grid support features. These wind turbines can have a gearbox or can be direct-driven [46].

Pros

- Simple to implement with low system production cost.

Cons

- Diode rectifier produces a large amount of harmonics (THD);
- Unidirectional power handling capability.

F2 Matrix Converter

The matrix converter concept has become increasingly attractive for wind power applications. Matrix converters offer the potential for significant size and weight reductions in power converter applications due to the absence of large energy storage elements, such as DC-link capacitors. Although the matrix converter includes six additional power switches, the absence of the DC-link capacitor may increase the efficiency and lifetime for the converter. The switching losses of the matrix inverter may be less than that of the back-to-back converter, because half of the switching becomes natural commutations. Provide practically sinusoidal waveforms of the input and output currents with negligible low order harmonics. Thermal stresses of the semiconductors in a matrix converter are lower than in a conventional converter [45 - 47]. However, the DC-link voltage cannot be boosted as that of back-to-back converter. Due to the absence of the DC-link, there is

no decoupling between the input and output of the converter. In ideal terms, this is not a problem but in the case of unbalanced or distorted input voltages, or unbalanced load, the input current and the output voltage also become distorted. Besides that, the modulation technique and commutation control are more complicated than those in the conventional PWM inverter. The protection of matrix converter in a fault situation is not as good as that of back-to-back converter [47].

Pros

Matrix converters have some significant advantages, such as:

- Sinusoidal input and output currents, absence of a DC-link capacitor, fewer IGBT switches, simple and compact power circuit, operation with unity power factor for any load, and regeneration capability [47];
- Offer the potential for significant size and weight reductions in power converter applications due to the absence of large energy storage elements, such as DC-link capacitors;
- Although the matrix converter includes six additional power switches compared to the back-to-back converter, the absence of the DC-link capacitor may increase the efficiency and lifetime for the converter;
- Negligible low order harmonics;
- Thermal stresses of the semiconductors in a matrix converter are lower than in a conventional converter [47].

Cons

- The DC-link voltage cannot be boosted. Without entering the over modulation range, the maximum output voltage of the matrix converter is over 0.85 times the input voltage;
- High conducting losses in the converter;
- Unbalanced or distorted input voltages, or unbalanced load, the input current and the output voltage also become distorted [49];
- Modulation technique and commutation control are more complicated;
- The protection of the matrix converter in a fault situation is not as good as that in the conventional inverter [48].

G2. Z-source converter

In 2002, Fung Zheng Peng proposed a new type of power conversion, which is called Z-source inverter. This inverter is applied to DC-to-AC and AC-to-AC energy conversion but the most application that used in ZSI is DC-to-AC power conversion. ZSI can overcome the limitations and theoretical barriers of the traditional inverters.

The basic ZSC topology consists of a special Z-network, which comprising two inductors (L1 and L2) and two capacitors (C1 and C2) connected in X shape, connected to the well-known three-phase bridge.

The DC source can be a battery, diode rectifier, thyristor converter, generator, an inductor, a capacitor, or a combination of those. Due to its low cost and high efficiency, it is well suited for wind-power generation system. However, its unidirectional nature makes it unpopular in DFIG system [48].

H2. Cycloconverter

The cycloconverter converts AC to AC directly without using intermediate DC-link. It is also called frequency converter. The high voltage AC (HVAC) and high voltage DC (HVDC) transmission systems are mainly used for power transmission. This type of converters have lower commutation and conduction losses, inherently bidirectional power flow capability and power circuit design is compact [49]. At the same time have some cons like an upper limit of output frequency, poor input power factor, and lower voltage transfer ratio and requires complex control circuitry [49].

Pros

- Lower commutation and conduction losses;
- Inherently bidirectional power flow capability.

Cons

- There is an upper limit of output frequency;
- Poor input power factor, lower voltage transfer ratio and requires complex control circuitry [49].

In order to achieve high voltage using low voltage switching devices, the multilevel converter topology uses a series of switching devices with low voltage DC sources. The renewable energy sources: wind turbine generators can be used as the multiple DC voltage sources. The proper control of the switching devices super imposed these multiple DC sources in a staircase in order to achieve high voltage at the output. Currently, there is an increasing interest in multilevel power converters, especially for medium voltage applications.

3.2.3.7 Control methods for PMSG

Due to PMSM's inherent advantages, like high power to weight ratio, low torque ripple, high efficiency, high power factor, are usually suitable for high performance servo drives. The general classification of the different control techniques for variable frequency control of PMSM drive is shown in Fig.3.10. These control methods can be divided into categories, (a) scalar (b) vector control and (c) new control techniques [50]. The scalar control technique is based on a simplified

model, which only valid for steady states. In this method the magnitude and frequency of voltage, currents, and flux linkage space vectors are controlled. The scalar control method is not suitable for transient performance. The scalar control without damper winding is not suited for PMSM, as it requires additional stabilization loop for stable operation. The stabilization loop can be formed with either of these methods, Rotor Speed perturbation, Input power or DC-link current perturbation or Flux and Power angle-stabilizing loop [51]. Therefore, scalar control of PMSM is only useful for an application, which not requires high dynamic performance. The second control method is known as vector control technique. In this method not only the magnitude and frequency of voltage, current and flux space vector is controlled, it also results in precise control of position of these space vectors. The vector control can be further subdivided into three categories: Field Oriented Control (FOC), Direct Torque Control (DTC) and Voltage Vector Control (VVC) [50-51]. The field-oriented control methods utilize the coordinate transformation of motor equation in a frame, which is, rotates in synchronism with permanent magnet flux. It allows decoupled control of, flux and torque producing component of stator current, and indirectly control motor flux and torque. The FOC uses d-axis and q-axis current controllers to get decoupled control of drive. The other vector control technique is direct torque control that allows direct control of motor flux and torque without the need of inner current control loops. The DTC uses hysteresis controller for controlling the flux and torque. This results in good dynamic performance of PMSM drive. However, the DTC suffers from various disadvantages, which include requirement of fast sampling time, need of two hysteresis controllers, variable switching frequency behavior and higher ripples in torque and flux [52].

A field orientation control (FOC) algorithm, which is the advanced scheme, is the most used technique in AC machine control applications such as a PMSG wind generation system. On the other hand, a direct torque control (DTC), is the new concept in WECSs and has many improvements in comparison with the FOC, such as the elimination of the current. Field oriented control (FOC) or vector control due to its ability of controlling the motor speed more efficiently, and the low economic cost to build an FOC system. Field oriented control also provides the ability of separately controlling the active and reactive power of the generator [50]. FOC technique has many drawbacks, such as high parameter dependence, and requires much computational resources. Furthermore, using mechanical speed sensors or observers is required to achieve FOC applications. Indeed, the rotor position is needed to give both current and voltage coordinates transformation [45].

DPC method produces a fast and robust power response without the need of complex structure and algorithms. One drawback, however, is its high-power ripple during a steady state. The active

and reactive power controllers and space-vector modulation (SVM) are combined to replace hysteresis controllers used in the original DPC drive, resulting in a fixed switching frequency of the power converter [51].

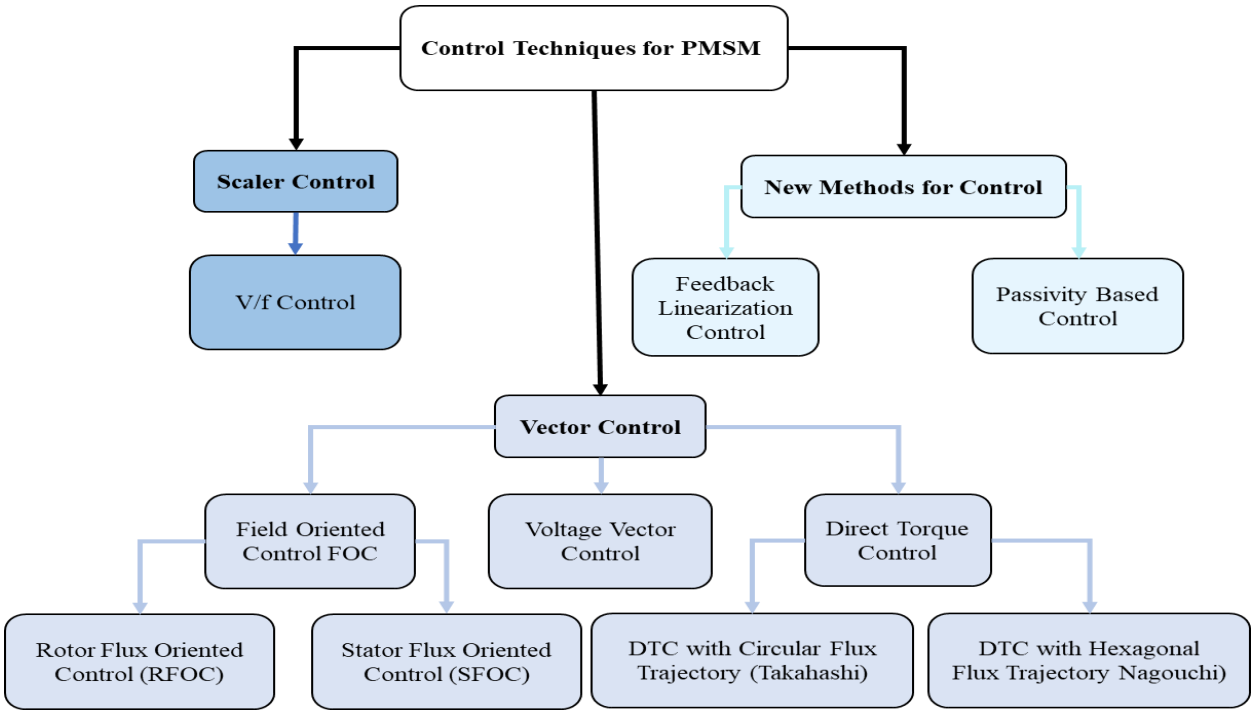

Fig.3.10 Classification of Different Control Techniques for PMSM Drive

3.6 Modeling of the wind turbine conversion chain based on PMSG

Wind energy captured by the blades was transformed into mechanic energy by wind turbine. The model studied is illustrated by Fig.3.11 that contains the wind model, an aerodynamic part and a mechanical model. The synoptic diagram summarizes the operation of such a plant.

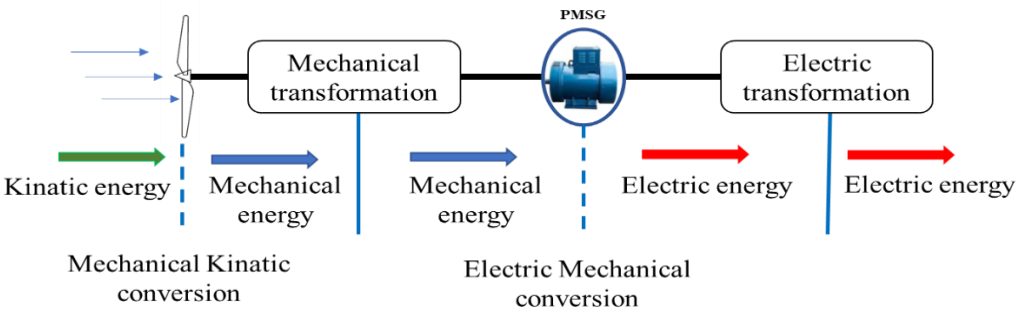

Fig.3.11 Simplified scheme of wind turbine.

3.3.1 Wind model

The wind speed model requires wind climate and geographical data of the concerned site and the period of the concerned year by the study [52]. The wind model is given by a Fourier series representation, which has as a signal consisting of a superposition of several harmonics. It is given by:

$$v = A_1 + \sum_{k=1}^{i} a_k \sin(\omega_k t) \tag{3.6}$$

Where A_1 : is the average value of the wind speed, a_k is harmonic amplitude of the order k, ω_k is pulse harmonic of order k.

3.3.2 Aerodynamic model

The principle of wind turbines in power generation is the transformation of the air kinetic energy into rotating mechanical power of the turbine rotor blades. At this moment soon enough the most common secondary wind turbine is the particular horizontal-axis propeller having three blades mounted on the top of a tower [53]. The power contained in the form of kinetic energy in the wind crossing at a speed *v*, surface A, is expressed by:

$$P_w = \frac{1}{2}\rho A v^3 \tag{3.7}$$

Where:

ρ :is the air density;

$A = \pi R^2$:is the wind turbine blades swept area in the wind;

v : is the wind speed.

The output mechanical power of wind turbine is

$$P_t = C_p * P_w = \frac{1}{2} C_p \rho A v^3 \tag{3.8}$$

Where power coefficient (Cp) represents the wind turbine power conversion efficiency. Cp is a non-linear function of Tip Speed Ratio (TSR or λ) and the blade angle β. Λ is defined as the ratio the tip speed of the turbine blades to wind speed. Λ is given by:

$$\lambda = R \frac{\Omega_t}{v} \tag{3.9}$$

Where R is blade radius, Ω_t is angular speed of the rotor. The expression for Cp(λ, β) can be described as:

$$C_p(\lambda, \beta) = \left(0.5 - 0.016 * (\beta - 2)\right) * \sin\left[(\pi * (\lambda + \frac{0.1}{18.5} - 0.3 * (\beta - 2))\right] - 0.00184 * (\lambda - 3) * (\beta - 2) \tag{3.10}$$

The theoretical maximum value of C_p is given by the Betz limit: $C_{p_max} = 0.593 = 59.3\%$

Fig.3.12 shows the variation of C_p as a function of λ, where we see that the maximum value of C_p = 0.5 is achieved for λ_{opt} = 9 and for β = 0. In order to maintain the power coefficient at its maximum we use the MPPT control.

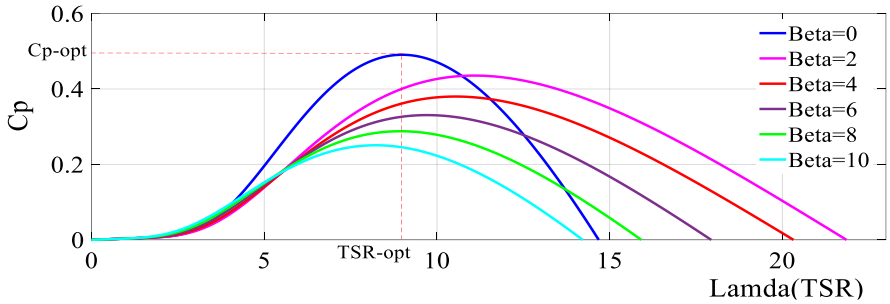

Fig.3.12 Power coefficient as a function of TSR

The rotor torque is obtained from the power received and the speed of rotation of the turbine:

$$T_t = \frac{P_t}{\Omega_t} = \frac{\rho \pi R^3 v^2}{2} C_t \tag{3.11}$$

Where Ct is the coefficient of torque. The coefficients of power and torque are related by the equation:

$$C_p(\lambda) = \lambda * C_t(\lambda) \tag{3.12}$$

3.3.3 Mechanic model

For the purpose of this simulation model, representing the fundamental resonance frequency of the drive train is sufficient and a two-mass model, as illustrated in Fig.3.13, can then model the drive train. The second resonance frequency is much higher and its magnitude is lower. All the magnitudes are considered in the fast shaft [28], [53]. Inertia J concerns the turbine side masses, while J_m concerns those of the electrical machine. These inertias do not always represent exactly the turbine and the electrical machine. If the fundamental resonance frequency comes from the blades, part of the turbine inertia is considered in J_m [53].

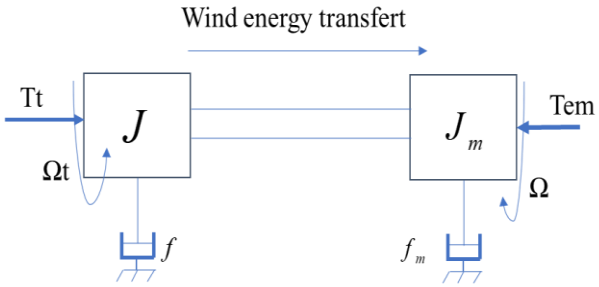

Fig.3.13 The mechanical coupling between the turbine and the electrical machine

Knowing the speed of the turbine, the torque captured by the turbine is therefore directly determined by: The differential equation, which characterizes the mechanical behavior of the turbine assembly and generator, is given by:

$$\Delta T = T_t - T_{em} = (J + J_m)\left(\frac{d\Omega_t}{dt}\right) + (f + f_m)\Omega_t \tag{3.13}$$

T_t Aerodynamic torque;

T_{em} Electromagnetic torque supplied by the generator;

J_m Inertia of the machine;

J Inertia of the turbine;

f_m Coefficient of friction of the machine;

f Friction of the blades.

We only have the mechanical parameters of the machine and the inertia of the wing. This is why in our application; we only consider the coefficient of friction associated with the generator (that of the airfoil is not taken into account).

$$J_{Tot} = (J + J_m) \approx J$$

$$f_{Tot} = (f + f_m) \approx f$$

With:

J_{Tot} Total inertia;

f_{Tot} Total friction coefficient.

Consequently, the model that characterizes the mechanical behavior of the wind chain is given by the following differential equation:

$$\Delta T = T_t - T_{em} = J\left(\frac{d\Omega_t}{dt}\right) + f\Omega_t \tag{3.14}$$

The speed value obtained by:

$$\Omega_t = \frac{\Delta T}{JS + f} \tag{3.15}$$

Fig.3.14 corresponding to this turbine modeling, it can be deduced easily from the equations given previously. The diagram shows that the speed of the turbine can be controlled by acting on two inputs: the angle of the blade β and the electromagnetic torque of the generator. The speed of wind is considered a disturbing input to this system [53].

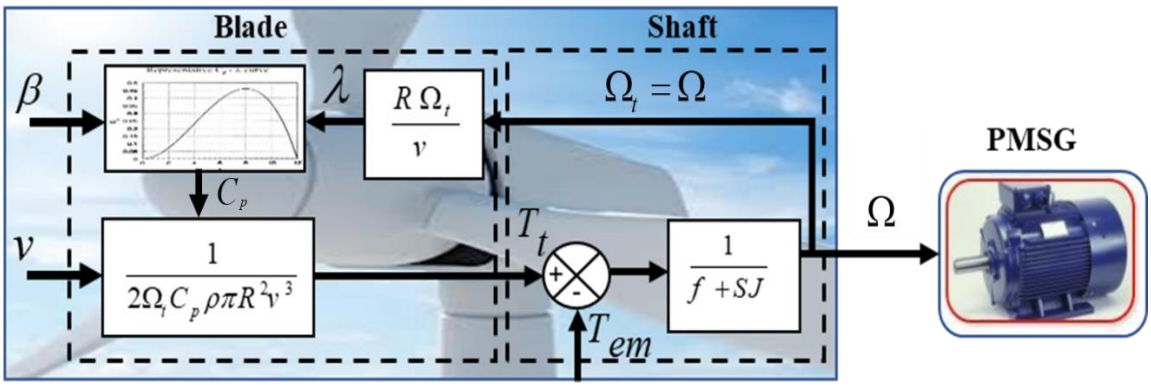

Fig.3.14 Block diagram of the turbine model

3.3.4 Modeling of PMSG

- **Electrical equations in the frame (abc)**

Matrix Voltages are expressed as a function of currents and flows by the following equations:

$$\begin{bmatrix} v_a \\ v_b \\ v_c \end{bmatrix} = R_s \begin{bmatrix} i_a \\ i_b \\ i_c \end{bmatrix} + \frac{d}{dt} \begin{bmatrix} \varphi_a \\ \varphi_b \\ \varphi_c \end{bmatrix} \tag{3.16}$$

Where:

$\begin{bmatrix} v_a & v_b & v_c \end{bmatrix}^t$:Stator phase voltage vector;

$\begin{bmatrix} i_a & i_b & i_c \end{bmatrix}^t$:Current vector of the stator phases;

$\begin{bmatrix} \varphi_a & \varphi_b & \varphi_c \end{bmatrix}^t$:Vector of the total fluxes;

R_s: Resistance of the stator phases.

The total flux in each phase can be written by the equations which follow

$$\begin{cases} \varphi_a = (L_s - M)\, i_a + \varphi_f \cos(\theta) \\ \varphi_b = (L_s - M)\, i_b + \varphi_f \cos\left(\theta - \frac{2\pi}{3}\right) \\ \varphi_c = (L_s - M)\, i_c + \varphi_f \cos\left(\theta + \frac{2\pi}{3}\right) \end{cases} \tag{3.17}$$

Where:

φ_{abc} : The flows of the axes (a, b, c);

φ_f : Flux of the permanent magnet;

Ls: the inductance of the stator phases;

M : PMSG mutual inductance between two adjacent phases (±2π/3 electrical shift);

L_c : (Ls- M): Cyclic inductance;

θ : The electrical angle designating the position of the rotor relative to the stator.

- **Electrical equations in Park's frame of reference (d q)**

PMSG model can be written in the d-q synchronously rotating reference frame, by the following equation system [53].

$$\begin{cases} V_d = R_s i_d + L_d \frac{di_d}{dt} - L_q i_q \omega_p \\ V_q = R_s i_q + L_q \frac{di_q}{dt} - L_d i_d \omega_p + \sqrt{\frac{3}{2}} \varphi_f \omega_p \end{cases} \tag{3.18}$$

Fig.3.15 shows the equivalent circuit of the PMSG on the dq-rotating reference frame.

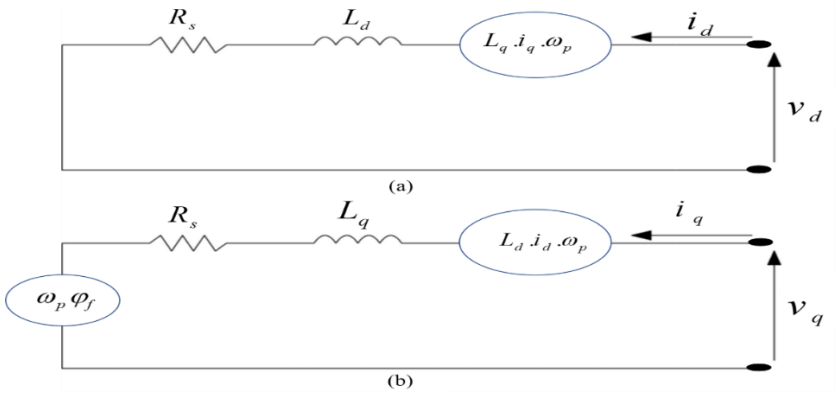

Fig.3.15 Equivalent circuit of PMSG in the synchronous frame

The model of the synchronous generator with permanent magnets thus obtained, can write in the following form:

$$\begin{cases} V_d = -R_s i_d - L_d \dfrac{di_d}{dt} + L_q i_q \omega_p \\ V_q = -R_s i_q - L_q \dfrac{di_q}{dt} - L_d i_d \omega_p + \sqrt{\dfrac{3}{2}} \varphi_f \omega_p \end{cases} \tag{3.19}$$

$\sqrt{\frac{3}{2}} \varphi_f \omega_p$: Electromotive force induced only on the "q axis;

ω_p: Electric angular velocity or electric pulsation;

$L_q i_q \omega_p , L_d i_d \omega_p$: Coupling terms between the axes (non-linearity terms).

The modified Park transformation used, retains the power in both "abc" and "dq" domains. Therefore, the electric power will be the same:

$$\begin{cases} P_e(abc) = T_{em} * \Omega \\ P_e(dq) = \sqrt{\dfrac{3}{2}} * \varphi_f * \omega_p * i_q \end{cases} \tag{3.20}$$

The "PMSG" model will be governed by the following system of equations [54]:

$$\begin{cases} V_d = -L_d \dfrac{di_d}{dt} + L_q i_q \omega_p \\ V_q = -R_s i_q - L_q \dfrac{di_q}{dt} + \sqrt{\dfrac{3}{2}} \varphi_f \omega_p \\ T_{em} = \sqrt{\dfrac{3}{2}} P \varphi_f i_q \\ T_m - T_{em} - T_f = J \dfrac{d\Omega}{dt} \end{cases} \tag{3.21}$$

Ω : Mechanical angular speed depend on the frequency and number of poles $\Omega = 2\pi \frac{f}{p}$;

P: Pairs of poles;

ω_p : Electric angular velocity or electric pulsation, $\omega_p = \Omega * p$;

T_m Engine torque driving the PMSG;

T_f Friction torque, $T_f = f\,\Omega$.

So, the Simulink based models of the drive train and the generator are given in Fig.3.16.

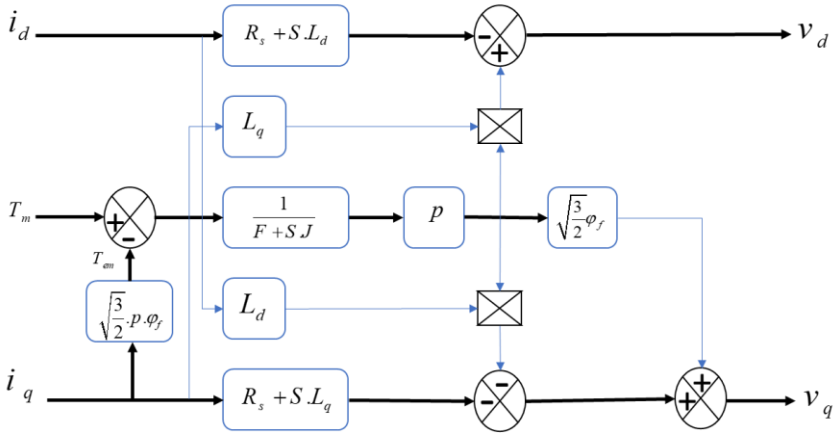

Fig.3.16 Block diagram of the PMSG model in d-q reference

3.4 System description for the proposed system for PMSG

The general structure of the vector control of PMSGs is schematized in Fig.3.17, the principle of vector control with voltage supply and current control makes it possible to impose the torque [58]. The torque is controlled by the component in quadrature, i_q^* is therefore proportional to the torque requested. The vector control then amounts to controlling the two components id and iq of the stator current by imposing the appropriate voltages v_d and v_q. Therefore, for impose the voltages v_d and v_q, it will suffice to impose the reference voltages v_d^* and v_q^* at the input of the converter. Using regulators PI for each of the current loop, obtaining reference voltages makes it possible to maintain the direct and quadrature currents close to their reference values i_d^* and i_q^*.

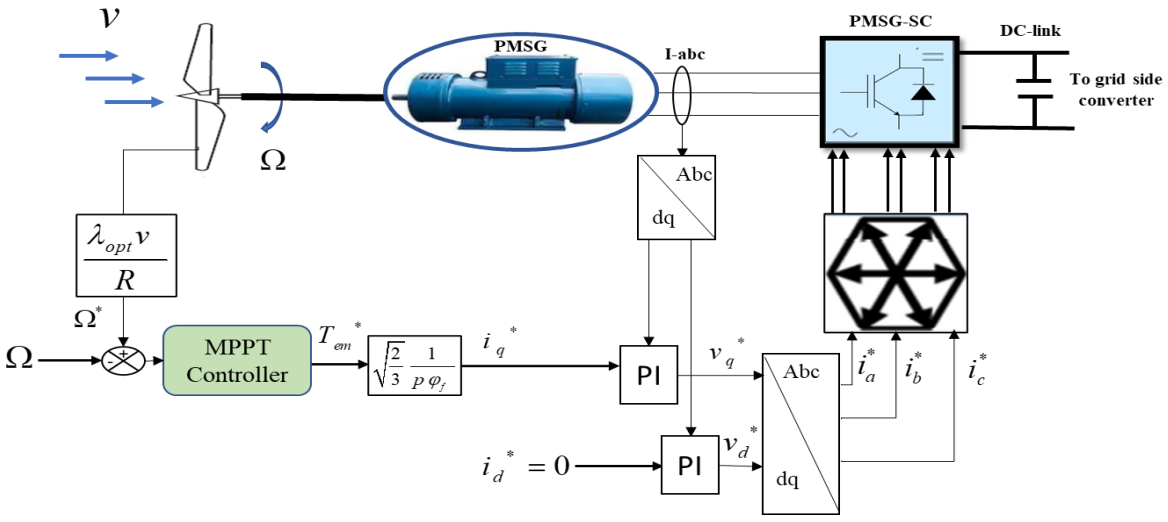

Fig.3.17 Global schematic on the generator side

3.4.1 Generator side controller

The generator side converter is mainly used to control the wind turbine speed in order to extract maximum power from the wind. In this case, the turbine should operate at maximum power coefficient. Therefore, it is necessary to keep the generator rotor speed at an optimum value of tip speed ratio. The PMSG rotor speed should be adjusted to follow the change of speed and consequently adjust the turbine speed at wind variations. The PMSG speed control can be implemented through the generator side converter [51]. This allows the generator to rotate freely depending on wind variation. Fig.3.17 shows the schematic control diagram of the generator side converter.

Generally, the MPPT control is applied when the wind speed is below the rated speed, and then, the pitch angle is constant. While if wind speed is greater than the rated speed, then the output power of the PMSG is controlled using pitch angle control.

This chapter presents a fuzzy logic controller (FLC) with a conventional PI to control a three-phase permanent-magnet synchronous generator-based wind turbine during wind speed variations.

For MPPT in WECS having three main algorithms are TSR, Power signal feedback (PSF) and Hill Climbing search method. However, this traditional technique used in WESC is having their own problems such as high frequency jitter, low precision and estimation levels of faults also falls down. There are many more active techniques are desperately trying to get MPPT point for WECS at higher standard levels. In proposed chapter the computer intelligence method used along with the Fuzzy logic control.

This study focusses on which MPPT controllers used to obtain maximum possible power in WECS, while applying the PI and fuzzy-PI controllers. We used the same conditions for both methods because it gave reasonable results. In this chapter, we will show how to build a fuzzy regulator to the speed control of the MSAP. Simulation results will also be presented and a comparison between the classic PI regulator and fuzzy-PI will be carried out for show the improvement of the dynamic behavior of the speed of the MSAP to demonstrate the performance of aforementioned WECS.

3.4.1.1 MPPT based PI control

In fact, when the wind speed is lower than the rated value, it is important for the WT to follow quickly the wind speed change in order to provide a maximum power to the grid. In other word operating point of WT changes rapidly, according to the change of the wind speed, so that is why it is necessary to integrate a MPPT strategy in to the WT in order to maintain its operating point around the optimal value. Which corresponds to λ_{opt} or C_{p-opt} of the 10 KW WECS model studied,

despite of the wind speed change. MPPT based PI the first proposed MPPT strategy structure is given in Fig.3.18.

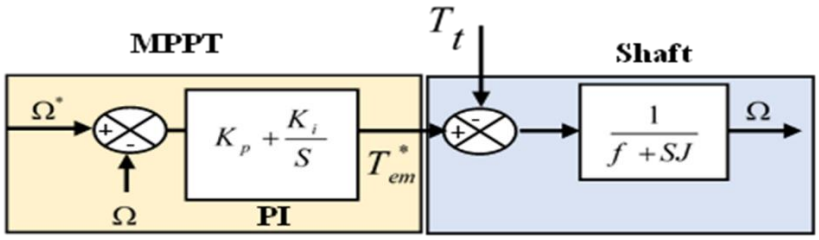

Fig.3.18 PI-based MPPT control

Adjusting the speed requires the addition of a PI corrector to optimize system performance. The dynamics of the system is governed by a first order differential equation, characterized by a time constant only:

$$\frac{\Omega}{\Delta T} = \frac{1}{f + JS} \tag{3.22}$$

3.4.1.2 MPPT based FL-PI control

In order to maximize the amount of energy produced from a wind turbine according to the wind speed fluctuations, the WECS needs a controller able of ensuring its operation mode around the optimal operating point. In this chapter, a MPPT strategy is proposed, to extract a maximum power from a variable speed wind turbine based on permanent magnet synchronous machine PMSG by using fuzzy logic control. The proposed strategy is based upon the monitoring and the judgement of the power rotational speed characteristic in the aim to find the optimum rotational speed upon the monitoring of the produced power [58]. The machine drive is used to convert the motion of rotation available at its shaft to a power electric. A converter side electrical machine is used to control the WECS. The basic structure converter side electrical machine of a fuzzy speed controller is given by Fig.3.19.

However, at the same time fast and dynamic response is also required and so fuzzy with Proportional integral controller (PI) is attached to the MPPT controller, which continuously tracks the maximum power based on all the environmental conditions.

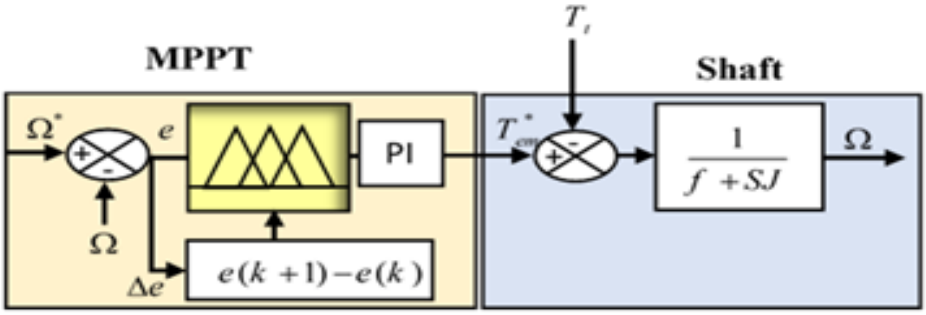

Fig.3.19 Fuzzy-based MPPT control

Designing a fuzzy regulator for controlling electric drives requires the choice of parameters. Fuzzification can be represented as membership function μ that associates with each element of the universe of discourse X, in the interval [-1, 1]. The universe of discourse is subdivided into five fuzzy sets characterized by the following standard designations (Negative Big noted NB; Negative Small noted NS; Equal Zero noted ZE; Positive Small noted PS; Positive Big noted PB) for the membership functions, we chose for each variable the triangular shapes and trapezoidal as shown in the following Fig.3.20 [9] [58].

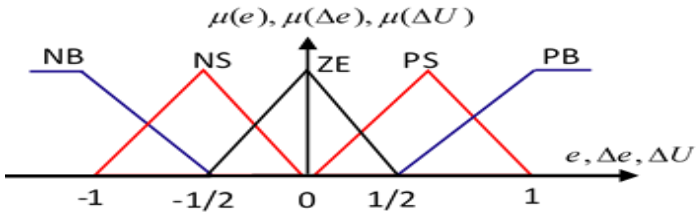

Fig.3.20 Membership functions of various variables

From the study of the behavior of the system, Fuzzy rule base is a collection of multiple IF-THEN rules; We can establish the ordering rules. These can be represented by the following inference matrix:

Table.3.5 Fuzzy rules inference matrix.

E Δe	NB	NS	ZE	PS	PB
NB	NB	NB	NS	NS	ZE
NS	NB	NS	NS	ZE	PS
ZE	NS	NS	ZE	PS	PB
PS	NS	ZE	PS	PS	PB
PB	ZE	PS	PS	PB	PB

The two inputs of the fuzzy controller are the speed error and its variation. The speed error noted e defined by defined by:

$$e = \Delta\Omega = \Omega^{*} - \Omega \tag{3.23}$$

The variation of the speed error noted Δe is defined by:

$$\Delta e = e(k+1) - e(k) \tag{3.24}$$

The output of the FL regulator corresponds to the electromagnetic torque denoted ΔU.

3.5 Model of three-phase rectifier

To achieve The PWM technique refers to a special switching scheme of the six power transistors of a 3-phase power converter. It generates minimum harmonic distortion to the current waveform. In the system presented in Fig.3.21, a SVPWM rectifier is used. This converter is supplied by three-phase voltage source and it provides a DC voltage. Neglecting the internal voltage drop during conduction, and switching transients during turn-on and turn-off, the rectifier can be modeled as shown in Fig.3.21.

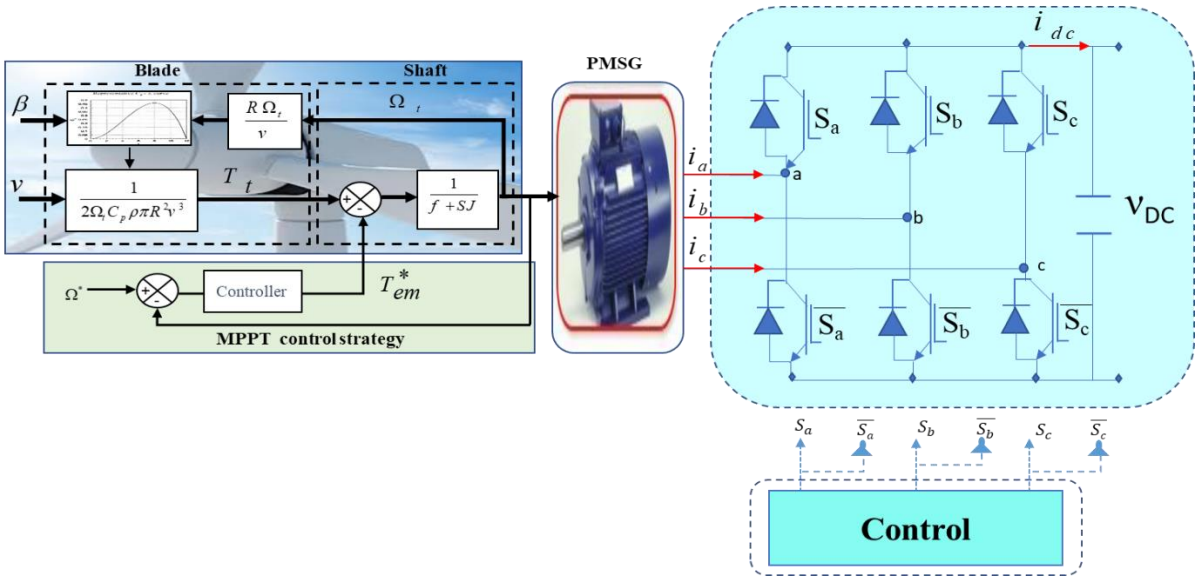

Fig.3.21 Generator side converter for wind turbine system

The relationship between the switching variable vector [a, b, c]^t and the line-to-line voltage vector [V_{ab} V_{bc} V_{ca}]^t is given by the following equation [52]:

$$\begin{bmatrix} V_{ab} \\ V_{bc} \\ V_{ca} \end{bmatrix} = V_{dc} \begin{bmatrix} 1 & -1 & 0 \\ 0 & 1 & -1 \\ -1 & 0 & 1 \end{bmatrix} \begin{bmatrix} S_a \\ S_b \\ S_c \end{bmatrix} \tag{3.25}$$

Where :

S_a, S_b, S_c: Switching state of the converter.

Wind Energy system with full power converter using Space Vector PWM inverter topology is implemented. A two level Space Vector PWM Inverter topology is selected here. The SVPWM technique is one of the most popular PWM techniques due to the use of higher DC bus voltage. The concept of SVPWM relies on the representation of AC bus quantities as space vectors. Space vector simultaneously represents three phase quantities as one rotating vector, hence each phase is not considered separately.

Space Vector Modulation (SVM) is one of the real-time modulation techniques and is widely used for digital control of voltage source inverters. This section presents the principle and implementation of the space vector modulation for the two-level inverter.

The circuit model of a typical two-level three-phase voltage source PWM inverter as depicted, The six power switches (three in upper leg and three in lower leg) are controlled by the switching variables $S_a, \overline{S_a}, S_b, \overline{S_b}$ S_c and $\overline{S_c}$ which decides the shape of the output. When an upper transistor is switched on, the corresponding lower transistor is switched off. The principle of SVM is based on the fact that there are only eight possible switch combinations for a three-phase inverter. The basic inverter switch states are shown in the table (000, 001, …. ,111) [53-56].

In this modulation technique the three phase quantities can be transformed to their equivalent two-phase quantity either in synchronously rotating frame or stationary frame. From these two-phase components, the reference vector magnitude can be found and used for modulating the inverter output. The process of obtaining the rotating space vector is explained in the following section, considering the stationary reference frame [53-56].

When this three-phase voltage is applied to the machine it produces a rotating flux and this rotating resultant flux can be represented as single rotating voltage vector. To implement the space vector PWM, the voltage equations in the abc reference frame can be transformed into the dq reference frame that consists of the horizontal (d) and vertical (q) axes as depicted Fig.3.22.

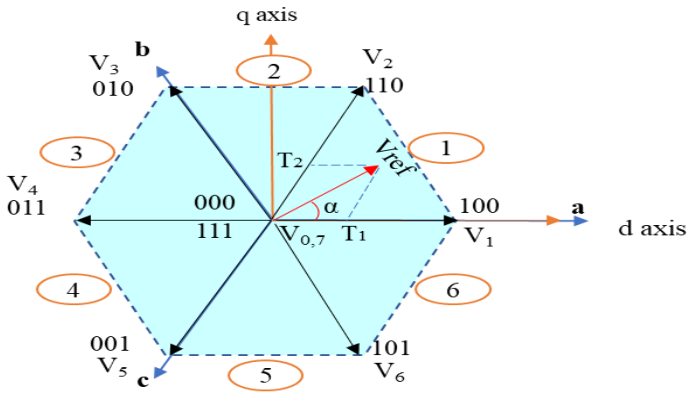

Fig.3.22 Basic switching vectors and sectors.

The SVPWM passes through four main stages, the first of which involves the calculation of vd, vq and vd,qref. The second stage concerns the calculation of the sector number. The third stage involves the calculation of the switching time signals, while during the final stage the switching sequences are calculated [58].

The active (P) and reactive (Q) powers of PMSG are respectively:

$$\begin{cases} p = v_d^* i_d^* + v_q^* i_q^* \\ Q = v_d^* i_q^* + v_q^* i_d^* \end{cases} \tag{3.26}$$

3.6 Results and discussion

In this chapter, we present a comparative study of two different MPPT methods for a wind energy system based on permanent magnet synchronous generator (PMSG). These techniques are: classical (PI) control and the robust (FL-PI). These methods have been developed with the aim of comparing their performance on the wind-system energy efficiency, according to the response time, the maximum power to be achieved and the system behavior during the optimal power point tracking MPP. For a better analysis study, we simulated the system under variable wind speed conditions.

A simulation is performed in MATLAB/Simulink for the proposed system in the aim to investigate the performances of the presented strategy. The characteristics of the simulated system are given in Table.3.6.

WECS is subjected to a wind profile given by Fig.3.23(a) of five seconds of time interval; Fig.3.23 (b, c and d) show respectively, the tip speed ratio, power coefficient, the PMSG speed obtained by the proposed strategies PI and FL-PI controllers respectively. The FL-PI controller is compared in similar operating conditions to the well-known PI control technique, which is widely used in the industry. Both controllers are tuned to reach similar transient response and overall performance in nominal case for a fair comparison. Next, the superiority of the FL-PI over conventional control technique is shown clearly in these results. The performances of the fuzzy regulator presented are evaluated at through an application on the synchronous machine with permanent magnet for the speed of rotation of the wind turbine drive, which corresponds to the optimum point linked to the optimum specific speed λ_{opt} and to the maximum power coefficient Cp_{max}. The rotational speed of the generator follows very well the immediate changes of the wind speed in order to bring the operating point around its optimal value where WECS is at its high level of efficiency. This is verified by the power efficiency and tip speed ration around their nominal value despite of the changes rapidly of the wind speed (Cp_{opt}=0.5, λ_{opt}=9). As showon, the parameters simulated of WECS exhibit the fluctuations for reason: the dynamic rapid of the system brought by the MPPT-FL-PI compared to the traditional PI strategy, the MPPT-FL-PI strategy allows WT to respond rapidly to wind speed changes in order to extract a maximum energy. In term of power coefficient, the proposed strategy captures 2% more energy than the PI strategy control.

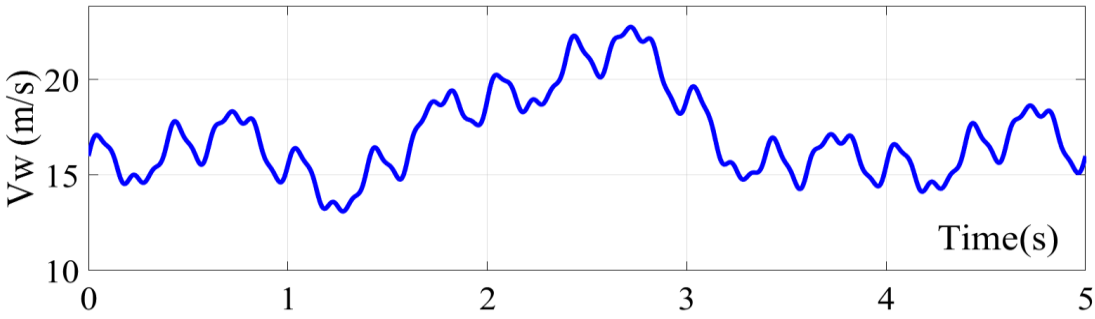

(a) Wind speed

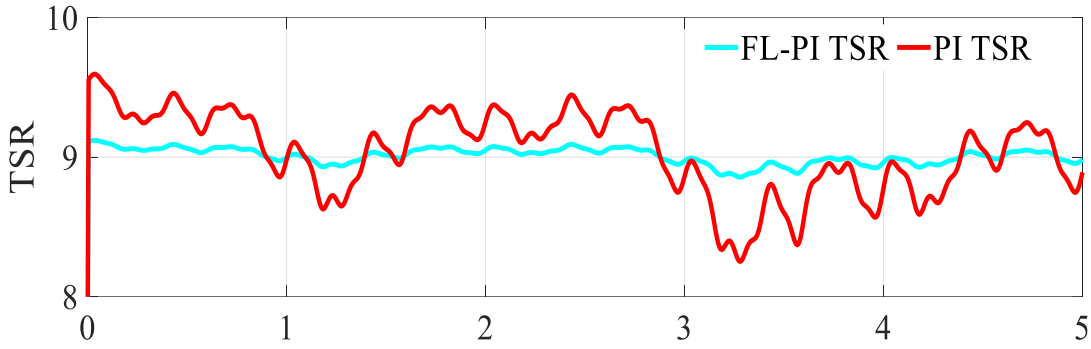

(b) PI and FL-PI TSR

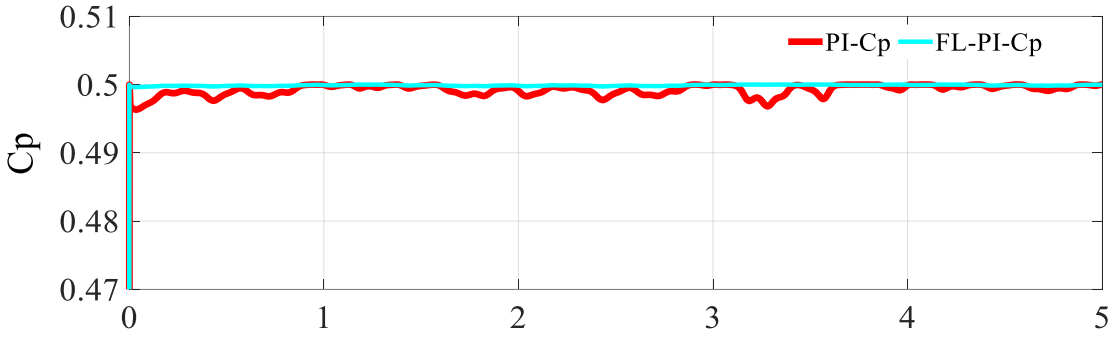

(c) PI and FL-PI power coefficient

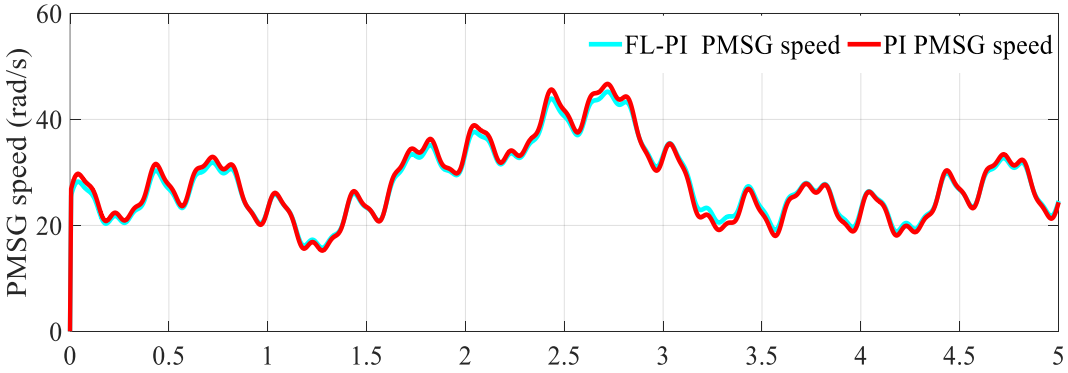

(d) PI and FL-PI PMSG speed

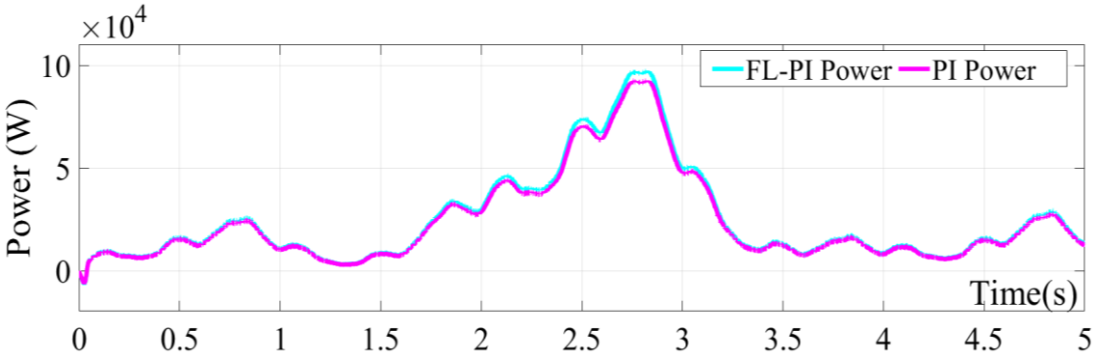

(e) The output power respense produiced by the PMSG generator

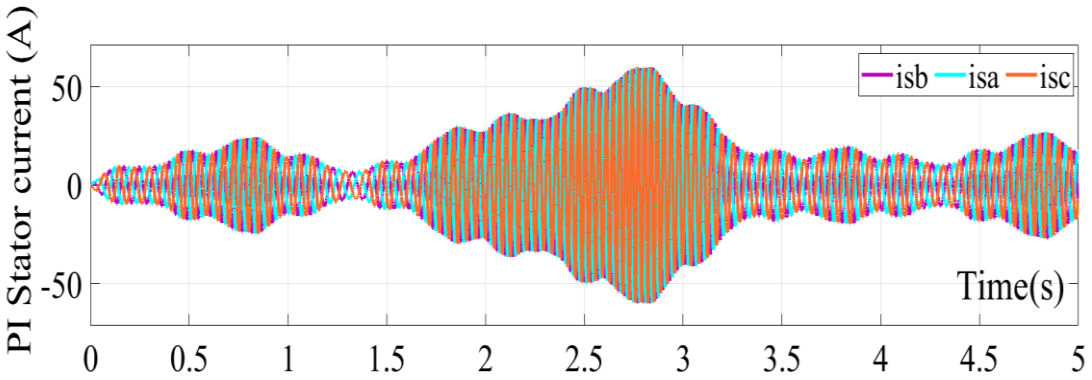

(f) PI three phase stator output current

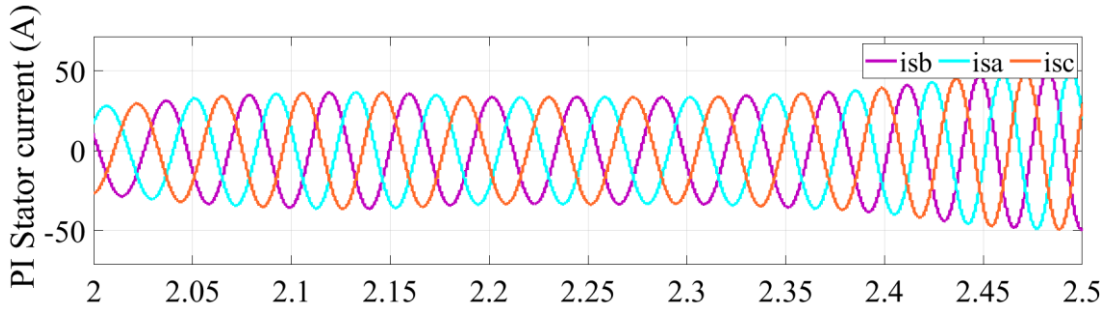

(g) Zoom of three PI three phase stator output current

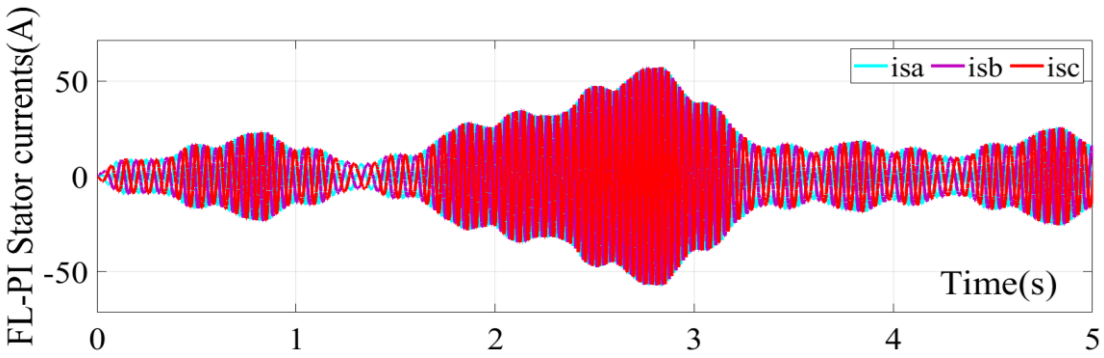

(h) FL-PI three phase stator output current

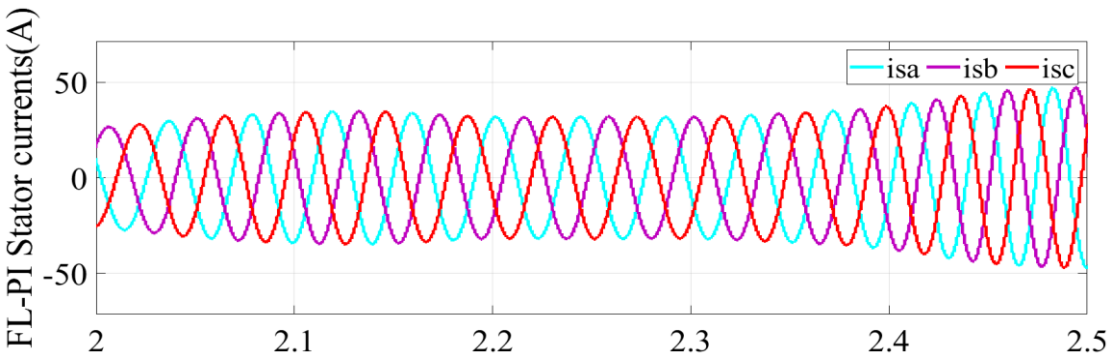

(i) Zoom of FL-PI three phase stator output current

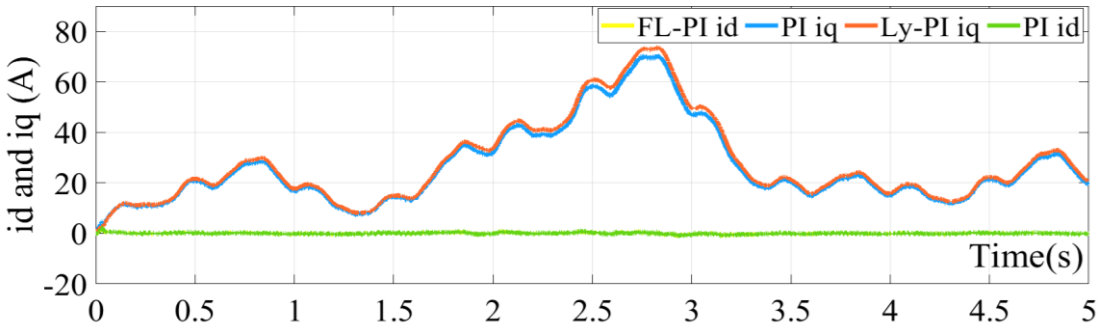

(j) Currents id & iq

Fig.3.23 Simulation result

Fig.3.23(from e to j) illustrate the wind turbine power, the three phase stator currents and id, iq currents for the two MPPT methods. As it can be seen in the figures, both of the two MPPT methods successfully track the optimum power point under fluctuating wind speed. But, the trajectory of the a FL-PI method is very close to the optimal profile compared with the PI MPPT method, thus in addition to higher dynamic response, the FL-PI method provides the best possible power efficiency for the WECS. Simulation results demonstrate superiority of a FL-PI method in tracking the MPP with the minimum possible time and the highest efficiency. It is followed by the PI method, which has nearly similar characteristic from the efficiency and time response.

3.7 Conclusion

As the WES has become a center of attraction for the researcher and highly researched area. A comparative and concise on different converter topologies, generators and control schemes has been achieved through this chapter. The different wind turbines along with the basic wind-energy system background are discussed. It also presented the various technical aspects related to WES, including types of electrical generator, topologies of power electronics converter and different control schemes. This chapter also recommends the use of multilevel converter in WES due to its advantageous features.

The main objective of this chapter was modelling and fuzzy control optimization of a Permanent Magnet Synchronous Generator (PMSG), as well as the contribution it could make in a variable

speed wind-power system. For this, we have dealt with the aspects that encompass the development of such a system: the state of the art of wind energy conversion systems, modelling, operational analysis and control.

This study allowed us to carry out a complete and global modeling of a wind power conversion. This modeling is distinguished mainly by the approach. Different which was made of the mechanical part which uses aerodynamic calculations for determine the relationships between wind speed, torque and propeller speed. It was all designed around a PMSG.

In this chapter, a comparative test of two MPPT controller design for a WECT is achieved to operate at the MPP. The MPPT controller plays a remarkable role to enhance the reliability and performance of the system. In order to operate the wind energy system at maximum efficiency and thus reduce losses, we compared the proposed MPPT construction with the PI controller. The MPPT controller implemented using FL-PI has a much better performance, the overall system efficiency, reliability and performance of the system have been improved for high-performance PMSM drives. A fuzzy controller is combined with PI, in this control system to cope with structured and unstructured uncertainties, which offer robustness to variation condition or parameters.

The simulation results corresponding to this control algorithm show that the variations in the speed of the generator are adapted to the variation in the speed of the wind. The extraction of the maximum power from the wind is always complete, in imposing a reference torque equal to the torque of the generator. While almost negligible error between the measured electromagnetic torque and estimated by PMSG. In this case, a maximum power coefficient and a speed ratio optimal have maintained, therefore the energy efficiency is almost optimal for the whole wind speed range.

Finally, the results obtained for the two MPPT control strategies (FL-PI and PI) show good static and dynamic performance, a desirable response time offered by the two techniques; which justifies the choice of the MPPT method for the control of the turbine.

The active power delivered by the stator has the same shape as the electromagnetic torque and the reactive power is zero since the machine operates at unity power.

The FL control strategy will be used as an alternative solution for systems operating with uncertainties and external disruptions in varying conditions unlike other control PI approaches. Results suggest good performance, steady state, and standstill conditions for output rotor speed tracking in transient, achieving the precision of control needed for high-performance. Comparison results against a conventional controller, FC controller shows better robustness to parameters variation and friction nonlinearities. It is noteworthy that this performance is achieved the

precision of control needed for high-performance, and their inherent parallelism makes them a good candidate for implementation in real-time PMSM drive systems.

Table.3.6 Parameters for a WECS

Parameters of the system	WECS Parameters
Inductance of the stator phases on the d, q axis	L_d=L_q=12.5 mH
Rotor inertia [kg/m^2]	J=16
Friction of the blades [kgm/rd]	f =0.01
Stator resistance [Ω]	R_s=1.137
Number of pole pairs	P=6
Radius of the blades [m]	R=3.5
Optimal Tip speed ratio	λ_{opt} =9
Air density [Kg/m^3]	ρ =1.2
Flux of the permanent magnet	φ_f =0.9
Flux maximal de l'aimant [Wb]	φ_{max} =0.15
Optimal power coefficient	0.5
Optimal TSR λ	9
PMSG rated power	10KW
Rated wind speed	20m/s
Pitch Angle, β	0°
Switching frequency f_z	3e^3
Kp1=Kp2	90
Ki1=Ki2	900

Parameters of the system	MPPT PI Parameters
Kp	**105**
Ki	180
FL-Kp	105
FL-Ki	180

Parameters of the system	PMSG PI Control Parameters
Kp1=Kp2	**90**
Ki1=Ki2	900

References

[1] DJERIRI, Youcef, et al. Commande directe du couple et des puissances d'une MADA associée à un système éolien par les techniques de l'intelligence artificielle. 2015. Doctoral thesis.

[2] KUMAR, Dipesh et CHATTERJEE, Kalyan. A review of conventional and advanced MPPT algorithms for wind energy systems. Renewable and sustainable energy reviews, 2016, vol. 55, p. 957-970.

[3] BABU, Bindhu et DIVYA, S. Comparative study of different types of generators used in wind turbine and reactive power compensation. IOSR Journal of Electrical and Electronics Engineering (IOSR-JEEE), 2017, p. 2278-1676.

[4] BAROUDI, Jamal A., DINAVAHI, Venkata, et KNIGHT, Andrew M. A review of power converter topologies for wind generators. Renewable energy, 2007, vol. 32, no 14, p. 2369-2385.

[5] KARTHI, K., RADHAKRISHNAN, R., BASKARAN, J. M., et al. A review of maximum power point tracking controls and wind electric generators. In : 2018 International Conference on Inventive Research in Computing Applications (ICIRCA). IEEE, 2018. p. 1122-1126.

[6] PENA, Ruben, CLARE, J. C., et ASHER, G. M. Doubly fed induction generator using back-to-back PWM converters and its application to variable-speed wind-energy generation. IEE Proceedings-Electric power applications, 1996, vol. 143, no 3, p. 231-241.

[7] SATTAR, A. A., MAREI, M. I., et BADR, A. O. Back-to-back converters with doubly fed induction generators for wind energy scheme. In : The 2010 International Conference on Computer Engineering & Systems. IEEE, 2010. p. 114-119.

[8] MEGHNI, Billel, SAADOUN, Abdallah, DIB, Djalel, et al. Effective MPPT technique and robust power control of the PMSG wind turbine. IEEJ Transactions on Electrical and Electronic Engineering, 2015, vol. 10, no 6, p. 619-627.

[9] M. E. Azzaoui and H. Mahmoudi, 'Fuzzy-PI control of a doubly fed induction generator-based wind power system', IJAAC, vol. 11, no. 1, p. 54, 2017, doi: 10.1504/IJAAC.2017.080819.

[10] YANG, Lihui, XU, Zhao, OSTERGAARD, Jacob, et al. Advanced control strategy of DFIG wind turbines for power system fault ride through. IEEE Transactions on power systems, 2011, vol. 27, no 2, p. 713-722.

[11] TORKI, Wafa, GROUZ, Faten, et SBITA, Lassaad. Vector control of a PMSG direct-drive wind turbine. In : 2017 International Conference on Green Energy Conversion Systems (GECS). IEEE, 2017. p. 1-6.

[12] ELBEJI, Omessaad, HAMED, Mouna Ben, et SBITA, Lassaad. PMSG wind-energy conversion system: Modeling and control. International Journal of Modern Nonlinear Theory and Application, 2014, vol. 2014.

[13] BAROUDI, Jamal A., DINAVAHI, Venkata, et KNIGHT, Andrew M. A review of power converter topologies for wind generators. Renewable energy, 2007, vol. 32, no 14, p. 2369-2385.

[14] YANG, Lihui, XU, Zhao, OSTERGAARD, Jacob, et al. Advanced control strategy of DFIG wind turbines for power system fault ride through. IEEE Transactions on power systems, 2011, vol. 27, no 2, p. 713-722.

[15] ELSAKKA, Mohamed M., INGHAM, Derek B., MA, Lin, et al. CFD analysis of the angle of attack for a vertical axis wind turbine blade. Energy Conversion and Management, 2019, vol. 182, p. 154-165.

[16] DURSUN, Emre Hasan et KULAKSIZ, Ahmet Afsin. Maximum power extraction from PMSG based VS-WECS by using variable Step-Size P&O Method. In: 2019 third International Symposium on Multidisciplinary Studies and Innovative Technologies (ISMSIT). IEEE, 2019. p. 1-5.

[17] ALI, Mustafa M., YOUSSEF, Abdel-raheem, ALI, Ahmed S., et al. Variable step size PO MPPT algorithm using model reference adaptive control for optimal power extraction. International Transactions on Electrical Energy Systems, 2020, vol. 30, no 1, p. e12151.

[18] MARTEN, David, WENDLER, Jan, PECHLIVANOGLOU, Georgios, et al. QBLADE: an open source tool for design and simulation of horizontal and vertical axis wind turbines. International Journal of Emerging Technology and Advanced Engineering, 2013, vol. 3, no 3, p. 264-269.

[19] BEAINY, Anissia, MAATOUK, Chantal, MOUBAYED, Nazih, et al. Comparison of different types of generator for wind-energy conversion system topologies. In: 2016 third international conference on renewable energies for developing countries (REDEC). IEEE, 2016. p. 1-6.

[20] THONGAM, Jogendra Singh et OUHROUCHE, Mohand. MPPT control methods in wind-energy conversion systems. Fundamental and advanced topics in wind power, 2011, vol. 15, p. 339-360.

[21] BARAN, Janusz et JĄDERKO, Andrzej. An MPPT control of a PMSG-based WECS with disturbance compensation and wind speed estimation. Energies, 2020, vol. 13, no 23, p. 6344.

[22] ELTAMALY, Ali M., ALOLAH, A. I., FARH, Hassan M., et al. Maximum power extraction from utility-interfaced wind turbines. New Developments in Renewable Energy, 2013, p. 159-192.

[23]S. H. Hosseini, A. Farakhor, and S. K. Haghighian, 'Novel algorithm of maximum power point tracking (MPPT) for variable speed PMSG wind generation systems through model predictive control', in 2013 8th International Conference on Electrical and Electronics Engineering (ELECO), Nov. 2013, pp. 243–247, doi: 10.1109/ELECO.2013.6713840.

[24]G. Ji and K. Ohyama, 'MPPT control of Variable Speed Wind Power Generation System using Switched Reluctance Generator and AC-AC converter', in 2020 23rd International Conference on Electrical Machines and Systems (ICEMS), Nov. 2020, pp. 1012–1016, doi: 10.23919/ICEMS50442.2020.9290911.

[25]A. Kadri, H. Marzougui, and F. Bacha, 'MPPT control methods in wind energy conversion system using DFIG', in 2016 4th International Conference on Control Engineering Information Technology (CEIT), Dec. 2016, pp. 1–6, doi: 10.1109/CEIT.2016.7929115.

[26]X. Zhi, D. Xiangjun, and L. Lei, 'MPPT for wind power system with switched reluctance generator', in 2018 13th IEEE Conference on Industrial Electronics and Applications (ICIEA), May 2018, pp. 1420–1424, doi: 10.1109/ICIEA.2018.8397932.

[27] Baljit Singh,A K Bhardwaj 'Performance Analysis of DFIG based Wind Turbine using Back to Back Converter'. Indian Journal of Science and Technology. June 2007, vol. 8, no 17, p. 0974-6846. DOI:10.15662/IJAREEIE.20156.0506132

[28] PENALBA, Markel, SELL, Nathan P., HILLIS, Andy J., et al. validating a wave-to-wire model for a wave energy converter—Part I: The Hydraulic Transmission System. Energies, 2017, vol. 10, no 7, p. 977.

[29] MOUSA, Hossam HH, YOUSSEF, Abdel-Raheem, and MOHAMED, Essam EM. State of the art perturb and observe MPPT algorithms based wind energy conversion systems: A technology review. International Journal of Electrical Power & Energy Systems, 2021, vol. 126, p. 106598.

[30] GOUABI, Hicham, HAZZAB, Abdeldjebar, HABBAB, Mohamed, et al. Experimental implementation of a novel scheduling algorithm for adaptive and modified P&O MPPT controller using fuzzy logic for WECS. International Journal of Adaptive Control and Signal Processing, 2021, vol. 35, no 9, p. 1732-1753.

[31] KUMAR, Dipesh and CHATTERJEE, Kalyan. A review of conventional and advanced MPPT algorithms for wind energy systems. Renewable and sustainable energy reviews, 2016, vol. 55, p. 957-970.

[32] A. E. Yaakoubi, A. Asselman, A. Djebli, and E. H. Aroudam, 'A MPPT Strategy Based on Fuzzy Control for a Wind Energy Conversion System', Procedia Technology, vol. 22, pp. 697–704, Jan. 2016, doi: 10.1016/j.protcy.2016.01.145.

[33] RAM, J. Prasanth, RAJASEKAR, N., et MIYATAKE, Masafumi. Design and overview of maximum power point tracking techniques in wind and solar photovoltaic systems: A review. Renewable and Sustainable Energy Reviews, 2017, vol. 73, p. 1138-1159.

[34] KAHLA, Sami, SOUFI, Youcef, SEDRAOUI, Moussa, et al. Maximum power point tracking of wind energy conversion system using multi-objective grey wolf optimization of fuzzy-sliding mode controller. International Journal of Renewable Energy Research, 2017, vol. 7, no 2, p. 926-936.

[35] ARDJAL, Aghiles, MANSOURI, Rachid, et BETTAYEB, Maamar. Fractional sliding mode control of wind turbine for maximum power point tracking. Transactions of the Institute of Measurement and Control, 2019, vol. 41, no 2, p. 447-457.

[36] H. Chaoui and P. Sicard, 'Adaptive Fuzzy Logic Control of Permanent Magnet Synchronous Machines With Nonlinear Friction', IEEE Transactions on Industrial Electronics, vol. 59, no. 2, pp. 1123–1133, Feb. 2012, doi: 10.1109/TIE.2011.2148678.

[37] AHMED, Ashraf, RAN, Li, et BUMBY, Jim R. New constant electrical power soft-stalling control for small-scale VAWTs. IEEE transactions on energy conversion, 2010, vol. 25, no 4, p. 1152-1161.

[38] MOHAMMADI, Ebrahim, FADAEINEDJAD, Roohollah, et MOSCHOPOULOS, Gerry. A study of power electronic based stall and electromechanical yaw power control strategies in small-scale grid-connected wind turbines. In : 2018 IEEE applied power electronics conference and exposition (APEC). IEEE, 2018. p. 2323-2329.

[39] MOHAMMADI, Ebrahim, FADAEINEDJAD, Roohollah, SHARIATPANAH, Hamid, et al. Performance evaluation of yaw and stall control for small-scale variable speed wind turbines. In : 2017 IEEE 30th Canadian Conference on Electrical and Computer Engineering (CCECE). IEEE, 2017. p. 1-4.

[40] NGUYEN, Luat T. Simulator study of stall/post-stall characteristics of a fighter airplane with relaxed longitudinal static stability. National Aeronautics and Space Administration, 1979.

[41] SHARIATPANAH, Hamid, FADAEINEDJAD, Roohollah, et RASHIDINEJAD, Masood. A new model for PMSG-based wind turbine with yaw control. IEEE transactions on energy conversion, 2013, vol. 28, no 4, p. 929-937.

[42] ANNOUKOUBI, Maha, ESSADKI, Ahmed, LAGHRIDAT, Hammadi, et al. Comparative study between the performances of a three-level and two-level converter for a Wind Energy Conversion System. In : 2019 International Conference on Wireless Technologies, Embedded and Intelligent Systems (WITS). IEEE, 2019. p. 1-6.

[43] GHENNAM, T., BOUHALI, O., MAIZI, D., et al. Theoretical study and experimental validation of a Wind Energy Conversion System control with three-level NPC converters. In : 2012 XXth International Conference on Electrical Machines. IEEE, 2012. p. 2178-2183.

[44] MOUALDIA, A., BOUDANA, Dj, BOUCHHIDA, O., et al. Direct torque control based multi-level inverter and artificial neural networks of wind energy conversion system. In: 2016 8th International Conference on Modelling, Identification and Control (ICMIC). IEEE, 2016. p. 49-54.

[45] DURÁN, Mario J., KOURO, Samir, WU, Bin, et al. Six-phase PMSG wind energy conversion system based on medium-voltage multilevel converter. In : Proceedings of the 2011 14th European Conference on

Power Electronics and Applications. IEEE, 2011. p. 1-10.

[46] EKSTRÖM, Rickard, EKERGÅRD, Boel, and LEIJON, Mats. Electrical damping of linear generators for wave energy converters—A review. Renewable and Sustainable Energy Reviews, 2015, vol. 42, p. 116-128.

[47] CÁRDENAS, Roberto, PEÑA, Rubén, WHEELER, Patrick, et al. Control of the reactive power supplied by a WECS based on an induction generator fed by a matrix converter. IEEE Transactions on Industrial Electronics, 2008, vol. 56, no 2, p. 429-438.

[48] JEGATHEESWARAN, R. and RAJESH, R. Variable speed wind-energy conversion system using PMSG & Z-Source inverter. In: 2015 International Conference on Innovations in Information, Embedded and Communication Systems (ICIIECS). IEEE, 2015. p. 1-7.

[49] BOUMASSATA, Abderraouf et KERDOUN, Djallel. Direct powers control of DFIG through direct converter and sliding mode control for WECS. In: 2015 3rd International Conference on Control, Engineering & Information Technology (CEIT). IEEE, 2015. p. 1-5.

[50] YARAMASU, Venkata, DEKKA, Apparao, DURAN, Mario J., et al. PMSG based wind-energy conversion systems: survey on power converters and controls. IET Electric Power Applications, 2017, vol. 11, no 6, p. 956-968.

[51] M. A. Abdullah, A. H. M. Yatim, and Chee Wei Tan, 'A study of maximum power point tracking algorithms for wind energy system', in 2011 IEEE Conference on Clean Energy and Technology (CET), Jun. 2011, pp. 321–326, doi: 10.1109/CET.2011.6041484.

[52] JUNG, Jin-Woo and DSTUDENT, P. H. PROJECT# 2 Space vector PWM inverter. Mechatronic Systems Laboratory, Dept. of Electrical and Computer Eng. The Ohio State University, 2005.

[53] RAJENDRAN, R. and DEVARAJAN, N. Analysis and FPGA realization of a pulse width modulator based on voltage space vectors. International Journal of Computer Applications, 2010, vol. 2, no 6, p. 46-51.

[54] BUJA, Giuseppe S. and KAZMIERKOWSKI, Marian P. Direct torque control of PWM inverter-fed AC motors-a survey. IEEE Transactions on industrial electronics, 2004, vol. 51, no 4, p. 744-757.

[55] Harrabi, N., De Almeida, J.S., Laboudi, K. (2021). Controller design approach for SVPWM-regulated AC/DC rectifier. European Journal of Electrical Engineering, Vol. 23, No. 5, pp. 353-360. https://doi.org/10.18280/ejee.230501

[56] SHANTHI, R., KALYANI, S., et THANGASANKARAN, R. Performance analysis of speed control of PMSM drive with sinusoidal PWM and space vector PWM fed voltage source inverters. In: 2017 International Conference on Innovations in Green Energy and Healthcare Technologies (IGEHT). IEEE, 2017. p. 1-10.

[57] LUO, Yi. Wind Turbine Site Selection Over Abandoned Mined Land. In: NAAMLP 32nd Annual Conference, Sept. 19-22, 2010, Scranton, PA. 2010. p. 2-16.

[58] LATRECHE, Mohammed-Tahar. Commande Floue de la Machine Synchrone à Aimant Permanant (MSAP) utilisée dans un système éolien. 2018. PhD Thesis.

Chapter 04: Grid Energy Storage Technology

4.1 Introduction 106
4.2 Grid energy storage 106
4.2.1 Pros of grid energy storage 107
4.2.2 Cons of grid energy storage 108
4.3 Energy storage technologies 109
4.3.1 Battery Energy Storage 109
4.3.2 Supercapacitors 109
4.3.3 Pumped hydro energy storage 110
4.3.4 Compressed air energy storage (CAES) 110
4.3.5 Thermal energy storage (TES) 110
4.3.6 Flywheel 110
4.3.7 Hybridization of energy storage systems HESS 111
4.3.8 Hydrogen storage 111
4.4 Specific requirements of grid energy storage 111
4.4.1 Types of batteries 112
4.4.2 Battery Characteristics 113
4.4.3 Battery Bank Size Calculation 114
4.5 Control of Bidirectional DC-DC Converter for Battery Storage 115
4.5.1 Model analysis 116
4.5.2 Design of battery control 117
4.6 Battery testing charging and discharging 118
4.6.1 Discharging mode 118
4.6.1Charging mode 119
4.6.1 Stop mode 120
4.7 Battery testing storage system simulation 120
4.8 Conclusion 121
References 122

Chapter 4: Grid Energy Storage Technology



Abstract

As more renewable energy is developed, energy storage is increasingly important and attractive; hence, finding and implementing cost-effective and sustainable energy storage and conversion systems is vital. While energy storage technologies have existed for decades, fast-ramping grid-level storage is still an immature industry and is experiencing relatively rapid improvements in performance and cost across a variety of technologies.

In this chapter, storage from various aspects including design features, advantages, disadvantages, and environmental impacts is assessed. In addition, batteries of various types are considered one of the most suitable approaches to store energy for different technologies and applications of batteries; however, environmental impacts of large-scale battery use remain a major challenge that requires further study. We proposed as energy storage devices, such as grid-connected batteries. This review reaffirms that batteries are not efficient for 100%, it also confirms that batteries industry can generate considerable amounts of environmental pollutants (hazardous waste, greenhouse gas emissions and toxic gases) during different processes.

Batteries use at a large scale or grid-scale, will have significant social and environmental impacts; hence, it must be compared carefully with alternatives in terms of sustainability, while focusing on research to quantify externalities and reduce risk.

4.1 Introduction

The main problem in connecting the RE energy to the grid is the fluctuations in the output power from RE system, energy storage devices can be used to overcome this issue. Energy storage has the potential to significantly increase the efficiency, stability, and resiliency of the electric power grid [1-3]. Today, electricity generation must always be in dynamic balance with grid, with the increasing role of variable generation and changing demand profiles or sudden problems, grid operators have limited resources to maintain this dynamic balance. Energy storage, if suitably deployed, gives the grid operators a flexible and fast responding resource to effectively manage variability in generation and demand [2-3].

Today, the stability of the electric power grid is maintained through real time balancing of generation and demand. Grid scale energy storage systems are increasingly being deployed to provide grid operators the flexibility needed to maintain this balance. Energy storage also imparts resiliency and robustness to the grid infrastructure. Over the last few years, there has been a significant increase in the deployment of large-scale energy storage systems [2-5]. This growth has been driven by improvements in the cost and performance of energy storage technologies and the need to accommodate distributed generation [6-8], as well as incentives and government mandates. Energy management systems (EMSs) and optimization methods are required to effectively and safely utilize energy storage as a flexible grid asset that can provide multiple grid services [7-9].

This chapter presents the impact of grid connected batteries storage of grid power systems with large amount of renewables infeed.

4.2 Grid energy storage

The electric grid must have the generation capacity to meet the demands of electricity consumers [10]. However, electricity demand varies greatly both daily and seasonally, and operating a RE to match grid that has broad peak-to-base spreads is a great challenge. Electricity providers must have enough installed power capacity to match peak demand and must continuously operate enough capacity to meet real-time demand [2], [8-10]. Many of these inefficiencies are caused by the perishable nature of energy within the electrical grid. Due to the lack of energy storage devices within the grid system, energy must be immediately delivered to and used by the consumer.

The power capacity for energy storage within the grid currently sits at 125 GW (the majority of which is in the form of pumped hydro plants), which is about 3% of global power capacity [4], [10]. Additional energy storage within the grid would allow many more plants to run closer to full capacity and reduce energy losses during electricity transmission. Energy storage is a key element in diversifying energy sources and adding more renewable energy sources into the energy market.

Grid energy storage also called large-scale energy storage is a collection of methods used for energy storage on a large scale within an electrical power grid [5-7]. As of 2020, the largest form of grid energy storage is dammed hydroelectricity, with both conventional hydroelectric generation as well as pumped storage hydroelectricity [8-10].

Energy storage can provide benefits and services such as load management, power quality and uninterruptable power supply to increase the efficiency and supply security. This becomes more and more important in regard to the energy transition and the need for a more efficient and sustainable energy system [8-10][11]. Numerous energy storage technologies (pumped-storage hydroelectricity, electric battery, flow battery, flywheel energy storage, supercapacitor etc.) are suitable for grid-scale applications, however their characteristics differ [7-9].

4.2.1 Pros of grid energy storage

There are many ways to utilize energy storage to provide benefits to the local electricity grid, depending on the size of the storage project and the technology, where usage will vary. Here are some of the benefits:

- **Peak power supply and emergency preparedness**

Vital needs can be met reliably even with no transmission or generation going on while non-essential needs are deferred. How much this affects any given utility varies significantly. In a summer peak utility, more solar can generally be absorbed and matched to demand. In winter peak utilities, to a lesser degree, wind correlates to heating demand and can be used to meet that demand[12-14]. Depending on these factors, beyond about 20–40% of total generation, grid-connected intermittent sources such as solar power and wind power tend to require investment in grid interconnections, grid energy storage or demand-side management enhances grid reliability and allows renewable sources to integrate.

- **Frequency regulation**

The electricity grid runs on alternating current (AC) that must operate within an accepted frequency range. Utilities must keep this frequency within a narrow band to prevent damage to electrical equipment. They do this by ramping generation assets either up or down. However, it can often take several minutes or longer to adjust some generation units that run on coal, nuclear, or natural gas, the traditional providers of this service [12]. This creates a unique opportunity for utilities to use energy storage as it can react in seconds rather than minutes or longer.

- **Backup power and impact of energy storage on island grid dynamics**

Some electricity customers have critical loads that must have a fully reliable electricity supply. If a grid outage occurs, these customers can utilize an on-site generator to power these loads

[12][13]. Now that energy storage is more affordable, facility managers are choosing battery storage to provide backup power instead of fossil fuel alternatives like a diesel generator.

As distributed generators increase their importance on the electric power system, more and more parameters have to be controlled in order to assure the proper operation of the utility. One of the main problems encountered with this kind of generation is the potential formation of islands which could keep working in a normal way even if the utility grid has failed. One solution to this problem is the application of energy storage.

4.2.2 Cons of grid energy storage

Any electrical power grid must match electricity production to consumption, both of which vary drastically over time. Any combination of energy storage and demand response has these disadvantages:

- **Environmental and health impacts caused by batteries**

Use Batteries may impact the environment during manufacturing, use, storage, treatment, disposal and recycling. Due to their a vast range of applications, a large number of batteries of different types and sizes are produced globally, leading to different environmental and public health issues. Pollutions caused by using batteries some metals and non-metals involved in battery manufacturing can threaten human health via different forms of exposure, such as inhalation, skin or eye contact, ingestion and injection [1-3].

- **Efficiency of the batteries**

The battery capacity and lifetime are affected by deep cycling and extended states of low charge.

- **Additional cost and complexity**

The initial and ongoing battery costs, the system's reliability and durability often suffer due to the inadequate and improper battery selection, as in most cases the choice is based on lowest price. Many approaches can be followed for the selection of a RE battery [2-4]. Cycle life, effect of rate of discharge, self-discharge rate, performance at extreme temperature, battery voltage and maximum current drain capacity in ampere-hours, watt-hours per weight, watt-hours per unit volume, maintenance requirements and cost per watt-hour are a few critical parameters which can be optimally combined to select the right battery for any particular RE installation, were due to: poor operation and maintenance procedures; an inadequate battery charging system; improper sizing of the battery; and inadequate information on the condition of the batteries [12-14].

In several RE plants, batteries were found to be damaged due to deep-discharge, aging and structural failure of the cell casing [3-5]. A few cases of excessive overcharging and the large number of operating cycles in five years of their operation were observed. In addition to these, cases of explosions caused by a build-up of hydrogen in the cells were also observed. Proper

battery operation in a RE system requires voltage-regulating protection circuitry to prevent overcharging and excessive discharging [2-5]. Permanent damage can be done with a battery if it is charged too fast and far too long. Similarly, forcing higher charging currents into a battery when it is fully charged will cause the battery to gas. Excessive discharging will cause the plates to disintegrate and should be avoided. A disadvantage of implementing battery storage systems is the initial cost. The price of batteries is decreasing across the board, with many financial experts claiming that there will actually be a clear economic benefit from adopting this technology over the next few years [13-15].

- **Energy lost**

Energy lost in round trip inefficiencies and additional infrastructure and space requirements.

4.3 Energy storage technologies

There is a wide variety of energy storage technologies that could be deployed to fulfill applications within electrical networks. These technologies have been reviewed by numerous other authors [3], [6-8]. In this section, we briefly describe each technology and provide a summary of the relevant information for use by energy storage developers, network and system operators, and regulators.

4.3.1 Battery energy storage

Battery Energy Storage (BES) can enable the transition to a sustainable and secure energy system based on renewable sources, with reduced greenhouse gas emissions and enhanced energy independence [14-16]. Batteries can store energy from on-peak renewable energy and release it when it is more needed in central, de-centralized and off-grid situations. Batteries can also offer grid support services like voltage control and frequency regulation, so maintaining grid stability and flexibility [12].

4.3.2 Supercapacitors

Supercapacitors store energy as an electrical charge and consist of a porous separator between two conductive electrodes and an electrolyte [6],[17]. They can achieve a higher energy density than capacitors due to the porous electrodes with high surface area. This technology can reach a much higher power rating than batteries with fast charge/ discharge cycles, but it also presents a high self-discharge [17-19]. It is attractive for short-term responses such as frequency grid services [9]. Supercapacitors have a long lifetime, their energy efficiency is heavily dependent on their discharge rate and dependent on construction and voltage, can vary from 52% to 96%; This illustrates the need to design energy storage technologies based on their intended applications. Supercapacitors have a high energy capacity cost in comparison with similar energy storage alternatives [6],[17].

4.3.3 Pumped hydro energy storage

Pumped hydro Energy Storage (PHES) is among the most mature, flexible, and efficient forms of large-scale energy storage [20]. The technology works by pumping water from low-altitude reservoirs to upper reservoirs to exploit the gravitational potential energy of the water. The discharging cycle releases the water from the high-altitude reservoir and extracts energy through a hydroelectric turbine [6]. The main drawbacks of this energy storage technology are the large initial costs of investment.

4.3.4 Compressed air energy storage (CAES)

Energy can also be stored in compressed air, in which a motor-compressor is used to pump air into a tank, which is then reversed when the energy is needed, turning the motor into a generator, and the compressor into a turbine. Recent advances, such as the new regenerative device from LightSail Energy, manages and utilizes the heat generated by the process, which has improved round-trip efficiencies into the 70 percent range. In compressed air energy storage (CAES), energy is stored in the form of high-pressure compressed air, which is then used to generate electricity via a turbine [6]. Globally, there are a handful of installations, with power capacities. CAES typically has capital costs varying, a cycle efficiency of 40% & 60%, and a lifetime of 20 & 40 years. Adiabatic CAES offers increased cycle efficiency (50% & 70%), but with capital costs. An extension of this approach is to use liquid air energy storage (LAES), which uses liquefied air or nitrogen as a storage medium [21]. LAES offers round trip efficiencies of 50% & 60%, but this can be significantly improved if waste heat is available. Liquid air can be stored in a tank, so it can be deployed on many more sites than CAES.

4.3.5 Thermal energy storage (TES)

Thermal energy storage (TES) comprises a collection of technologies that store energy in thermal form (heat or cold) either directly or indirectly through energy conversion processes. Grid-scale TES technologies include cryogenic energy storage [6] and pumped thermal electricity storage. TES currently accounts for approximately 55% of global non-pumped hydro installations, and its installed power capacities. The existence of grid integrated systems makes it attractive for wholesale market services coupled with its overall system efficiency and high energy density. TES is the least cost energy storage technology, with sensible thermal energy storage. Other classes in its family are latent heat storage generally and the most expensive thermochemical energy storage [22]. TES technologies have response times of a few minutes to tens of minutes and are therefore suited for energy- rather than power- led applications.

4.3.6 Flywheel

Flywheel energy storage puts excess energy into a heavy spinning rotor, which, due to its large inertia, maintains a very constant speed. These are often used in a vacuum enclosure which

eliminates air resistance, resulting in higher efficiency. Flywheels store kinetic energy in a rotating disk and were among the first commercialized storage technologies to be used in electric power systems. The defining characteristic of this technology is its high-power and low-energy density. Flywheel energy storage also has a fast response and can deliver rated power within one second, enabling participation in services that require fast response. This technology has a low environmental impact [22], a long lifetime, and high round trip efficiency (approximately 85%). The disadvantage of flywheel storage is the high capital cost of energy and a self-discharge rate as high as 20% of the stored energy per hour.

4.3.7 Hybridization of energy storage systems HESS

A hybrid energy storage system (HESS) refers to the combination of multiple energy storage technologies with the aim of exploiting their individual advantages and mitigating their drawbacks. The most common configuration in the literature merges high-power, fast-response devices with high-capacity technologies to address one or more services [6],[23]. However, the criteria for selecting hybrid technologies can also account for a number of additional characteristics, such as individual response time, cycle efficiency, cycle lifetime, self-discharge rate, initial investment costs, operation and maintenance costs, location, and potential revenue streams [6], [23-25]. As the capital cost of investment required for hybridizing a system might be higher than for a single-energy storage technology, a number of approaches, such as active or passive coupling architecture, control techniques, or relative sizing methodologies can be considered to maximize the technical and economic benefits of hybridization. The optimal sizing of HESS is a planning process to determine the power and energy ratings of each storage device by allocating their cost of power and cost of energy in the most efficient and useful way according to the system's objectives [25],[26].

4.3.8 Hydrogen storage

Hydrogen storage utilizes excess electric power to produce hydrogen and oxygen from water by means of electrolysis. Energy can be retrieved by running them back through a fuel cell, or by direct combustion of the hydrogen-oxygen combination to power a gas turbine or other type of engine[23].

4.4 Specific requirements of grid energy storage

- The amount of photovoltaic electricity produced throughout the day varies from a maximum during peak sunshine hours to zero during the night. Some energy applications function satisfactorily during sunshine hours therefore get power directly from the PV array. Other applications require a continuous supply of energy, irrespective of the time of the day, and hence need a reliable energy storage device [1-5]. Also, the main problem in connecting the wind energy to the grid is the fluctuations in the output power from wind farms. Energy storage devices can be

used to overcome this issue. The energy storage system (ESS) is used to achieve good reliability and high efficiency. The storage devices store the energy during maximum power generation and deliver the power based on the demand, providing uninterrupted power supply [12-15].

- The electrical grids need a stable system that provides a balance between supply and distribution.
- Anti-islanding protection allows the inverter to disconnect when it identifies a problem with the power grid or during maintenance periods [12-14]. Battery storage is becoming increasingly popular throughout the RE. This is particularly true in parts of the country that are impacted by frequent electrical outages, whether due to natural disasters or otherwise. A big reason why storage is popular in these areas is due to storage's ability to island.
- This type of energy storage can balance the intermittent of the power supply, which is caused by renewable energy sources, or by a malfunction, failure unforeseen, component failures… etc. The combination of an energy storage system can contain advantages such as regulating frequency and voltage in electrical networks, describes the key to the penetration of renewable energy such as photovoltaic systems and the wind turbine connected to the electricity grid [14],[17].

This chapter aims to select a battery technology for a test application, The methodology for battery is composed a characteristics integrated model, battery bank size, control of bidirectional DC-DC converter for battery storage, design of battery control and battery testing charging and discharging modes.

4.4.1 Type of batteries

A wide range of batteries with different chemistries exists such as in Table.4.1 [28]:

Table.4.1 Main chemistries for different battery types

Type	Energy Efficiency (%)	Cycle Life (cycles)
Lead acid	70-90	200-2000
Zinc Bromide	70	1000
Sodium-sulfur NaS	80-90	500-2500
Lithium-ion Li-ion	75-90	500-2000
Li Polymer	70	>1200
Nickel-Cadmium Ni-Cd	60-90	500-2000
Nickel-metal Hydride Ni-MH	70	500-1000
Vanadium Redox flow VRB	80	100-150

4.4.2 Battery Characteristics

The use of batteries in RE systems differs from the use of batteries in other common battery applications. For RE systems, the key technical considerations are that the battery experience of a long lifetime under nearly full discharge conditions. Common rechargeable battery applications do not experience both deep cycling and being left at low states of charge for extended periods of time.

- **Battery Lifetime and Maintenance**

The lifetime of a battery may be specified in several different ways depending on the application and hence on which mechanism is most significant. For applications in which the battery is regularly charged and discharged, the most appropriate measure of lifetime is the number of charge/discharge cycles over which the battery maintains a given fraction of its capacity [2-7]. Since batteries inherently involve chemical reactions that are reactive, the materials used in batteries are susceptible to alternate reactions that degrade battery performance. Improper use of the battery can greatly accelerate battery aging and further decrease the number of cycles over which a battery can be used. Battery life is defined either in years (if it remains fully charged or in of cycles under a given set of conditions (including temperature and DOD) [10-14].

- **Battery safety and disposal**

Most battery systems, including those used in renewable energy systems, contain corrosive or dangerous chemicals and the safety regulations for each type of battery should be carefully checked. Additional safety concerns relate to their ability to produce large current. Finally, for lead-acid battery systems, the evolution of hydrogen is a potential issue. Batteries should not be thrown away as most batteries contain toxic and/or corrosive material [14].

- **Cut-off voltage**

In many battery types, including lead acid batteries, the battery cannot be discharged below a certain level or permanent damage may be done to the battery. This voltage is called the "cut-off voltage" and depends on the type of battery, its temperature and the battery's rate of discharge [12-14].

- **Self-discharge**

Self-discharge refers to the fact that even in the absence of a connected load, the discharge reaction will proceed to a limited extent and the battery will therefore discharge itself over time. The rate of self-discharge depends primarily on the materials involved in the chemical reaction and on the temperature of the battery [12-16].

- **Cold cranking current**

The maximum amount of current a battery can provide for a short period of time is called the cranking current [14][17]. This parameter is often specified for transport applications, in which

the battery must provide enough current to start a large engine. However, it is typically not an important parameter in RE systems.

- **Battery State of Charge SOC**

A key parameter of a battery in use in a RE system is the battery state of charge (BSOC). The BSOC is defined as the fraction of the total energy or battery capacity that has been used over the total available from the battery [5-9]. Battery state of charge (BSOC or SOC) gives the ratio of the amount of energy presently stored in the battery to the nominal rated capacity. A common way to measure the BSOC is to measure the voltage of the battery and compare this to the voltage of a fully charged battery. However, as the battery voltage depends on temperature as well as the state of charge of the battery, this measurement provides only a rough idea of battery state of charge [10-16].

- **Depth of discharge DOD**

In many types of batteries, the full energy stored in the battery cannot be withdrawn without causing serious, and often irreparable damage to the battery [5-8]. The depth of discharge (DOD) of a battery determines the fraction of power that can be withdrawn from the battery. For example, if the DOD of a battery is given by the manufacturer as 25%, then only 25% of the battery capacity can be used by the load. Nearly all batteries, particularly for renewable energy applications, are rated in terms of their capacity. However, the actual energy that can be extracted from the battery is often (particularly for lead acid batteries) significantly less than the rated capacity [12-15]. This occurs since, particularly for lead acid batteries, extracting the full battery capacity from the battery dramatically reduced battery lifetime. The depth of discharge (DOD) is the fraction of battery capacity that can be used from the battery and will be specified by the manufacturer.

- **Daily depth of discharge**

In addition to specifying the overall depth of discharge, a battery manufacturer will also typically specify a daily depth of discharge. The daily depth of discharge determined the maximum amount of energy that can be extracted from the battery in a 24-hour period [12-14]. Typically, in a larger scale PV system, the battery bank is inherently sized such that the daily depth of discharge is not an additional constraint. However, in smaller systems that have a relatively few days storage, the daily depth of discharge may need to be calculated.

4.4.3 battery bank size calculation

Solar or wind energy needs to be stored somewhere and typically this is done using deep-cycle batteries. For many installations of one or two solar panels, one large battery has enough storage capacity, but for larger systems it may be necessary to connect multiple batteries to create a battery bank. To work out how much battery storage capacity you need, the batteries are generally

connected to the DC bus, under these conditions, the number of cells in series is directly set by the DC bus voltage [27]:

$$N_{bs} = \frac{V_{dc}}{V_{bn}} \tag{4.1}$$

N_{bs} Number of batteries connected in series,

V_{bn} Nominal voltage of a battery (V).

With the aim of preventing deep discharges and limiting the phenomena of "gassing" (This situation arises when an electric current is continued to be applied to the battery while it is charged), the energy stored in the battery is subject to the following constraints:

$$E_{bat,\min} \leq E_{bat} \leq E_{bat,\max} \tag{4.2}$$

$E_{bat,\max}$: Maximum authorized storage energy, (Wh)

$E_{bat,\min}$: Minimum authorized storage energy, (Wh)

Here we assimilate the maximum energy , max to the nominal capacity of the battery C_{bn} which can be expressed in Ah as in Wh. Thus, the minimum capacity (minimum energy) is determined from the DOD depth of discharge.

$$E_{bat,\min}(t) = (1 - DOD)\,C_{bn} = SOC\;C_{bn} \tag{4.3}$$

State of charge

$$SOC(t) = \frac{E_{bat}}{C_{bn}} \tag{4.4}$$

4.5 Control of Bidirectional DC-DC Converter for Battery Storage

Energy storage for RE inverter system traditionally is applied in the stand alone off-grid system considering the RE is not available during all the day and energy storage system like the battery is used to temporarily store the extra energy from the RE to provide energy when there is no low energy [16-18]. As for the grid-connected system, battery storage is not really necessary considering the grid as a limitless battery bank that can provide electricity continuously apart from the costing reason the consumer need to invest [16][18]. However, with the dropping cost in RE system installation and increasing electricity price, the interest towards storage system in the grid connected RE system is changing. From our perspective, having a battery storage system is meaningful only if the energy from the battery can be used in an advantageous manner which allows for better self-consumption and reduction in the cost of purchasing electricity from the grid. For that in term of storage capacity, it does not need to have such a big capacity, which is able to provide backup electricity for several days, but just enough to function as a buffer to protect consumer from a higher electricity price. In order to ensure the above battery storage system is

functioning effectively, power flow management is a critical aspect to be investigated [19]. The RE inverter system must ensure that the time and amount of power charged and discharged to or from the battery are right. In this context a bidirectional power flow control enables the power to be directed as required within the system. From a broad perspective, a study on the topology and related controlling aspects of the RE conversion system is important to achieve an efficient power conversion with energy storage capability and satisfy the power quality requirement [17-19].

The use of bidirectional DC-DC converter for interfacing the battery storage with the inverter system is widely investigated. The main advantage of the bidirectional converter is its ability to realize a bidirectional power flow by functioning either as a buck or boost converter depending on the triggered switch at any time. As shown in Fig.4.1, the output of the converter is directly connected to the DC bus capacitor of the inverter and current is discharged from the battery during the boost converter mode and recharged back to the battery during the buck mode.

4.5.1 Model analysis

The buck-boost chopper is used for the battery storage. It is considered a stage adaptation, and it makes it possible to carry out the charging and discharge given its reversibility of current. So, it step-up the voltage for the charge, and step-down voltage for the discharged. [10] [16] The model of the buck-boost chopper associated with the batteries is shown in Fig.4.1.

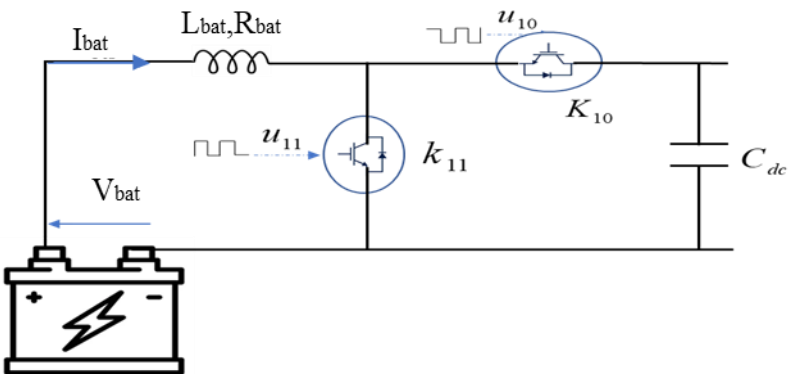

Fig.4.1 Bidirectional DC-DC

During operation, the converter can be either in a current mode control which makes it possible to control the amount of power flowing out/in from/to the battery, or in a voltage mode control to help stabilize the DC bus voltage. When the inverter system changes from grid-connected environment to standalone mode due to grid fault, the DC-DC boost converter and the bidirectional DC-DC converter alternately control the DC bus [16].

The two switches "K11" and "K10" form a switching cell. Their operation will therefore be complementary [12]. If we associate two connection functions $U_{11}$and U_{10} representing respectively the conduction state of switches "K11" and "K10", we obtain:

$$\{U_{11} = 1 - U_{10} \tag{4.5}$$

The main function of a charge controller in the system is to regulate the voltage and current from the source voltage into a rechargeable battery. The minimum function of a source charge controller is to disconnect the source when the battery is fully charged and keep the battery fully charged without damage. A charge controller is important to prevent battery overcharging, excessive discharging to protect the life of the batteries in the system. Power electronic circuit is used in a charge-controller to get higher efficiency, availability and reliability. The use of power electronics circuits such as various DC to DC converter topologies like bidirectional buck-boost converter. Depending on the state of the two switches "K11" and "K10", two configurations are possible:

- **Configuration 1: K11 closed and K10 open**

$$L_{bat}\frac{di_{bat}}{dt}+R_{bat}i_{bat}=V_{bat} \tag{4.6}$$

- **Configuration 2: K11 open and K10 closed**

$$L_{bat}\frac{di_{bat}}{dt}+R_{bat}i_{bat}=V_{bat}-V_{dc} \tag{4.7}$$

4.6.2 Design of battery control

The main purpose of using the bidirectional converter with the battery is to keep the DC bus voltage constant. In this case, it is not important to check the state of charge or discharge of the battery because the DC bus voltage can be stable and minimize the voltage ripples of the capacitor. When charging, switch K_{11} is activated and the converter works as a Boost (booster). Otherwise, in the event of a discharge, switch K_{10} is activated and the converter operates as a buck. Fig.4.2 shows the control that has been applied to the bidirectional chopper, and which contains two control loops, one on voltage control, and the other on current control. When the DC bus voltage is lower than the reference voltage, switch K_{11} is activated and vice versa for switch K_{10}. In the DC-controller methodology reference voltage of the DC bus Vdc* is compared with the DC bus voltage sensed voltage vdc. When error obtained is used by the PI, the output reference battery current I_{bat}*is compared with the battery current sensed I_{bat}. When error obtained is used by the hysteresis controller input, the output of the controller command the switches K_{11} and K_{10}.

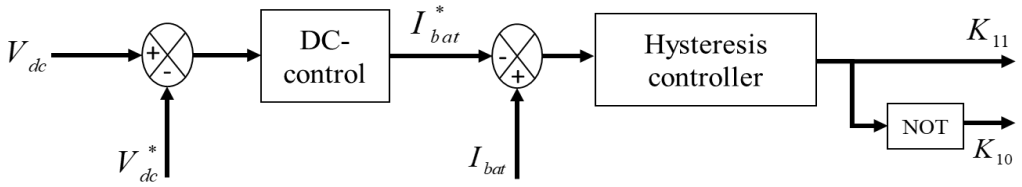

Fig.4.2 Battery control

4.6 Battery testing charging and discharging

The power battery example illustrates a 24 V, 10 Ah Lithium-Ion battery and the state of charge (SOC) of the battery is 0.5 (50 %). The battery is charged when the state of charge (SOC) of the battery goes over 0.5 (50 %). To charge the battery and the current goes negative. The battery is discharged by the constant DC voltage, when the SOC drops under 0.5 and the current goes positive.

4.6.1 Charging mode

When the grid is failing or in maintenance, the batteries will charge and supply from the voltage sources. The charging mode of the battery is given by the following tests, including voltage curve, SOC of the battery and Battery voltage characteristic for different charge currents. As in Fig.4.3.

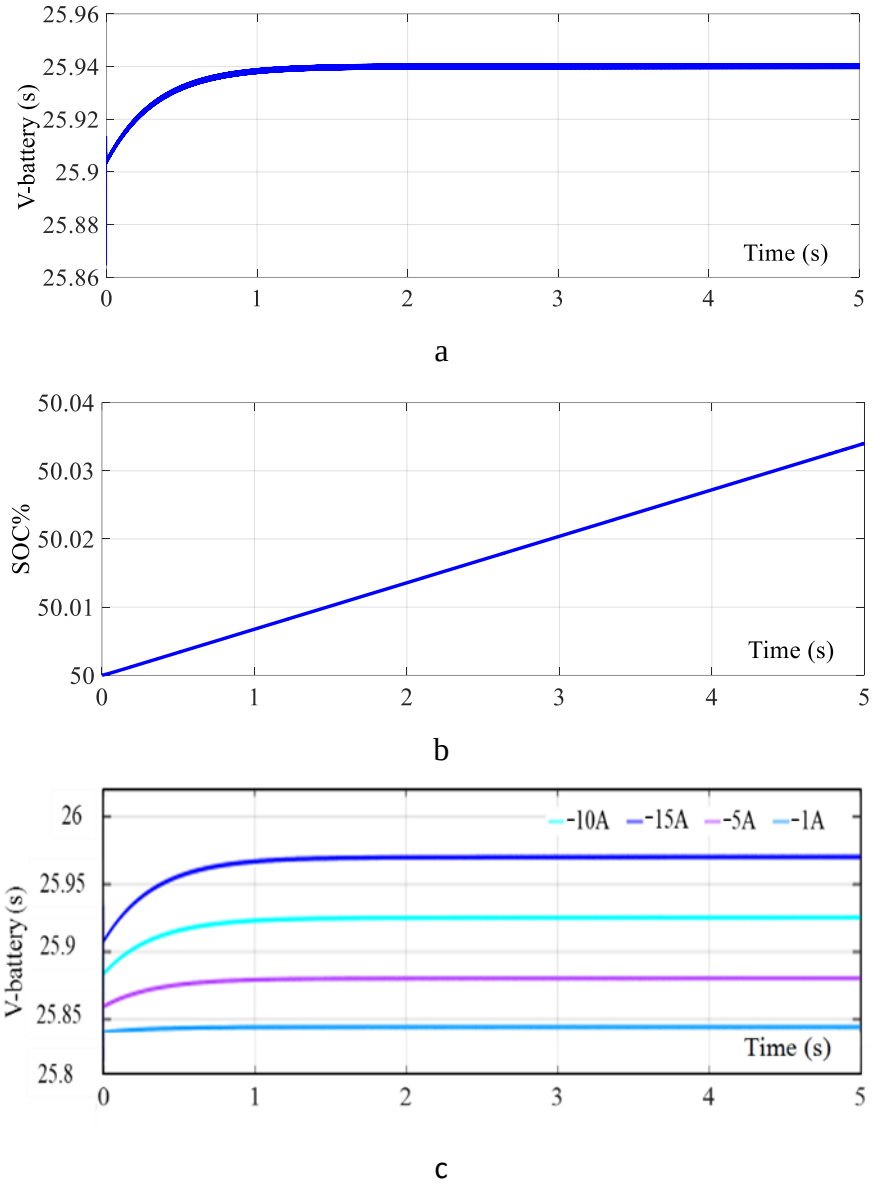

Fig.4.3 a. Voltage curve in charging mode, b. SOC curve in charging mode and c. Battery voltage characteristic for different charge currents.

When charging mode, the battery increases the voltage curve found that the battery voltage stable linear growth. At the same time, When the charge starts, the SOC state curve also accurately reflects the charge process on the impact of SOC. Charging process, SOC linear increase. Fig.4.3 shows the charge characteristic of the battery used the voltage evolution for different charge currents. We notice that the higher charge current is importantly, the faster the battery charge.

4.6.2 Discharging mode

When the voltage sources are disabled, in trouble or maintenance, the batteries will supply the grid.

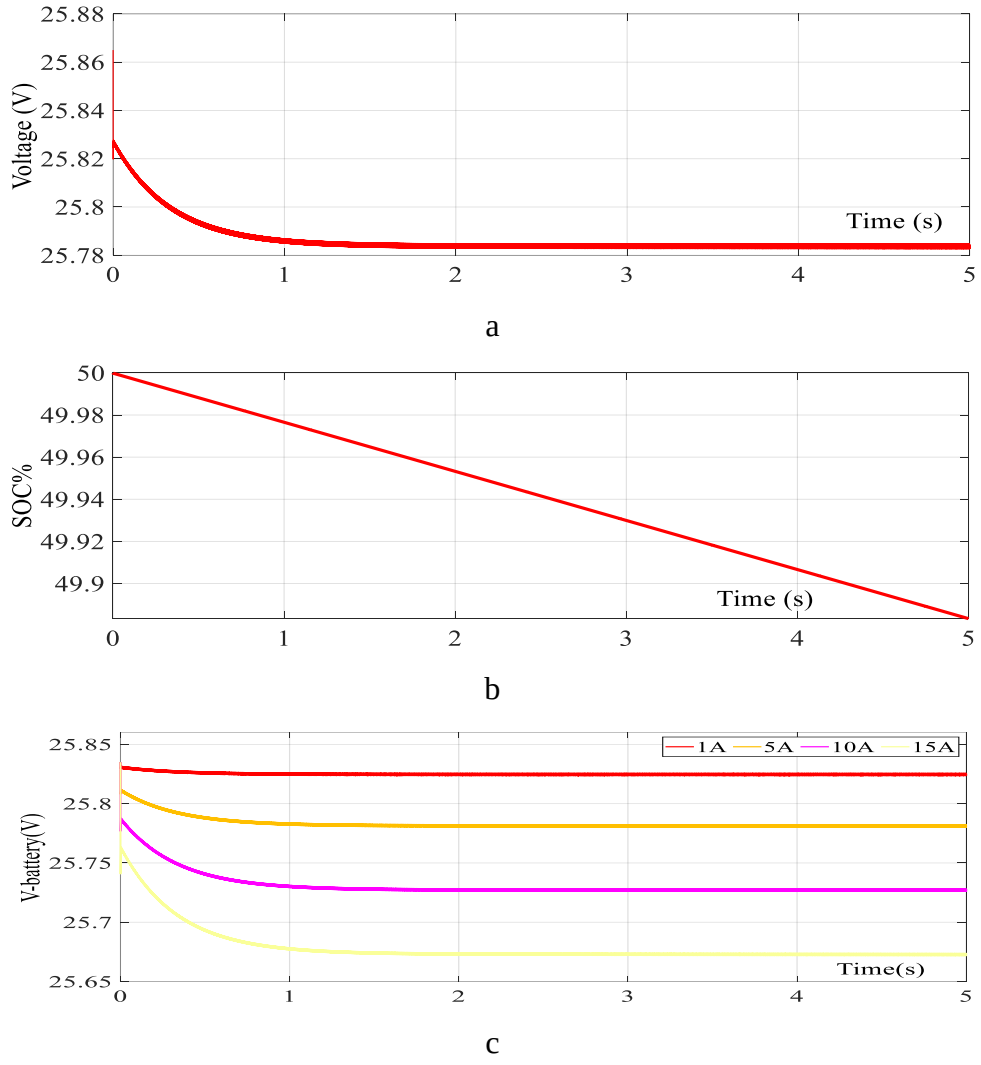

Fig.4.4 a. Voltage curve in discharging mode, b. SOC curve in discharging mode and c. Battery voltage characteristic for different discharge currents.

When discharging mode, the battery decreased voltage curve, found that the battery voltage is reduced. At the same time, When the discharge starts, the SOC state curve also accurately reflects the discharge process on the impact of SOC, discharging process, SOC linear decrease. Fig.4.4 shows the discharge characteristic of the battery used the voltage evolution for different discharge currents. We notice that the higher discharge current is important, the faster the battery discharge.

4.6.3 Stop mode

When the grid is ideal and the sources are enabling, the batteries will disconnect from the DC-link. When the charge is stopped and the discharge is stopped, the battery open circuit.

4.7 Battery testing storage system simulation

The inclusion of the storage system was simulated in both isolated operating mode and parallel mode (charge and discharge) and under different constraints such as variations of the mode.

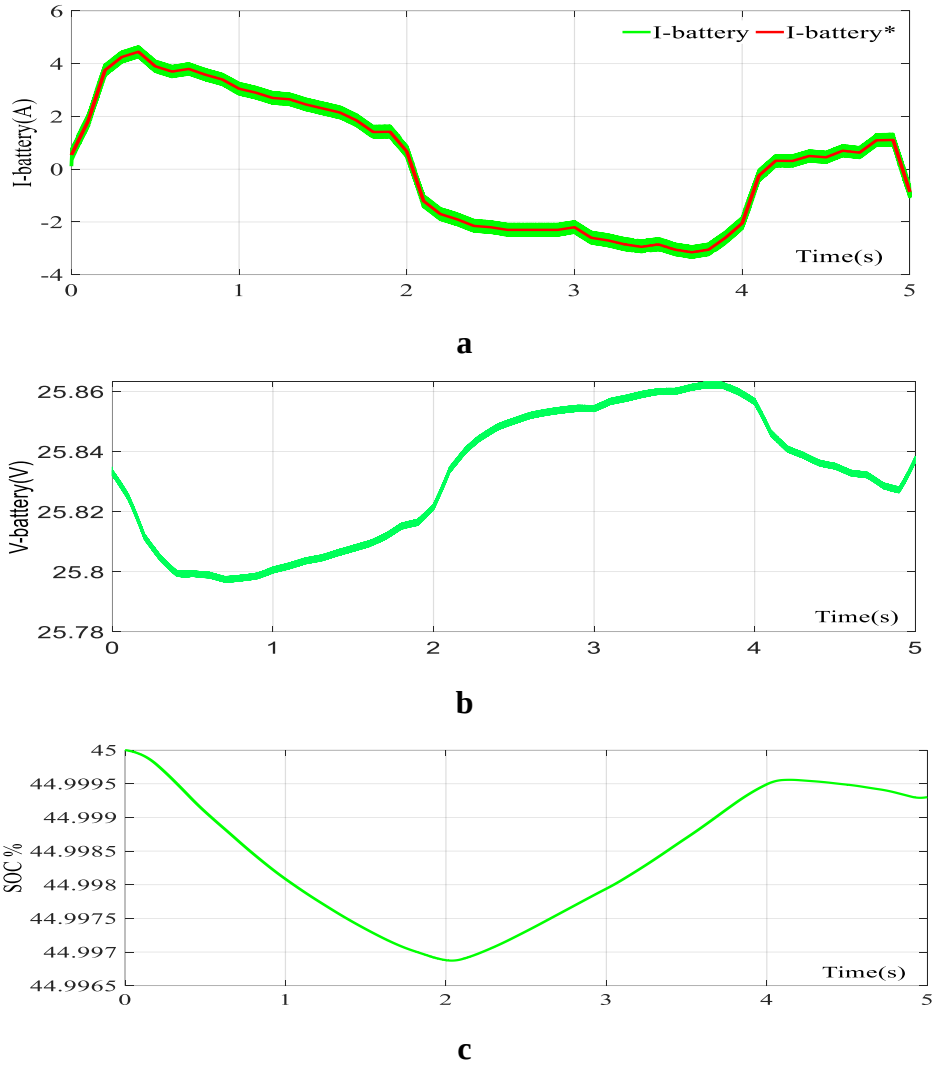

Fig.4.5 a. battery current, b. Voltage curve c. Battery SOC characteristic

Fig.4.5 shows the evolution of the battery current, we notice that the current is regulated to its reference value. The simulation results reflect that the charging and discharging of the li-ion battery has complex characteristics, and the model of battery can provide accurate results for battery SOC estimation. By observing the charge-discharge curve of the battery, it can be found that the voltage changes rapidly in the initial and final stages of charge-discharge in the intermediate process. As shown in Fig.4.5 SOC state curve also accurately reflects the charge and discharge process on the impact of SOC, charging process, SOC linear increase. During the discharge process, SOC is gradually reduced in each discharge period as shown in Fig.4.5.

4.8 Conclusion

Energy storage technology has potential to transform the electricity infrastructure in ways that can fundamentally alter the delivery of energy. While this transformation is at a nascent stage, researchers need to develop tools that can efficiently use the full range of applications and services that energy storage systems can provide to the electric grid. EMSs play a critical role in the effective utilization of energy storage as a flexible grid asset that can provide multiple grid services and ensure safe operation of energy storage systems.

In this chapter, we have made an attempt to provide a comprehensive review of grid energy storage and optimization tools that are needed for efficient operation of energy storage in the existing grid. The industry needs robust system energy storage and optimization methods that have the flexibility to accommodate multiple storage technologies and new applications and also the ability to operate on evolving market structures. The regulatory environment for energy storage is evolving quickly. This complex regulatory environment, which is a function of location and market structure, makes it difficult to develop generic approaches that meet the needs of a majority of systems. Even with regulatory reforms that make for a level playing field for new technologies including energy storage, storage valuation/optimization continues to be a challenging problem. While there has been significant progress, there are a number of areas requiring additional research:

- The characteristics of the charge/discharge profile, as well as the state of charge profile, can greatly impact the lifetime of electrochemical energy storage systems. Better models are needed so that the battery energy storage optimization can effectively capture the impact to the overall return on investment.
- In fact, adding home battery storage to a grid-tied RE system is most useful either the grid is unreliable and goes down frequently or extreme weather events are common.
- If we installed batteries in the RE system, we don't need the grid. we can draw energy from the batteries to tackle the situation. So, Grid-tied is the backup of the backup. It is like a giant battery. The advantages of on-Grid Systems; We do not have to buy an expensive battery back-up system to store any energy, this utility is a 100% efficient battery in itself.
- In grid-connected RE systems batteries are not needed, since all the power generated by the RE plant is uploaded to the grid for direct transmission, distribution and consumption. Hence, the generated RE power reduces the use of other energy sources feeding the grid like hydro, whose saving act as energy storage in the system, providing the same function of power regulation and backup as a battery would deliver in a stand-alone system. Since grid-connected systems do not need batteries, they are more cost effective and require less maintenance and re-investment as

stand-alone systems do. This concept together with the cost reduction, technology development, environmental awareness, right incentives and regulations has unleashed the power of RE.

References

[1] PRASAD, A. Rajendra et NATARAJAN, E. Optimization of integrated photovoltaic–wind power generation systems with battery storage. Energy, 2006, vol. 31, no 12, p. 1943-1954.

[2] DAUD, M. Zalani, MOHAMED, Azah, WANIK, MZ Che, et al. Performance evaluation of grid-connected photovoltaic system with battery energy storage. In : 2012 IEEE International conference on Power and Energy (PECON). IEEE, 2012. p. 337-342.

[3] NOTTROTT, A., KLEISSL, Jan, et WASHOM, Byron. Energy dispatch schedule optimization and cost benefit analysis for grid-connected, photovoltaic-battery storage systems. Renewable Energy, 2013, vol. 55, p. 230-240.

[4] KOLLER, Michael, BORSCHE, Theodor, ULBIG, Andreas, et al. Review of grid applications with the Zurich 1 MW battery energy storage system. Electric Power Systems Research, 2015, vol. 120, p. 128-135.

[5] JIN, Yin, ZHAO, Wenchun, LI, Zhixin, et al. Modeling and Simulation of Lithium-ion Battery Considering the Effect of Charge-Discharge State. In : Journal of Physics: Conference Series. IOP Publishing, 2021. p. 012003.

[6] GREENWOOD, David, WALKER, Sara, WADE, Neal, et al. Integration of High Penetrations of Intermittent Renewable Generation in Future Electricity Networks Using Storage. In : Future Energy. Elsevier, 2020. p. 649-668.

[7] HANNA, R., KLEISSL, J., NOTTROTT, A., et al. Energy dispatch schedule optimization for demand charge reduction using a photovoltaic-battery storage system with solar forecasting. Solar Energy, 2014, vol. 103, p. 269-287.

[8] JACKSON, Tara M., WALKER, Geoffrey R., et MITHULANANTHAN, Nadarajah. Integrating PV systems into distribution networks with battery energy storage systems. In : 2014 Australasian Universities Power Engineering Conference (AUPEC). IEEE, 2014. p. 1-7.

[9] BENLAHBIB, Boualam. Supervision d'un système hybride éolienne-photovoltaïque connecté au réseau électrique. 2019. Thèse de doctorat.

[10] LAWDER, Matthew T., SUTHAR, Bharatkumar, NORTHROP, Paul WC, et al. Battery energy storage system (BESS) and battery management system (BMS) for grid-scale applications. Proceedings of the IEEE, 2014, vol. 102, no 6, p. 1014-1030.

[11] DEHGHANI-SANIJ, A. R., THARUMALINGAM, E., DUSSEAULT, M. B., et al. Study of energy storage systems and environmental challenges of batteries. Renewable and Sustainable Energy Reviews, 2019, vol. 104, p. 192-208.

[12] NATHAN, M. Swami, RAJASEKARAN, R., et RANI, P. Usha. Rules based functional control of bidirectional DC-DC converter for stand-alone PV with hybrid energy storage system. In : 2015 International Conference on Innovations in Information, Embedded and Communication Systems (ICIIECS). IEEE, 2015. p. 1-6.

[13] BYRNE, Raymond H., NGUYEN, Tu A., COPP, David A., et al. Energy management and optimization methods for grid energy storage systems. IEEE Access, 2017, vol. 6, p. 13231-13260.

[14] JOSSEN, A., SPATH, V., DORING, H., et al. Battery management systems (BMS) for increasing battery life time. In: 21st International Telecommunications Energy Conference. INTELEC'99 (Cat. No. 99CH37007). IEEE, 1999. p. 56.

[15] LAWDER, Matthew T., SUTHAR, Bharatkumar, NORTHROP, Paul WC, et al. Battery energy storage system (BESS) and battery management system (BMS) for grid-scale applications. Proceedings of the IEEE, 2014, vol. 102, no 6, p. 1014-1030.

[16] RASIN, Zulhani et RAHMAN, M. F. Control of bidirectional DC-DC converter for battery storage system in grid-connected quasi-Z-source pv inverter. In : 2015 IEEE Conference on Energy Conversion (CENCON). IEEE, 2015. p. 205-210.

[17] MANE, Jaya Aniruddha et JAIN, A. M. Design, modelling and control of bidirectional DC-DC converter (for EV). In : 2015 International Conference on Emerging Research in Electronics, Computer Science and Technology (ICERECT). IEEE, 2015. p. 294-297.

[18] Lawder, Matthew T., Bharatkumar Suthar, Paul WC Northrop, Sumitava De, C. Michael Hoff, Olivia Leitermann, Mariesa L. Crow, Shriram Santhanagopalan, et Venkat R. Subramanian. « Battery energy storage system (BESS) and battery management system (BMS) for grid-scale applications ». Proceedings of the IEEE 102, no 6 (2014): 1014-30.

[19] HAIZHOU, Zhai. Modeling of Lithium-ion Battery for Charging/Discharging Characteristics Based on Circuit Model. International Journal of Online Engineering, 2017, vol. 13, no 6.

[20] REHMAN, Shafiqur, AL-HADHRAMI, Luai M., et ALAM, Md Mahbub. Pumped hydro energy storage system: A technological review. Renewable and Sustainable Energy Reviews, 2015, vol. 44, p. 586-598.

[21] LUND, Henrik et SALGI, Georges. The role of compressed air energy torage (CAES) in future sustainable energy systems. Energy conversion and management, 2009, vol. 50, no 5, p. 1172-1179.

[22] BOLUND, Björn, BERNHOFF, Hans, et LEIJON, Mats. Flywheel energy and power storage systems. Renewable and Sustainable Energy Reviews, 2007, vol. 11, no 2, p. 235-258.

[23] ZÜTTEL, Andreas. Materials for hydrogen storage. Materials today, 2003, vol. 6, no 9, p. 24-33.

[24] DIVYA, K. C. et ØSTERGAARD, Jacob. Battery energy storage technology for power systems—An overview. Electric power systems research, 2009, vol. 79, no 4, p. 511-520.

[25] HEMMATI, Reza et SABOORI, Hedayat. Emergence of hybrid energy storage systems in renewable energy and transport applications–A review. Renewable and Sustainable Energy Reviews, 2016, vol. 65, p. 11-23.

[26] FIORENTI, Simone, GUANETTI, Jacopo, GUEZENNEC, Yann, et al. Modeling and experimental validation of a hybridized energy storage system for automotive applications. Journal of Power Sources, 2013, vol. 241, p. 112-120.

[27] GASSAB, Samir. Modélisation d'une centrale à énergie renouvelable photovoltaïque-éolienne. 2018. PhD Thesis

[28] PROVAZI, Kellie, CAMPOS, Beatriz Amaral, ESPINOSA, Denise Crocce Romano, et al. Metal separation from mixed types of batteries using selective precipitation and liquid–liquid extraction techniques. Waste Management, 2011, vol. 31, no 1, p. 59-64.

Chapter 05: Grid-connected Hybrid Renewable Energy System based PV/Wind

5.1 Introduction 125
5.2 Synthesis of hybrid systems architectures with PV, WES sources and batteries connected to the grid 125
5.2.1DC-Coupled systems 126
5.2.2AC-Coupled systems 127
5.2.3 The proposed configuration of hybrid system 127
5.2.4 What services can batteries provide in our work? 128
5.3 Originality of the proposed configuration 129
5.3.1 Hybrid PV-WES-side Power Control 130
5.3.2 Hybrid grid-side Power Control 130
5.3.3 Hybridization of the WT / PV power 130
5.4 Simulation results and discussions 131
5.4.1 Dynamic behavior of hybrid PV-WT 131
5.4 Conclusion 136
References 137

Chapter 5 : Grid-connected Hybrid Renewable Energy System based PV/Wind



Abstract

This chapter deals with power control of a PV-Wind hybrid generation system for the interconnection operation with the electric grid system. The proposed system consists of a solar array, DC/DC converter, DC/AC converter and a variable-speed wind generator, wind-side converter connected to grid interface inverter. Power control strategy is applied to extract the maximum power available from varying condition of solar irradiance and wind speed while maintaining power quality at a satisfactory level. The grid interface three-phase three-levels NPC inverter transfers the energy drawn from the PV array and wind turbine into the grid by keeping common the DC-voltage constant.

This chapter aims to examine the dynamic behavior of the hybrid PV-WT model under different operating conditions. The model is implemented using MATLAB/Simulink shows a good dynamic performance of hybrid PV-WT under different operating conditions.

5.1 Introduction

Actually, the energy demand is increasing rapidly while the conventional energy resources are depleted. As a result, the world is looking for alternative energy sources [1–4]. There are promising sources of hybrid-distributed generation, such as the wind generator, solar PV, fuel cell, biomass, geothermal, tides, and wave generator. Wind generator and solar PV are the most commonly used [5]. The integration of hybrid PV-WT system into electrical grid can improve the reliability of renewable power generation to supply the grid and minimizing the overall cost [3-5]. Wind and solar PV technology are gaining much attention of researchers and investors as an alternative source of electric energy. The intermittent nature of RE resources such as wind and solar, hybrid combinations of these resources with their efficient generation technology can make the whole system more reliable and improve the system performance [6].

Generally, hybrid energy system converts all individual system's output into electrical energy form. The final output is ready to supply the electrical grid. Good reliability and improved operational performance can be achieved by proper selection of technology and unit sizing while hybridization and designing of such systems [7]. The integral and the essential part of a Hybrid Renewable Energy System (HRES) is the capacity and the types of storage. Using high-capacity storage, energy can be used for a long period, but the response time is slow. Access-based storage can be used for gaining fast response. With proper storage and renewable energy resources, any kind of combination of RES technology could make hybrid power system [8-10].

This chapter reviews the literature on principles of wind energy and solar photovoltaic (PV), it is used as a hybrid renewable energy system with different configuration schemes of integration and motivation using advance control system techniques.

The chapter deals on application of multilevel converter topologies in hybrid PV-Wind power system. An abridged study based on three level inverters, which leads us to justify our choice (Neutral point clamped). Simulation results show good performances (low THD current, sinusoidal wave form) by adding RL-filter before the grid. Besides, we have presented a simulation study based on variable irradiation, constant temperature (25C°), wind speed then variable temperature.

5.2 Synthesis of hybrid system architectures, PV-Wind energy sources, including batteries connected to the grid

There are many configurations available in the literature to form a hybrid system from renewable energy sources. For our integration technique we choose between DC and AC description schemes.

5.2.1 DC-Coupled systems configuration

This architecture shown in Fig.5.1 consists of a single DC bus line, where coupling different components of the system takes place. In this architecture, the RES producing DC power can be connected directly or through a DC/DC converter depending on the DC bus voltage.

The considered system consists of: Photovoltaic (PV) panels, Wind Energy Conversion System (WECS), and Battery Energy Storage (BES). Solar photovoltaic can connect to common DC-link directly or through DC/DC chopper. Similarly, DC batteries also may connect to main bidirectional chopper DC/DC converter for an appropriate voltage level. The WECS includes the Wind Turbine (WT) based on Permanent Magnet Synchronous Generator (PMSG), the stator phase winding of PMSG is connected to the AC/DC converter, DC side of WES converter is connected to the one common DC-bus. In this type of hybrid system configuration, the different renewable sources, photovoltaic and wind turbine are interfaced to the main DC-link. Then, DC-bus can also supply DC/AC inverter to the utility grid. DC coupling is controlled because there is a need of synchronization to integrate different RE sources.

In order to obtain the maximum power conversion from the WES, the Maximum Power Point Tracking Algorithm (MPPT) has been applied to control the PMSG. The PV panel system is connected to the DC/DC boost converter. To control this converter system, MPPT algorithm is also applied in order to achieve the maximum power from PV source. The battery bank is connected to the DC bus through bidirectional DC/DC converter, to implement the proper charging and discharging strategies of the battery bank [5-10].

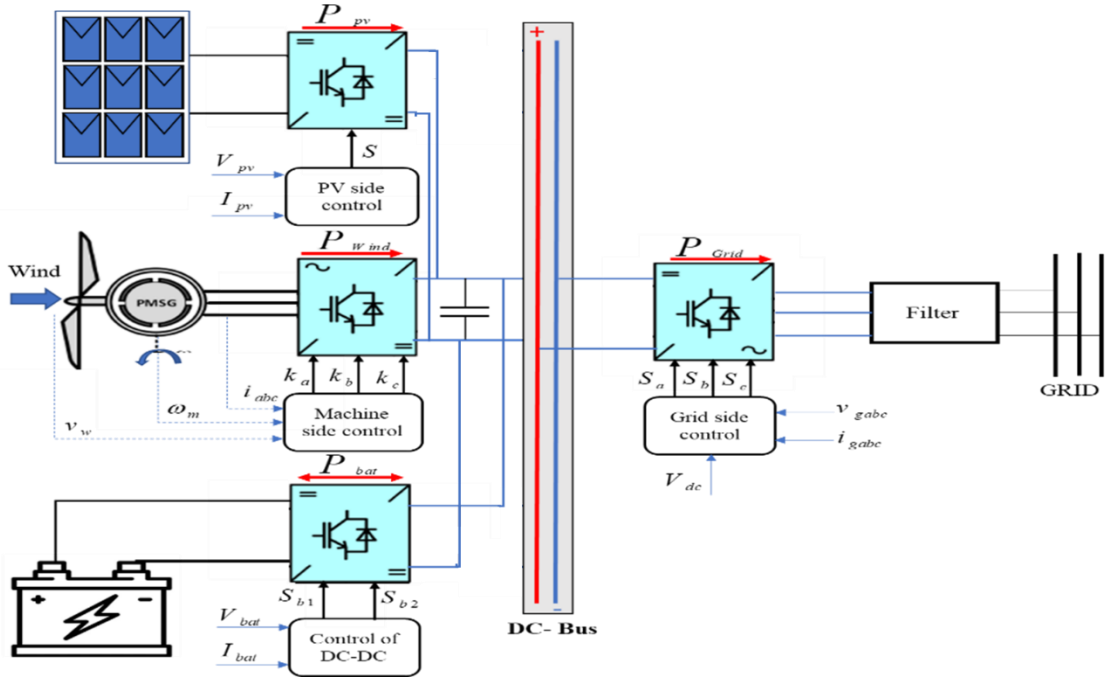

Fig.5.1 HRES configuration with common DC-bus

5.2.2 AC-Coupled system configuration

In this type of AC-Coupled systems as illustrated in Fig.5.2, a grid connected hybrid renewable energy system with a common AC-bus. Different renewable sources, like photovoltaic and wind turbine, are connected to a main power frequency AC-bus by power electronic interfacing circuits. AC buses are used for the hybridization of the wind source with ultimate AC outputs. A PV source with DC outputs need DC/AC converter while this AC output is joined to a utility grid system. In this configuration, several individual DC/AC converters are applied instead of one common DC/AC converter. It means that each individual energy system uses a separated converter system; Battery Energy Storage (BES) can be connected to common AC-link through DC/AC converter after using a bidirectional DC/DC to put into practice the battery bank's recommended charging and draining procedures. Where all AC sides are connected to the common AC-bus. To control wind and PV sources, MPPT algorithms are also applied [5-10].

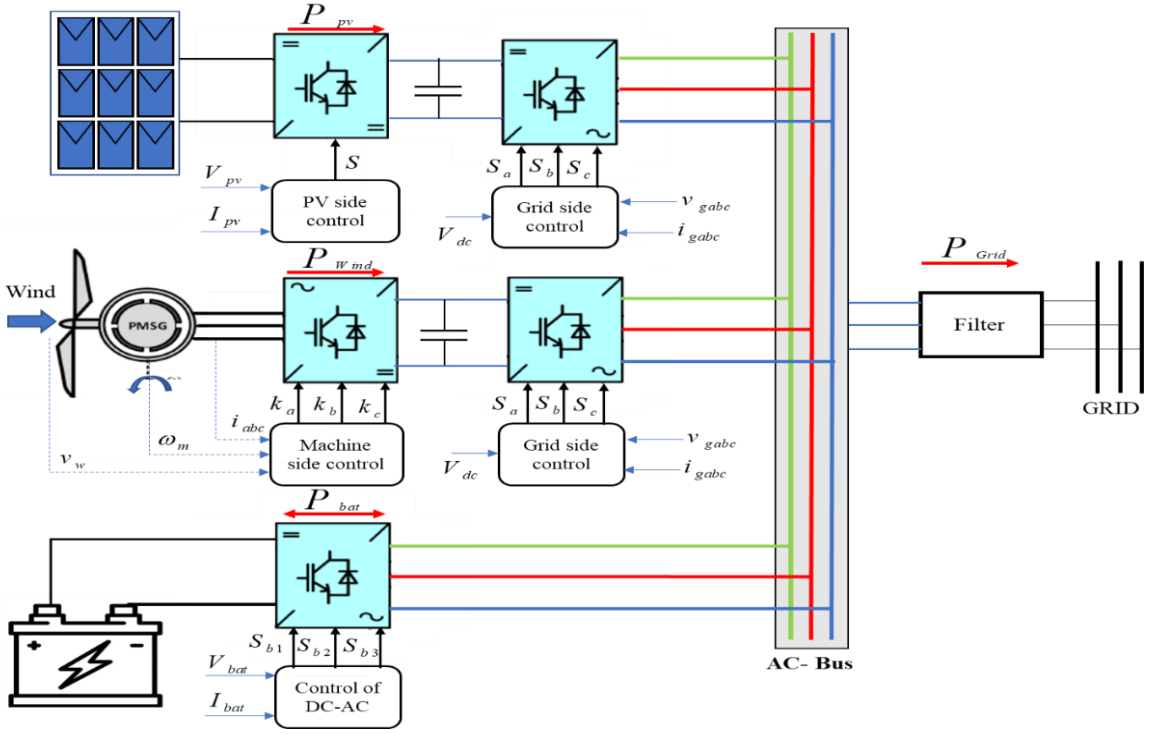

Fig.5.2 HRES configuration with common AC-bus

5.2.3 The proposed configuration of HRES

Fig.5.3 shows the proposed configuration applied to a combined hybrid energy system integrating three main subsystems PV, WECS including storage system with three level inverter and control units. PV and WEC systems are used as a primary energy source and the batteries as a backup energy storage. All three energy systems are connected in parallel to the common DC-bus. The output from the DC side combined in parallel using a three-phase NPC inverter to

provide the desired power to the grid. Two MPPT techniques are employed for PV and WEC systems and an additional DC-DC, bidirectional buck-boost DC-DC converter is used in buck mode to charge and in a boost mode to discharge the batteries.

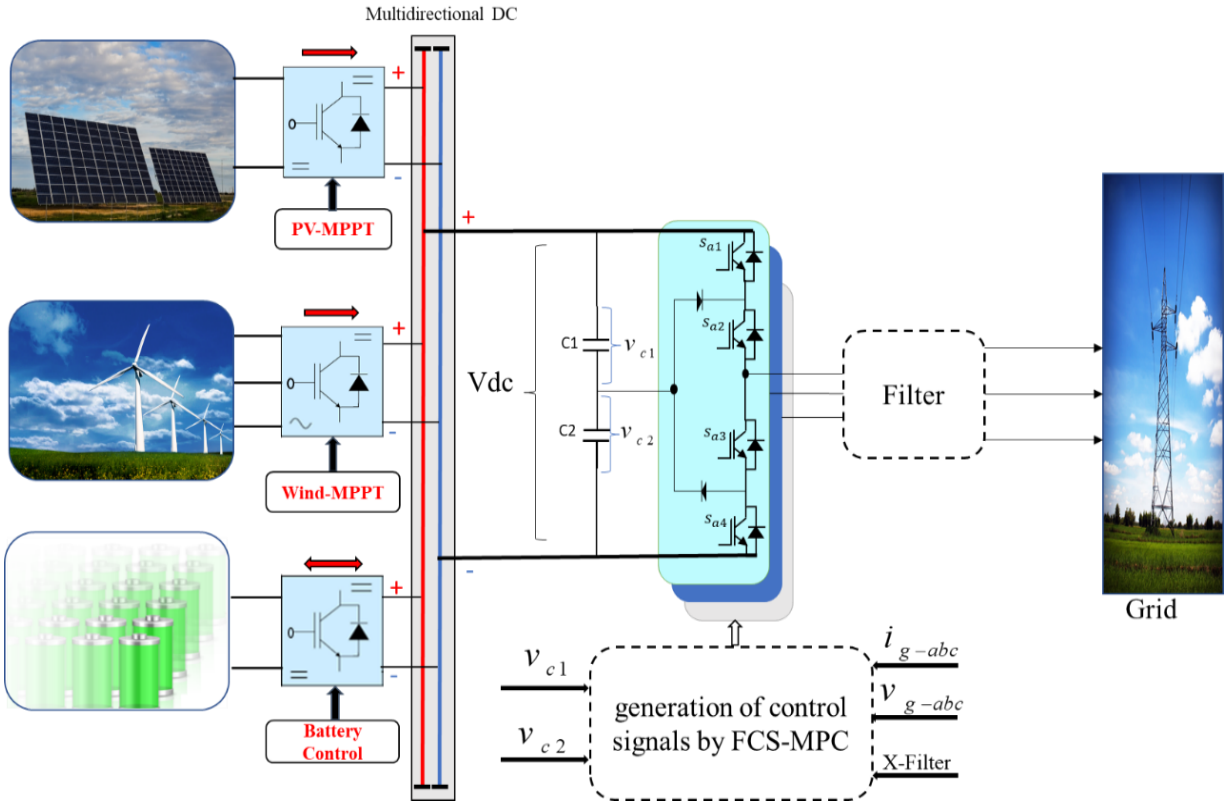

Fig.5.3 Synoptic diagram of the hybridization of PV-Wind including storage power plant

5.2.4 What services can batteries provide in our work?

a- Anti-islanding protection is a required function of grid-connected systems. The objective is to disconnect the solar modules and WEC systems during power outages of the grid. Disconnection isolates potential problems to avoid damage to PV and WECS components and promotes safe conditions for performing maintenance. Therefore, it is necessary to implement grid support functions in the control loops. Grid-connected RE systems must satisfy several requirements to contribute to the normalized operating grid under perturbations. Given the variable nature of renewable energy resources, energy storage is a necessary component of a distributed PV system to provide reliable power during a grid outage. Distributed storage has the potential to supply electricity during grid outages.

This scenario has a very high cost, requires a very high level of integration with other system components, typically less mature than many other types and requires an even more robust and thorough approach to maintenance. Integrating batteries into a grid requires additional balance-of-system equipment, in addition to safety equipment, such as fuses, current fault protection, etc.

If the inverter is fitted with anti-islanding protection, it simply means that it has an islanding detection and can sense when the grid is down. That way, it can stop feeding power back to the grid and protect the utility workers.

An anti-islanding inverter might seem like a small detail, but it's important because:

- Anti-islanding ensures the safety of workers fixing the grid during an outage, keeps the grid equipment safe. The grid infrastructure is set up in such a way that it will shut down when it detects a severe problem. Without system anti-islanding protection, the hybrid system will continue to send voltage back to the grid, which could damage the grid hardware and lead to other costly losses.
- Anti-islanding prevents inverter damage. System islanding could cause damage to inverters, rendering them non-functional. Anti-islanding exists to protect the inverters from overload and save the system from costly damages.

b- Intermittency has always been an issue limiting the growth of renewable energy, but the development of hybrid energy systems (Wind-Photovoltaic) well suited to grid-connected or decentralized generation can solve several energy supply problems [11]; these systems require geographical places, which can provide these types of sources. Other solutions of hybrid systems, which does not depend on the geography is very significant to improve PV-Wind power quality. In addition to the storage energy system with a hybrid system, battery storage may not be the economic resource to help integrate renewable energy to the grid[12].

5.3 Originality of the proposed configuration

Solar PV system is integrated with wind energy system to get a hybrid system as shown in Fig.5.4. It is composed of PV arrays, DC-DC converter, with PV-MPTT, a PMSG based wind turbine system with AC-DC converter, MPPT algorithm and DC-AC three phases inverter grid connection. Wind turbine system is connected to DC-bus, whereas the hybrid system is connected to CPI via RL filter and voltage source inverter (VSI).

The hybrid renewable energy system ensures continuous power flow to the grid. The proposed P&O based MPPT for a solar PV system, and FL-PI MPPT comprises for a wind turbine. Wind turbine is connected in parallel to a common PWM inverter through their individual AC-DC converter. The only adaptation needed is the requirement to maintain the DC-bus voltage constant. Both solar PV and wind are connected in parallel to a common PWM inverter through DC-AC inverter. DC-voltage is measured and controlled based DC-link controller. The output is fed into another controller, to generate the pulses for DC-AC NPC converter. The NPC converter output voltage is variable according to the FSC-MPC output algorithm. Hence, PLL control has been implemented to maintain the output voltage

synchronization. The low harmonic distortion of voltage and current at the inverter output is achieved by using an output filter.

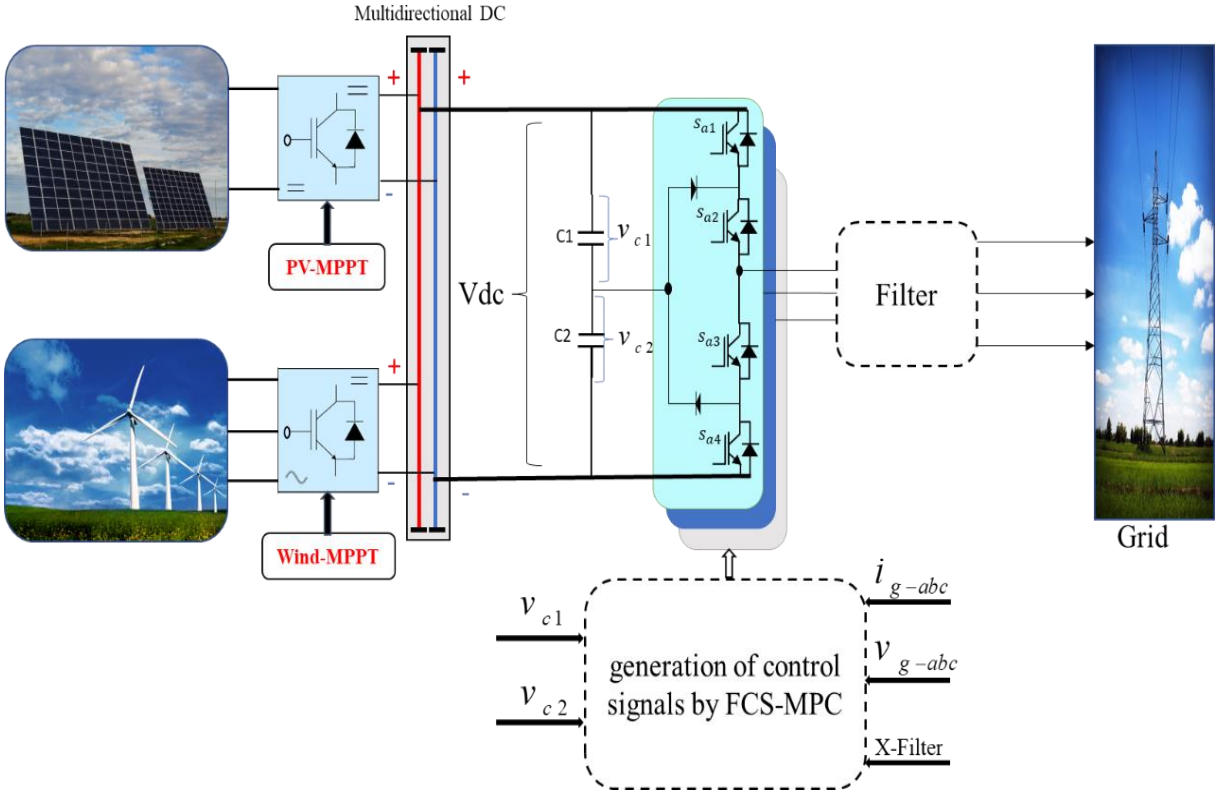

Fig.5.4 Architecture of the power hybrid system

5.3.1 Hybrid PV-WES-side Power Control

The control scheme of PV side converter is presented in chapter 2; however, the control scheme of wind side converter is presented in chapter 3.

5.3.2 Hybrid grid-side Power Control

Grid-side inverter has the same control structure as that of PV-grid-side converter shown in chapter 2, where DC-link control take the P_{hyb} instead the P_{PV} such as given by the expression (5.1). The common DC-voltage is maintained constant.

$$I_{PVg} = \frac{2P_{hyb}}{3\,V_{\max}} \tag{5.1}$$

5.3.3 Hybridization of the PV/WT power

Hybrid PV-wind generation system can offer higher reliability to maintain continuous power than any other individual power generation system. After having modeled, simulated and optimized of the two systems, PV and wind power separately, the hybridization of these two systems is supposed to be accomplished upstream of the DC bus. The phase which presents clearly this hybridization is located downstream in the DC-bus, it is although the injecting process of the total power into the grid via a DC-bus and inverter. According to the Fig.5.4

above, the inverter connected to the grid must inject the total power used by the two systems. The total power will be given by the sum of the wind and PV powers as in (5.2) [13]. So, we can estimate the wind power from this equation.

$$P_{hyb} = P_{PV} + P_{WT} \tag{5.2}$$

P_{PV} : The total power of the PV system;

P_{WT} : The total power of the WEC system;

P_{hyb} : The total power of the whole hybrid system.

5.4 Simulation results and discussions

The block diagram of integrated PV-WT system is shown in Fig.5.4. The system is simulated using MATLAB/SIMULNK. It is composed of 10 kW PV and a10 kW WT, which supplying the grid. Firstly, the dynamic behavior of this system is analyzed under different operating conditions. Digital simulation studies were performed for converter systems with a wind turbine based PMSG and PV panels. Many simulation studies were conducted to show performance of HRES system under various conditions.

5.4.1 Dynamic behavior of hybrid PV-WT

The first test; the temperature is assumed to be 25°C with high wind speed such as in Fig.5 5(a). The dynamic performance of hybrid PV-WT grid connected system is studied under different operating conditions such as solar irradiation and wind speed. Solar irradiation and wind speed signals are shown in Fig.5.5(b) and Fig.5.5(c), respectively. The output power of PV depends on solar irradiation and ambient temperature. Solar irradiation has the major influence on the performance of the PV system. The output power is directly proportional to the insolation level; it is depicted in Fig.5.5(d); it decreases when solar irradiation decreased. Therefore, the output power of the PV system is fluctuated according to the variation of the irradiation. The output power of WT depends on wind speed. WT power output varies due to change in wind speed. The pitch angle is activated at zero without changing the beta angle of the blade. The power fluctuations in PV or WES are a result of variations in weather conditions. The power achieved by the hybrid systems (wind and photovoltaic) illustrated in Fig.5.5(d) is injected to the grid; the reactive power of the grid inverter is shown in Fig.5.5(e).

Fig.5.5(f) represents the common DC-voltage; it is maintained at reference 762V with drastic changes in wind and solar conditions. The current and voltage waveforms are shown in Fig. 5.5(g, h & i), they show how the current grid amplitude increases compared to the grid current seen in chapter 2.

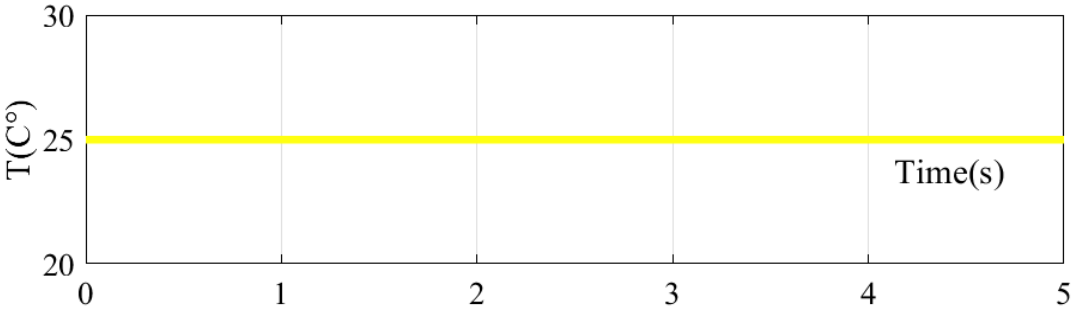

(a) Ambient temperature

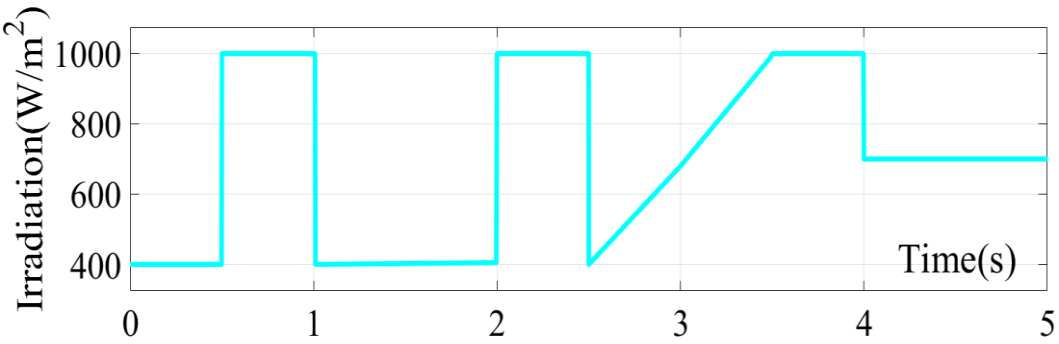

(b) Solar irradiations

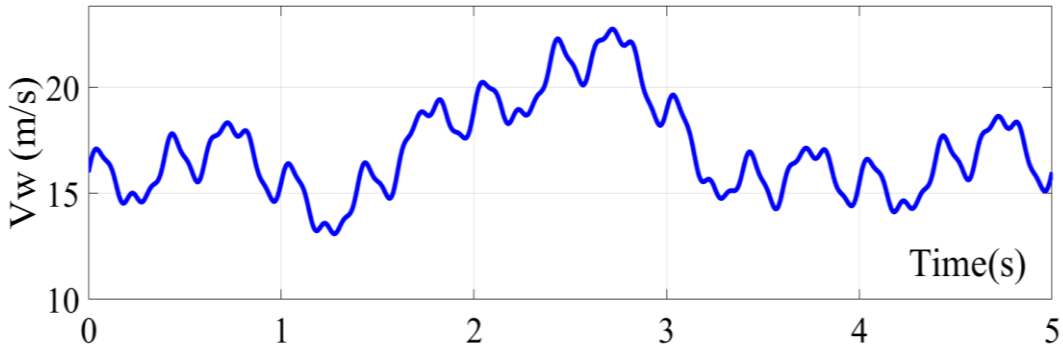

(c) Wind profile

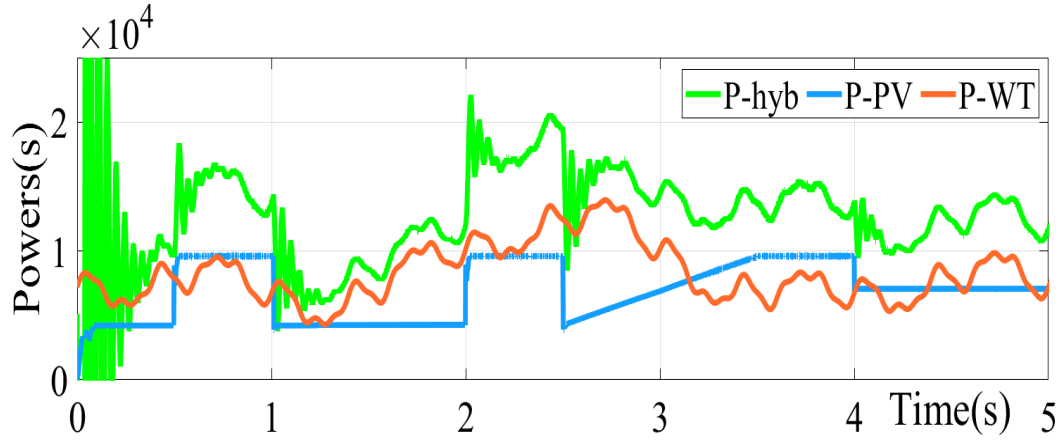

(d) Active powers of PV, WT and the total HRES power

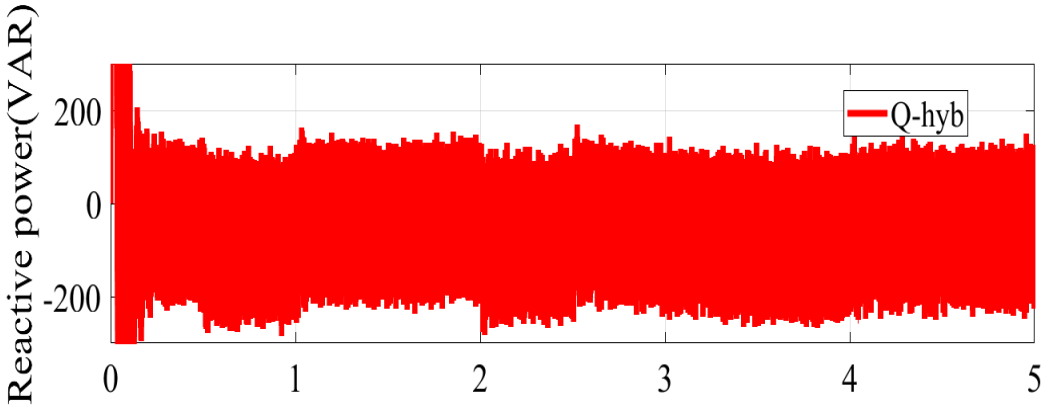

(e) Reactive power of HRES

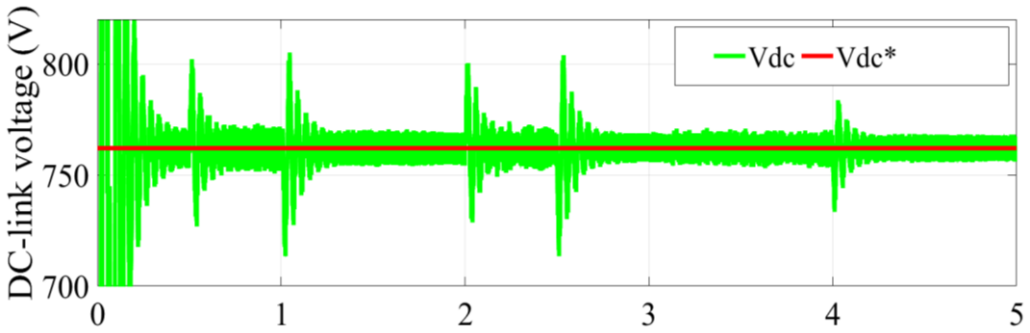

(f) DC-voltage of HRES

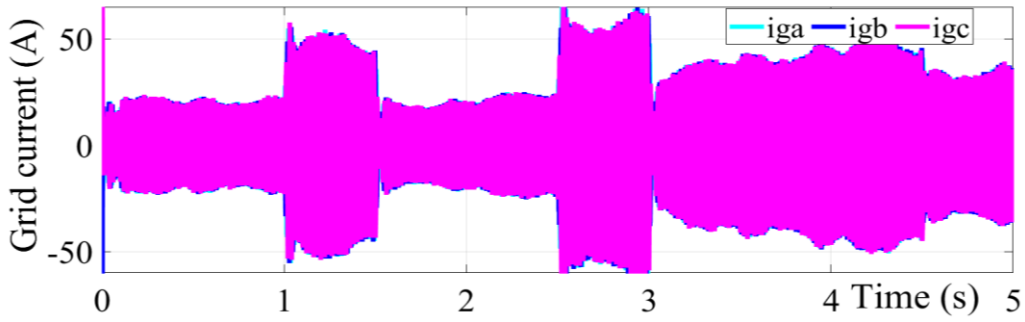

(g) Grid current injected by HRES

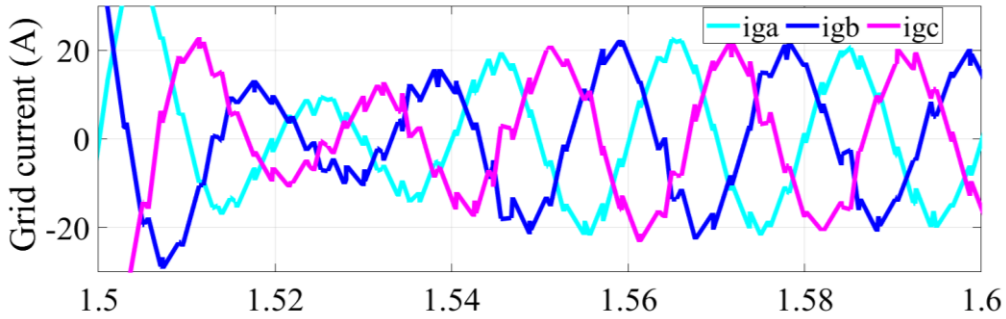

(h) Zoom of grid current injected by HRES

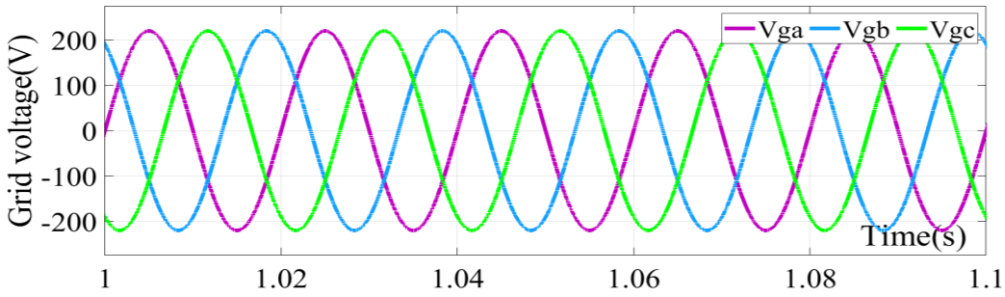

(i) Zoom of grid voltage source

Fig.5.5 Simulation results for constant temperature

In the second test, the temperature is assumed variable as in Fig.5.6(a). Fig.5.6(b) shows the active power extracted at a nearly unity power factor from the hybrid PV-wind generator. The active power has varied smoothly compared to the irradiance, temperature and wind speed variations. PV array voltage traces the desired level well response to solar radiation and temperature changes.

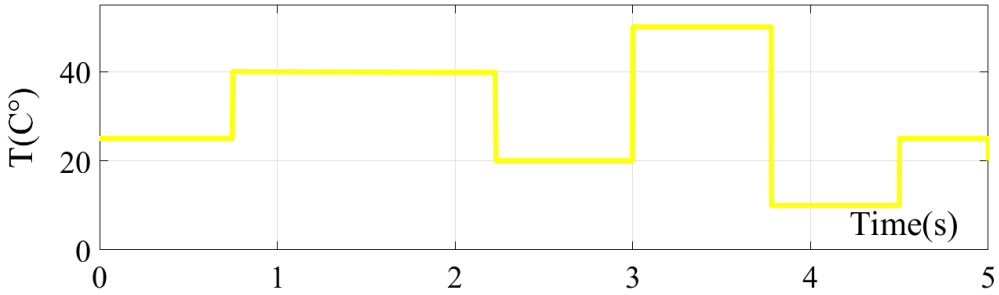

(a)Variable temperature

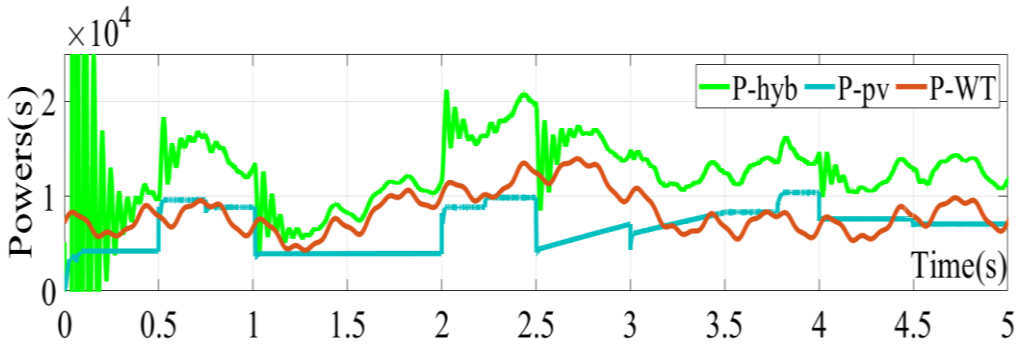

(b) Active powers of PV, WT and the total HRES power

Fig.5.6 Simulation results for variable temperature

Neutral-point voltage imbalance is one of the main problems of multilevel-level neutral-point clamped inverters that impedes their industrial application. In order to solve this problem, a neutral-point voltage balancing method based on finite set model predictive control (FCS-MPC) is proposed in this thesis, thus, DC-link capacitor voltages are balanced.

This method shows that a simple control loop maintains the voltage balance in different operating conditions as illustrated in Fig.5.7(a, b and c).

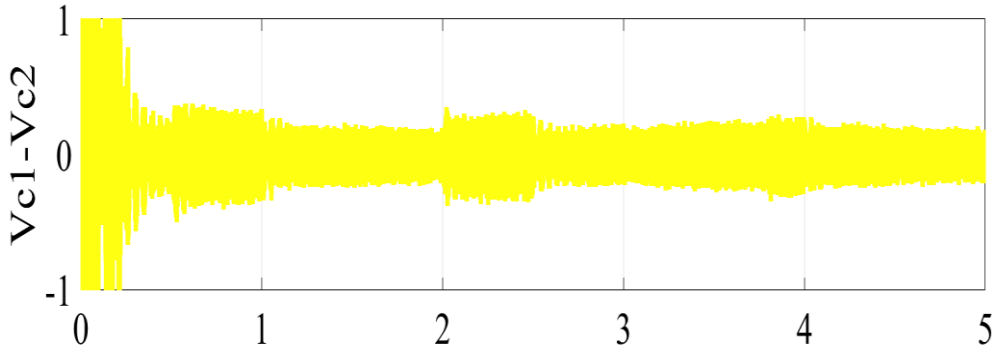

a) Voltage difference (Vc1 – Vc2)

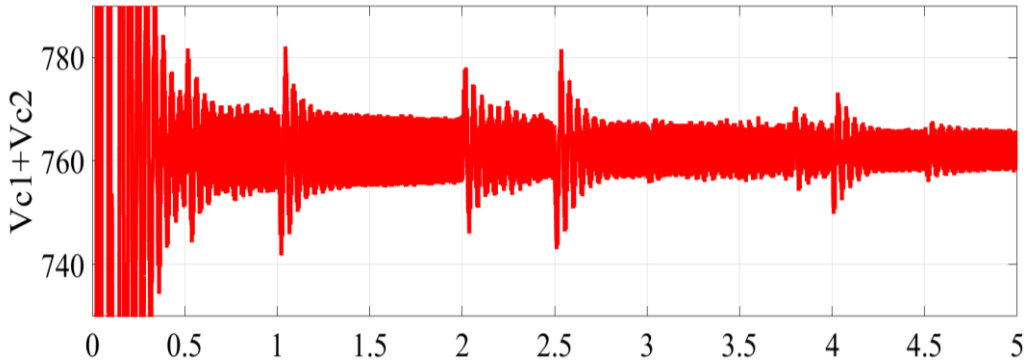

b) DC-voltage (Vc1 + Vc2)

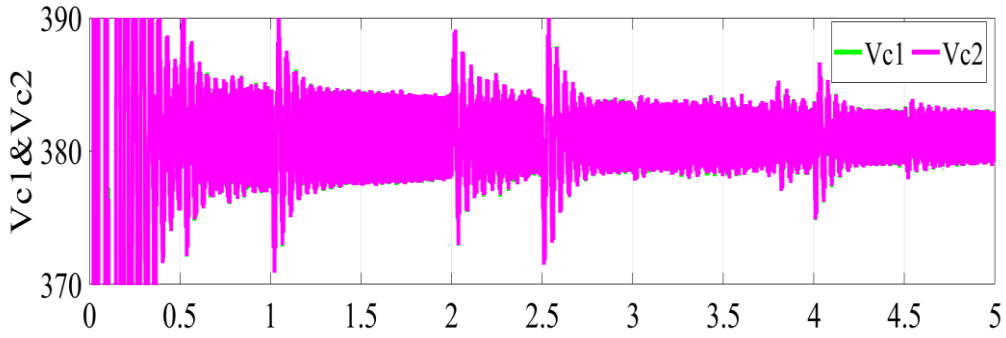

c) DC-voltages (Vc1&Vc2)

Fig.5.7 Simulation result for the voltage balancing

Wind/PV hybrid system is in nearly the unity power factor operation under the wind speed, solar radiation condition and temperature as shown in Fig. 5.8 (maintain the reactive power to the zero level). The harmonic distortions have been increased. Using the FFT analysis tool in Simulink, the THD of the output current waveforms was recorded. The results show the current harmonics supplied by the inverter, in which case the THD value was between (7 % and 11%)

for abnormal operation (change of weather condition such as solar radiation, wind or temperature).Where, THD value is above the IEEE standard of 5%.

As the low pass filter eliminated the low order harmonics well, some higher order harmonics were still seen, but with small magnitudes. The THD for the current waveform during the normal operating condition was between (4 % and 6%).

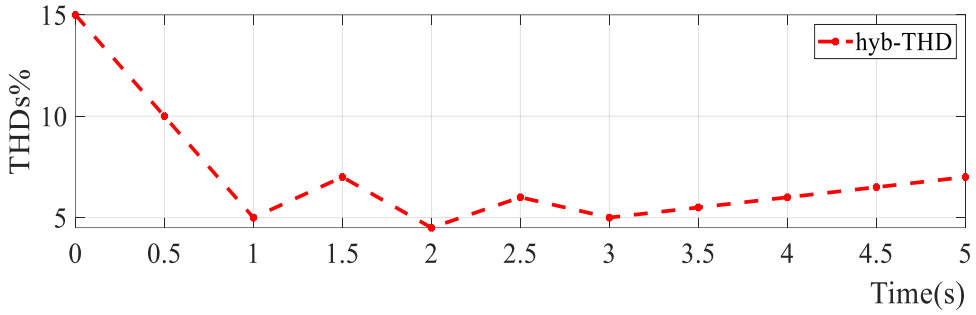

Fig.5.8 THDs of HRES

4.5 Conclusion

This chapter has provided the basic concepts of hybrid system, photovoltaic and wind turbine. Different integration schemes are illustrated shown by different schematic diagrams of hybrid renewable energy system. In this chapter, a hybrid PV-WES grid connected was modeled and simulated using Matlab/Simulink. The dynamic performances of the hybrid system at different weather conditions are analyzed. In PV system, Perturb & Observe MPTT technique was used to satisfy the maximum power of PV arrays at different weather conditions. WES generates maximum power using FL-PI, PMSG generates power's stability due to their control ability. This can increase the power quality and causes transient stability. Finally, the advance control work using FCS-MPC, which has been done in this field, is illustrated. Motivation and challenges are also mentioned to improve the interest. Challenges are carried out to develop the advance techniques to overcome the different technical issues, like MPPT, DC-link voltage, synchronization, voltage fluctuations, reliability and stability of HRES.

In this chapter, simulation study for PV-WES based NPC grid connected is presented. Several tests were studied in order to understand more deeply the behavior of power control of the system in steady and transient, which depends on weather conditions.

The modeling and simulation study was carried out based on MATLAB/Simulink. The simulation results showed the excellent performances of PV/Wind hybrid control in response in solar intensity conditions and wind speed.

The simulation tests assure that the power control algorithm could work under sever and variable conditions, which could guarantee a good power performances (short response time, good tracking, low power error and good power quality) and get a nearly unity power factor.

References

[1] KIM, Seul-Ki, KIM, Eung-Sang, et AHN, Jong-Bo. Modeling and control of a grid-connected wind/PV hybrid generation system. In: 2005/2006 IEEE/PES Transmission and Distribution Conference and Exhibition. IEEE, 2006. p. 1202-1207.

[2] ABBASSI, Rabeh, HAMMAMI, Manel, et CHEBBI, Souad. Improvement of the integration of a grid-connected wind-photovoltaic hybrid system. In : 2013 International Conference on Electrical Engineering and Software Applications. IEEE, 2013. p. 1-5.

[3] YOUNSI, Sami, JRAIDI, Moncef, HAMROUNI, Najib, et al. Modelling and control of hybrid renewable energy system connected to AC grid. International Journal on Computer Science and Engineering, 2011, vol. 3, no 12, p. 3854.

[4] RADWAN, Amr Ahmed A., YASSER, A.-RI Mohamed, et JIANG, Xichen. A hybrid wind-photovoltaic generation system modeling and performance evaluation. In : 2019 IEEE 7th International Conference on Smart Energy Grid Engineering (SEGE). IEEE, 2019. p. 129-133.

[5] BENLAHBIB, Boualam. Supervision d'un système hybride éolienne-photovoltaïque connecté au réseau électrique. 2019. Thèse de doctorat.

[6] FAIZ, Asghar et REHMAN, Abdul. Hybrid renewable energy systems: Hybridization and advance control. In : 2015 Power Generation System and Renewable Energy Technologies (PGSRET). IEEE, 2015. p. 1-5.

[8] GAJEWSKI, Piotr et PIEŃKOWSKI, Krzysztof. Control of the Hybrid Renewable Energy System with Wind Turbine, Photovoltaic Panels and Battery Energy Storage. Energies, 2021, vol. 14, no 6, p. 1595.

[9] BENHALIMA, Seghir. Modélisation et contrôle des systèmes éoliens-solaire intégrés au réseau VSC-HVDC. 2019. Thèse de doctorat. École de technologie supérieure.

[10] MURUGAN, Bala et MANOHARAN, S. Optimal power flow management control for grid connected photovoltaic/wind turbine/diesel generator (GCPWD) hybrid system with batteries. International Journal of Renewable Energy Research (IJRER), 2013, vol. 3, no 4, p. 819-826.

[11] NOTTROTT, A., KLEISSL, J., et WASHOM, B. Storage dispatch optimization for grid-connected combined photovoltaic-battery storage systems. In : 2012 IEEE Power and Energy Society General Meeting. IEEE, 2012. p. 1-7.

[12] ZHANG, Yang, CAMPANA, Pietro Elia, LUNDBLAD, Anders, et al. Comparative study of hydrogen storage and battery storage in grid connected photovoltaic system: Storage sizing and rule-based operation. Applied energy, 2017, vol. 201, p. 397-411.

[13] GASSAB, Samir. Modélisation d'une centrale à énergie renouvelable photovoltaïque-éolienne. 2018. Doctoral thèses.

Chapter 6 : General Conclusion and Perspectives

6.1 Report of the thesis.....138
6.2 Perspectives.....141

Chapter 6 : General Conclusion and Perspectives



6.1. Report of the thesis

The research work of this thesis presents a contribution to the control and optimizing the behavior and energy performance of two energy systems totally renewable, In this work, we presented different stages of the study of the functioning of the hybrid systems using renewable energy sources PV and wind, with the electrical network.

The first chapter deals with a three-phase two-stage grid tied PV (photovoltaic) system. The first stage is a boost converter, which serves the purpose of MPPT (maximum power point tracking) and feeding the extracted solar energy to the DC link of the PV inverter, whereas the second stage is a three-level voltage source converter (VSC) using Neutral Point Climped (NPC) inverter serving as PV inverter which feeds power from a boost converter into the grid.

The input voltage of a boost converter is adjusted according to MPPT algorithm and the output voltage of boost converter, which is also the DC link voltage of VSC is also kept adaptive according to CPI voltage condition. In overall, the proposed system is operated such that both the input and output voltages of boost converter are adjusted according to sensed variables of the circuit. The boost converter feeds the power to the DC link of VSC, which then feeds that power into the three-phase grid at unity power factor with respect to CPI. A P&O based MPPT technique is used and a PLL control is proposed for the control of the VSC. The amplitude of the reference grid currents is estimated using a PV Feedforward (PVFF) term and a Fuzzy logic controller DC link voltage error. A set of unit vectors is estimated from grid voltages to synchronize output currents of VSC. The estimated reference grid currents are compared with sensed grid currents and FCS-MPC current controller is used to generate switching logic for VSC.

The performance of proposed system has been demonstrated for a wide range of CPI voltage variation. A simple and novel adaptive DC link voltage control approach has been proposed for control of grid tied VSC. The DC link voltage is made adaptive with respect to CPI voltage which helps in the reduction of losses in the system. Moreover, a PV array Feedforward term is used which helps in fast dynamic response. An approximate linear model of DC link voltage control loop has been developed and analyzed considering Feedforward compensation. The PV array Feedforward term is so selected that it is to accommodate for change in PV power as well as for CPI voltage variation.

The Feedforward Fuzzy Logic (FF-FL) controller is validated under Matlab/Simulink 2019. The presented results indicated that the FF-FL controller significantly improves the dynamic response of PV system compared to the PI controller, and the (FF-FL) controller can further reduce overshoot caused by disturbance. The THDs of the grid currents and voltages are found less than 5% (within IEEE standard). The simulation results have confirmed the feasibility of the proposed control algorithm.

Finaly, the FCS-MPC algorithm is developed with the aim to achieve a perfect control of the powers injected into the grid using a three-level NPC inverter as part of renewable energy system. According to the discrete-time model of the power conversion system, its future behavior is first predicted at the future sampling time (k+1)Ts. Thereafter, a specified cost function is formulated as a function of the line currents and the two DC-bus voltages quadratic errors. Accordingly, the

opportune switching state which minimizes the cost function is determined and applied at the next switching time (k+1)Ts . Moreover, the control of power flow from the NPC inverter to the grid is assured by the FCS-MPC algorithm and with the RL filter. Additionally, the output current of the inverter has a sinusoidal waveform so that the THD level is below the limits of international standards (<<5%). Furthermore, the voltage balancing control is effectively achieved in the model.

In the second chapter, two MPPT strategies, the conventional PI and the fuzzy-PI controllers were designed and developed for a standalone WECS. These control strategies allow to maximize the output power of the WECS. The simulation results demonstrate that the Fuzzy-PI Controller provides high performance and shows very good dynamic as compare to the PI controller under fluctuating of wind speed.

Renewable energy sources like PV provide direct power in the form of DC supply, but the power developed by the WECS is in the form of AC supply. Integration in AC faces many problems like synchronizing the phase, amplitude and frequency of the voltages and currents generated. This complexity can be overcome by integrating PV and Wind in the DC supply form. SVPWM technique improves the quality of current and reduces the harmonics efficiency. In this thesis, SVPWM technique is applied for successful conversion of power.

The fourth chapter illustrated the difficulty in evaluating the role of energy storage. Although there is a large body of literature aimed at assessing both technical and economic issues associated with storage integration, there is a lack of coherence in the modeling approaches used and recommendations drawn from the community. These discrepancies arise in large part due to the versatility of storage resources and the market and regulatory structures that determine storage economics.

As a result, market and regulatory challenges are becoming equally pressing. This survey points to a critical need for new models that can provide insight into the interplay between the technical, economic and regulatory issues. In addition to previously discussed gaps in the current literature, there are well-known barriers to energy storage adoption, such as: technological maturity, cycle efficiency, as well as capital, operating and maintenance costs, The balancing and power quality requirements for accommodating non-dispatchable, intermittent renewable energy sources in the power grid are changing as the penetration level increases. It is useful to point out that energy storage alone is not an all encompassing solution for addressing the myriad of challenges associated with renewable energy integration. Research on grid-level energy storage system must focus on the improvement of battery performance, including operating voltage, cycle life, energy and power densities, safety, environmental friendliness, and cost improve the energy density, reduce the cost, and develop safe battery systems.

In this thesis, a small scale hybrid PV-WT grid connected is designed for a rated power of 10 kW from PV system and 10 KW from WECS. The system consists, one side, of solar PV array, DC-DC converter. Anothor side, of wind generator, wind-side converter, and grid interface three-phase three-level NPC inverter. Based on the results obtained from computer simulations the following conclusions can be made :

That the extraction of the maximum power from PV arrays and wind turbine system are obtained using MPPT system. The P&O MPPT algorithm has been implemented for the PV system and FL-PI MPPT has been implemented for WECS. The proposed system has been simulated in MATLAB-SIMULINK environment. From the simulation results, it is found that, to obtain grid voltage, grid current and balancing at nearly unity power factor, the grid side parameters have to be tuned properly by designing the FCS-MPC and proper modulation scheme for grid inverter interface.

This work offered an amended DC-link voltage controller founded on an adaptive DC-link controller with the feed forward term. The proposed controller is self-tuned so that the following limitations are satisfied: no overshoot and fast dynamic response. The proposed and analyzed FCS-MPC principles for a three-phase, three-level NPC grid-tied inverter elaborated the way to execute the FCS-MPC algorithm. This control strategy can effectively realize the three-level grid-performance. Besides that, both control methods (FF and FCS-MPC) appeared to exhibited the complementary and mutual influence that is represented by a low grid current THD value during steady state operation.

6.2. Perspectives

At the end of the results and observations presented in this thesis, perspectives interesting factors likely to contribute to the improvement of the hybrid system studied are possible. These perspectives can be summarized by the following points :

From theoretical point of view

- Other cost functions to improve the FCS-MPC performances of the hybrid system from different perspectives.
- Additionnal renewable source of energy can for example be used to ensure the continuity of the power supply in the event that the two RES sources operated as well as storage batteries will no longer be able to meet the user's energy demand.
- Investigation of other multilevel inverter (level or topology), DC/DC multilevel converter to improve the PV production system or AC/DC multilevel rectifier for WECS.

- Control and analysis of hybrid systems with power control of a wind and solar hybrid generation system for interconnected operation whith an electric distribution system, and that is through an investigation of Energy Management System (EMS), wich leads to reduce energy consumption, this has several benefits**.**

From practical point of view

- Altogether, the results presented in this manuscript remain theoretical results. As future work, the experimental validation of the entire hybrid system is the most considered perspective where the different control strategies developed will be implemented on microcontroller boards, such as dSPACE board adequate for setting practical implementation of the studied hybrid system.

Scientific Production during the PhD

International Conferences :

[1] **Nadjah Attik**, Abd Essalam Badoud, Rahmani Lazhar « Detailed Study of Inverter Control for Three Phase Grid Connected Solar PV System » International Conference on Sustainable Renewable Energy Systems and Applications Tebessa, Algeria, Dec. 04-05, 2019

[2] **Nadjah Attik,** Abd Essalam Badoud, Farid Merahi, « Fuzzy-PI MPPT Control Method based Wind Energy Conversion System » International Conference on Innovative Applied Energy (Smart Exhibition) (DZENERGY 2021), (DZENERGY 2021)

[3] **Nadjah Attik**, Abd Essalam Badoud, Farid Merahi, Abdelbaset Laib, Rahmani Lazhar «An improved DC-link control for dual-stage grid connected PV system using three-level NPC inverter » 19th IEEE International Multi-Conference on Systems, Signals & Devices SSD'2022

[4] **Nadjah Attik**, Abd Essalam Badoud, Farid Merahi, Abdelbaset Laib, Rahmani Lazhar « Performance Analysis of Four Level NPC Inverters using FCS-MPC Voltage Balancing Method » 19th IEEE International Multi-Conference on Systems, Signals & Devices SSD'2022

Journal Papers :

[1] **Nadjah Attik**, Abd Essalam Badoud, Farid Merahi, Abdelbaset Laib, Yahia Ayat « DESIGN OF AN EFFECTIVE CONTROL FOR GRID-CONNECTED PV SYSTEM BASED ON FS-MPC» FACTA UNIVERSITATIS Series: Electronics and Energetics Vol. 34, No 1, March 2021, pp. 21-35 https://doi.org/10.2298/FUEE2101021A

Abstract

This thesis is a contribution to the problem of hybridization of renewable energy systems, more precisely, a hybrid system composed of photovoltaic and a wind turbine system. This system is supposed to be equipped with power electronic converters and storage system (batteries). The first objective is to extract the maximum power from each source. To do this, our approach is based on tracking of maximum power point, P&O method is used, this technique with a dual purpose, is applied to the PV system. In order to achieve the maximum power form wind turbine for different wind speed, MPPT controller is implemented on the rectifier side for the extraction of maximum power. MPPT controller is implemented using Fuzzy Logic-Proportional Integral (FL-PI) control technique. When the wind speed increases, the real power generated by the Permanent Magnet synchronous Generator (PMSG) based WECS increases accordingly to MPPT controller. The potential to use DC directly from WECS requires proper rectification of power (from AC to DC). In the rectification process, the basic Space Vector Pulse Width Modulation (SVPWM) technique is applied to the WECS designed with (PMSG). This content is involved in a DC-link control using the Feed Forward-Fuzzy Logic (FF-FL) method to control the first conversion stage. It is associated with the second stage predictive current control strategy Finite Control Set Model Predictive Control (FCS-MPC) applied to three-phase three-level inverter, based grid connected hybrid PV-wind system.

In this thesis, the first processing step extracts the maximum power from hybrid system field to feed the DC-link stage. To maintain a suitable power intermission control, it must keep the DC-link voltage at its reference value, then assessment the amplitude of the grid currents. Simple regulators have an extended time to respond and considerable voltage ripples over steady-state, Feed Forward technique overcomes these issues. The selectors of adaptive DC-link voltage controller are used to assure a high efficiency of the system, the thesis proposed an adaptive DC-Voltage Feed Forward by adjusting reference DC-Voltage according to CPI (common point of interconnection) voltage. The fuzzy logic with optimal number of rules as well as the membership functions is used to compensate the DC-Link losses.

To compensate the current undesirable harmonic with a unity power factor, Finite Control Set-Model Predictive Control (FCS-MPC) is suggested for current control of three-phase three-level Neutral-Point Clamped (NPC) inverter in terms of evaluated cost function that reduces the error current.

Keywords: Hybrid system (PV-Wind), Permanent Magnet Synchronous Generator (PMSG), Three-phase three-level Neutral-Point Clamped (NPC), Feed Forward-Fuzzy Logic (FF-FL), Fuzzy Logic-Proportional integral (FL-PI), Grid connected converters and Finite Set Model Predictive Current Control (FCS-MPC).

Résumé

Cette thèse est une contribution à la problématique de l'hybridation du système à énergies renouvelables, plus précisément, un système hybride composé d'un système photovoltaïque et d'une turbine éolienne. Ce système est censé être équipé de convertisseurs d'électronique de puissance et d'un système de stockage (batteries). Le premier objectif est d'extraire le maximum de puissance à partir de chaque source. Pour ce faire, notre approche est basée sur la poursuite du point de puissance maximale, la méthode P&O a été utilisée, cette technique à double finalité, est appliquée au système PV. Pour atteindre la puissance maximale formée à différentes vitesses de turbine éolienne, le contrôleur MPPT est mis en œuvre du côté du redresseur pour l'extraction de la puissance maximale. Le contrôleur MPPT est mis en œuvre à l'aide de la technique de contrôle Logique Floue Proportionnel Intégrale (FL-PI). Lorsque la vitesse du vent augmente, la puissance réelle générée par le système de conversion à énergie renouvelable (SCER) basé sur le Générateur Synchrone à Aimants Permanents (GSAP) augmente à l'aide du contrôleur MPPT. La possibilité d'utiliser le courant continu directement à partir du SCEE nécessite une rectification appropriée (du courant alternatif au courant continu) de l'alimentation. Pour le processus de redressement, la technique de modulation de la largeur d'impulsion du vecteur spatial (SVPWM) de base du SCEE est conçue avec un GSAP. Ce contenu est impliqué dans un contrôle de liaison DC utilisant la méthode (FF-FL) pour contrôler le premier étage de conversion associé à la stratégie de contrôle du courant prédictif du deuxième étage FCS-MPC appliquée pour un onduleur triphasé à trois niveaux, basé sur le système hybride PV -éolien connecté au réseau.

Dans cette thèse, la première étape de traitement extrait le maximum de puissance du system hybride pour alimenter l'étage DC-Link. Pour maintenir un contrôle d'interruption de puissance adapté, il faut maintenir la tension du circuit intermédiaire à sa valeur de référence puis évaluer l'amplitude des courants du réseau. Les régulateurs simples ont un temps de réponse prolongé et des ondulations de tension considérables sur l'état stable, la technique Feed Forward surmonte ces problèmes. Les sélecteurs du contrôleur adaptatif de tension de liaison DC sont utilisés pour assurer un rendement élevé du système, la tension de liaison DC est adapté par la technique Feed Forward à la tension de liaison DC de référence en fonction de la tension PCI (point commun d'interconnexion). La logique floue avec un nombre optimal de règles ainsi que les fonctions d'appartenance sont utilisées pour compenser les pertes de liaison DC.

Pour compenser l'harmonique indésirable de courant avec un facteur de puissance unitaire, la commande prédictive à ensemble de commande fini (FCS-MPC) est suggérée pour le contrôle du courant de l'onduleur triphasé à point neutre (NPC) à trois niveaux en termes de fonction de coût évalué qui réduit le courant d'erreur.

Mots-clés : Système hybride (PV- éolien), Generateur synchrone à aimants permanent (GSAP), Onduleurs de tension à point neutre (NPC) triphasé à trois nineaux, Feed Forward-Fuzzy Logic (FF-FL), Fuzzy Logic-Proportional intégral (FL-PI), Convertisseurs connectés au réseau et La commande prédictive à ensemble de commande fini (FCS-MPC).

ملخص

هذه الأطروحة مساهمة في مشكلة تهجين نظام الطاقة المتجددة. بتعبير أدق، نحن نعتبر نظامًا هجينًا يتكون من الألواح الشمسية الكهروضوئية وتوربينات الرياح. من المفترض أن يكون هذا النظام مزودًا بمحولات ونظام تخزين (بطاريات). الهدف هو تطوير استراتيجيات التحكم لاستخراج الطاقة القصوى المتاحة من المصادر المدروسة ولتحسين نظام الطاقة الكلي .الهدف الأول هو استخراج أقصى طاقة من كل نظام. للقيام بذلك، يعتمد نهجنا على تتبع أقصى نقطة طاقة، تم استخدام طريقة Perturb and Observe (P&O) يتم تطبيق هذه التقنية ذات الغرض المزدوج على الألواح الشمسية. من أجل تحقيق أقصى قدر من الطاقة، يتم تشكيل توربينات الرياح بسرعات مختلفة، يتم تنفيذ وحدة التحكم MPPT على جانب المعدل لاستخراج أقصى طاقة. يتم تنفيذ وحدة تحكم MPPT باستخدام تقنية التحكم .Fuzzy Logic - Proportional Integral (FL-PI) عندما تزيد سرعة الرياح تزداد الطاقة الحقيقية التي تولدها WECS القائمة على PMSG بمساعدة وحدة التحكم MPPT .تتطلب القدرة على استخدام طاقة التيار المستمر مباشرة من WECS التصحيح المناسب (من التيار المتردد إلى التيار المستمر) لمصدر الطاقة. لعملية التصحيح، تم تصميم تقنية تعديل عرض نبض متجه الفضاء (SVPWM) الخاصة بـ WECS بمولد متزامن مغناطيسي دائم.

يشارك هذا المحتوى في عنصر تحكم رابط DC باستخدام طريقة Feed Forward-Fuzzy Logic (FF-FL) للتحكم في مرحلة التحويل الأولى، المرتبطة باستراتيجية التحكم في التيار التنبؤي للمرحلة الثانية المطبقة في عاكس ثلاثي المراحل ثلاثي المستويات، يعتمد على الشبكة الهجينة الكهروضوئية- نظام الرياح. في هذا الصدد، تستخرج خطوة المعالجة الأولى الحد الأقصى من الطاقة من حقل النظام الهجين لتغذية DC-linkللحفاظ على تحكم مناسب في انتقال الطاقة، يجب التحقق من جهد وصلة التيار المستمر بالقيمة المرجعية ثم تقييم سعة تيارات الشبكة. المنظمون البسيطون لديهم وقت طويل للاستجابة وتموجات جهد كبيرة على الحالة المستقرة، وتقنية Feed forward تتغلب على هذه المشكلات. تُستخدم محددات وحدة التحكم في الجهد DC-link التكيفية لضمان كفاءة عالية للنظام، وقد اقترحنا جهد ارتباط DC متكيف إلى الأمام عن طريق ضبط جهد ارتباط DC المرجعي وفقًا لجهد CPI(نقطة التوصيل البيني المشتركة). يتم استخدام المنطق الضبابي مع العدد الأمثل من القواعد بالإضافة إلى وظائف العضوية للتعويض عن خسائر ارتباط DC.

للتعويض عن التوافقي غير المرغوب فيه الحالي مع عامل قدرة الوحدة، يمكن للعمل المقترح أن يؤدي استراتيجية التحكم التنبؤية الحالية لنموذج التحكم المحدود لنموذج التحكم التنبئي يُقترح FCS-MPC للتحكم الحالي في العاكس ثلاثي المستويات ثلاثي المستويات من حيث التقييم دالة التكلفة التي تقلل الخطأ بين التيار المتوقع والتيار المرجعي. يُقترح التحكم التنبئي لنموذج التحكم المحدود (FCS-MPC) لإظهار الكفاءة الديناميكية العالية للمحولات متعددة المستويات.

كلمات مفتاحية: نظام هجين (PV-Wind)، مولد متزامن مغناطيسي دائم (PMSG)، محولات جهد نقطي محايد ثلاثي الأطوار بثلاثة مستويات (NPC)، تغذية أمامية -المنطق الضبابي (FF-FL)، المنطق الضبابي- التكامل النسبي (PI- FL)) ،المحولات المتصلة بالشبكة والتحكم التنبئي ذي المجموعة المحدودة (FCS-MPC).